FINAL REPORT

on

ACCELERATED / ABBREVIATED TEST METHODS FOR PREDICTING LIFE OF SOLAR CELL ENCAPSULANTS

TO

JET PROPULSION LABORATORY CALIFORNIA INSTITUTE OF TECHNOLOGY

FOR THE

ENCAPSULATION TASK OF THE LOW-COST SOLAR ARRAY PROJECT

The JPL Low-Cost Solar Array Project is sponsored by the U. S. Department of Energy and forms part of the Solar Photovoltaic Conversion Program to initiate a major effort toward the development of low-cost solar arrays. This work was performed for the Jet Propulsion Laboratory, California Institute of Technology by agreement between NASA and DOE.
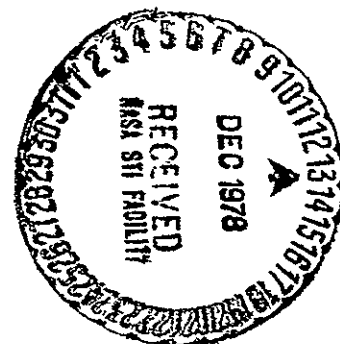
Period Covered:

October 25, 1977 through April 30, 1978

Prepared April 30, 1978

by

J. M. Kolyer, Principal Investigator
N. R. Mann, Statistician
J. Farrar, Project Manager

Rockwell International

FINAL REPORT
on

ACCELERATED / ABBREVIATED TEST METHODS FOR PREDICTING LIFE OF SOLAR CELL ENCAPSULANTS

TO
JET PROPULSION LABORATORY
CALIFORNIA INSTITUTE OF TECHNOLOGY

FOR THE
ENCAPSULATION TASK OF THE LOW-COST SOLAR ARRAY PROJECT

The JPL Low-Cost Solar Array Project is sponsored by the U. S Department of Energy and forms part of the Solar Photovoltaic Conversion Program to initiate a major effort toward the development of low-cost solar arrays. This work was performed for the Jet Propulsion Laboratory, California Institute of Technology by agreement between NASA and DOE.

Period Covered.

October 25, 1977 through April 30, 1978

Prepared April 30, 1978

by

J. M. Kolyer, Principal Investigator
N. R. Mann, Statistician
J. Farrar, Project Manager

Rockwell International

Autonetics Strategic Systems Division
Electronic Systems Group
3370 Miraloma Avenue
P O Box 4192
Anaheim, CA 92803

ACKNOWLEDGMENTS

ABSTRACT·'

Accelerated and abbreviated test methods were developed for pre-
dicting the outdoor lifetime of solar cell encapsulants. Encapsulants are
clear materials applied as covers to protect the cells from environmental
hazards.

An important principle is that encapsulants should be tested in a
total array system allowing realistic interaction of components. Therefore,
micromodule test specimens were fabricated with a variety of encapsulants,
substrates, and types of circuitry. Interactions, sometimes favorable, were
observed between these components. One common failure mode was corrosion of
circuitry and solar cell metallization due to moisture penetration. Another
was darkening and/or opacification of encapsulant. However the power output
remained high despite drastic visual changes. '

A Test Program Plan was proposed. It includes multicondition
accelerated exposure, which was demonstrated to give successful predictions
for property changes. Another method was hyperaccelerated photochemical
exposure using a solar concentrator. It simulates 20 years of sunlight
exposure in a short time period of one to two weeks.

The study was beneficial in identifying some cost-effective encap-
sulants and array designs. It was shown that silicon junctions are remark-
ably resistant to moisture and contaminants With corrosion-resistant
circuitry, the encapsulant could be a low-cost plastic which protects cells
from dust, abrasion, and mechanical shock.

CONTENTS

CONTENTS' (continued)

CONTENTS (continued)

CONTENTS (continued)

CONTENTS (continued)

ILLUSTRATIONS

ILLUSTRATIONS (continued)

ILLUSTRATIONS (continued)

TABLES

TABLES (continued)

TABLES (continued)

GLOSSARY AND DEFINITIONS

Term	Definition
A_{360}	Absorbance of UV light at 360 or 600 nm, which is $\log_{10}(\frac{1}{T})$ where T is the transmittance
Abbreviated Exposure	Outdoor (natural) exposure for considerably less than 20 years
Accelerated Exposure	Indoor exposure to light from a xenon lamp, filtered through Pyrex and water to attenuate short wavelength UV and infrared. All equipment was contained in a cabinet
ATR-FTIR	Attenuated Total Reflectance by Fourier Transform Infrared Spectroscopy (analytical method)
ATR-IR	Attenuated Total Reflectance by Conventional Infrared Spectroscopy (analytical method)
cm	centimeters
Contact	Collector, grid, or "finger" of titanium-silver on the upper surface of the solar cell
CUV	Cumulative UV light energy received by a sample
Desert Sunshine	Desert Sunshine Exposure Tests, Inc., Box 185 Black Canyon Stage, Phoenix, AZ
DSC	Differential Scanning Calorimetry (analytical method)
EMMA	Equatorial Mount with Mirrors for Acceleration, used at Desert Sunshine for exposure of samples
EMMAQUA	EMMA with intermittent water spraying of samples
EMMA(QUA)	Both EMMA and EMMAQUA

Term	Definition
ESCA	Electron Spectroscopy for Chemical Analysis (analytical method)
FET	Field Effect Transistor (A4T4391)
45°S	Abbreviated exposure outdoors on racks tilted 45° from vertical and facing south
FTIR	Fourier Transform Infrared Spectroscopy (analytical method)
IR	Infrared radiation, above 700 nm
ISWPR	International Symposium on the Weathering of Plastics and Rubber, June 8 and 9, 1976, Institution of Electrical Engineers, London WC2R OBL
IV curve	A plot of current vs. voltage for an operating solar cell
JPL	Jet Propulsion Laboratory
Lexan	Lexan No. 8740 polycarbonate film, not UV-stabilized, nominally 127 μm (5 mils) thick, from General Electric
mm	millimeter
mW	milliwatts
Miami or Phoenix	Exposure to the weather on racks tilted at 45° and facing south in Miami FL, or Phoenix AZ
nm	nanometers
NOCT	Nominal operating cell temperature (for solar cells in modules)
OCLI	Optical Coating Laboratory, Inc., City of Industry, CA
Outdoor Exposure	Miami, Phoenix, or EMMA(QUA) exposure
P	Property, specifically fraction of original transmittance at 360 nm in our mathematical modeling

Term	Definition
Polystyrene	Biaxially-oriented clear polystyrene film, nominally 127 µm (5 mils) thick, from Catalina Plastics, Glendale, CA
Pottant	A protective, insulating material in which an electronic device, e.g., a solar cell, is "potted" or embedded
Power point	That point on the IV curve of a solar cell at which the power (product of I and V) is at a maximum
psi	pounds per square inch
Solar cell	N120CG-9, by OCLI. Responds to light from approximately 0.4 to 1.2 µ'
Sylgard 184	Transparent silicone rubber, produced by Dow Corning Corp.
Tedlar	Tedlar 100BG30 TR (poly(vinyl fluoride)) film, treated on both sides to improve adhesion, nominally 25 µm (1 mil) thick, from du Pont
Tg	Glass transition temperature
TGA	Thermogravimetric Analysis (analytical method)
UTS	Universal Test Specimen (described in text)
UV	Ultraviolet radiation, 295-400 nm for sunlight at sea level
V	Volts
Weathered	Subjected to either natural or artificial weathering
Weathering	Exposure to either natural or artificial weather conditions

SUMMARY

The objective was to define methodology for making confident predictions of long-term encapsulant performance at any exposure site in the U.S.A. To meet the goals of the LSA Project, solar cell encapsulants must provide protection for 20 years.

Accelerated testing with Universal Test Specimens (UTS's) was conducted in order to expose candidate encapsulants in a realistic array-system environment. The UTS was a micromodule whose utility and convenience were demonstrated in our tests. Materials used as components of the UTS's were varied widely to establish a broad data base for modeling and prediction purposes.

Our first UTS system was designed to concentrate degradation effects in the encapsulant component. However, these UTS's proved too durable except for the moisture-sensitive cell contacts. These did fail during accelerated exposure due to moisture attack on the metallization. Sylgard 184 did not prevent this attack, which occurred more rapidly in Miami than predicted in the fixed-condition tests Failure analysis showed that cell contacts degraded and then thermal and moisture cycling outdoors encouraged lifting from the silicon surface.

The second set of UTS systems included degradable components except for the cells. Expectations had been that moisture-sensitive cells would lose power more rapidly for those encapsulants whose degradation allowed faster permeation by water. However, the cells were unexpectedly moisture-resistant due to better solder coverage of the contacts than found in the earlier cells. Therefore, solar cell power, the property being monitored, decreased little

during accelerated exposure. Encapsulants darkened or opacified, yet the power output remained high. Subsequent steam exposure greatly darkened and opacified encapsulants and large power losses occurred.

Despite the inability to obtain UTS property data extensive enough for predictions, such data was obtained on separately-exposed plastic films, one of which (Lexan) had been used on UTS's.

These data were used to demonstrate prediction methodology, and successful predictions were made for property changes of the films in Phoenix and Miami. This was an important result of the program.

Multiconditional accelerated exposure proved valuable for disclosing failure modes and pinpointing which of the weather factors (UV, temperature, moisture) was responsible. The multicondition method is essentially a set of controlled experiments. For example, two sets of conditions varied only in UV level. Thus, basic mechanisms were exposed. For example, thermal degradation and hydrolysis could be distinguished from photochemical effects. Single-condition exposures only show what happens but not why. The multicondition method has been adopted by JPL in investigating the degradation of plastic materials as encapsulants.

Hyperaccelerated photochemical exposure was demonstrated by concentrating sunlight 1400 times with a solar furnace. For these tests, transparent plastic films were placed under flowing water in a quartz vessel. The amount of acceleration was as expected, since property vs. time and intensity data indicated that the mechanism was unchanged. A week of such exposure deposits the equivalent of 20 years of UV light.

The UV-visible spectrum of sunlight is unchanged by front-surface mirrors. However, the solar furnace facility had some back-surfaced glass

mirrors. These reflected negligible UV at 295-300 nm due to absorption by glass. Consequently the solar intensity was 700 suns instead of 1400 at the lower end of the wavelength range of terrestrial sunlight. Quartz absorbs no UV-visible light, and 5 cm. of water begins to absorb infrared light at about 1.3 microns. Thus, hyperaccelerated exposure with front-surface mirrors subjects materials to the true UV-visible spectrum of sunlight, and the problem of imperfect solar simulation with lamps is avoided.

A Test Program Plan was developed based on the experience of testing UTS's and plastic films. It is intended to predict the 20-year outdoor performance of any encapsulant material in an array environment.

Prediction methodology involved determining degradation rate constants under 24 conditions of accelerated exposure. Then these values were integrated with weather data to determine the parameters of an appropriate mathematical model. Extrapolation of a linear data plot, according to the model, afforded long-term predictions.

Our accelerated conditions, with an acceleration factor of 8, were maintained for about 2 months, simulating 16 months outdoors. Therefore, materials with a 1-2 year lifetime were included· the plastic films Lexan and polystyrene. If a material with a 20 year lifetime had been tested, we could not have checked the predictions. Thus, the acceleration factor was too low for a 20 year material

Performance of UTS components varied widely from material to material. Solar cells proved very moisture-resistant when Ti/Ag contact metallization was protected by a solder coat. Encapsulant degradation products had no effect on cells Darkening or partial opacification of the cover encapsulant had surprisingly little effect on power output. The cells had little response to blue light, and visual clarity is not essential for light transmission. A few cells were cracked but continued to perform normally.

Without solder coating, cell metallization was degradable. The losses in power for Sylgard-encapsulated UTS's were about 11% in Phoenix and 31% in Miami after 1.5 years. These data are consistent with the known mechanism of moisture attack on the corrosion-sensitive Ti/Ag couple.

Field effect transistors (FET's) encapsulated in Sylgard 184 showed no large increases in leakage current under normal exposure conditions. Thus, there was no ionic degradation of the P/N junction. However, FET's beneath other encapsulants, especially Parylene C, gave high leakage currents in 1-3 months outdoor exposure. Steam exposure also caused high leakage currents.

Circuitry used initially was gold-plated Mo/Mn fired on ceramic substrates. It was very weather-resistant. Thick-film copper circuitry (25-36 microns) also appears reliable for photovoltaic systems.

In contrast, copper-plated Mo/Mn circuitry corroded during 1-3 months of Miami exposure or 12 days steam exposure. The result was decreased power output from the solar cells.

Substrates of three types were tested Ceramic substrates (96% alumina) were highly weather-resistant. Enameled steel performed well except for breaks in the enamel; it could be a cost-effective candidate Glass-reinforced (G-10) epoxy showed surface degradation on outdoor degradation, but it did not warp.

Pottant/cover materials were the main subject of our tests. The weather-resistant materials were·

Sylgard 184
acrylic lacquer
Tedlar film
polyurethane (protected from UV)

Materials which degraded considerably were·

> Parylene C
> polyurethane (uncovered)
> nitrocellulose lacquer
> Lexan
> polystyrene

Failure modes of the above materials included

> Darkening
> Opacification
> Cracking, embrittlement
> Loss of surface gloss
> Delamination (of glass cover from polyurethane)

<u>Favorable synergism</u> of array components was noted. For example, Sylgard supported an embrittled Lexan cover, and glass protected polyurethane from UV/light.

I. INTRODUCTION

A. OBJECTIVE OF THE STUDY

Encapsulation is necessary to protect solar cells and interconnects from natural hazards which can reduce power output It is important to identify these hazards and to learn how they degrade solar cell performance. The overall goal of the encapsulation task can be summarized as follows

> "To select or develop a cost-effective encapsulation
> system which protects solar cell·arrays for 20 years
> of outdoor exposure."

> Rockwell International's contract had one specific goal·
> "To develop a methodology for predicting the performance
> of solar cell encapsulants for periods of up to
> 20 years."

B. UNIVERSAL TEST SPECIMEN (UTS)

We wished to expose condidate encapsulants in a realistic array-system environment. Therefore, a micromodule or UTS was designed for use in accelerated weathering tests. It comprised a circuit board bearing three pairs of solar cells and three FET (field effect transistor) chips.

C PROBLEMS IN ACCELERATED/ABBREVIATED TESTING

It is difficult to simulate or accelerate the degradation processes which occur in outdoor exposure. Nevertheless, technologists have attempted to do so for many years with various methods and types of equipment. There has been much speculation on the value of results obtained. Many materials people still have no confidence in accelerated testing of any kind However, decisions usually are made with imperfect data, which is better than no data.

1

There are two ways of predicting performance of a material or system over 20 years of outdoor exposure. The first method is abbreviated testing, in which some property is measured for a year or two of natural exposure to give a property(P)-vs.-time(t) curve which is then extrapolated. At the moment, our judgment is that this method by itself is not practical because (1) sensitive analytical methods must first be developed; and (2) extrapolation from 1-2 to 20 years is questionable when the shape of the P vs. t curve is unknown. For example, P may drop suddenly in a catastrophic failure as when a UV stabilizer has been consumed. However, when abbreviated data is consistent with accelerated data, it increases confidence in the latter.

The second method is accelerated testing. This includes (1) tests of the oven aging or "pressure cooker" type to accelerate thermal pyrolysis, hydrolysis, and oxidation reactions and (2) exposure to continuous and/or intensified UV-visible light to speed photochemical degradation. The former tests have been extensively developed for electronic devices. However, UV-exposure tests are chiefly applied to paints, plastics and textiles and are a controversial subject. Although lamps are convenient light sources, their spectra (Figures 1 and 2) imperfectly match the spectrum of terrestrial sunlight. Therefore, comparison tests must be conducted in natural sunlight to ensure the mechanisms are identical. One solution is to use natural sunlight and achieve acceleration by concentration with front-surface mirrors as practiced by Desert Sunshine Exposure Tests Inc. It is precisely for this reason that many select EMMA exposure to the less expensive and more convenient Weather-Ometer exposures. That front-surface aluminum mirrors (Alzak) do reflect the true UV-visible spectrum of sunshine is seen in Figure 3.

2

TYPICAL OUTPUT SPECTRA

WAVELENGTH (NANOMETERS)
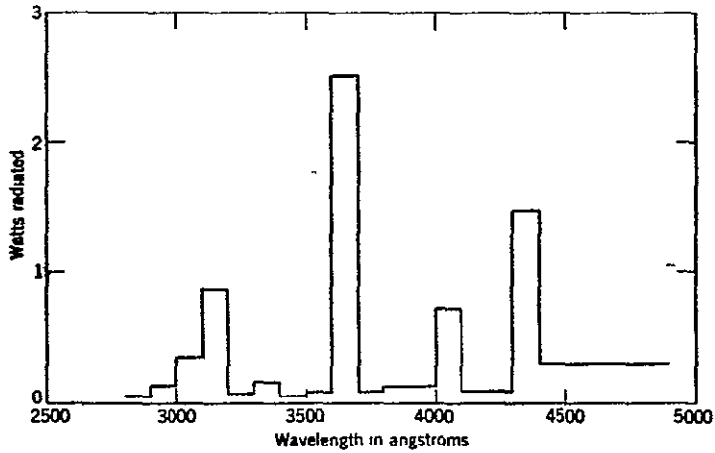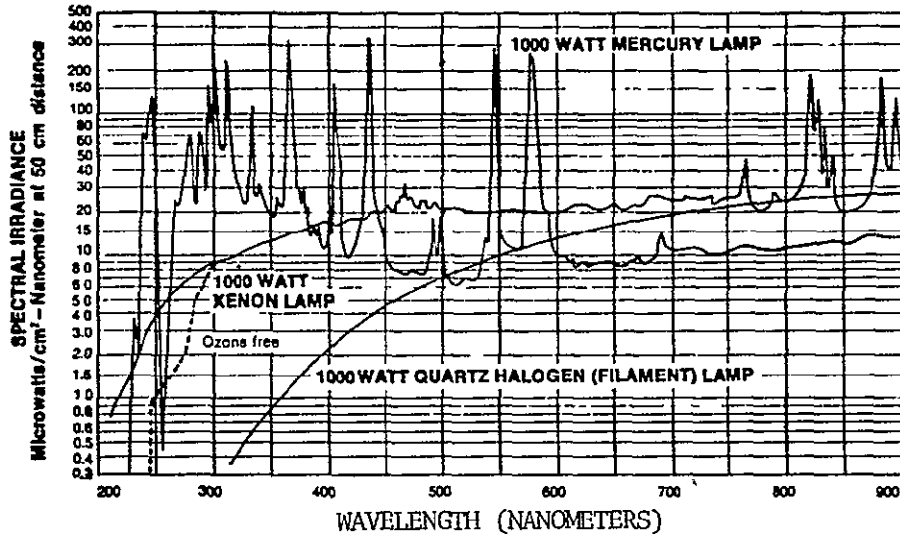
Energy distribution in spectrum of sunlamp 275-RS

Figure 1. Spectra of Lamps Used in
Accelerated Weathering Tests

3
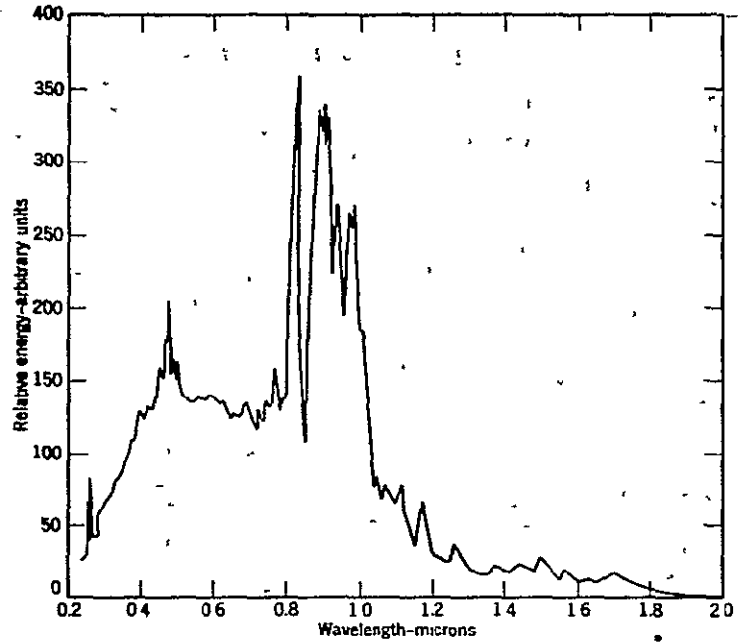
Spectral energy distribution of typical 5-KW Xenon lamp Electrode radiation excluded
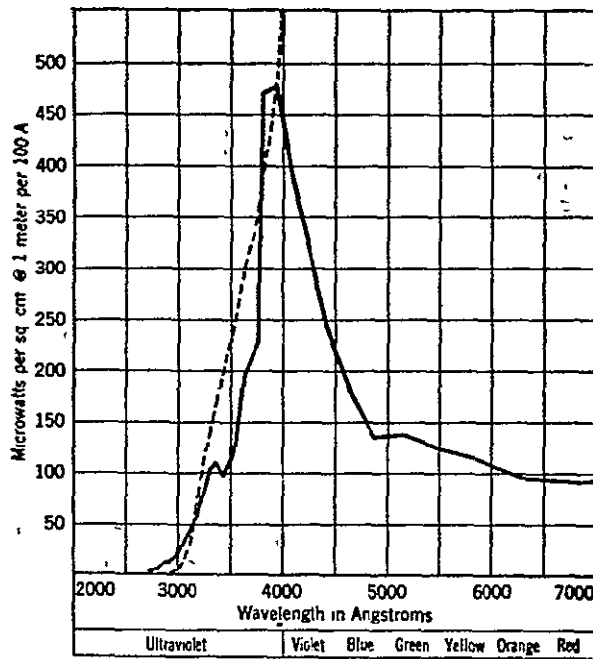
National Sunshine Carbon with Corex filter compared with natural sunlight. Solid line, with Cortex D filter Dotted line, natural sunlight.

Figure 2. Spectra of the Two Light Sources Used in Weather-Ometers vs. the Spectrum of Sunlight

4
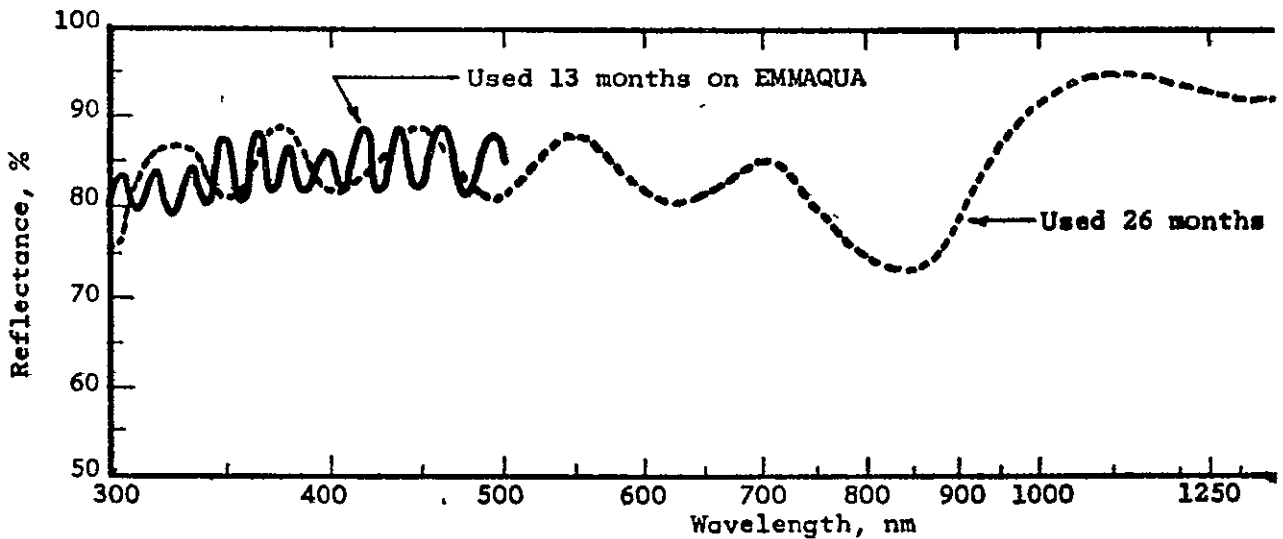
Figure 3. TOTAL HEMISPHERICAL SPECTRAL REFLECTANCE OF ALZAK

In the interests of cost and expediency, there is a need for a simple "black box" - an artificial weathering cabinet - which will subject samples to "20 years of typical weather." Such devices are sold commercially. They use sunlamps for solar simulation. However, as emphasized continually in the literature on artificial weathering, the results of such exposure are neither reliable nor credible. The most weather-resistant materials may pass such a test. However they are usually expensive. On the other hand, cost-effective candidates tend to fail. Premature failure results from degradation by

(1) high temperatures, and

(2) short UV wavelengths

Neither condition occurs in natural outdoor exposures. Hence, unrealistic over-testing must be avoided in identifying cost-effective plastics. Furthermore, a one-condition "black box" test does not disclose the relative importance of each weather factor - UV light, temperature, and moisture.

5

D. EXPERIMENTAL APPROACH

We devised a multicondition time-compression technique to disclose failure modes and clearly identify the controlling weather factor(s). Samples in the multicondition accelerated exposure cabinet were exposed to 18 conditions of UV light intensity, temperature, and moisture as shown in Figure 4. In addition, there were 6 conditions in darkness.

Since all artificial sunlight sources are suspect (Reference 1), we included natural exposure tests at 45°S to corroborate the multicondition data using a xenon lamp. We also included EMMA and EMMAQUA tests. These are expensive but can provide supporting information in a shorter time than natural exposure.

The above three methods, along with the conventional Weather-Ometer time-compression method, are shown pictorially in Figure 5.

Rate data for each of the sets of conditions in the multicondition accelerated test were to be combined with weather data to predict performance outdoors. Reference 2 gives a detailed account of the conceptual procedure. Appendix B of the present report illustrates reduction to practice. Lack of detailed outdoor UV data (Reference 1) is a major difficulty with this approach. Nevertheless, predictions of property changes were remarkably good

We also investigated hyperaccelerated photochemical exposure with natural sunlight to deposit 20 years of UV energy on samples. This was done because graphical extrapolation for predicting property levels is difficult even when properties can be precisely measured, which is not true for most plastics' properties (References 3 and 4)

In summary, our experimental approach was to emphasize multicondition accelerated exposure but to integrate results of all the above tests in making predictions.

6

Figure 4

MULTICONDITION ACCELERATED EXPOSURE

0 pct R H.

50 pct R. H

100 pct R H.

Xenon Lamp

Shutter

Low Temperature ◄——— | ———► High Temperature
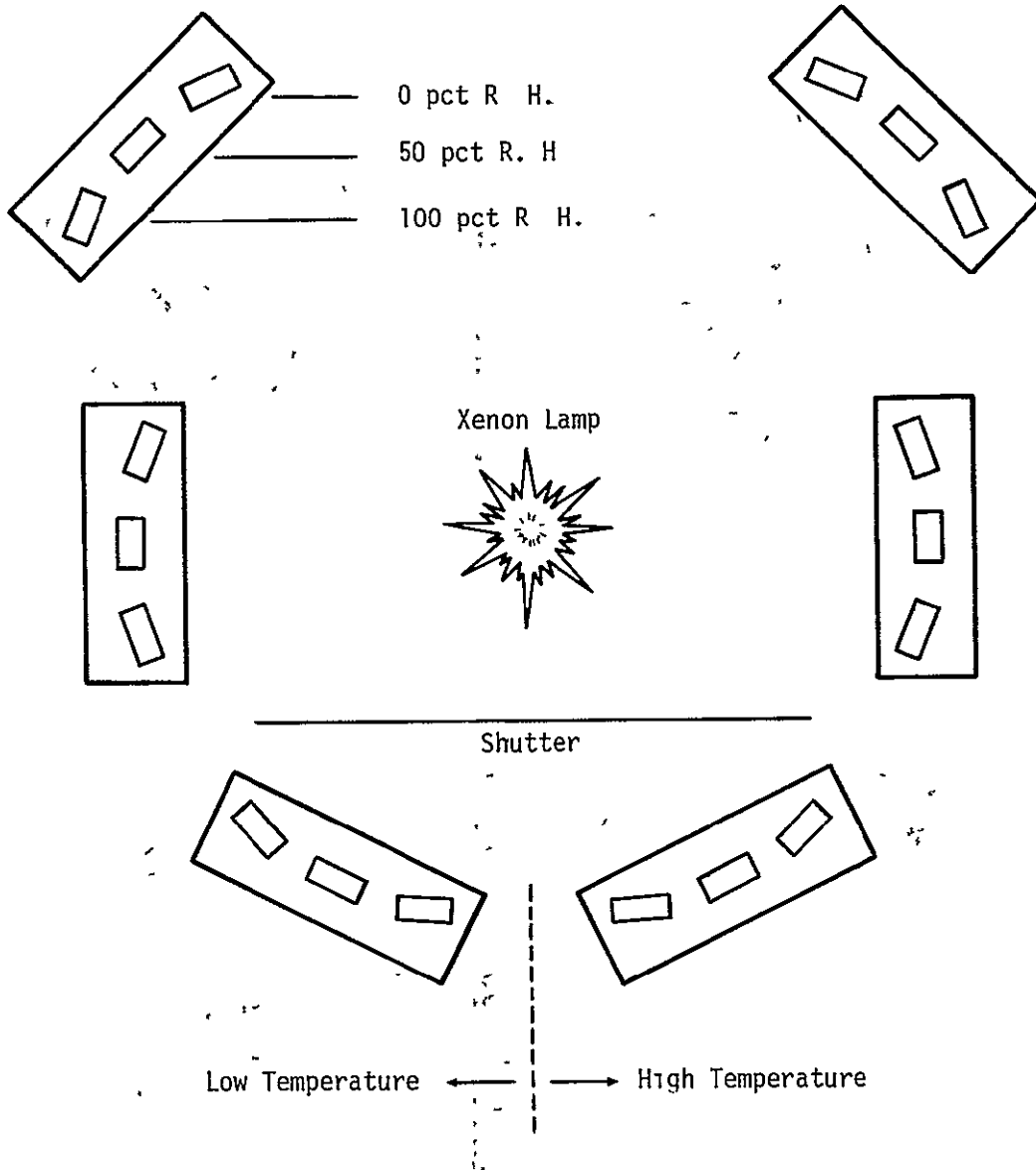
Figure 5

METHODS OF EXPOSURE TESTING

45°
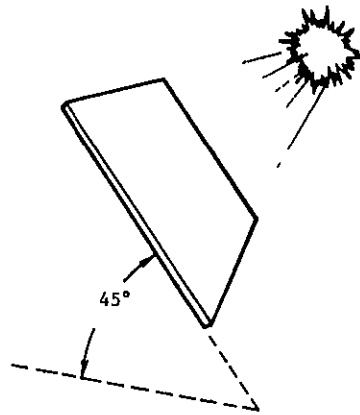
CONVENTIONAL OUTDOOR EXPOSURE
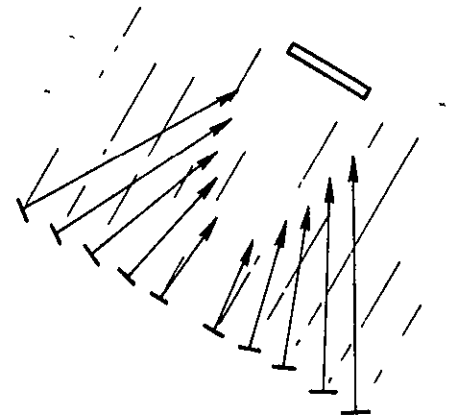
SUNLIGHT CONCENTRATION
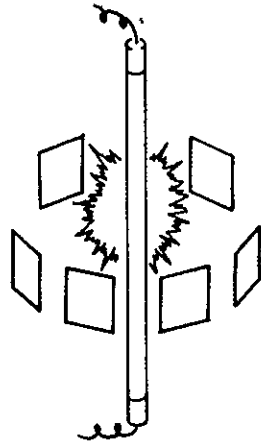
TIME - COMPRESSION
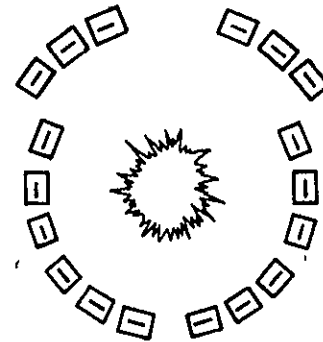
MULTICONDITION TIME - COMPRESSION

E. ORGANIZATION OF THE REPORT

The main body of this report is concerned with (1) the micro-module or UTS (description, use in a Test Program Plan, and performance of materials/components), and (2) prediction methodology and mathematical modeling techniques.

Full descriptions of experimental procedures, the means of UTS fabrication, the exposure methods, and complete tabulations of exposure test data are given in Appendix A. Details of prediction calculations appear in Appendix B.

-Results obtained in the second year are emphasized; the first year's study is covered in the Interim Report (Reference 2).

II. THE UNIVERSAL TEST SPECIMEN (UTS)

UTS's were developed as an evaluation technique for encapsulants.
UTS's allow direct measurement of the effect of encapsulant degradation
(e.g., discoloration, opacification) on electrical performance of the cells.
Also, it is necessary to know how effectively encapsulants protect solar
cells and interconnects when each array component is subjected to mechanical
and thermal stresses resulting from proximity to the other components.
That is, the UTS allowed encapsulants to be evaluated in the environment of
a total array system so that failure modes are realistically displayed and
both system and component degradation rates determined.

The UTS consisted of six 1x2 cm solar cells and three tiny FET's
(transistor chips) attached to a 3x10 cm. circuit board. The FET's were
placed between each pair of solar cells to detect ionic contaminants.
Figure 6 is a photograph of a UTS encapsulated with Sylgard 184 transparent
silicone rubber. Several other materials were also tested. Figure 7
diagrams the components of a UTS.

Various failure modes are listed in Table 1 Delamination did not
occur in our tests without steam exposure. However, it was cited as a problem
in early module buys by JPL. Presumably our stress-free design (no frame)
avoided delamination.

Thus, the UTS was intended to be a convenient vehicle for testing en-
capsulants in the meaningful context of an array system. Its small size was
advantageous for accelerated exposure tests. Equipment such as EMMA/EMMAQUA
or laboratory weathering cabinets cannot accomodate large samples.

10
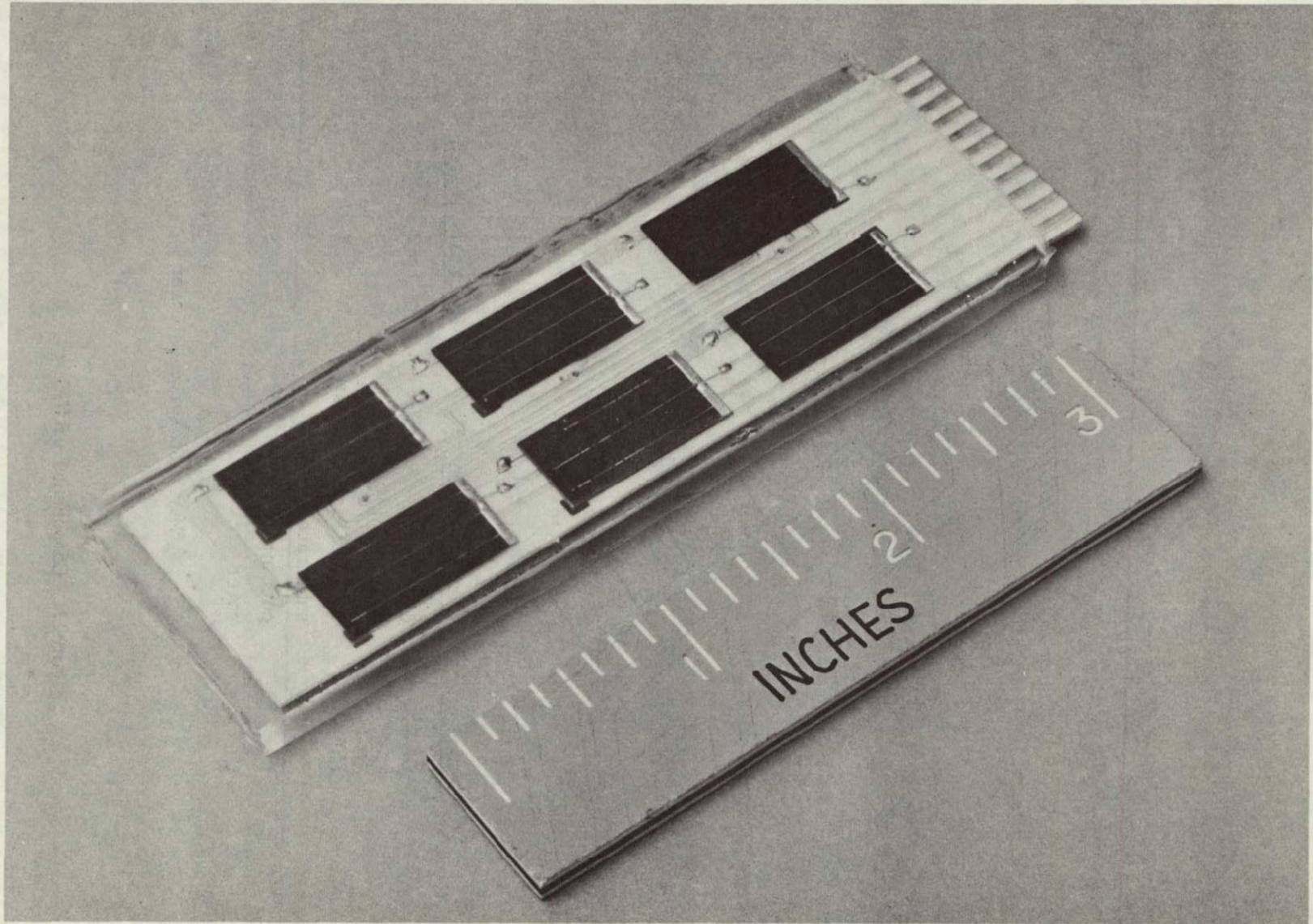
Figure 6.   Universal Test Specimen (UTS) Encapsulated with Sylgard 184
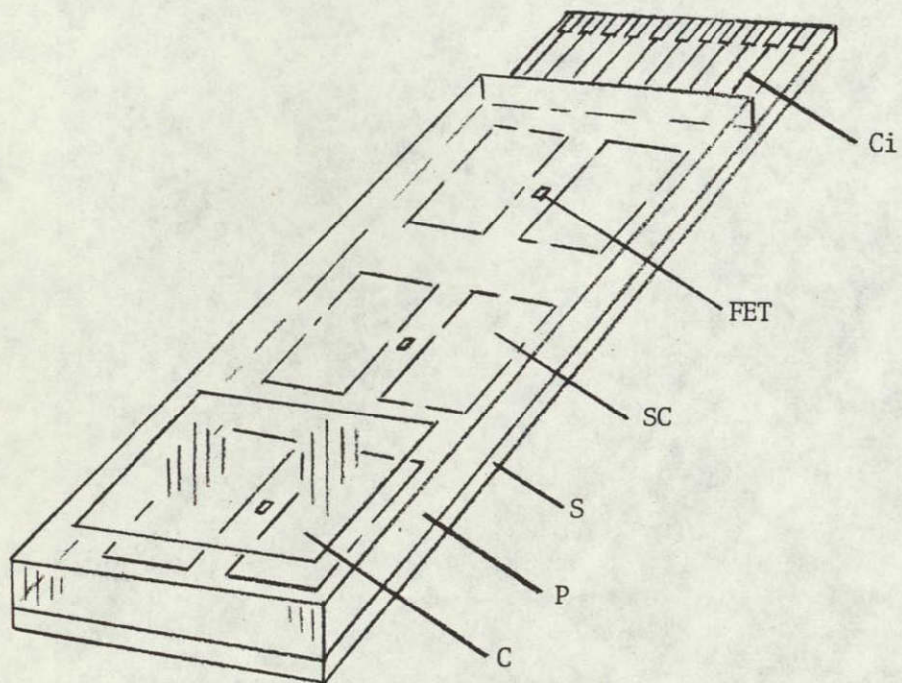
Component	Identification	Materials Tested
Ci	circuitry	4
SC	solar cell	1
FET	field effect transistor	1
S	substrate	3
P	pottant*	9
C	cover	3

*May also serve as cover.

Figure 7. Components of UTS

III. TEST PROGRAM PLAN USING UTS'S

A. GENERAL PROCEDURE

The ultimate product of this contract was a Test Program Plan supported by data. It is shown schematically in Figure 8. Recommended exposure periods and requirements for number of samples are given in Table 2. However, the nature of the material and the climate at the exposure sites of interest will determine the test conditions. For plastics, the glass-transition temperature, Tg, must be known. Polymers degrade more rapidly above Tg since they behave like viscous liquids rather than glassy solids. Therefore, a Tg determination is shown in Figure 8, it influences the test conditions.

We emphasized the testing of plastic materials. They are prime candidates for low-cost encapsulation because of easy processability. Also, we emphasized acceleration of photochemical degradation because realistic degradation by UV light is a difficult problem in accelerated testing. On the other hand, programs for temperature/humidity testing of electronic devices have been extensively developed, e g , References 5 and 6.

B. TESTS

1. Hyperaccelerated Exposure with Highly-Concentrated Sunlight

This procedure is the first step in the Plan. Our exposures in a solar furnace are reported in detail in Appendix A. Efficient cooling is required. We immersed the samples in water, because moisture does not accelerate yellowing of Lexan and polystyrene. Alternately, a small and inexpensive solar furnace is commercially available (Reference 7). The mirrors in this device are front-surfaced, as desired to reflect all the UV in sunlight.

14
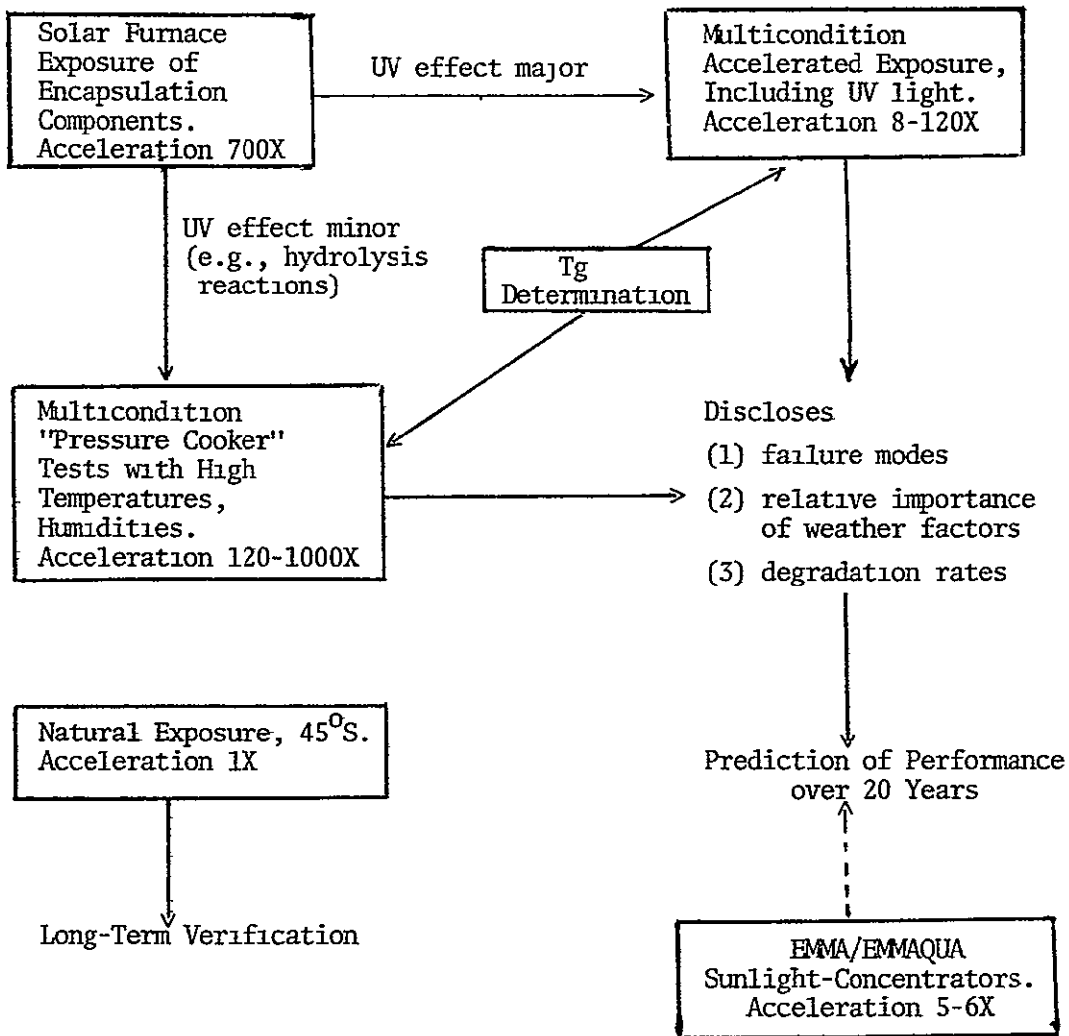
Figure 8   Test Program Plan Sequence

Table 2

Exposure Periods and Number UTS's Required

(One-Year Program)

Exposure	Number of Conditions	Exposure Periods, Days	Total Number UTS's Required
Multicondition	24	5,10,20,40,80,135	24
Solar Furnace	3	1, 2, 3, 6, 10	15
"Pressure Cooker"	6	5, 10, 40, 100	24
Tg Determination	1	0	0
EMMA, EMMAQUA	2	30,60,90,120,240,365	12
Natural (45°S) (3 sites)	3	30,60,90,120,240,365	18

2. Multicondition Accelerated Exposure

a. With UV Light

If hyperaccelerated exposure shows that UV light is a major factor, multicondition accelerated exposure should be carried out. We used the conditions shown in Table 3 to obtain degradation rates for materials with a short outdoor lifetime. This allowed comparison of predictions with natural weathering results during a 1-2 year program. Twenty-four fixed conditions were maintained in order to compile extensive rate data

Later testing required only 8 key conditions. These were sufficient to disclose failure modes, to clarify the relative importance of the basic weather factors, and to screen out weak candidates.

16

Table 3

Accelerated Conditions

UV Intensity Relative to Noon Summer Sunlight	Air Temperature °C	UTS Temperature °C	Relative Humidity %	
1.00	26	43	0	*
			50	
			100	*
	60	72	0	*
			50	
			100	*
0.66	18	28	0	
			50	
			100	*
	55	64	0	
			50	
			100	*
0	40	40	0	
			50	
			100	
	72	72	0	*
			50	
			100	*
Alternating (1.00 for 12 hrs., 0 for 12 hrs.)	26 (light) 7 (shade)	43 7 (shade)	0	
			50	
			100	
	60 (light) 44 (shade)	72 44 (shade)	0	
			50	
			100	

*Eight key conditions for a simplified procedure.

A xenon lamp was used despite its imperfect solar simulation. Even when it is used to rank the stability of materials, the results are often distorted Unnatural acceleration is induced by UV wavelengths below about 295 nm., where the solar spectrum cuts off at sea level (Reference 8). These unnaturally-low wavelengths are typical of mercury vapor sunlamps often used in exposure testing. Visible light can also cause polymer degradation. Examples are as follows. Vinyl acetate copolymers are degraded by light at 385-415 nm. Kevlar, aromatic polyamide, is degraded by visible and UV light (Reference 4). Wool is yellowed by UV light (below 311 nm) and bleached by visible (violet) light (Reference 9).

Consequently, the solar spectrum should be matched across the entire wavelength range. Xenon arcs give the best overall solar simulation (Reference 2). However their spectrum includes the undesirable wavelengths below 295 nm. mentioned above. Our experience with Lexan yellowing showed that a 1.8 mm. thick filter of Pyrex 7740 was not sufficient for attenuating UV at about 300 nm (see Reference 2). Unless it is known that a material is degraded by wavelengths only above 310 nm., Pyrex filters should be thickened until Lexan yellows at the outdoor rate using data of Reference 2. Filtration of xenon light was not required for polystyrene which degraded at 319 nm. (Reference 10); our xenon lamp gave expected rates for both yellowing and loss of tensile strength.

Weather-resistant materials with outdoor lifetimes greater than 20 years will pass the hyperaccelerated exposure test. If significant degradation occurs, multicondition accelerated exposure will verify long lifetime and allow specific predictions for various climates. Suppose hyperaccelerated exposure at $35^{\circ}C$ produces 40% loss in tensile strength after depositing 20 years of cumulative UV energy. Then, if 50% loss of strength were defined as the failure point, the material would pass this test. However, what would be the effect of a NOCT of $60^{\circ}C$? Also, what is the role of moisture? The material should be subjected to multicondition exposure with UV light but obviously at greater stresses than shown in Table 3. Also, longer times than those shown in Table 2 may be required. Degradation should be accelerated to minimize uncertainties of extrapolating property vs. time data. Extrapolation of accelerated data should coincide with predictions based on hyperaccelerated exposure. Internal consistency of calculations will increase the credibility of predictions.

b. **Without UV Light**

This multicondition exposure involves variation only of moisture and temperature in "pressure cooker" and oven-aging tests. None of these were conducted. However, they are commonly used in industry for testing plastic-packaged electronic devices (References 11 and 12). The objective is to determine degradation rates at several elevated temperatures and different humidity levels. The data is then extrapolated to operating temperature via an Arrhenius plot.

3. **EMMA and EMMAQUA**

These devices are essentially low-powered solar furnaces. Since they use natural sunshine, solar simulation is assured They provide only one-condition exposure and are costly. Hence their use is optional, as indicated by the dotted line in Figure 8. EMMA and EMMAQUA exposures are recommended to corroborate photochemical degradation rates determined by the xenon lamp (multicondition) exposures.

4. **Tg Determination**

For thermoplastic materials, the glass transition temperature should be determined by DSC, TMA, dynamic mechanical testing, torsion pendulum, or other methods. Materials tend to degrade by unnatural failure modes and at unrealistically-rapid rates above the T_g. We observed this for both Tedlar and an acrylic lacquer Data obtained under conditions in which the T_g is exceeded should be used with caution. These comments do not pertain to all materials, e.g., elastomers such as Sylgard 184.

C. ANALYTICAL METHODS

Once the controlling failure mode has been determined (the "weak link" in the parlance of reliability testing), some property must be selected

which falls continuously to a level defined as failure. Suppose embrittlement/ loss of integrity of a plastic encapsulant cover were the failure mode. Then a number of mechanical or extrinsic properties, e.g , tensile strength, might be followed. Alternately, intrinsic properties, e.g., molecular weight, can be used. A secondary property, such as a spectral change, might be related to the preceding strength-related property. This correlation was, done successfully for Lexan yellowing vs. loss of tensile strength.

Analytical methods were reviewed in the Interim Report (Reference 2).

D. DATA ANALYSIS

The monitored property should be expressed on a scale of 1 (no degradation) to 0 (complete degradation), with the selection of an arbitrary failure point, e.g., 0.5. This variable is "P" (for "property").

With "t" being exposure time in days, the following plots (Reference 13) should be tried.

(1) Using probability paper, P on the probability scale vs. t on the linear scale (normal model).

(2). Same but with $\log_{10}(t)$ (lognormal model)

(3) $\log_{10}\left[\log_{10}(\frac{1}{P})\right]$ vs. t (exponential model).

(4) $\log_{10}\left[\log_{10}(\frac{1}{P})\right]$ vs. $\log_{10}t$ (Weibull model).

(5) $\log_{10}P$ vs. $\log_{10}t$ $(P \sim t^n)$.

The method of plotting that gives the best line should be selected. Other models may be tried if necessary (see "Prediction Methodology" section of this report). Note that degradation mechanisms are specific to each material or to a class of closely-related materials. If P falls to 0.5, the following values would be reached if degradation followed the exponential model $(P \sim e^{-t})$ as plotted in Figure 9·

Test	Equivalent Years of Exposure	P, if P = 0.50 at 20 years	P, if P = 0.50 at 10 years
Multicondition (135 days, acceleration factor 8)	3	0.9945	0.966
Natural, 45°S	1	0.9997	0.998
Hyperaccelerated	20	0.5000	0.018
EMMA/EMMAQUA	5	0.9795	0.883

Thus a very sensitive and precise analytical method is needed for a 20-year material or even a 10-year material in all tests but the hyper-accelerated exposure.

On the other hand, a Weibull model with $\beta = 0.5$ might fit the data. Here, $P \sim e^{-0.5t}$ as shown by the dashed line in Figure 9. Then the following values of P would be reached in the above tests

Test	Equivalent Years of Exposure	P, if P = 0.50 at 20 years	P, if P = 0.50 at 10 years
Multicondition	3	0.938	0.692
Natural	1	0.984	0.912
Hyperaccelerated	20	0.500	0.018
EMMA/EMMAQUA	5	0.883	0.490

If the analytical method is precise, usable data will certainly be obtainable for either a 10-year material or a 20-year material. In practice, the multicondition test must be increased in severity and/or duration to obtain decreases in P large enough to be measurable and provide degradation rate data.

The four tests are intended to reinforce one another. That is, the data plots for P vs. t for equivalent exposure conditions should fall along a single line. In other words, the data of all the tests should be combined in making a prediction. It might be argued that hyperaccelerated exposure

21
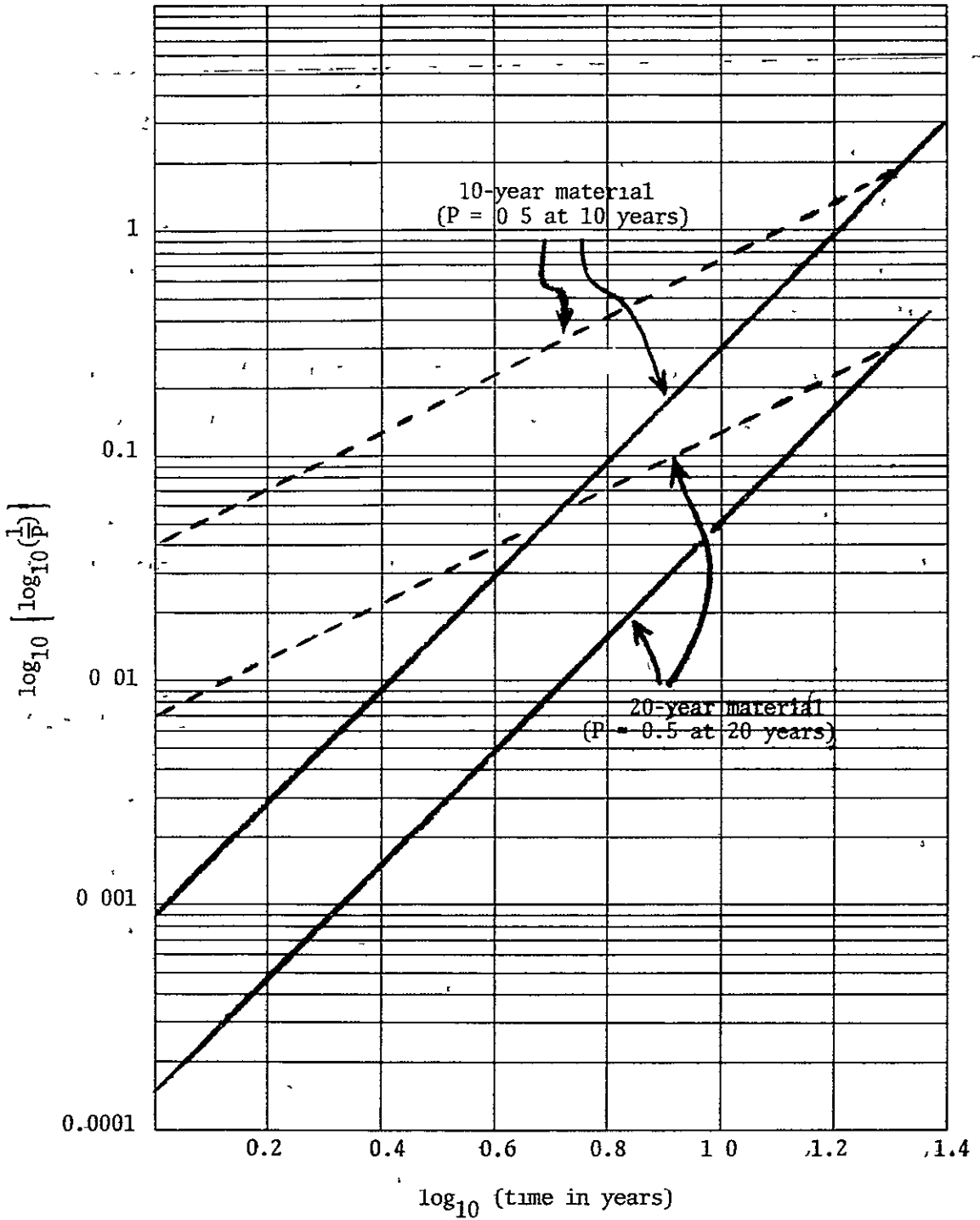
Figure 9 Weibull Plots for Materials with 10 or 20 Year Lifetimes

$$\text{————} \quad P \sim e^{-t}$$
$$\text{————} \quad P \sim e^{-0.5t}$$

alone would be sufficient when a material degrades negligibly, but this test does not disclose failure mechanisms as does multicondtion exposure. Also, a material might be stable to UV light but degrade by thermal hydrolysis, for example. Furthermore, interpretation involves assumptions about outdoor UV levels even if photochemical degradation is the predominating mechanism. Therefore, the purpose of hyperaccelerated photochemical exposure is to indicate whether the subsequent multicondition accelerated exposure should or should not include UV light

In summary, the credibility of predictions made by this Test Program Plan derives from the synthesis of complementary test methods.

An important application of this Test Program Plan may be for improving array design. Multicondition exposure is essentially a set of controlled experiments intended to disclose the reasons for failure. Deficiencies may then be corrected and the design retested.

IV. PERFORMANCE OF UTS COMPONENTS

A. SOLAR CELLS

The solar cells were very moisture-resistant when the Ti/Ag contacts were protected by a solder coat. Solder-coated metallization resisted 100% relative humidity at 72°C for 61 days followed by steam at 100°C for 31 days. There was no obvious effect of encapsulant degradation products on the cells.

Without solder coating on the contacts, an average power loss of 43% was observed after 72 days exposure at 80°C and 100% relative humidity (Reference 2).

Power loss observed in the solar cells was surprisingly low as encapsulants became dark in color or opaque. For example, the loss was as little as 10% despite darkening of polyurethane encapsulant to the point of visual opacity. The opaque (milky) acrylic lacquer caused as little as 15% power loss. A few cells cracked but continued to perform normally. A similar observation has been made with full-scale modules in tests at JPL.

Disparities in performance between paired solar cells were generally not great in accelerated exposure but were sometimes very large in steam exposure. One reason is that the Cu-plated Mo/Mn circuitry on the ceramic substrate often corroded to failure.

The feasibility of taking _in situ_ power readings during multi-condition exposure was demonstrated (see Appendix A). Electrical connection was made with tape cables soldered to the edge contacts of the UTS's. Assuming a conservative time-compressed "acceleration factor" of 8, observations over 1 year would give performance vs. time relationships simulating 8 years of outdoor exposure.

24

The only available long-term outdoor exposure data are for the UTS's encapsulated with Sylgard 184 (Table 4). The greatest power loss occurred in the wet climate of Miami, presumably due to moisture-induced degradation of the Ti/Ag metallization (not protected by solder on these cells).

In outdoor exposures for up to 90 days, Miami's moist climate seemed responsible for significant power reduction for the encapsulant systems (other than Sylgard 184) using the ceramic substrate and also for the nitro-cellulose lacquer cover (data in Appendix A). These power losses are attributed to corrosion of circuitry

B. FIELD EFFECT TRANSISTORS (FET'S)

In outdoor exposure, FET's encapsulated in Sylgard 184 continued to give low leakage currents after 1.5 years. With other encapsulants, especially Parylene C, very high leakage currents were found after 1-3 months exposure. Hydrogen chloride evolution produced by photodegradation of Parylene C could explain the response.

In accelerated exposure, FET's encapsulated in Sylgard 184 gave low leakage currents after 72 days. After steam exposure, the currents increased but less so than for most other encapsulants tested. FET's encapsulated in a polyurethane gave particularly high leakage currents after steam exposure. Values of up to 100,000 times the original value were observed, indicating the presence of ionic hydrolysis products.

C. CIRCUITRY

Gold-plated Mo/Mn circuitry fired on ceramic substrates was very weather-resistant and remained bright after 72 days of accelerated exposure or 1.5 years of outdoor exposure. In contrast, 2.5 microns of copper over

Table 4

Retention of Maximum Power by Solar Cells

in UTS's Exposed Outdoors

Exposure Time, Days	Miami, 45°S	Phoenix, 45°S	EMMA	EMMAQUA
5	100	103	101	97
10	100	108	99	101
15	97	102	-	-
30	98	103	95	100
60	93	87	-	-
90	99	90	100	97
150	99	94	97	99
210	85	90	88	96
300	78	95	83	92
420	82	100	93	99
540	69	89	83	91

NOTE   Values are the average percent of original power for the
6 solar cells of the UTS.

Mo/Mn corroded extensively after 12 days of steam exposure and showed evidence of corrosion, in terms of loss of power of attached solar cells, after 1-3 months Miami exposure.

Copper circuitry about 25-36 microns thick on enameled steel or epoxy substrates was dulled or stained after 61 days in steam but did not corrode to failure. Therefore, properly protected thick-film copper circuitry appears reliable for photovoltaic systems

D. SUBSTRATES

Enameled steel and ceramic (96% alumina) were highly weather-resistant. However, glass-reinforced epoxy substrates degraded on weathering. This is evidenced by "fiber bloom" which represents loss of surface resin. However, warpage did not occur.

The effects of accelerated exposure followed by steam exposure on substrates are summarized in Table 5.

E. POTTANT/COVER

Sylgard 184 as pottant proved highly weather-resistant after 540 days exposure under all four conditions, it remained elastomeric and nearly water-white. Internally it was quite clear, but microroughness (dulling) of the surface was apparent after 420 or 540 days EMMAQUA exposure. A 25 micron sliver was microtomed from the surface after 420 days EMMAQUA exposure. It was examined by transmission IR spectroscopy using a Beckman Model IR 4240 grating instrument and compared with an unweathered control. The spectra of the two were essentially identical. Both showed a moderately strong bond at 2.7-2.8 microns but no hydroxyl absorption in the 2.9-3 1 micron region.

Table 5

Effect on Substrates of Accelerated Exposure for 61 Days
Followed by Steam Exposure for 31 Days

Substrate	Observed' Effects
Ceramic	None
Enameled Steel	Slight rusting at corners and very slight rusting at back edges.*
Epoxy	No warping. Bleaching and fiber bloom (loss of resin at surface) under most severe conditions.

*Immersion of a substrate in 1% NaCl for 32 days resulted in appreciable rusting only at the corners, where enamel coverage was imperfect.

The Lexan cover cemented on Sylgard 184 degraded but remained intact even when embrittled because it was supported by the pottant. This exemplifies a favorable interaction of components

The acrylic coating and the polyurethane pottant, when protected by a glass cover from degradation by UV, showed promising weather-resistance. A cross-linked acrylic coating such as Acryloid AT63 (80¢/lb., dry basis) should be still better (Reference 14)

Nitrocellulose lacquer degraded rapidly as we anticipated. It afforded a good illustration of the advantage of our multicondition exposure procedure in disclosing the relative importance of weather factors in degradation. See Figure A2 of Appendix A, for convenience, the nine photographs will be referred to as #1, 2, and 3 from left to right across the top, #4, 5, and 6 across the middle, and #7, 8, and 9 across the bottom The following

conclusions are drawn by comparing these photographs. Figures A4, A14, and A24 also are referred to.

(1) The most pronounced visible degradation (blistering) is caused by

   (a) More UV - #6 worse than #9
                #5 worse than #8

   (b) Higher temperatures - #6 worse than #4

   (c) Increased humidity - #6 worse than #5
                      #4 worse than #3
                      #7 worse than #2
                      #9 worse than #8

(2) Blistering is proportional to light intensity. Compare #9 with #7, showing a relatively fine "orange peel" texture, and with #6.

(3) Photograph #3 represents NOCT at noon in a dry, desert climate. Photograph #4 represents NOCT at noon in a moist climate such as Miami. These results illustrate the dramatic differences in encapsulant performance possible for dry vs. wet sites.

(4) Incidentally, referring to Figure A4, the effect of humidity in causing loss of gloss of the polyurethane encapsulant is clearly shown.

(5) The nitrocellulose lacquer was degraded by moisture alone, with no previous UV exposure, at $100^\circ C$ (Figures A14 (right column) and A24). However, previous UV exposure without moisture caused greater degradation in subsequent steam exposure. Therefore, weather factors can have a sequential effect.

(6) Under prolonged exposure, an encapsulant can become <u>less</u> opaque. For example, see Figures A14, A21, and A24 for nitrocellulose lacquer originally exposed at 0 rel. UV, $72^\circ C$,

and 100% R.H. There remained less material after 31 days of steam exposure than after 12 days. Consequently, the solar cell power dropped to about 50 percent of original at 12 day-, steam exposure and rose to about 95% at 31 days. The same effect is seen for nitrocellulose lacquer originally exposed to 0.66 rel. UV, 64°C, and 100% R H. (Figures A14, A21, and A24) and also for acrylic lacquer originally exposed to 0.66 rel. UV, 64°C, and 100% R.H. (Figures A14, A18, and A24).

Tables 6-8 summarize performance of nine array systems during accelerated/steam exposure. Degradation outdoors was much less severe, see Appendix A for data

Steam exposure was used in an attempt to force the failure of the moisture-resistant cells. The cell metallization survived but the steam temperature (100°C) could produce unrealistic results in terms of encapsulant degradation For example, 100°C is considerably over the Tg of the acrylic lacquer (63°C). Therefore, a hydrolysis reaction may have been forced to occur resulting in a milky appearance This reaction is improbable under conditions of normal exposure.

The Lexan studied was not UV-stabilized, since we desired degradation data for predicting purposes Gradual yellowing proceeded at a rate which decreased in the order accelerated exposure (xenon lamp) >> EMMAQUA > EMMA > Phoenix $\simeq$ Miami Yellowing is ascribed to a photo-Fries rearrangement (Reference 15) This color change involved transmission loss only at the violet end of the visible spectrum where the solar cells responded negligibly. Therefore, yellowing did not affect electrical performance This absorbance change was readily and precisely measured and useful for mathematical modeling studies discussed under "Prediction Methodology "

Table 6. Summary of Performance of Encapsulant Systems
after Accelerated (Xenon Lamp) Exposure for 61 Days

Encaps. System No.*	Solar Cell Power Loss	Corrosion of Copper Circuitry	Degradation of Encapsulant Cover or Pottant	Debonding of Glass Cover
1	Up to 4% loss	Dull		
2		Dull	Yellowed by light	
3				0% except for 0 rel. UV,72°C, 100% R.H. (10% debonded)
4			Darkened by high light + high temp.	
5				
6				0% except for 0 rel.UV, 72°C, 100% R.H. (5% debonded)
7	25% under high light + high temp.	Dull	Deep brown, surface ridged	
8	Up to 6% loss		Yellowed by light, dull surface	
9				0% except for 0 rel.UV, 72°C, 100% R.H. (10% debonded)
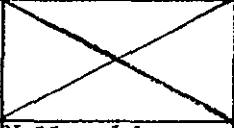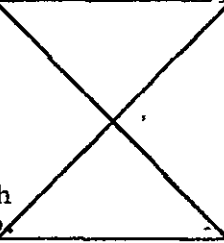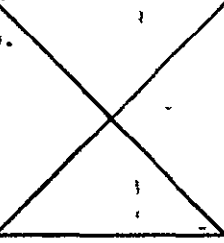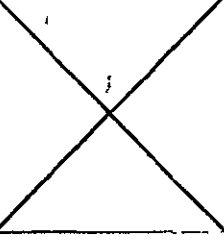
*Encapsulant System No.	Substrate	Pottant/Cover
1	Ceramic	None
2	"	Parylene C
3	"	2B74 (polyurethane) + glass
4	Steel	1B73 (acrylic)
5	"	Sylgard 184
6	"	2B74 + glass
7	Epoxy	Nitrocellulose lacquer
8	"	2B74
9	"	2B74 + glass

Table 7 Summary of Performance of Encapsulant Systems after Accelerated (Xenon Lamp) Exposure (61 Days) Followed by Steam Exposure (12 Days)

Encaps. System No.*	Solar Cell Power Loss	Corrosion of Copper Circuitry	Degradation of Encapsulant Cover or Pottant	Debonding of Glass Cover
1	Up to 100% power loss after steam exposure, attributed to corrosion of thin Cu plating on circuitry	Dull before steam exposure	╳	╳
2		Dull before steam exposure	Yellowed by light. Lost integrity by high light + high temp.	╳
3				Av. 48% debonded after steam
4	Up to 72% loss, attributed to opacity after steam exposure	Dull after steam exposure	Darkened by high light + high temp. Milky after steam exposure	╳
5	Up to 8% loss			╳
6	Up to 7% loss One cell failed (unexplained)			Av. 23% debonded after steam
7	Up to 72% loss, attributed to opacity after steam exposure	Dull before steam exposure	Severely degraded before steam, then further blistered	╳
8	Up to 10% loss		Cloudy, darkened	╳
9	Up to 9% loss			Av. 48% debonded after steam

*Encapsulant System No.	Substrate	Pottant/Cover
1	Ceramic	None
2	"	Parylene C
3	"	2B74 (polyurethane) + glass
4	Steel	1B73 (acrylic)
5	"	Sylgard 184
6	"	2B74 + glass
7	Epoxy	Nitrocellulose lacquer
8	"	2B74
9	"	2B74 + glass

32

Table 8. Summary of Performance of Encapsulant Systems after Accelerated (Xenon Lamp) Exposure (61 Days) Followed by Steam Exposure (31 Days)

Encaps System No.*	Solar Cell Power Loss	Corrosion of Copper Circuitry	Degradation of Encapsulant Cover or Pottant	Debonding of Glass Cover
1	Up to 100% loss after steam exposure, attributed to corrosion of thin Cu plating as well as Mo/Mn circuitry beneath	Dull before steam exposure	✕	✕
2		Dull before steam exposure	Pale brown. Lost integrity by high light + high temp.	✕
3		Much dark staining	Deep yellow	Av. 87% debonded after steam
4	Up to 100% loss, attributed to opacity after steam exposure	Dull after steam exposure	Milkiness increased from 12 to 31 days steam exposure	✕
5	Less than 10% except for once cell	Dull under some conditions		✕
6	Two cells failed. One lost 17%, other lost <10%.	Much dark staining	Yellow at edges in some cases	Av. 70% debonded after steam
7	Up to 83% loss, attributed to opacity after steam exposure	Dull before steam exposure	Partly lost over cells between 12 and 31 days steam exposure	✕
8	Up to 21% loss, attributed to darkening	(Circuitry not visible)	Dark red-brown, sometimes nearly opaque	✕
9	Up to 17% loss	Much dark staining	Brown at edges in some cases	Av 82% debonded after steam

*Encapsulant System No.	Substrate	Pottant/Cover
1	Ceramic	None
2	"	Parylene C
3	"	2B74 (polyurethane) + glass
4	Steel	1B73 (acrylic)
5	"	Sylgard 184
6	"	2B74 + glass
7	Epoxy	Nitrocellulose lacquer
8	"	2B74
9	"	2B74 + glass

Further observations on Lexan yellowing were made in Reference 2. Yellowing could be correlated with tensile strength loss, but only for samples exposed to weather in the same manner   The optical and mechanical changes proceeded by independent mechanisms.

Reference 2 also briefly discusses chain-scission, which results in embrittlement, and loss of surface gloss. The latter was moisture-related. For effect of outdoor exposure on molecular weight distribution, see Appendix A.

Reference 16 gives a brief review of Lexan degradation, including further references.

Many plastics develop a protective surface layer, analogous to the oxide layer on aluminum, during outdoor exposure. This is true for Lexan, poly(methyl methacrylate), and poly(vinyl chloride) (Reference 17). Therefor, results with thin films should be extrapolated to heavier sections with caution.

Tedlar is du Pont's poly(vinyl fluoride) film   Its weather-resistance is well known and the fact is supported by our data. Our most severe exposure conditions were 1.5 years on the EMMA and EMMAQUA. At an acceleration factor of 5, this represents about 8 years normal outdoor exposure. The samples had negligible color, tensile breaking stress was about 80% of original, and tensile elongation was about 75% of original. These results were for unsupported film. As a UTS cover, Tedlar also remained colorless and flexible.

ATR-FTIR indicated a low level of surface carbonyl groups on weathered Tedlar. This level developed early in exposure and then did not increase further. A possible explanation is oxidation of hydrocarbon sequences in the polymer or of additives, e.g , lubricant

If the operating temperature is not too high, Tedlar may well endure 20 years as a cover material (Reference 18).

All the preceding materials were tested on UTS's. Lexan and Tedlar were exposed as unsupported films. Polystyrene film was studied to provide additional data for mathematical modeling purposes Polystyrene degrades rapidly in sunlight and samples were exposed at Miami only. The rates of yellowing and of embrittlement were similar to those of Lexan but somewhat higher. See the Interim Report (Reference 2) for data.

Polystyrene after accelerated exposure showed evidence of progressive carbonyl formation in ESCA tests (see Appendix A). These results agree with earlier data obtained by ATR-IR (Reference 2).

Two polystyrene properties, absorbance at 360 nm. (representing yellowing) and tensile strength, were modeled and successfully predicted See the following "Prediction Methodology" section.

V. PREDICTION METHODOLOGY

A. MODELING THE DEGRADATION OF MATERIALS/ARRAYS

A failure distribution is a mathematical description of lifetime or degradation rate for a single material or a system.

Degradation is followed by recording the cumulative number of failures or the decreasing level of a particular property The latter method has the advantage of requiring few samples and often may be the only practical technique A problem with either procedure for following degradation is in distinguishing among nonsymmetric distributions such as the Weibull or lognormal. Such distributions differ significantly in the early and late phases of degradation where data points often are scarce

Fortunately, variances in our data were small due to replication. Thus, mathematical models could be selected. The data sometimes diverged from the model but they did so in a consistent pattern In our accelerated test, there were relatively few time intervals but a large number of weathering conditions. Therefore, the most important criterion for selecting a model was its consistent success in fitting data over a variety of conditions Another criterion was its ability to fit data for more than one property Merely examining the squared deviations of data from graphical lines representing the various models was inadequate for choosing among the models. A purely objective selection of models can be made only if all the mechanisms of degradation, as well as their interactions, have been rigorously described mathematically. This will seldom occur in practice.

B. TYPES OF STATISTICAL FAILURE MODELS

See Reference 2 for a general discussion of mathematical models.

1. Exponential Distribution

The exponential distribution is widely used because of its simplicity
and its inherent association with the well-developed theory of Poisson processes.
This model assumes that the increment of property lost, as a fraction of
remaining property level, is constant for any small increment of time during
the degradation. That is, over any small time interval the property degrades
by a fixed percent of its previous level, a reversal of the "compound-
interest law." The exponential model is a special case of the Weibull model
with shape parameter $\beta = 1$. The exponential model has been used by Kamal
(Reference 19) to model the degradation of plastics in an artificial weather-
ing chamber under controlled conditions. However, it is not clear whether
the exponential curve was the best model for fitting the data or whether it
was used because of its convenience.

Suppose data for property level "P" are plotted against time "t"
and they fit the exponential model. Then a plot of $\ln(\frac{1}{P})$ or $\log_{10}(\frac{1}{P})$ vs.
t or of $\ln\left[\ln(\frac{1}{P})\right]$ or $\log_{10}\left[\log_{10}(\frac{1}{P})\right]$ vs. $\ln(t)$ or $\log_{10}(t)$ will be linear.
In the first case the slope may vary, but in the second case (Weibull plot)
it is always unity.

2. Weibull Distribution

The increment of property lost, as a fraction of remaining property
level, is a power function of time The Weibull model is an asymptotic
extreme-value function Therefore, it implies that failure occurs because
of a weakest link or severest flaw of many links or flaws. A four-parameter
Weibull model was used by Clark and Slater (Reference 20) for the degradation
of polymers at several outdoor test sites.

37

Besides the usual scale parameter λ and shape parameter β, parameters were added to define an induction period ("i") and a minimum level of degradation $(\alpha/(1 + \alpha)$·

$$P = \frac{e^{-\lambda(t-i)^{\beta}} + \alpha}{1 + \alpha}$$

where P (fraction of original property) is defined as being unity when t-i is zero or less than zero.

The data modeled by Clark and Slater appeared to be based on single observations and their model fitted reasonably well sometimes but poorly otherwise.

3. Lognormal Distribution

In a lognormal distribution, the increment of property lost, as a' fraction of remaining property level, first increases and then decreases. It can be shown to approach zero at initiation and at long times. When ' failure occurs by fatigue cracks, the lognormal failure model implies that crack growth is randomly proportional to crack size. For polymers, if tensile strength loss should follow the lognormal model, it might be postulated that the amount of chain-scission is randomly proportional to the cumulative UV received.

4. Empirical Models

Empirical models are less desirable than the above distributions. They tend to be more complex, of narrower applicability, and difficult to explain mechanistically. Empirical models are exemplified below.

C. APPLICATION OF MODELS TO OUR DATA

1. Weibull and Lognormal Models

a. Accelerated Data

Both Weibull and lognormal models fit our data. The Weibull model was more convenient for making predictions. It fitted accelerated data for yellowing of polystyrene (see Appendix B). However, the lognormal model gave the most consistent fits for yellowing of Lexan and for cumulative weight loss of polystyrene by TGA The plots are illustrated in Reference 2. The TGA plot is the first indication that a property other than transmittance at 360 nm. follows the asymptotic lognormal model.

b. Outdoor Exposure Data

Initially, the asymptotic lognormal model appeared to fit the film transmittance data obtained from exposures in Phoenix and Miami. Subsequently, there appeared to be a divergence from this model. Data on Lexan films exposed at Phoenix in the fall fit a model appropriate for all outdoor degradation. This data set, the EMMA and EMMAQUA data, and the winter-start data all follow a linear plot on lognormal probability paper (Figures 10 and 11). However there is a change of slope after five months. This is true of the fall and winter initiation data for Lexan exposed both in Phoenix and Miami. For Lexan with exposure initiated in summer, the time before change of slope is two months both in Miami and Phoenix. For polystyrene exposed in the fall at Miami, the time until change of slope is four months. There is no explanation for this phenomenon since the cumulative UV is different in all examples.

Figure 12 shows the Phoenix exposure data presented as Weibull plots, which may be compared with the lognormal plots of Figure 11. The data points

39

Figure 10   Lognormal Plots of Outdoor Exposure Data for
Lexan and Polystyrene at Miami, 45°S.

P = fraction of original transmittance at 360 nm.

0.05
0.10
0.30
0.50
0.70
0.80
0 90
0.95
0.98
0.99

————•————•——— = fall-initiated Lexan exposure.
····O······O··· = summer-initiated Lexan exposure.
——-□——--□—- = winter-initiated Lexan exposure.
——-X————X—- = fall-initiated polystyrene exposure

1   2   3   4   5   6   7

ln (time days)

40
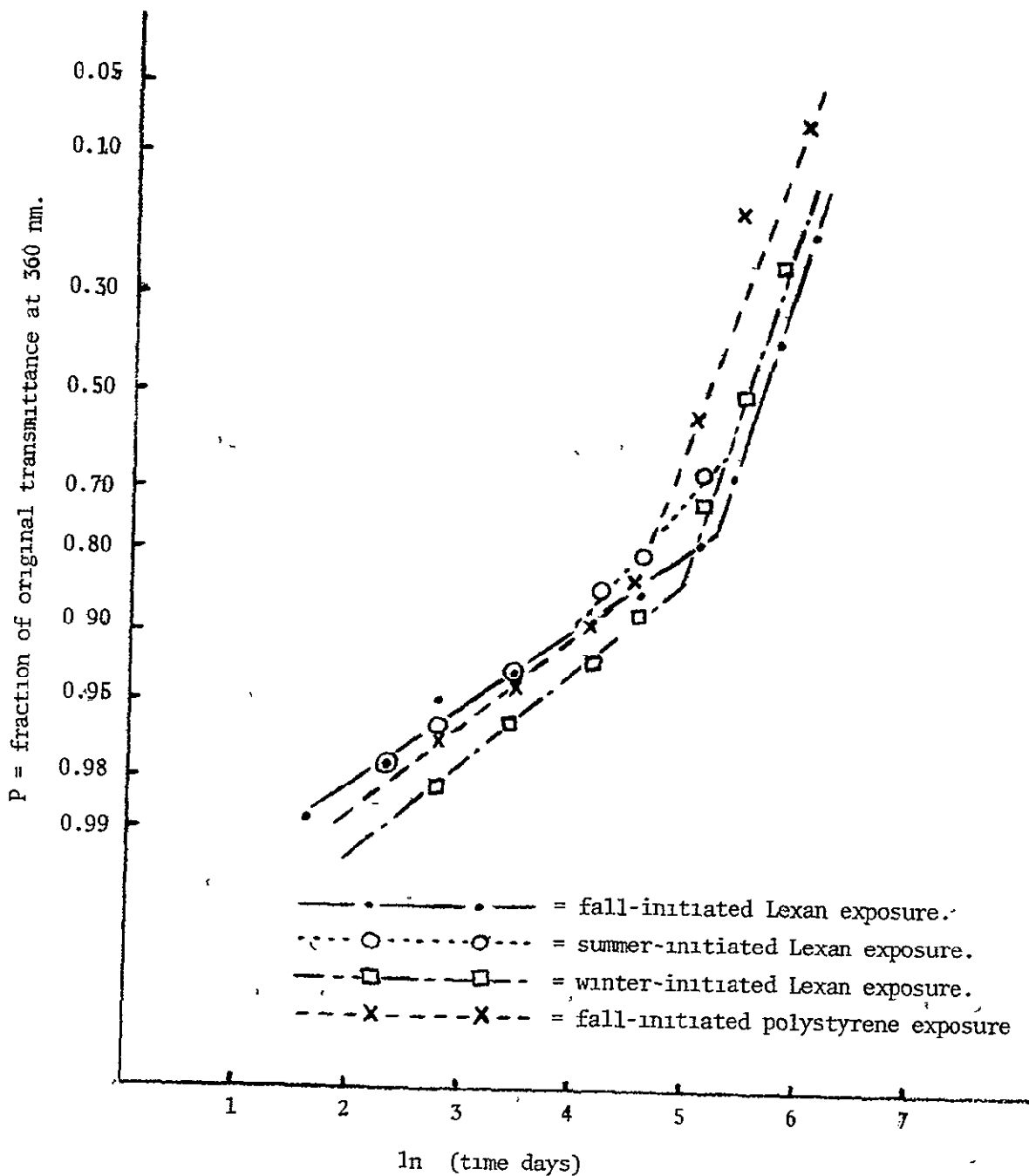
Figure 11. Lognormal Plots of Outdoor Exposure Data for
Lexan at Phoenix, 45°S and EMMA/EMMAQUA.

P = fraction of original transmittance at 360 nm.

ln (time, days)

• = EMA
O = EMMAQUA
□ = fall-initiated exposure, 45°S.
△ = summer-initiated exposure, 45°S.
● = winter-initiated exposure, 45°S.

41
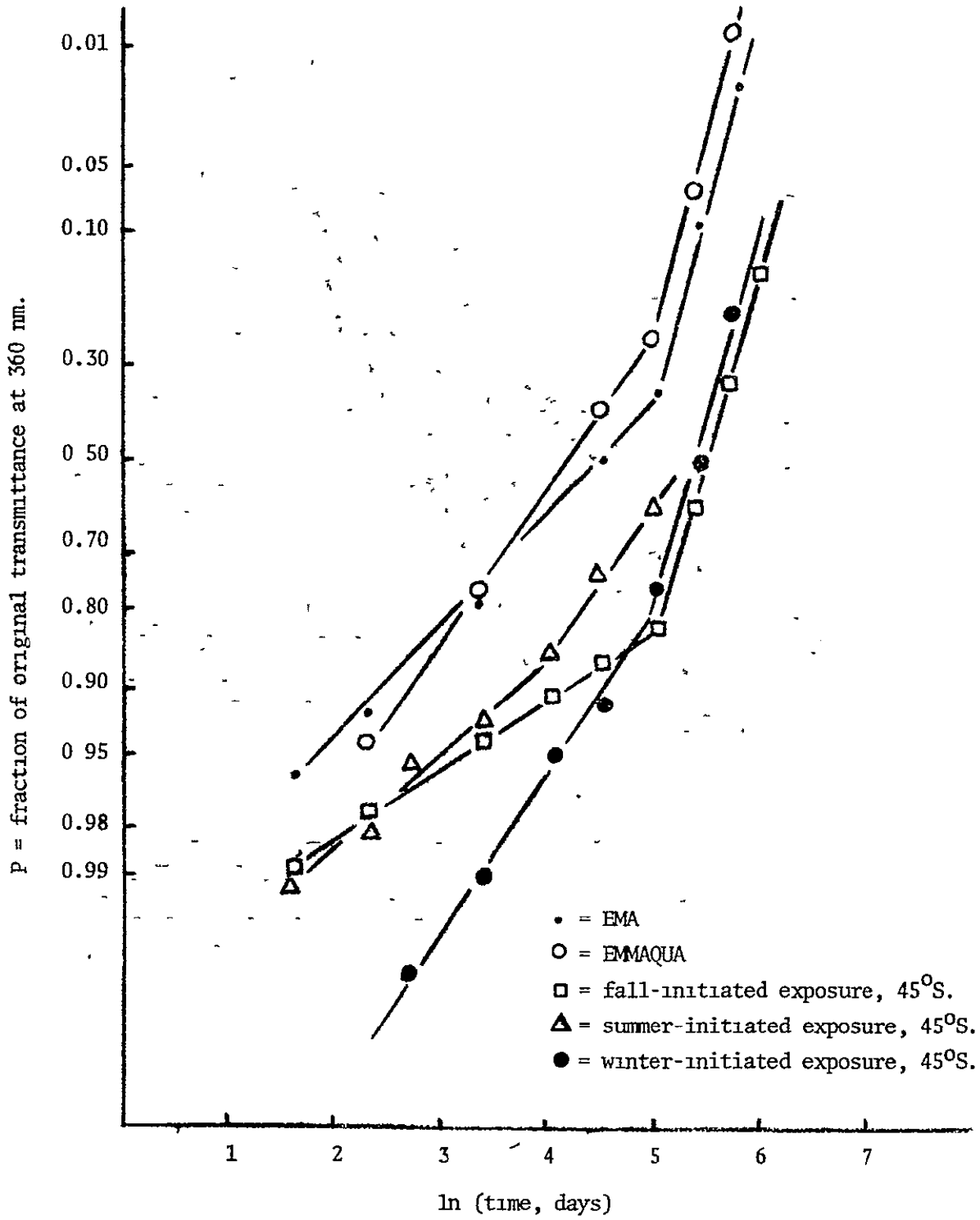
Figure 12   Weibull Plots of Outdoor Exposure Data for
Lexan at Phoenix, 45°S and EMMA/EMMAQUA.
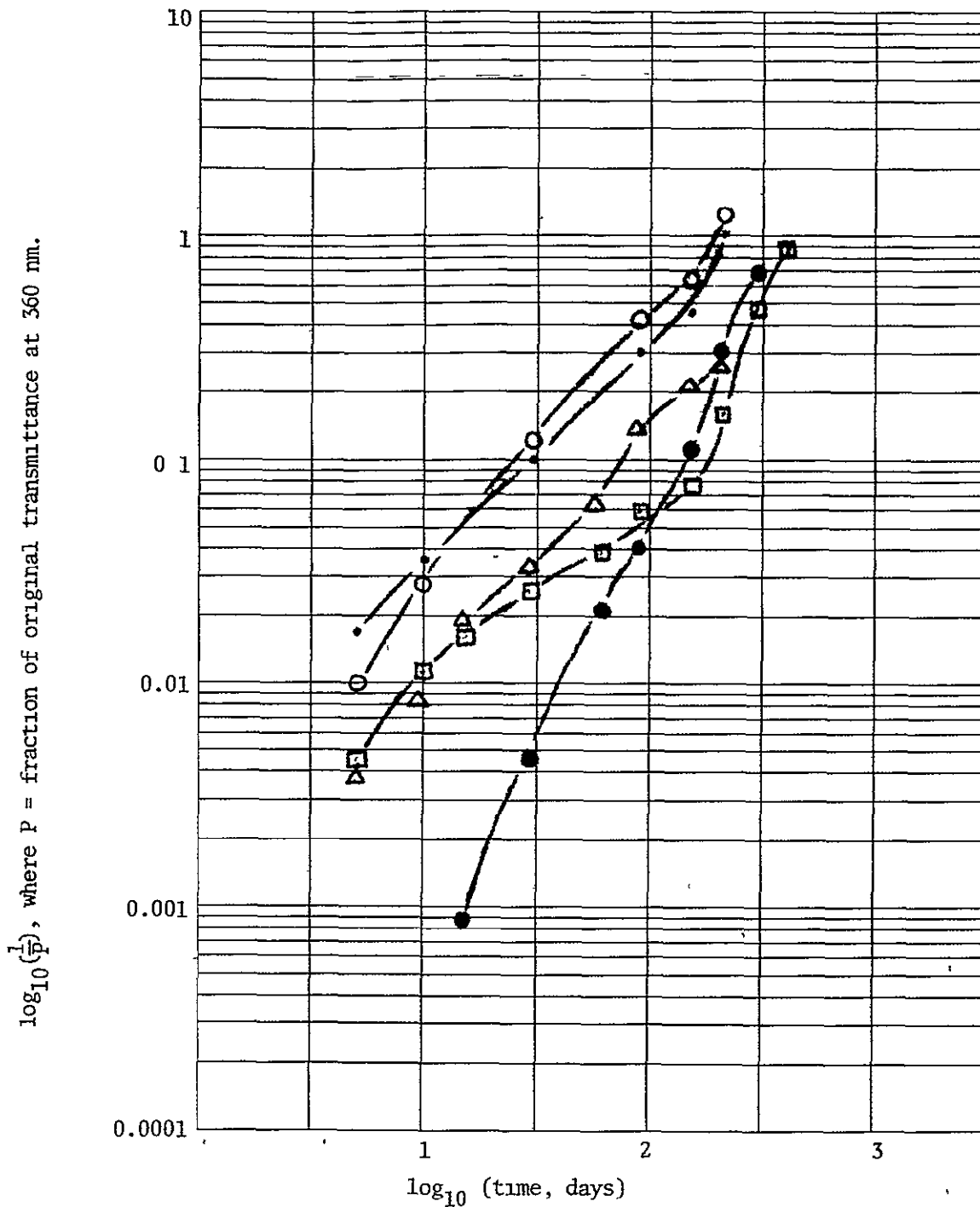
$\log_{10}(\frac{1}{P})$, where P = fraction of original transmittance at 360 nm.

$\log_{10}$ (time, days)

● = EMA

O = EMMAQUA

□ = fall-initiated exposure, 45°S.

△ = summer-initiated exposure, 45°S.

◗ = winter-initiated exposure, 45°S

42

plotted to fit the Weibull model define curves rather than consistently defining lines with sharp inflections. Thus, by the criterion of consistency mentioned above, the lognormal model appears preferable as a way of presenting and-extrapolating data. This example illustrates the important "internal consistency" principle in mathematical modeling.

2. Empirical Models

    a. Empirical Curve-Fitting Using Accelerated Exposure Data

An example of empirical curve-fitting is shown in Figure 13. The following equation was selected from Reference 21:

$$y = ae^{b/x}, \text{ where b is less than 0}$$

$$\text{linear form} \quad \ln y = \ln a + b/x$$

The quantity $\log_{10}\left[1000 \log_{10}(\frac{1}{P})\right]$ was defined as y, and ln (time, hours) was defined as x. A suitable value of "a" was found by trial and error to be 3.55. Then, using the value of $\log_{10}(\frac{1}{P})$ found for 24 hours, "b" was calculated to be -1.21. Thus, the linear form of the equation became.

$$\ln\left\{\log_{10}\left[1000 \log_{10}(\frac{1}{P})\right]\right\} = 1.27 - 1.21/\ln t,$$

where t = time in hours and P = fraction of original transmittance at 360 nm.

The factor of 1000 was used for convenience and subsequently removed. Figure 13 shows that a good fit was achieved. This is a Weibull plot. If $\ln\left\{\log_{10}\left[1000 \log_{10}(\frac{1}{P})\right]\right\}$ were plotted on the ordinate and 1/ln t on with abscissa, a straight line would result, with slope -1.21.

Other accelerated data sets showed a consistent pattern of deviation from this model, the curves, exhibiting increasing and then decreasing slopes as y increases. Thus, the empirical model was excellent for one data set but did not have general applicability.
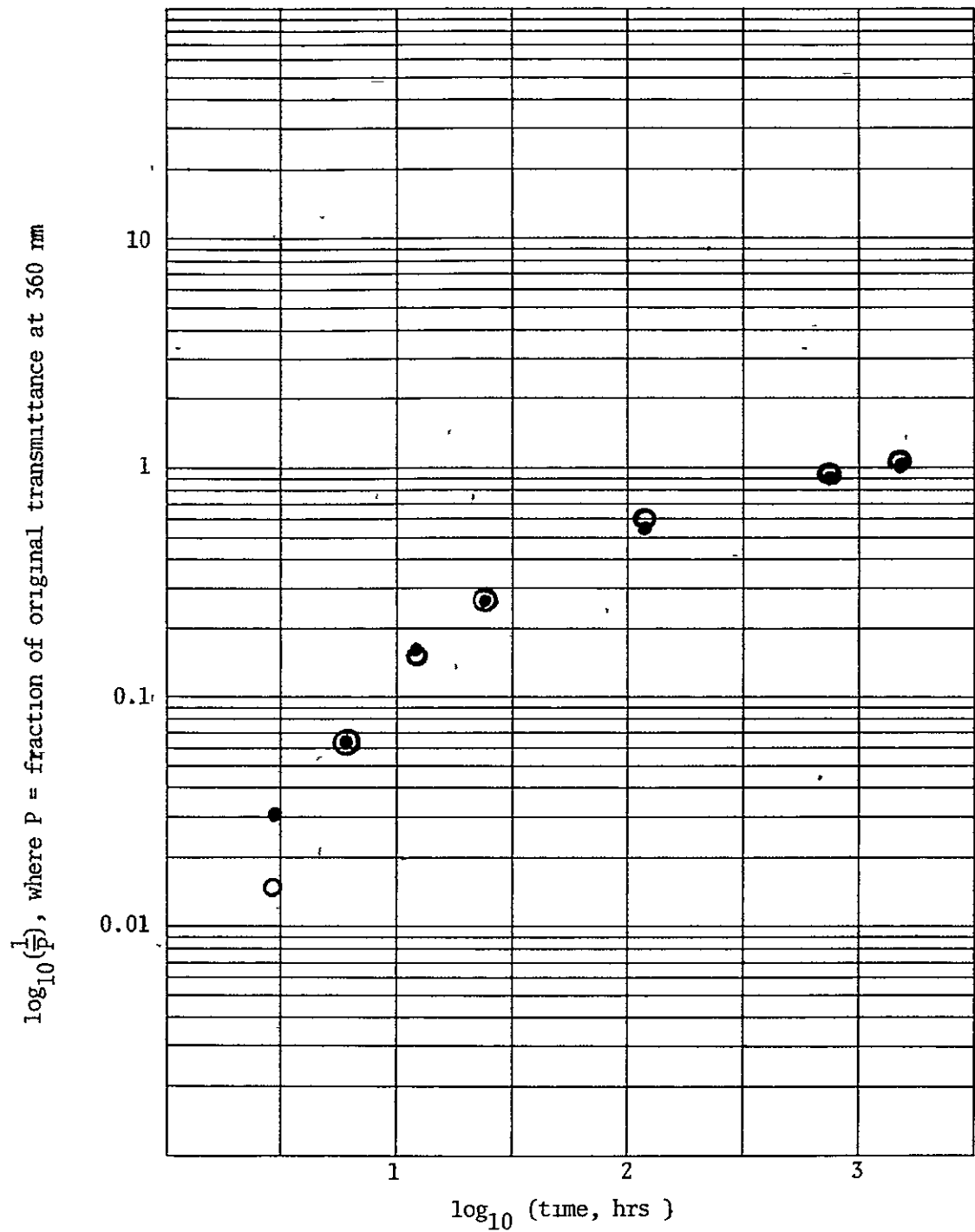
Figure 13   Absorbance Data for Accelerated Exposure of Lexan
(1 00 rel   noon UV, 26°C, 0% relative humidity)

• = Found

○ = Calculated (see text)

44

b. Computer Treatment of Outdoor Absorbance Data

An empirical equation for CUV (cumulative ultraviolet light) was fitted to UV data from Reference 22 and 45°S total insolation data from Reference 23. This equation was a complicated function of sines, representing the rise of UV intensity in summer and the drop in winter. Table 9 shows that calculated CUV data agreed well with the assumed data. Note that the actual values for 300 nanometer UV light are unknown at this time.

Assuming the Weibull equation shown in Table 10, twenty iterations with a least-squares curve fitting program gave the Weibull parameters shown in Table 10 and the calculated absorbance values shown in Table 11. The agreement between observed and calculated values is good, especially for longer exposure times.

Values of β of 1.4-2.0 suggest an "autocatalytic" photochemical reaction. That is, the rate of chromophore formation increases with exposure because the increasingly-yellow material absorbs more and more UV light. The same suggestion is given by the slope in plots of outdoor data vs. an exposure factor (see Appendix A).

An empirical equation involving no assumed UV values also gave a good fit for up to 420 days for exposure data starting on 9/12/76. The rise and fall of UV intensity during the year is expressed as a sine function.

$$\ln\left[\log_{10}\left(\tfrac{1}{P}\right)\right] = C_1 + C_2 \ln t + C_3{}^t + C_4 \sin\left[\left(\tfrac{2\pi}{365}\right)(t + 256 + C_5)\right],$$

where P = fraction of original transmittance at 360 nm

$$\begin{aligned}
t &= \text{exposure time in days} \\
C_1 &= -6.313 \\
C_2 &= 0.635 \\
C_3 &= 0.0057 \\
C_4 &= -0.2722 \\
C_5 &= 58.93
\end{aligned}$$

Table 9

Cumulative UV Values Used in Computer Treatment
of Absorbance Data for Lexan Exposed at Phoenix, 45°S

Exposure Time, days	Cumulative UV, Relative Values		
	Start 9/12/76	Start 12/22/76	Start 6/21/77
30	267	106	349
60	472	182	726
90	515	404	964
150	666	1035	1165
210	1071	1815	1335
300	2176	2785	2160
420	3445	3160	3670

Table 10

Weibull Parameters Found for Absorbance Data
for Lexan Exposed at Phoenix, 45°S

Equation: $100 \log_{10}(\frac{1}{P}) = \lambda \ (CUV/1000)^{\beta}$,

where P = fraction of original transmittance at 360 nm.

Date Exposure Started	Values by Least-Squares Curve Fitting Program			
	λ	95% Confidence Limits for λ	β	95% Confidence Limits for β
9/12/76	15.1	13.7 - 16.6	1.44	1.36 - 1.53
12/22/76	11.3	9.5 - 13.0	1.76	1.62 - 1.91
6/21/77	15.2	12.8 - 17.6	2 04	1.38 - 2.69

Table 11

Calculated vs. Observed Values for Absorbance Data

for Lexan Exposed at Phoenix, 45°S

Exposure Time, days	$\log_{10}(\frac{1}{P})$, where P = Fraction of Original Transmittance at 360 nm.					
	Start 9/12/76		Start 12/22/76		Start 6/21/77	
	Calc'd	Observed	Calc'd	Observed	Calc'd	Observed
30	0.0225	0.0271	0.0021	0.0048	0 0178	0.0339
60	0.0512	0.0402	0.0056	0.0224	0.0791	0.0666
90	0.0582	0.0601	0.0227	0.0394	0.1411	0.1411
150	0.0842	0 0772	0.1195	0 1158	0.2073	0.2152
210	0.1672	0.1577	0.3223	0.3147	0 2736	0.2702
300	0 4652	0.4813	0.6867	0.6958		
420	0.9030	0 8975	0.8579	0.8534		

D. PREDICTION OF PROPERTY CHANGES FOR PLASTIC FILMS

1. Procedure

The plan for predicting weatherability is described in Reference 2. Degradation rate constants were determined for various combinations of UV intensity, temperature, and humidity in an accelerated test. Then, using weather data for an exposure site, the changes' in encapsulant properties were calculated.

Battelle have conducted a detailed analysis of environmental variables (Reference 24). Statistical data were used to obtain frequencies, durations, and transitions for the simultaneous occurrence of various combinations of environmental variables. The simultaneous occurrence of specific levels of air temperature, relative humidity, and insolation could be represented as an "environmental cell," shown graphically as a geometric cube

Insolation

Relative Humidity

Air Temp.
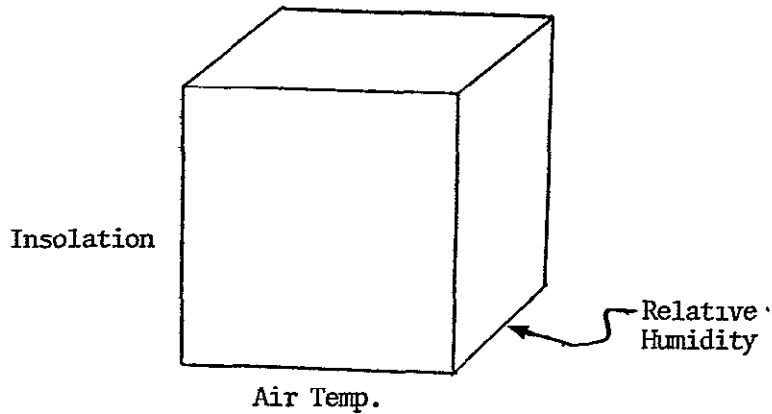
At any given time, the values of a particular combination of temperature, relative humidity, and insolation are defined by the coordinates of a point which lies in exactly one of the environmental cells. When values of the environmental variables change with time, the point moves from cell to cell. Three-hourly measurements for a given geographic location were used to obtain the list of successive cell code numbers which can be computerized and analyzed. Aggregated information is used to provide frequency and duration histograms.

Environmental cell statistics are used to generate 20-year forecasts of the expected number of exposure hours, E, for each cell.

$$E = \frac{NKT}{H}$$

where N = observed number of occurrences of a cell in a historical time period H

K = 3 hours

T = forecast time period

By establishing the generalized rate constants of encapsulant degradation for each cell, total degradation can be computed for 20 years of exposure. The changes in encapsulant properties with time in our accelerated test can be related in "environmental cells" in the same manner.

48

Our plan assumes that degradation rates are a unique function of temperature (T), relative humidity (RH), and ultraviolet light deposited (UV). Therefore, rates were determined for 24 static experimental conditions These data were used to calculate the generalized rate constants for any (T, RH, UV) condition, i.e., for any arbitrary set of environmental cells. The rate constant k_i for condition i (or cell i) is

$$k_i = f\ (T_i,\ RH_i,\ UV_i).$$

This plan has been successfully fulfilled

Assumptions were

(1) The xenon lamp used in accelerated exposure indeed represents July noon sunlight as evidenced by our spectroradiometric measurements.

(2) UV intensity varies with season and time of day according to certain graphical data from Reference 22.

Assumption (2) is the critical one. It was necessary to make such an assumption because "the amount of UV radiation received at a given location in the United States is poorly known and is virtually impossible to estimate accurately" (Reference 24).

For full details see Appendix B and Reference 25.

For convenience, the steps in making a prediction are summarized in simple outline form in Figure 14.

2   Yellowing of Polystyrene

Predictions assumed that the xenon lamp truly represented noon sunlight in terms of UV intensity   A Weibull model with $\beta = 0.9$ was found to fit the accelerated data and was assumed to pertain to outdoor weathering

FIGURE 14

PREDICTION METHODOLOGY

1. SELECT MODEL EQUATION

   WEIBULL: $\log_{10}\left(\dfrac{1}{p}\right) = \left(\dfrac{\lambda}{2.3}\right) t^{\beta}$

2.

   RELATIVE HUMIDITY.   ↑UV   TEMPERATURE   ENVIRONMENTAL CELL WITH $\dfrac{\lambda}{2.3}$ = ___ β = ___
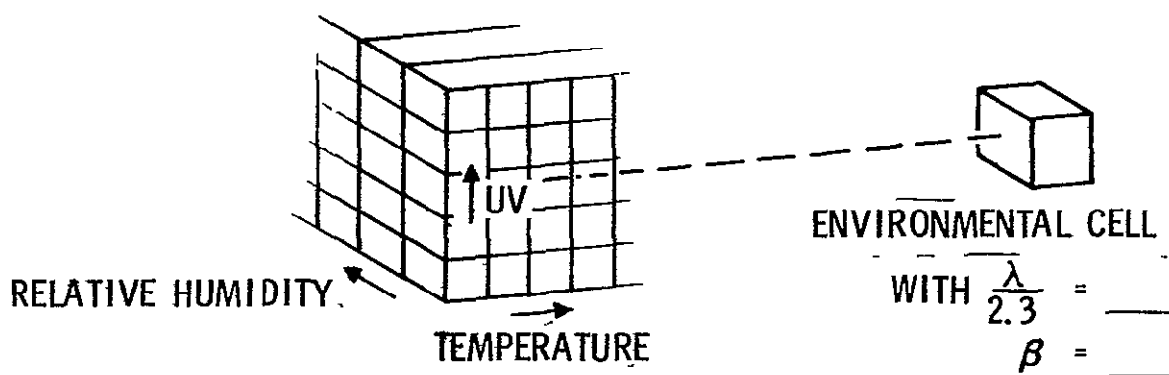
3. "TYPICAL DAY" OF EACH MONTH: 7-9 AM, 9-11 AM, 11 AM - 1 PM, 1-3 PM, 3-5 PM. OBTAIN WEATHER DATA.

4. ASSIGN VALUES OF $\dfrac{\lambda}{2.3}$ AND β TO EACH TWO-HOUR PERIOD, USING ENVIRONMENTAL CELL MATRIX.

5. FIND $\dfrac{\lambda}{2.3}$ AND β FOR TYPICAL DAY OF EACH MONTH.

6. SUM INCREMENTS OF DEGRADATION OVER MONTHS OF THE EXPOSURE PERIOD.

50

Also, it was necessary to assume a schedule of variation of UV during the year from literature data. Considering these assumptions, the predictions were very successful (Figure 15).

The accelerated data for polystyrene also were fitted to a log-normal model. The following results were obtained

Exposure Time in Miami (45°S), Days	% of Original Transmittance at 360 nm	
	Predicted	Found
30	0.96	0.97
60	0.89	0.91
90	0.87	0.83
150	0.59	0.55
210	0.16	0.16
300	0.02	0.07

Selection of the better model, Weibull or lognormal, is not obvious in this case. See the above section "Selection of a Mathematical Model."

3. Yellowing of Lexan

A mismatch between the spectra of the xenon lamp and the sun caused hyperacceleration of yellowing. Hence the accelerated data had to be adjusted. Therefore, the form of the curve of yellowing vs. time and not the absolute values is significant.

Figures 16 and 17 show data through 300 days. A Weibull model with $\beta = 1.0$ was assumed for these calculations. However, longer times (420, 540 days) showed that a higher value of β, about 1.3, was required. Recalculation with $\beta = 1.3$ (see Appendix A) gave good agreement of observed and calculated values through 540 days.

Figure 15

POLYSTYRENE YELLOWING IN MIAMI

y-axis: $A_{360} - A_{600} - 0.0139 = \log_{10}\left(\frac{1}{P}\right)$, where P = fraction of original transmittance at 360 nm

x-axis: $\log_{10}$ (exposure time, days)

● = Found
O = Predicted
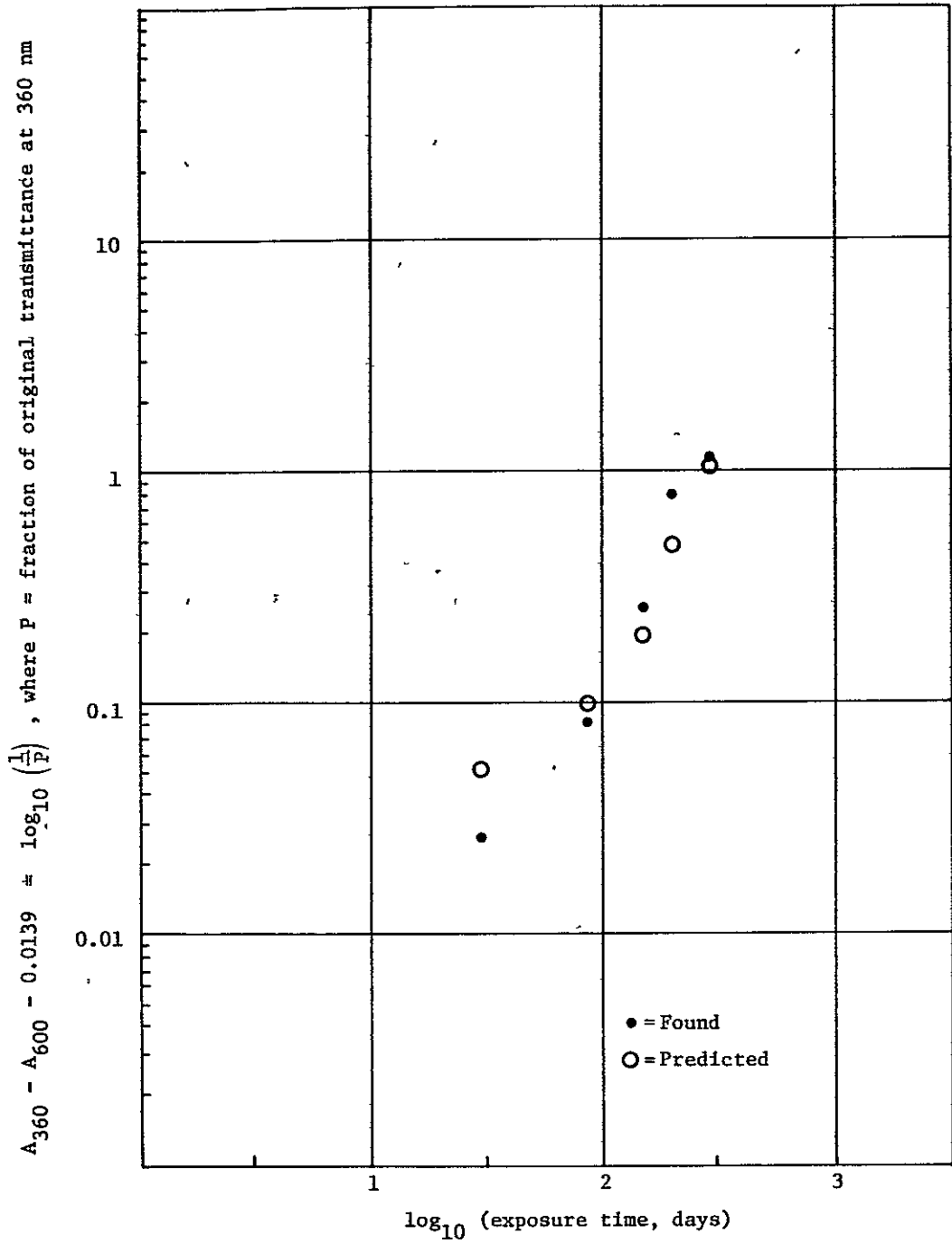
Figure 16

LEXAN YELLOWING IN PHOENIX
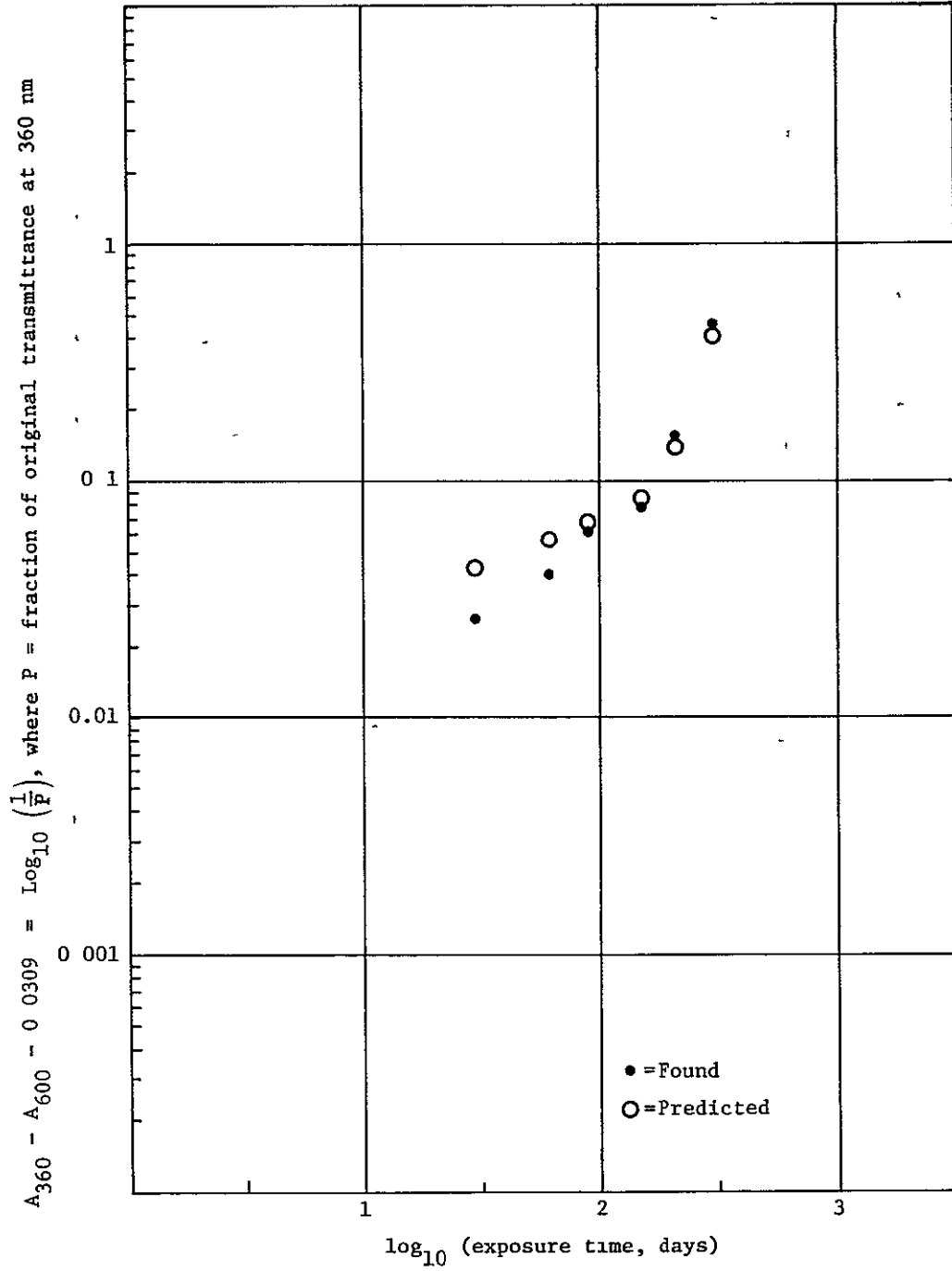
Figure 17

LEXAN YELLOWING IN MIAMI

$A_{360} - A_{600} - 0.0309 = \log_{10}\left(\frac{1}{P}\right)$, where P = fraction of original transmittance at 360 nm

$\log_{10}$ (exposure time, days)

● =Found

◯=Predicted

54
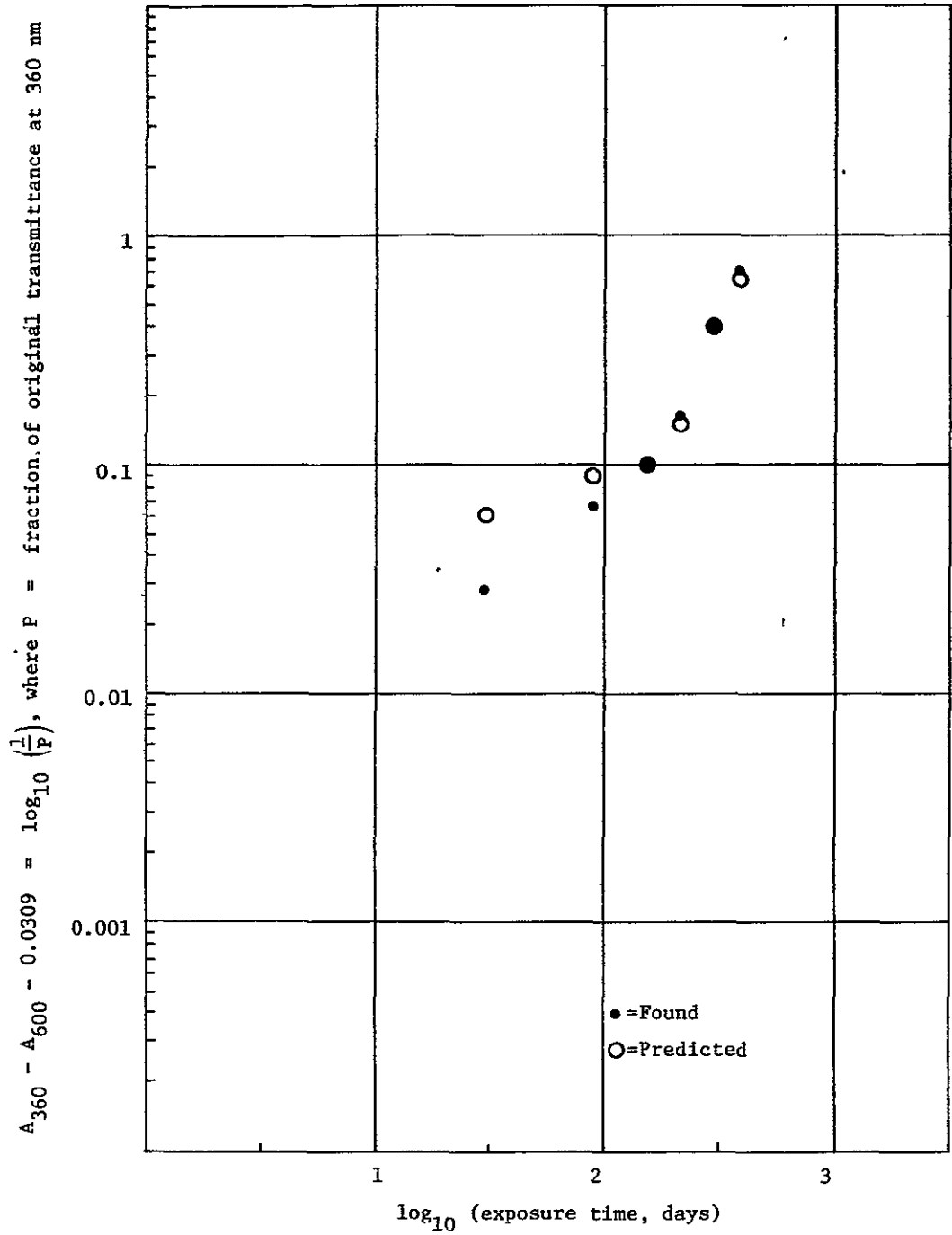
4. Loss of Tensile Strength of Polystyrene

A Weibull model with $\beta = 0.9$ was assumed, as done for the yellowing of polystyrene. Predictions were successful (Figure 18).

An example of the use of the relationship of yellowing and tensile strength loss, discussed in Appendix A, is shown in Figure 19. After 210 days exposure in Miami, samples showed an absorbance value of 0.777, and this corresponded to 42% of original breaking stress. Subsequently, tensile strength was determined and found to be 39% of original, which is in good agreement.

5. Loss of Tensile Strength of Lexan

Agreement was fair only at the 300 day point. Yellowing of Lexan proceeded under the lamp at about 20X the rate for noon sunshine. The reaction involves a molecular rearrangement without chain scission Loss of tensile strength reflects chain-scission and is independent from yellowing. Each process has its own activation spectrum.

6. Tedlar Properties

Tedlar has shown insufficient changes in absorbance at 360 nm (corrected by absorbance at 600 nm) to allow a quantitative prediction, but the negligible change after the presumed equivalent of 8 years natural exposure on the EMMA/EMMAQUA suggests only a slight absorbance increase in 20 years.

The losses in both tensile strength and elongation (a standard measure of toughness) have stabilized at 25% between 0.8 year and 1.5 years on the EMMAQUA. The level of surface carbonyl groups seems to have stabilized similarly Our results are consistent with du Pont's data (Reference 26).

55

Figure 18

LOSS OF TENSILE STRENGTH OF POLYSTYRENE IN MIAMI

y-axis: $\log_{10}\left(\frac{1}{P}\right)$, where P = fraction of original breaking stress

x-axis: $\log_{10}$ (exposure time, days)

● = Found
O = Predicted
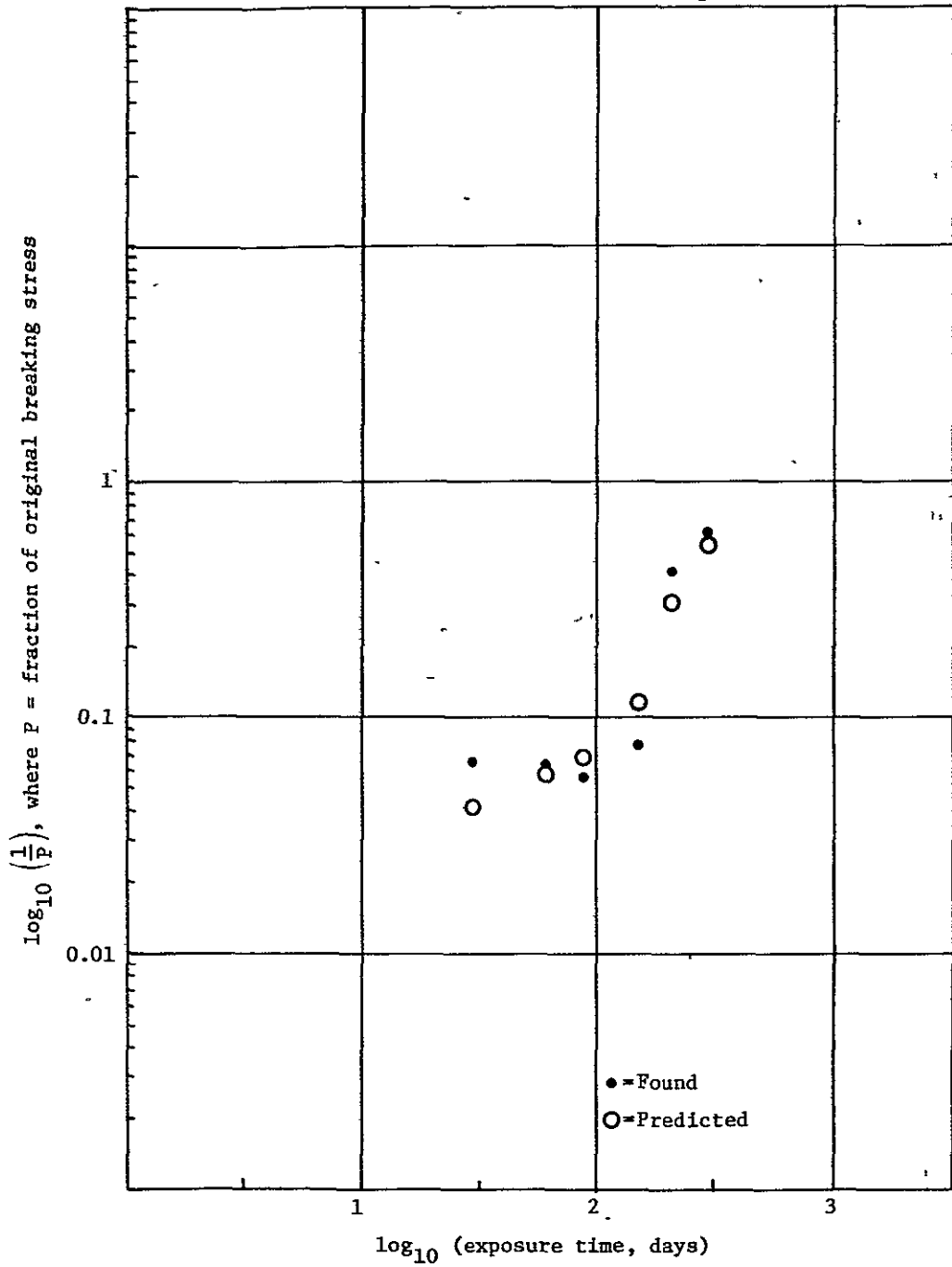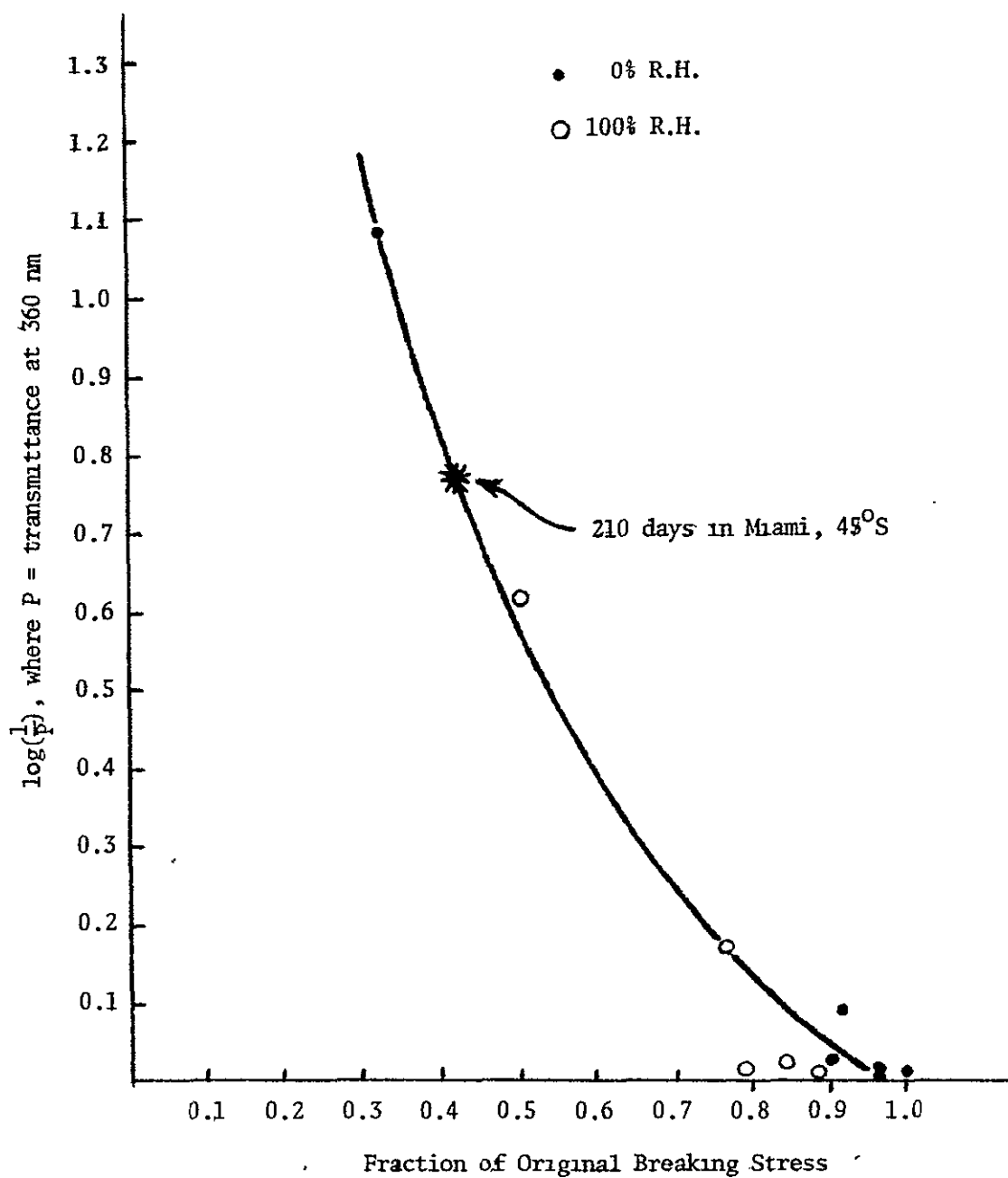
Figure 19. Relation of Transmittance at 360 nm and Tensile Breaking Stress for Polystyrene (from Accelerated Exposure Data)

Hyperaccelerated exposure with sunlight, e.g., at an intensity of 1000X, would be necessary to make a 20-year prediction.

E. OTHER PREDICTIONS

1. Solar Cell Power

An attempt was made to predict the rate of moisture-induced degradation of solar cell contacts for the silicone-encapsulated UTS's. No degradation was predicted for 5 years based on 'accelerated data (Figure 20), but significant power loss (31%) was observed for Miami exposure after 1.5 years. The "moisture-pumping" action of daily "baking" and nightly dew-soaking might explain this result. This is an example of an unsuccessful prediction based on lack of knowledge, in this case of the effect of temperature/humidity cycling. The solar cells used under encapsulants other than Sylgard 184 were very moisture-resistant. Survival at 72°C and 100% relative humidity for 2 months suggests, by the rule of thumb that reaction rate doubles for each 10°C rise in temperature, a lifetime of at least $2x2^3$ = 16 months under the most humid conditions at an average "kinetic temperature" of 40°C. Further, the following month of survival in steam at 100°C suggests an additional minimum lifetime of $1x2^6$ = 64 months. The total is 16 + 64 = 80 months, or a minimum lifetime of about 7 years.

If the above prediction is correct, darkening/opacifying of encapsulants should control solar cell power. Accelerated data indicate that the power should remain at over 90% of original for all the array systems under conventional (45°S) exposure for at least 1.5 years, assuming an "acceleration factor" of 9. Similarly, the acrylic lacquer (System #4) and the glass/polyurethane encapsulants (Systems #3, 6, and 9) are predicted to remain unchanged after 1.5 years. The only accelerated
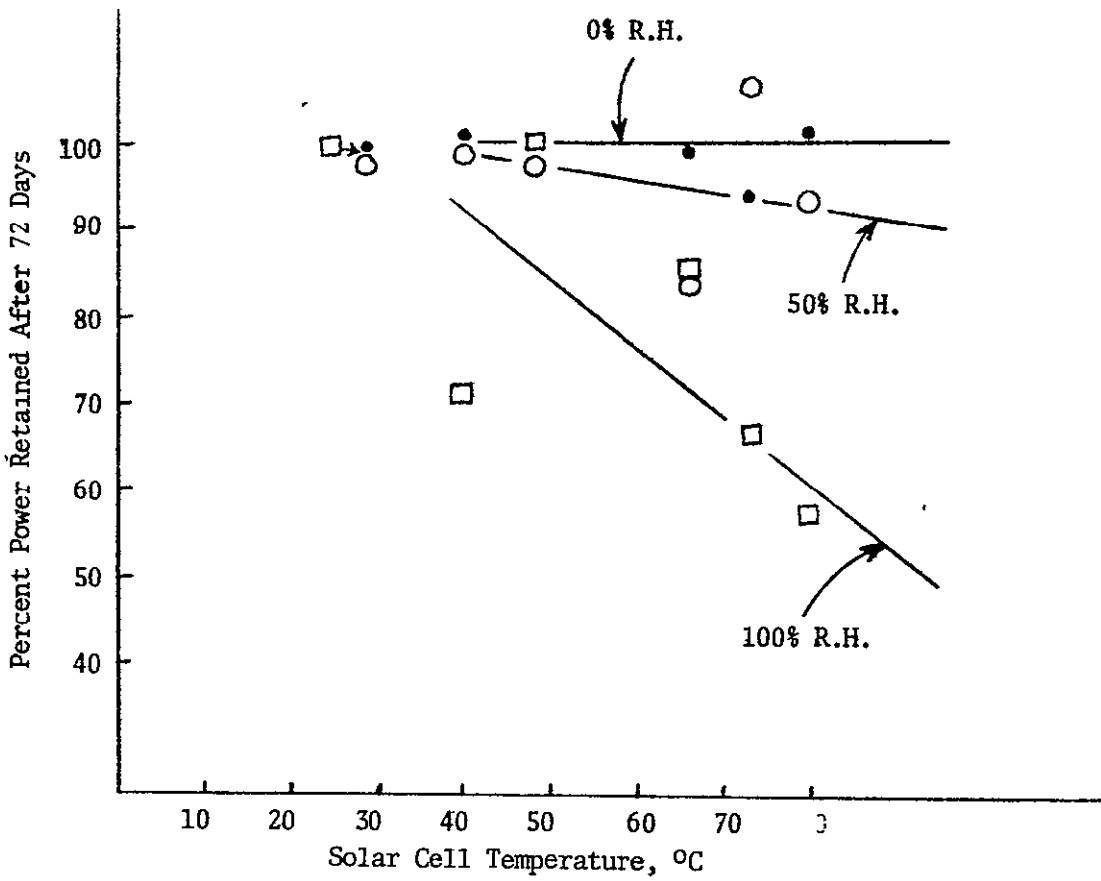
Figure 20. Effect of Moisture and Temperature on Power Output of Solar Cells in UTS's During Accelerated Exposure

conditions that degraded the acrylic lacquer were at a UTS temperature of $72^{\circ}C$, which exceeds the Tg of $63^{\circ}C$ as determined by DSC. Similarly, Tedlar was degraded only above its Tg ($57^{\circ}C$ by DSC) in accelerated exposure (Reference 2). On the other hand, severe degradation of nitrocellulose lacquer (System #7) is predicted at 1.5 years

Continued outdoor exposure would be necessary to check these predictions.

2. Loss of Gloss of Lexan Cover on Sylgard-Encapsulated UTS's

Loss of gloss of Lexan films was found to be moisture-related as well as temperature-related in accelerated exposure with the xenon lamp. Relevant data are presented in Table 12 and Figure 21. In EMMAQUA exposure, the fact that the UTS was warmer than the surrounding air caused the Lexan UTS cover to lose gloss before 90 days while unsupported Lexan lost its gloss between 150 and 210 days.

A rough calculation, involving a number of assumptions (Appendix A), predicted severe loss of gloss of the Lexan UTS cover in Miami in about 3 years. In agreement, the observed loss of gloss at 1.5 years (the longest available exposure) was only slight.

Table 12

ACCELERATED DATA REPRESENTING LOSS

OF GLOSS OF LEXAN

UV Intensity vs. Noon Sunlight	Air Temp., °C	Relative Humidity, %	$\log(\frac{1}{P}) \times 10^4$, where P = fraction of original transmittance at 600 nm, after 768 hours accelerated exposure	
1.00	26	0 50 100	34 24 326	
	60	0 50 100	-12 279 3039	
0.66	18	0 50 100	106 58 56	(161)* (88)* (85)*
	55	0 50 100	2 228 1297	(3)* (345)* (1965)*
0	40,80	0,50,100	very low	
0, 1.00 alternating	26, 7	0 50 100	-14 328 207	(14)** (0.6)**
	60,44	0 50 100	5 113 661	(0 4)** (0 2)**

*At UV intensity 1.00, assuming linear effect of light.

**Ratio to result with continuous light.

Figure 21   Effect of Temperature and Relative Humidity
on Loss of Gloss of Lexan
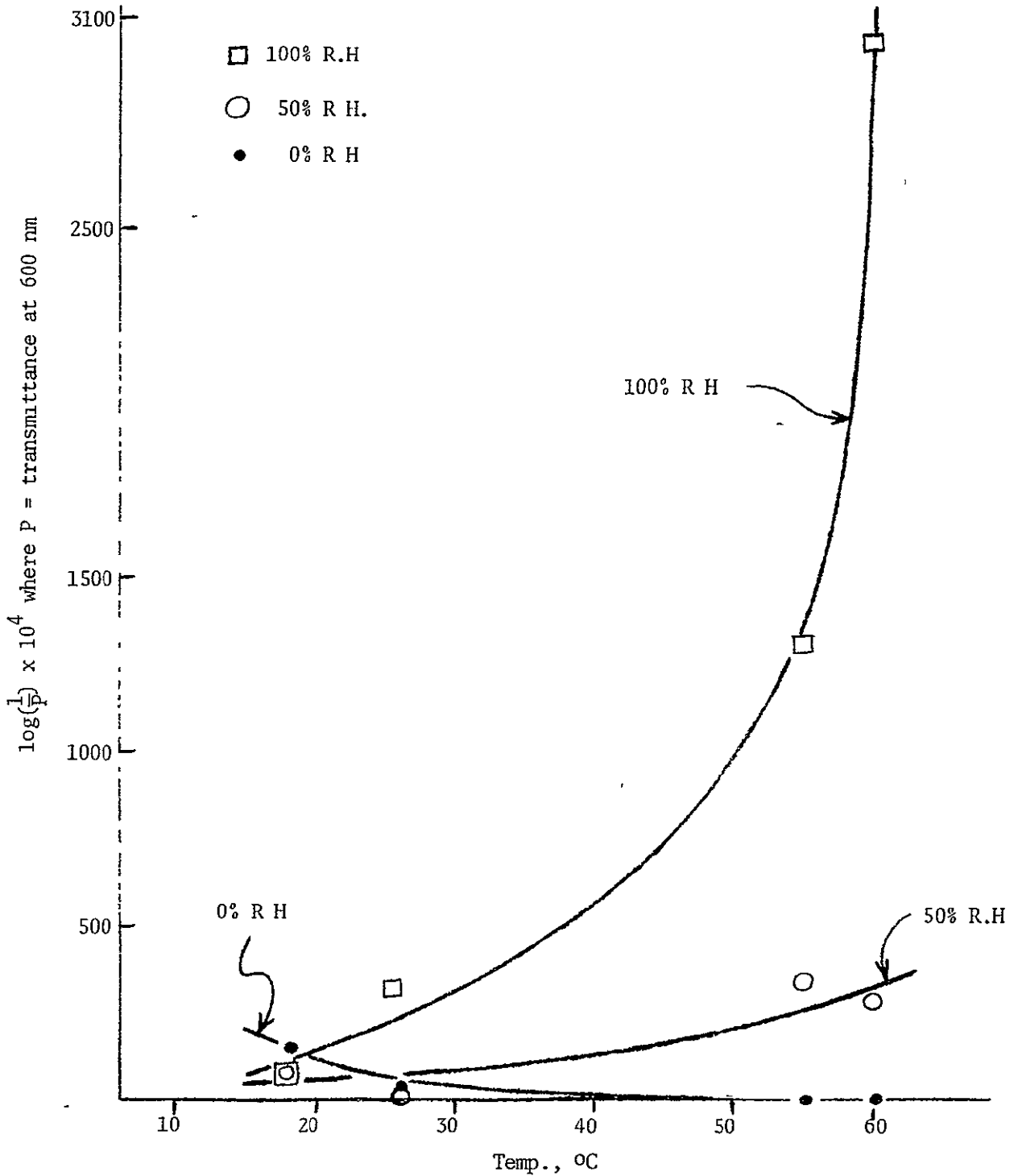
VI. CONCLUSIONS

The real dilemma in accelerated testing can be stated as follows·
"How can failures be forced to occur in a relatively short period of time
and yet ensure that parts have not been overstressed?"

"Overstressing" implies that test conditions are so severe that they
force an unnatural failure mechanism, one that would never occur under normal
conditions of use. Overstressing has been used to advantage in military pro-
curements to screen out electronic parts and components. The object is to
achieve high reliability at almost any cost. The needs of the LSA program
are quite different and considerably more difficult, namely to achieve
adequate reliability at the lowest possible cost. Expressed differently, it
is not acceptable to screen out encapsulants by exacting tests. These pass
only high-reliability candidates, ones likely to be more expensive. Probably
what would happen is that only hermetically-sealed systems would pass. For
weather-resistant plastics, tests could pass the expensive FEP and fail more
cost-effective materials such as Tedlar or acrylics. Defense agencies such
as Rome Air Development Center (RADC) are exploring the possibilities of
reducing test requirements. Such action would permit the use of plastic-
encapsulated devices in military hardware. This example is part of the
perennial quest for cost-reliability trade-offs.

On the other hand, if only mildly accelerated tests are used, system
failures will not occur in encapsulated solar cells for long periods of time.
Under such circumstances, is it possible to extrapolate or deduce from prop-
erty changes what will eventually occur and when? Clearly it is a question
of credibility.

With the above considerations as background, our main conclusions are:

(1) Data obtained by artificially weathering polymer films could
     be extrapolated with considerable confidence. Hyperaccelerated
     UV exposure appears ideal for testing films, including those
     intended as UV filters to protect underlying pottant.

(2) On the other hand, tests with micromodules (UTS's) did not pro-
     vide good predictions because solar cell power was the property
     monitored, and the cells themselves were rugged and little
     influenced by encapsulant degradation. This experience
     illustrates the difficulty of choosing a meaningful property
     to monitor and then defining the property level which con-
     stitutes failure. The property must fall continuously during
     exposure and be precisely measurable.

(3) Multicondition accelerated exposure and hyperaccelerated photo-
     chemical exposure are new and important procedures   Table 13
     summarizes the relative advantages of test methods.

The Test Program Plan (see section III, above) incorporates these
methods in a complementary synthesis.

Other conclusions are

If corrosion-resistant metallization is used, solar cells are in-
herently weather-resistant. Then, the encapsulant's role is to protect the
cells from soiling and mechanical shock rather than from moisture attack.

Degradation of encapsulants causes power generation loss but to a
lesser degree than expected. Considerable darkening and/or opacification
can be tolerated without reducing power more than 10 percent.

Table 13

Accelerated/Abbreviated Test Methods

Method	Exposure Time Required to Predict 20-year Behavior	Uses Natural Sunlight	Discloses Failure Modes	Shows Relative Effect of Weather Factors	Provides Extensive Degradation Rate Data
Conventional Outdoor Exposure	20 years	Yes	Yes	No	No
Conventional Weather- Ometer	2-3 years	No	Yes	No	No
EMMA/EMMAQUA 8X Sunlight Concentrators	2-3 years	Yes	Yes	No	No
Multicondition Accelerated Exposure (Accel. Factor about 8)	2-3 years	No	Yes	Yes	Yes
Hyper- accelerated Photochemical Exposure	1 month	Yes	Yes	No*	No**

*Yes, with the addition of thermal/hydrolytic ("pressure cooker") hyper-accelerated exposure as proposed in the Test Program Plan but not demonstrated.

**Yes, by including enough sets of conditions in the photochemical and thermal/hydrolytic hyperaccelerated exposure tests.

65

Favorable synergism was noted, e.g., silicone rubber supported an embrittled-Lexan polycarbonate "dust cover," and a glass cover acted as a UV filter to protect underlying polyurethane.

Micromodules with Sylgard 184 encapsulant showed every indication of having a 20-year encapsulant life in our exposure tests. Delamination was no problem because of stress-free design and mounting.

Whether a hermetic seal is needed to exclude all moisture from solar cells has not been established. When the moisture question is resolved, the functions of the encapsulant will be to exclude dirt, provide a cleanable surface, and protect cells from mechanical shock.

Potentially cost-effective materials were noted. These include aromatic polyurethane (13¢/ft.^{2}/0.010 inch) when protected from UV by glass or UV-grade Tedlar, Tedlar film (4¢/ft.^{2}/0.001 inch), crosslinked acrylic lacquer (2.3¢/ft.^{2}/0.003 inch), enameled steel for substrate (29¢/ft.^{3}/0.030 inch), and copper for circuitry (2.9¢/ft.^{2}/0.001 inch).

In summary, we believe that the problems inherent in accelerated/abbreviated testing can and will be overcome. Our work has demonstrated some solutions and suggested others. Predictions sufficiently "credible" for evaluation of new array designs or improvement of present designs can be based on our Test Program Plan and the principles outlined above.

VII. RECOMMENDATIONS

The primary recommendation is that our Test Program Plan be followed in selecting candidate encapsulants. Specifically, we recommend that predictions of weather-resistance be made by utilizing the following principles

(1) Hyperaccelerated tests, with a solar furnace or with ovens and autoclaves, must be carried out to corroborate extrapolations from the accelerated tests. In practice, extrapolations can be risky, and Figures 22 and 23 show a hypothetical example. The four data points for 5 months precisely fit a lognormal model (Figure 22). However they can easily be construed to fit a Weibull model also (Figure 23). The usual experimental errors permit no distinction and can favor the wrong model. At 20 years, where $\log_{10}$ (time, days) = 3.86, the lognormal extrapolation gives $\log_{10}(\frac{1}{P})$ = 0.86 or P = 0.14, and the Weibull extrapolation gives $\log_{10}(\frac{1}{P})$ = 1.44 or P = 0.04. Degradation may follow neither model but rather the dotted curve in Figure 22 which resembles the one for Lexan in accelerated exposure. At 20 years, the dotted curve in Figure 22 gives $\log_{10}(\frac{1}{P})$ = 0.45, or P = 0.35.

Consider the consequences of extrapolation. Suppose property P is tensile strength and 1/3 retention is required for encapsulant integrity. Then the dotted curve (Figure 22) would represent a 34 year life, the lognormal model (Figure 22) would represent a 6.1 year life, and the Weibull model (Figure 23) would represent a 2.4 year life!

67
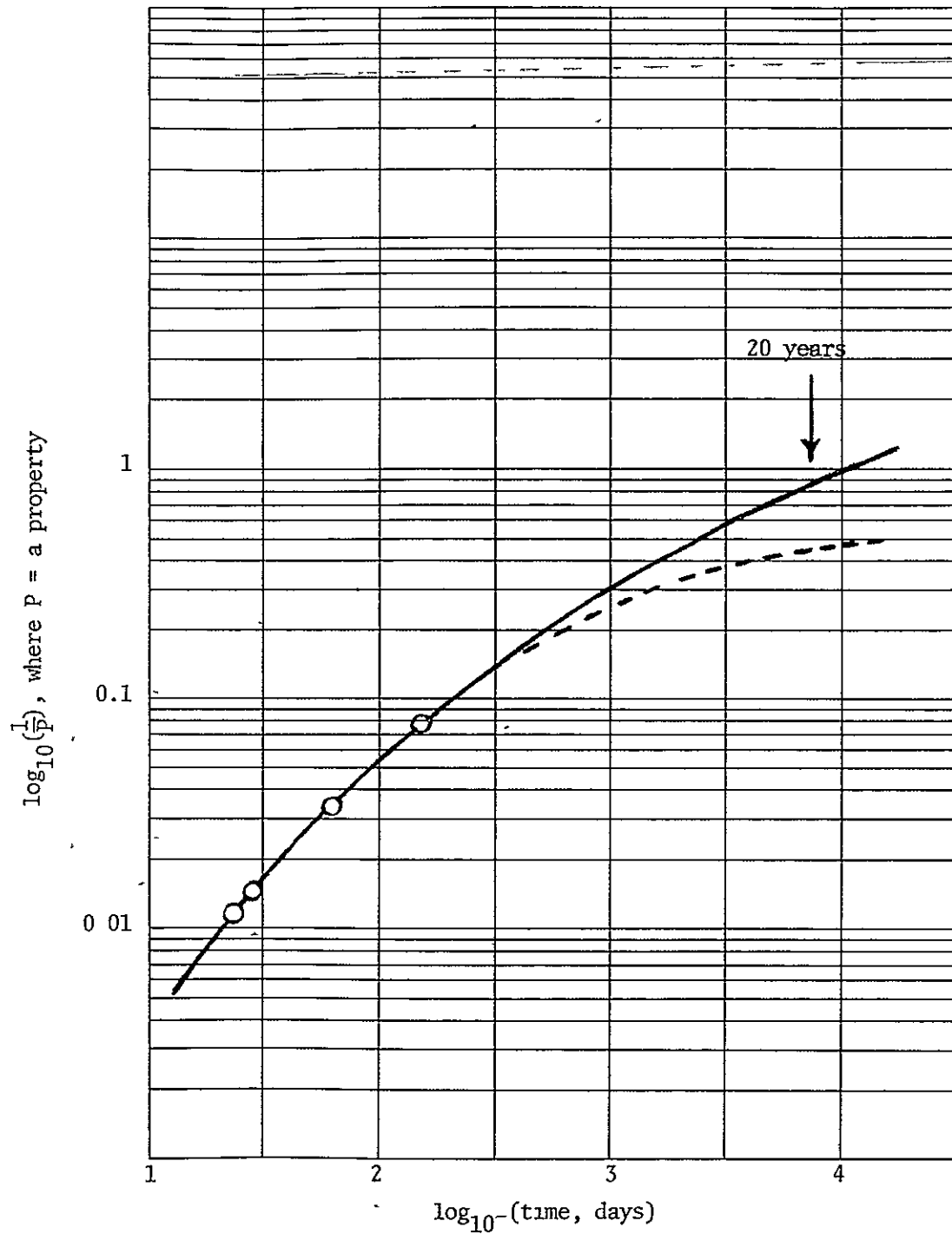
Figure 22. Hypothetical Data Points Extrapolated
by Lognormal Model

68
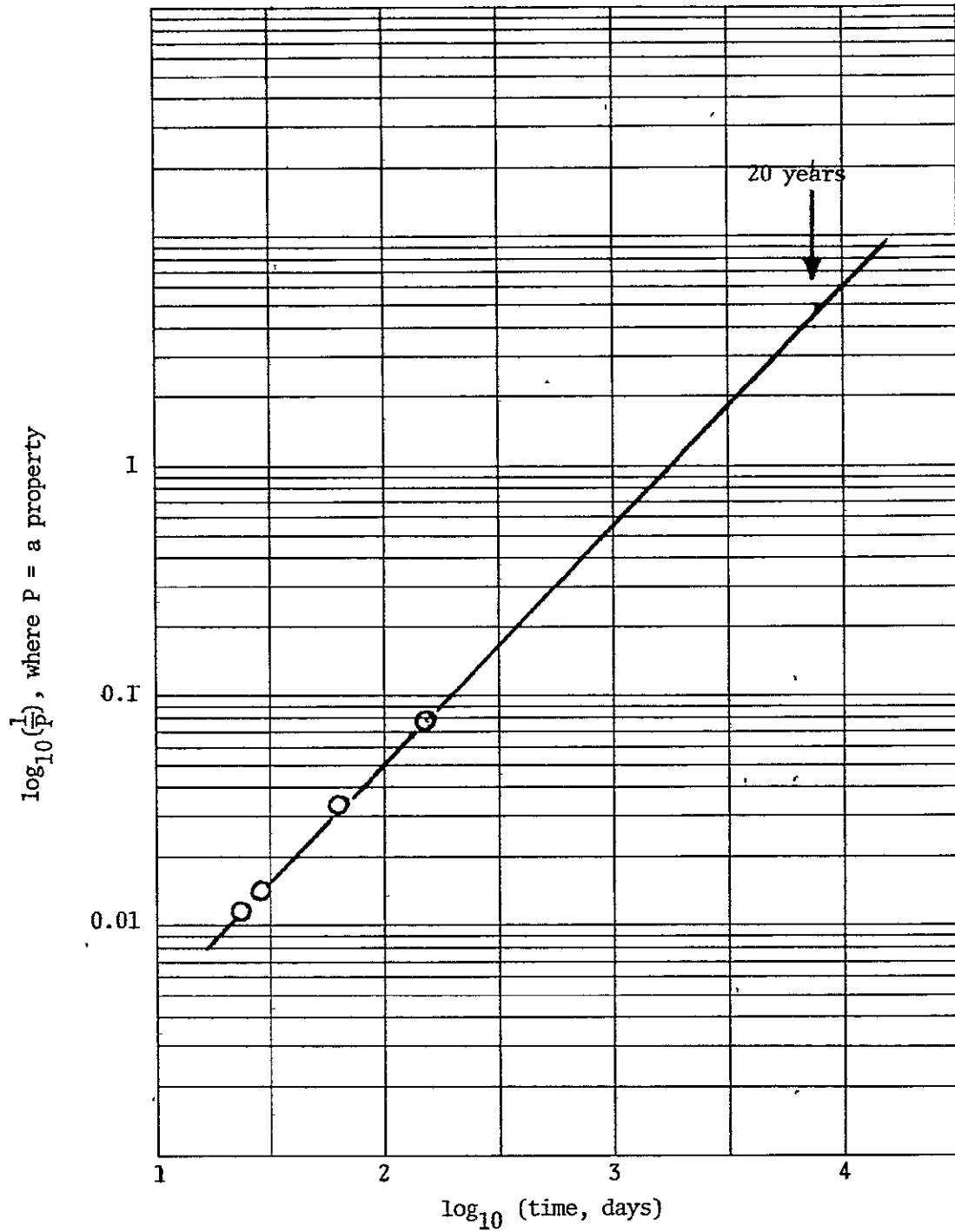
Figure 23. Hypothetical Data Points Extrapolated
by Weibull Model

Hyperaccelerated sunshine exposure should be applied to transparent plastic films which contain UV absorber to protect underlying material. These are of current interest for low-cost array designs. Our tests show that sunlight can be concentrated 1400X to accelerate degradation of such films.

(2) To avoid the solar simulation problem with lamps, natural sunshine should be used for hyperaccelerated tests. Indications are that the outdoor exposure testing services, which usually test plastics, coatings, and textiles, have recognized the potential importance of hyperaccelerated sunlight exposure and plan to introduce it as a commercial test method. Current work at JPL involves accelerations of up to 100 with mercury lamps which requires that activation spectra of degrading materials be known

(3) Accelerated and hyperaccelerated tests should be done at increasing stress levels to detect the threshold of over-stressing. Degradation rates at temperatures above Tg are probably not suitable for extrapolation because the mechanism is likely to change for many plastics   Below the stress threshold, data can be extapolated down to operating stresses by the Arrhenius equation or by some other mathematical model which gives a linear plot.

(4) Multicondition exposure should be conducted. The advantages of this technique, which is essentially a set of controlled experiments to show <u>why</u> degradation occurs, have been discussed above. The relative importance of weather factors is made clear.

(5) Precise data are required for predictions. As new analytical methods continue to be developed, they should be applied to module testing. For example, the SEM-SIMS (scanning electron microscopy - secondary ion mass spectrometry) technique can give chemical structure information for organic material at surfaces (Reference 27). Chemiluminescence is another interesting new technique (Reference 28).

(6) The criterion of internal consistency was mentioned above as an important principle for selecting mathematical models. That is, the model which most consistently fits data sets obtained over a wide range of exposure test conditions should be selected. This principle should be applied to life predictions from accelerated/abbreviated tests. Diverse tests should be conducted. Then, if their predictive results are internally consistent, credibility in the overall prediction is greatly enhanced In other words, mutual corroboration of data from different sources is advantageous. For example, data obtained with a photochemical acceleration of 8X should extrapolate to the 20-year value obtained directly with an acceleration of 1000X.

(7) Extensive information on outdoor, "real-world" operating con-
ditions should be utilized in translating accelerated test data
to predictions. The need for routine outdoor UV spectrophoto-
metric data has been mentioned. Dynamic/erratic factors should
be estimated and superimposed on the results of our Test Program
Plan, which predicts inherent weatherability only. Thus, our
static temperature/humidity conditions produced an optimistic
prediction for lifetime of Ti/Ag solar cell contacts presumably
because cyclic conditions of outdoor exposure caused separation
of contacts from the silicon surface. Also, mechanical stresses,
e.g., those imposed by the mounting frame of commercial modules,
must be accounted for. It must be remembered that the micro-
environment, not the macroenvironment, controls degradation of
a material. To illustrate, the corrosion rate of contacts or
interconnects will depend not on the relative humidity at a
local weather station but on the moisture level at the metallic
surface. This level could be very high at night due to dew-
soaking. We recommend that a moisture sensor, such as the
Panametric Mini-Mod-A, be embedded in encapsulants to monitor
water level continuously.

(8) The micromodule must be a vehicle for exposing encapsulants in
as realistic an array environment as possible. Our UTS's were
designed with this end in mind.

(9) Test results with micromodules should be correlated with data
obtained on commercial modules. Scale-up problems even with
relatively simple chemical manufacturing processes are well
known. By analogy, one must ascertain that the same failure

72

modes occur in both micro- and macromodules. Furthermore, the environment must be the same in regard to angle of presentation to the weather, internal geometry, thickness of layers, and mechanical stress fields.

(10) Metallization is subject to corrosion and may be the "weak link" in modules. We recommend that our prediction methodology be applied to solar cell contacts and interconnects Again, these components should be exposed in an array system environment for which our UTS design would be appropriate. Resistive elements, rather than FET's, could serve as corrosion monitors.

VIII. NEW TECHNOLOGY

Three innovations have been reported to the Government (NASA, Technology Utilization Officer). The Government has the right to decide to file patent applications on these. The innovations are·

(1) Accelerated Weathering Test Procedure (Multicondition Accelerated Exposure; see section III.B.2, above), reported August 4, 1976, Letter Submittal No. 76AG12669.

(2) Test Specimen for Solar Cell Encapsulants (Universal Test Specimen; see section II, above), reported August 4, 1976, Letter Submittal No. 76AG12669.

(3) Method for Highly-Accelerated Outdoor Exposure Testing of Plastics and Other Materials (Hyperaccelerated Exposure with Highly-Concentrated Sunlight, see section III.B.1., above), reported February 2, 1978, Letter Submittal No. 78ESG10219.

REFERENCES

1. Trubiroha, P., "Irradiance, Temperature, and Humidity in Artificial Weathering Devices," ISWPR, pgs. B2.1 - B2.11.

2. Kolyer, J. M., and Mann, N. R., Interim Report, JPL Contract 954458, ERDA-JPL-954458-77/2, Distribution Category UC-63, October 24, 1977.

3. Butters, G. and Marks, G. C., "Techniques for Predicting the Weathering Performance of Rigid PVC," ISWPR, pgs. D6.1 - D6.9.

4. Davis, A and Head, B. C., "Future Prospects for Accelerated Weathering of Polymeric Materials," ISWPR, pgs. C1.1 - C1.7.

5. Best, G. E., Bretts, G. R., McLean, H. T., and Lampert, H. M., "The Determination and Analysis of Aging Mechanisms in Accelerated Testing of Selected Semiconductors, Capacitors, and Resistors," Physics of Failure in Electronics, Vol. 3, RADC Reliability Series (Rome Air Development Center, Air Force Research and Technology Division), edited by M. F. Goldberg and J. Vaccaro, pgs. 61-79, April 1965.

6. Walsh, T., "A Technique for Controllable Acceleration and Prediction of Degradation Mechanisms of Electronic Parts," Physics of Failure in Electronics, Vol. 4, RADC Reliability Series (Rome Air Development Center, Air Force Research and Technology Division), edited by M. F. Goldberg and J. Vaccaro, pgs. 59-73, April 1965.

7. Anonymous, "Energy and Power Systems" (describing the solar-powered generator, also available as a testing device, produced by Omnium-G, Anaheim, CA), Industrial Research, pg. 67, October 1977.

8. Kinmonth, R. A., "A Correlation Review - Published Results from 1962 - 1977, Part II," Atlas Sun Spots (published by Atlas Electric Devices Co.), Vol. 6, Issue 16, autumn 1977.

9. Launer, H. F., "Effect of Light upon Wool. Part IV   Bleaching and Yellowing by Sunlight," Textile Research Journal, pgs. 395-400, May 1965.

10. Kolyer, J. M., "Stability of Materials Under Worldwide Climatic Conditions," Conference on Aerospace Transparent Materials and Enclosures, Atlanta, GA, November 18-21, 1975, Technical Report AFML-TR-76-54, pgs. 405-432.

11. Bevington, J. R., et al, "Reliability Evaluation of Plastic Integrated Circuits." Report No. RADC-TR-71-8, January 1971.

12. Anonymous, "No Room for Failure. A Reliability Assurance Program for Motorola Plastic Linear Integrated Circuits," published by Motorola Semiconductor Products, Inc., Phoenix, AZ, October 1975.

13. Ferris-Prabhu, A. V., "Forecasts from Limited Data," Machine Design, pgs. 123-129, January 20, 1977.

14. Private communication, Rohm and Haas Co., March 7, 1978.

15. Davis, A. and Golden, J. H., J. Macromol. Sci.. Rev. Macromol. Chem. C3, pg. 49 ff, 1969.

16. Kambour, R. P., "Mechanistic Aspects of Crazing and Cracking of Polymers in Aggressive Environments," General Electric Co. Technical Information Series Class 1, Report No. 77CRD169, August 1977.

17. Marechal, J-Ch., and Eurin, Ph., "The Prediction of PVC Weathering," ISWPR, pgs. D7.1 - D7.10.

18. Dr. J. Wilson, du Pont Co , Wilmington, DE, private communication, April 3, 1978.

19. Kamal, M. R., "Effect of Variables in Artificial Weathering on the Degradation of Selected Plastics," Polymer Engineering and Science, pgs. 333-340, October 1966.

20 Clark, J. E. and Slater, J. A., "Outdoor Performance of Plastics III, Statistical Model for Predicting Weatherability," National Bureau of Standards Report 10 116, October 30, 1969.

21. Daniel, C. and Wood, F. S., Fitting Equations to Data, Wiley - Interscience, 1971, pg. 22.

22. Koller, L. R., Ultraviolet Radiation, 2nd Edition, Wiley, 1965.

23. Zerlant, G. A , Proceedings, Institute of Envionmental Sciences, 21st Meeting, April 13-16, 1975, pg. 13.

24. Thomas, R. E. and Carmichael, D. C., Final Report on Terrestrial Service Environments for Selected Geographic Locations, to Jet Propulsion Laboratory for the LSSA Project, ERDA/JPL-954328-76/5, Distribution Category UC-63, June 24, 1976, pg. 84.

25. Kolyer, J. M., "Prediction of Weather-Resistance of Transparent Plastics by Multicondition Accelerated Exposure," Conference on Aerospace Transparent Materials and Enclosures, Long Beach, CA, April 24-28, 1978, Technical Report to be issued.

26. Anonymous, Bulletin TD-31, Glazing and Solar Energy, 4-Mil Tedlar Property and Usage Information, published by du Pont Company, Plastic Products and Resins Department, Wilmington, DE, received April 1978.

27. Leys, J. and Ruscica, R , "New Dimension in Problem Solving," Industrial Research/Development, March 1978, pgs. 114-119.

28. Nathan, R. A., "Chemiluminescence for the Determination of the Kinetics and Mechanism of Jet Fuel Oxidative Degradation," Final Report, Contract N00019-73-C-0360 for Naval Air Systems Command, Department of the Navy, March 1974.

APPENDIX A

APPENDIX A

MATERIALS, METHODS, AND DATA

I. PREPARATION OF UTS'S

A. Preparation of Sylgard-Encapsulated UTS's

Full details are given in the Interim Report (Reference Al).

B. Selection of Other Encapsulant Systems

Array components were selected after trials to verify the practicability of fabricating a total of 150 UTS's. The chosen materials are listed in Table Al, and their dimensions and properties are detailed in Table A2.

During exposure tests, we did not want failure to occur from thermal cycling alone, i.e., without the effect of other weather factors. Therefore, thermal cycling from -40 to +100°C was performed on candidate encapsulants using solar cells mounted on ceramic substrates. It was found that rigid epoxies as encapsulants cracked themselves or cracked the solar cell. Such materials could not be used for our experiments.

Polyurethane pottants were not affected by thermal cycling, nor were thin coatings of sprayed-on acrylic polymer or nitrocellulose lacquer. Parylene C coating was also successful.

Table A3 lists the nine array systems selected for test. One system (No. 1) has no protective encapsulant and served as a control. Three other systems (Nos. 3, 6 and 9) use the same pottant/cover but on different substrates in order to demonstrate how substrates influence degradation. The bond of Humiseal 2B74 to the glass cover was purposely mediocre to encourage delamination. The general object of the selections was to give a considerable variety of degradable systems, thus assuring ample degradation data.

79

To allow comparisons, one component sometimes was varied with the others held constant. For example, in Table A3, three systems (Nos. 3, 6 and 9) use the same pottant/cover but different substrates, and Nos. 8 and 9 use the polyurethane pottant with or without a glass cover.

C. Procedures for UTS Preparation

Circuits were applied to ceramic (alumina) by thick-film techniques, whereas photoetch of clad laminates was used to prepare the epoxy substrates. Application of copper circuitry to enameled steel required some process development. Of several approaches tried, the best proved to be thick-film copper (Cermalloy 7029) screened on and fired in an oven.

Referring to Table A3, the encapsulants were applied as follows. Parylene C was polymerized from the vapor phase of the monomer at room temperature by the standard technique (Reference A2). The polyurethane was vacuum-degassed on one minute, poured in place, allowed to cure at room temperature for 20 hours, and postcured at $77^{O}C$ for 2 hours. The degassing was important to avoid bubbles. The acrylic lacquer was sprayed, after diluting 1·1 with thinner, in 10 coats, with drying at $66^{O}C$. Note that the Tg of this lacquer was $63^{O}C$ by DSC, at which temperature stress relief occurred. The nitrocellulose lacquer was sprayed in 10 coats at package consistency, with drying at room temperature. Sylgard 184 was vacuum-degassed for 5 minutes, poured in place using a sheet of Lexan temporarily taped over the UTS as a mold, allowed to cure at room temperature for 20 hours, and then postcured at $100^{O}C$ for 2 hours.

II. EXPOSURE PROCEDURES

A. Outdoor Exposure

For the UTS's with nine different array systems, exposure began at
Miami (45°S) on October 31, 1977 and at Phoenix (45°S, EMMA, EMMAQUA) on
October 23, 1977. Exposure periods were 30, 60, 90 and 180 days. Returned
UTS's were electrically tested and examined for changes in appearance.

Exposure procedures for the Sylgard-encapsulated UTS's were similar
and are described fully in Reference A1.

B Accelerated Exposure

Reference A1 gives the detailed procedure. Exposure continued for
61 days. The eight exposure conditions are given in Table A4. The prop-
erty monitored was current (in milliamperes) produced by the solar cells
at 0.350 volts, which is close to the power point and gives a good relative
estimation of power as shown in Table A5 for Sylgard-encapsulated UTS's.
In this way we obtained several data points vs. time of exposure. Tape
cables from the UTS's were plugged into a rotary switch allowing con-
venient measurement of all solar cells per UTS in operation. All data
were expressed in terms of a reference cell at a fixed distance from the
lamp. UTS's exposed under the two dark conditions of Table A4 were tested
using a 75 watt reflector flood lamp as shown in Figure A1. A standard
cell was measured before and after each UTS tested, and results were
expressed as percent of standard cell performance. All UTS's after steam
exposure were also tested this way.

Steam exposure was continued for a total of 31 days. The UTS's were
suspended above boiling deionized water at atmospheric pressure. Steam
exposure was conducted because the cells used in this test, unlike the

81 '

cells attached to the silicone rubber encapsulated UTS's had a uniform coating of solder on the Ti-Ag grid lines (contacts). This coating excluded moisture. It is moisture penetration that causes hydrogen evolution by the Ti-Ag couple, separation at the Ti-Si interface, and decreased power (References A1 and A3)

III. EFFECT OF EXPOSURE ON UTS'S

See Reference A1 for the earlier data obtained on Sylgard-encapsulated UTS's.

A. Multicondition Accelerated Exposure

   1. Accelerated Exposure for 61 Days

      a. Changes in Appearance

      Changes in appearance of encapsulant and circuitry are detailed in Tables A6 and A7 and summarized in Table A8. Figures A2-A4 show visible changes of particular interest.

      b. Changes in Electrical Properties

      Complete data on relative solar cell power during the 61-day exposure are shown graphically in Figures A5-A13.

      Note that the _in situ_ solar cell power data are approximate. The Figures illustrate scatter in values during "plateaus" of performance vs. time.

   2. Steam Exposure for 12 Days, Following Accelerated Exposure

      a. Changes in Appearance

      Changes in appearance of encapsulant and circuitry are detailed in Tables A9 and A10 and summarized in Table A11. Figure A14 shows visible changes of particular interest.

      b. Changes in Electrical Properties

      Complete data on relative solar cell power during steam exposure, including the 12-day point, are shown graphically in Figures A15-A23.

82

The effect of length of circuitry path leading to the solar cells is shown in Table A12. There was a high correlation between longer path and reduced power for the ceramic substrate, because a longer path provided more opportunity for corrosion to increase resistance of the thinly Cu-plated Mo/Mn line.

The originally high resistance of the Cu-plated Mo/Mn lines is presumably due to the thinness of the Cu. Consequently, on probing the cells attached to short lines, the power output was less than 111 percent of original. However, probing cells attached to longer lines showed up to 146 percent of original power. "Probing" consisted of making direct contact to the bus bar and back metallization of the cell.

FET data are given in Table A13.

3. Steam Exposure for 31 Days, Following Accelerated Exposure

   a. Changes in Appearance

   Changes in appearance of encapsulant and circuitry are detailed in Tables A14 and A15 and summarized in Table A16. Figure A24 shows visible changes of particular interest.

   b. Changes in Electrical Properties

   Complete data on relative solar cell power during steam exposure are shown graphically in Figures A15-A23.

   The effect of length of circuitry path leading to the solar cells on the power of the cells is shown in Table A17. As at 12 days, the longer path on the ceramic substrate allowed more opportunity for corrosion to impede the flow of current from solar cells.

   FET data are given in Table A18.

B. Hyperacceleration by Highly-Concentrated Natural Sunlight

These tests were conducted at the White Sands Missile Range in
February 1978. The plastic films under test were immersed in rapidly
flowing water (5 liters/minute) in a quartz vessel (7.8 x 5.2 x 25 cm. ID,
2 mm. wall thickness). The light passed through 5.2 cm. water, which
absorbs essentially all energy of wavelength above 1.3 microns (about 17
percent of the solar constant). Calorimetric readings were made on light
actually passing through the sample, which was placed against the back
inner surface of the vessel. The water entered the vessel at about $14^{o}C$
and exited at about $35^{o}C$. The water-immersion method is valid because
air and water have little effect on the photochemical yellowing reactions
(Reference A1).

Absorbance data are given in Table A19. The best of these data,
obtained at 1400 suns (33 cal./cm.^{2}/sec.), are plotted in Figure A25.
Points from accelerated testing are included for comparison. Within
experimental error, there appears to be no real difference in the slopes
of lines through the experimental data, and the order of magnitude of
acceleration is as expected The 4 hour exposure of Lexan gave about the
same degree of yellowing as attained in 280 days of natural exposure
(tilted 45°, facing south) near Phoenix starting in September. Similarly,
the 4 hour exposure of polystyrene equaled 150 days of exposure in Miami
starting in October

Tensile test results on the films exposed to 33 cal./cm.^{2}/sec. are
shown in Tables A20 and A21.

After 4 hours in the solar furnace at 1400 suns, the breaking stress
of polystyrene was 84% of original and A (increase in absorbance at 360 nm)

84

was 0.26. The same results were obtained in outdoor exposure in Miami

for 150 days. Therefore, hyperacceleration produces the same degradation

of optical and mechanical properties as natural sunlight. Furthermore,

after 120 hours under the xenon lamp, the tensile strength of polystyrene

was 76% of original and A was 0.20. This correlation is close, and xenon

exposure is considered to simulate sunlight in this case. These equivalen-

cies are summarized below.

4 hrs. at 1400 suns = 120 hrs. under xenon lamp = 150 days in Miami.

On the other hand, Lexan yellows much faster than it loses strength

under xenon lamp exposure as seen below·

Light Source	Exposure Time	Conditions	A*	Fraction of Original Tensile Strength
Xenon Lamp	768 hours	35 C, 100% R.H.	1.1	0.52
Phoenix, 45°S	300 days	Ambient	0.48	0.27
EMMA	150 days	8 x sunlight	0.45	0.27
EMMAQUA	150 days	8 x sunlight + water spray	0.64	0.31
Solar Furnace	4 hours	1400 suns	0.46	0.26

$*\log_{10}(\frac{1}{P})$, where P = fraction of original transmittance at 360 nm.

The solar furnace gave the "natural" ratio between tensile strength

and A rather than the unnatural ratio given by xenon lamp exposure. Note

that higher numbers for A represent greater degradation (yellowing), while

lower fraction of original tensile strength represent greater degradation

of this property. Therefore, for the xenon lamp, A = 1.1 and tensile

fraction = 0.52 are in "unnatural" ratio.

C. Outdoor Exposure (45°S, EMMA, EMMAQUA)

   1. Changes in Appearance

   The Sylgard-encapsulated UTS's appeared similar after 420 or 540

days of exposure. The exposed Sylgard 184 encapsulant was slightly

dusty on the surface in all cases. The EMMAQUA caused dulling of the

surface. On the other hand, the Sylgard was quite clear internally.

The Tedlar cover remained glossy, colorless, and flexible in all cases.

The Lexan became yellow on exposure but maintained its integrity after

the 45°S exposures. Unsupported Lexan samples were brittle and

retained only about 25% of original tensile strength after 300 days

in Phoenix or Miami. Such a low tensile strength indicates complete

loss of integrity. Lexan cemented to the Sylgard 184 on UTS's was

intact after 540 days This is an example of favorable interaction

of encapsulant components. After EMMA exposure, the Lexan was deep

yellow, rough-surfaced, and showed one or two large cracks. During

EMMAQUA exposure, the Lexan cover was almost completely lost by 420

days. However, there was no visible effect of exposure on the ceramic

substrate or gold-plated circuitry. Assuming an acceleration factor

of 5, 540 days of EMMA(QUA) exposure represents about 8 years of nor-

mal exposure.

   For the other UTS's, observations on the appearance of encapsulant

and circuitry after exposure for 30, 60 and 90 days are given in

Tables A22 through A27.

86

2. Changes in Electrical Properties

The changes in electrical properties for Sylgard-encapsulated UTS's through 300 days exposure were reported in Reference A1. Data after 420 and 540 days exposure are given in Tables A28 and A29. The greatest power loss occurred in Miami, which has a moist climate. Degradation is attributed to moisture-induced lifting of contacts from the silicon surface (Reference A3).

For the other UTS's, FET data after exposure for 30, 60 and 90 days are given in Tables A30 through A32 and solar cell power data are given in Tables A33 through A41. Note that the method of measuring current at 0 350 volts gave about the same results, in terms of percent power retained, as the power point data.

IV. EFFECT OF EXPOSURE ON PLASTIC FILMS

A. Lexan (Grade 8740)

1 Relation of Absorbance Change and UV Light Deposited

Tables A42-A44 give complete outdoor exposure absorbance data for Lexan. Lexan yellowed more rapidly, as judged by absorbance at 360 nm, when outdoor UV was more intense (see Figure A26). Seasonal UV data are from Reference A4.

Figure A27 shows that when cumulative UV deposited is used, it gives a better plot than calendar time. At 150 days, the calendar-time plot gave an unexpectedly high absorbance corresponding to increased UV intensity in early spring.

The superiority of using "cumulative UV deposited" over "calendar time" is emphasized in Reference A5· "It is believed that if all

87

weathering tests, laboratory or outdoor, were timed as a matter of UV deposited on the test surface rather than by the clock, calendar, or toal solar radiation, ... a big step would be taken toward the goal of achieving repeatable or reproducible results which also provide good correlation."

It is important to remember that data for the exact wavelength range responsible for degradation are needed for good correlation. These data are unavailable at present, though both Desert Sunshine (Phoenix) and South Florida Test Service (Miami) are preparing to routinely record intensity readings at several points on the UV spectrum.

Data from Reference A4 could be used to estimate cumulative UV received by samples vs. time, but better results were obtained using early seasonal degradation rate data to estimate "exposure factors." Then absorbance data could be plotted into one approximate line regardless of the time of year when exposure-was started (Figures A28 and A29). The method was as follows.

First, an exponential model was assumed. It roughly fits facts, simplifies calculations, and corresponds to a simple photochemical reaction. The accumulated chromophore (colored species) is directly proportional to absorbance. It is also directly proportional to the total UV energy received in the appropriate wavelength region.

Next, early seasonal absorbance data were used to estimate "monthly rate factors" (Table A45). These factors were plotted vs. month of the year, and a smooth curve was drawn through the points for each of the two sites. These data imply that Phoenix has more UV variation than Miami at about 300 nm, the wavelength region causing yellowing of Lexan.

Finally, the "exposure factor" for a given sample was calculated by averaging the "monthly rate factors" for the months of exposure and multiplying by the number of days of exposure. For example, the sample exposed in Phoenix for 300 days starting on 12/22 was outdoors during January ("Monthly rate factor" = 1.0), February (2.0), March (2.7), and so on through October (1.8). The average of the "monthly rate factors" is (1.0 + 2.0 + 2.7 + ... 1.8)/10 = 2.7, and 2.7 x 300 = 810. $\log_{10}(810) = 2.91$, at which time $\log_{10}(\frac{1}{P}) = 0.6958$, and this point will be found plotted in Figure A28.

Convergence of data points (Figures A28 and A29) by this method is far closer than had been attained using "exposure factors" assumed from UV data in the literature. An exponential model (Weibull plot with slope = 1) had been assumed in handling the seasonal effects. However, the later data points fall into a line with slope of about 2, i.e., $P = e^{-\lambda (UV)^2}$. The significance is that chromophore concentration is proportional to the square of UV light deposited on the sample.

2. Correlation of Absorbance Increase (Yellowing) and Tensile Strength Loss

This subject is discussed under "Prediction Methodology" above. Additional data plots are presented in Figures A30 and A31. Although yellowing and tensile strength loss proceed by different mechanisms (rearrangement of atoms in the molecular chain for the former, scission of the chain for the latter), results continue to correlate as samples degrade However, the relationship is different for natural exposure (Figure A30) than for EMMA/EMMAQUA exposure (Figure A31) at higher levels of degradation. Below about 0.2 breaking stress, EMMA/EMMAQUA

exposure accelerated yellowing relatively more than it accelerated tensile strength loss. Therefore, absorbance measurements afford an indirect estimate of loss of strength for a series of weathered samples, providing that all samples were exposed in the same manner.

3. Gloss Retention, Tg, Tensile Strength

Loss of gloss, which was associated with both UV and moisture, was discussed in Reference A1 and also in the "Prediction Methodology" section of this report.

Decrease of Tg during exposure is discussed in Reference A1.

Tensile strength data received since the Interim Report (Reference A1) was written are presented in Table A46.

4. Changes in Molecular Weight and Molecular Weight Distribution

Results are given in Table A47.

The solar furnace exposure was estimated to have subjected the sample to as much UV at 330 nm., the wavelength believed to cause chain scission of Lexan, as 700 days of Phoenix 45°S exposure. Therefore, the number average molecular weights were roughly inversely proportional to the UV light energy deposited on the samples.

B. Polystyrene

1. Absorbance at 360 nm

Full data are given in Reference A1 and integrated in the "Prediction Methodology" section, above, and in Appendix B.

2. Tensile Strength Loss

The above comments also pertain to this property.

3. Carbonyl Formation

Data by ATR-IR are presented in Reference A1.

A series of polystyrene samples had been exposed under 1.00 noon sunlight UV intensity, 60°C, and 100 percent relative humidity in the accelerated test. These were examined by electron spectroscopy for chemical analysis (ESCA). Data are plotted in Figures A32 and A33. It is seen that too few data points were available to distinguish between a Weibull and lognormal model. As discussed in the "Prediction Methodology" section, above, more data would be required to choose between the two models. The evidence of progressive carbonyl formation agrees with attenuated total reflectance infrared spectroscopy (ATR-IR) results obtained earlier (see Reference A1).

C. Tedlar (Grade 100 BG 30 TR)

   1. Absorbance at 360 nm.

   After 540 days of outdoor exposure, including the EMMA and

EMMAQUA, Tedlar showed no visual color, and the absorbance at 360 nm.

showed little or no increase (Table A48).

   2. Tensile Properties

   Data for samples exposed through 300 days were reported in

Reference A1. Data for the samples exposed for 540 days are given in

Table A49.

   3. ATR-FTIR on Surface

   ATR-FTIR spectra were obtained with a Nicolet 7199 FTIR instrument

using a germanium crystal. There were significant changes in the

spectrum of Tedlar during weathering (Figures A34 - A36). Note the

change in relative intensities of the absorption bands at 830, 1030,

and 1090 cm.$^{-1}$. The absorption band at 1650 cm.$^{-1}$ is attributed to

a carbonyl group. FTIR transmission spectra also indicated negligible

carbonyl in the unweathered material and the same low level after 90

or 540 days of EMMAQUA exposure. Early leveling off of the carbonyl

content might result from oxidation of a low level of hydrocarbon

sequences in the polymer or of small amounts of additives, e.g.,

lubricant.

REFERENCES

A1. Kolyer, J. M., and Mann, N. R., Interim Report on JPL Contract No. 954458, ERDA-JPL-954458-77/2, Distribution Category UC-63, October 24, 1977.

A2. Anonymous, "Parylene Conformal Coatings," Union Carbide brochure F-43427A, 1974.

A3. Bishop, C. J., "Investigation into the Mechanism of Degradation of Silver-Titanium Contacts," Final Report, Contract NASW-1859, NASA Headquarters, July 1970.

A4. Koller, L. R., Ultraviolet Radiation, Second Edition, John Wiley and Sons, NY, 1965.

A5. Scott, J. L. (Desert Sunshine Exposure Tests, Inc.), "Seasonal Variations - Nemesis of Repeatable/Reproducible Accelerated Outdoor Durability Tests?" Paper presented at the Federation of Societies for Coatings Technology Symposium, Cleveland, Ohio, March 9-11, 1977.

A6. Wilson, Dr. J., du Pont Co., Wilmington, Del., private communication, April 3, 1978.

94
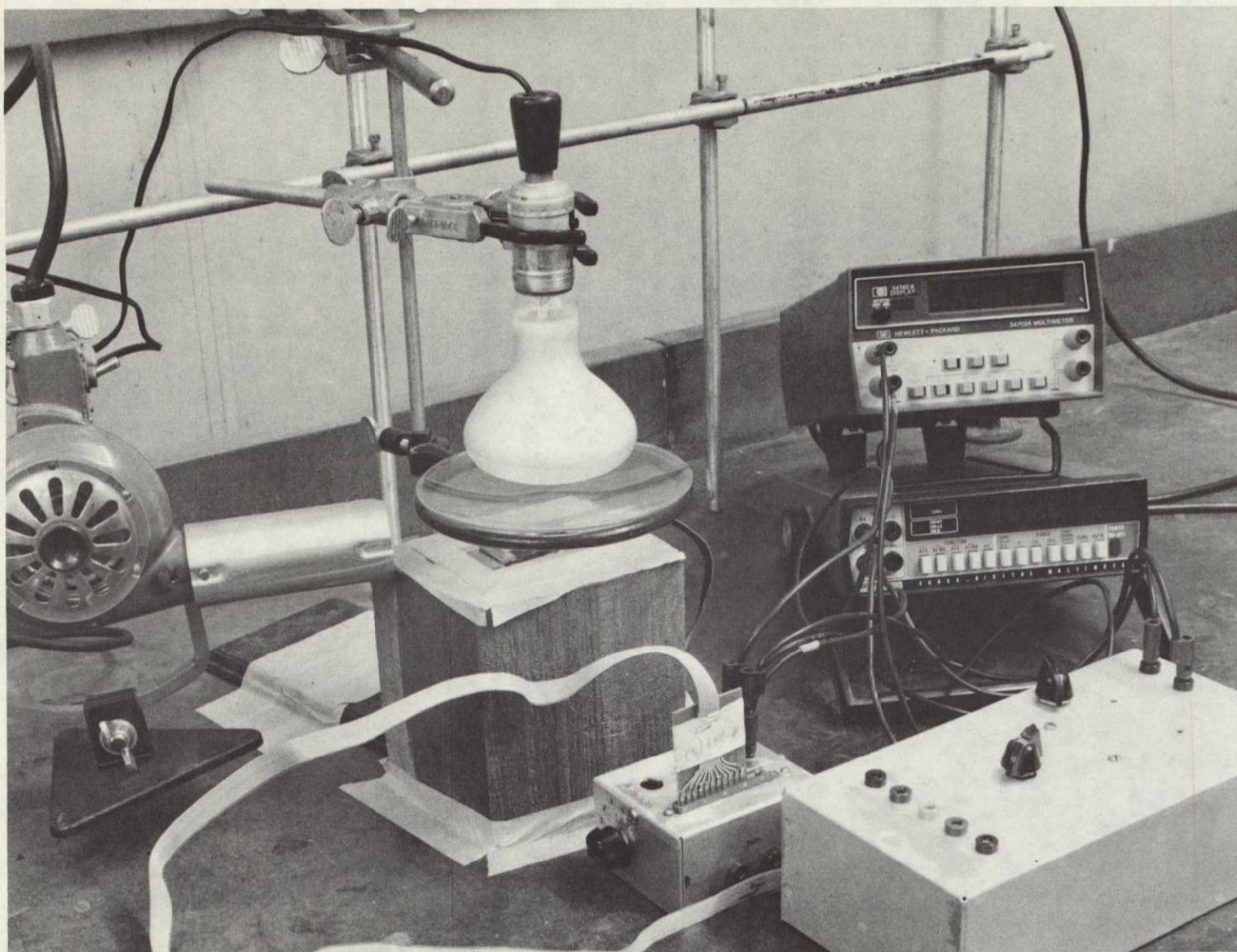
FIGURE A1. DETERMINATION OF POWER OF SOLAR CELLS ON A
UTS (UNDER LAMP) WITH TAPE CABLE. METERS
READ CURRENT AND VOLTAGE.
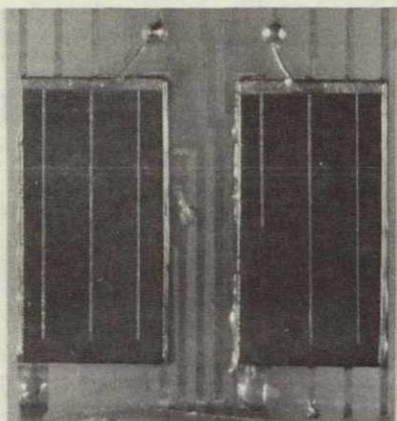
UNEXPOSED
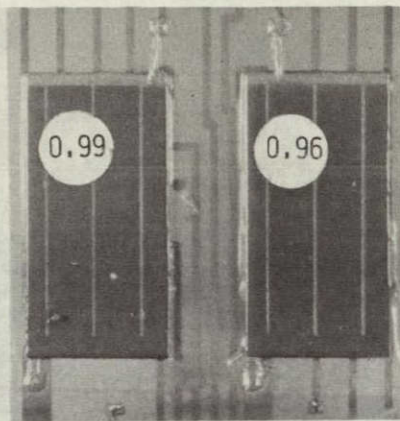
0.66 REL. UV,
28°C, 100% R.H.
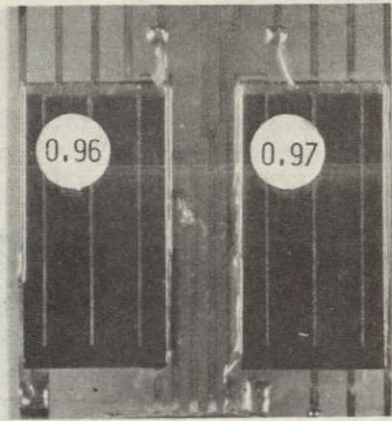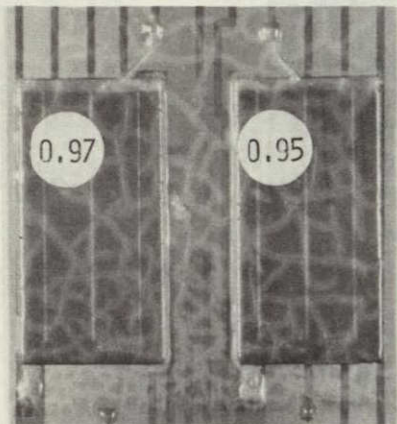
1.00 REL. UV,
43°C, 0% R.H.
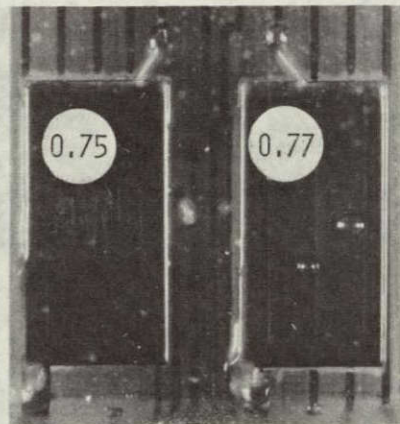
1.00 REL. UV,
43°C, 100% R.H.

1.00 REL. UV,
72°C, 0% R.H.
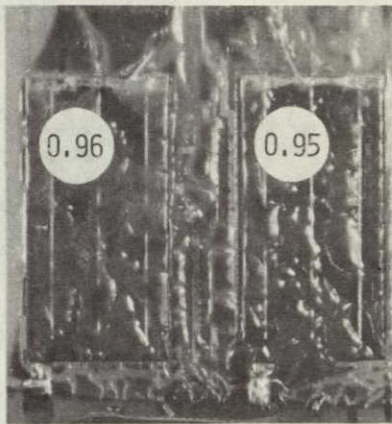
1.00 REL. UV,
72°C, 100% R.H.
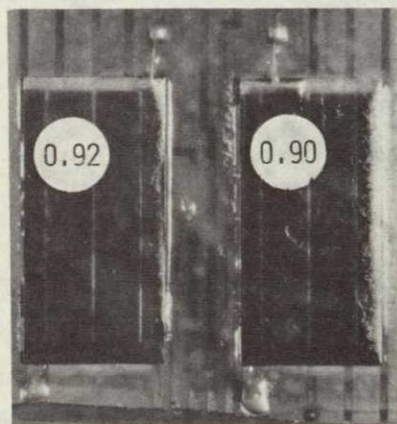
0.66 REL. UV,
64°C, 100% R.H.
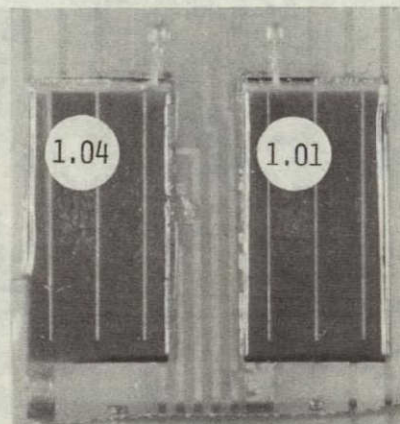
0 REL. UV,
72°C, 0% R.H.
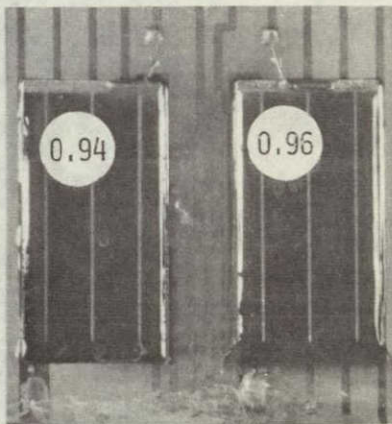
0 REL. UV,
72°C, 100% R.H.

FIGURE A2. ENCAPSULANT SYSTEM #7 (NITROCELLULOSE LACQUER ENCAPSULANT,
EPOXY SUBSTRATE) AFTER 61 DAYS ACCELERATED EXPOSURE
NOTE: FRACTION OF ORIGINAL POWER IS SHOWN FOR EACH CELL.

95
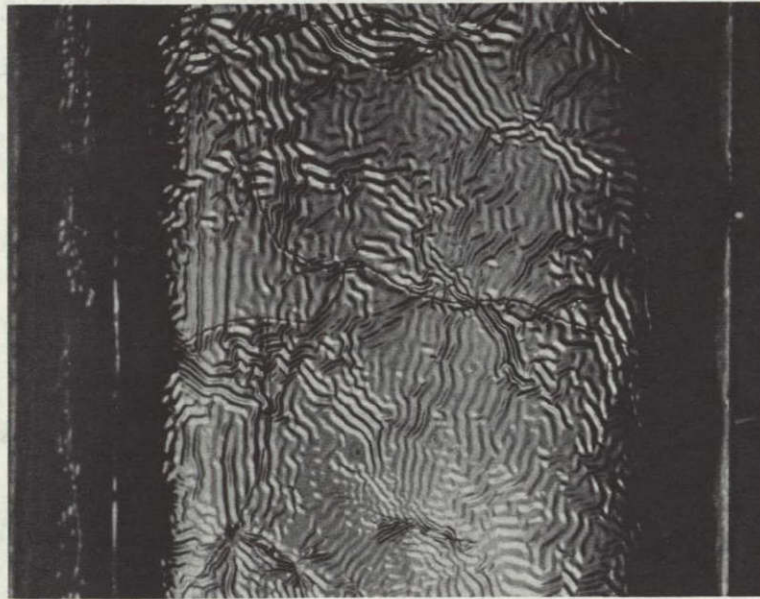
Figure A3. Encapsulant System #7 (Nitrocellulose Lacquer, Epoxy Substrate) After 61 Days Accelerated Exposure. Conditions: 0.66 UV, 64°C, 100% R.H., Magnified 10X
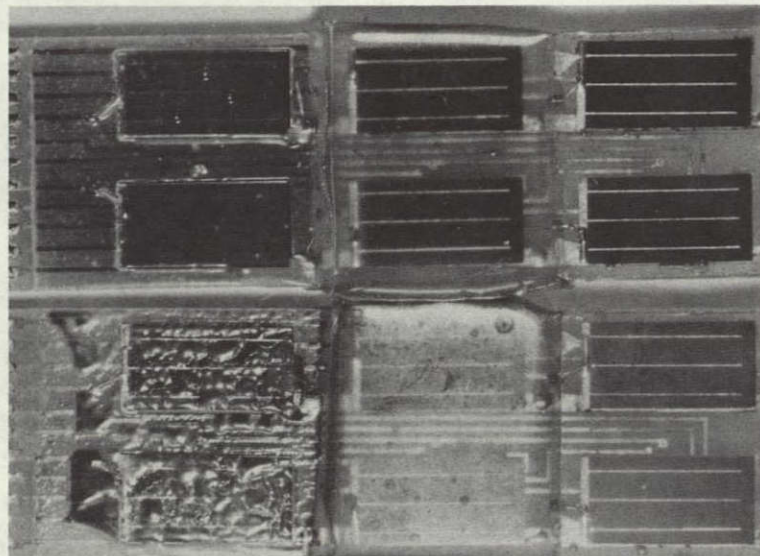
Figure A4. Encapsulant Systems #7-9 (Epoxy Substrate) After 61 Days Accelerated Exposure. Conditions: 1.00 Rel. UV, 72°C. Above: 0% R.H. Below: 100% R.H. Encapsulant Covers, left to right: nitrocellulose lacquer, 2B74, 2B74 + glass.

Figure A6. Change in Solar Cell Power
During Accelerated Exposure:
Array System 2*
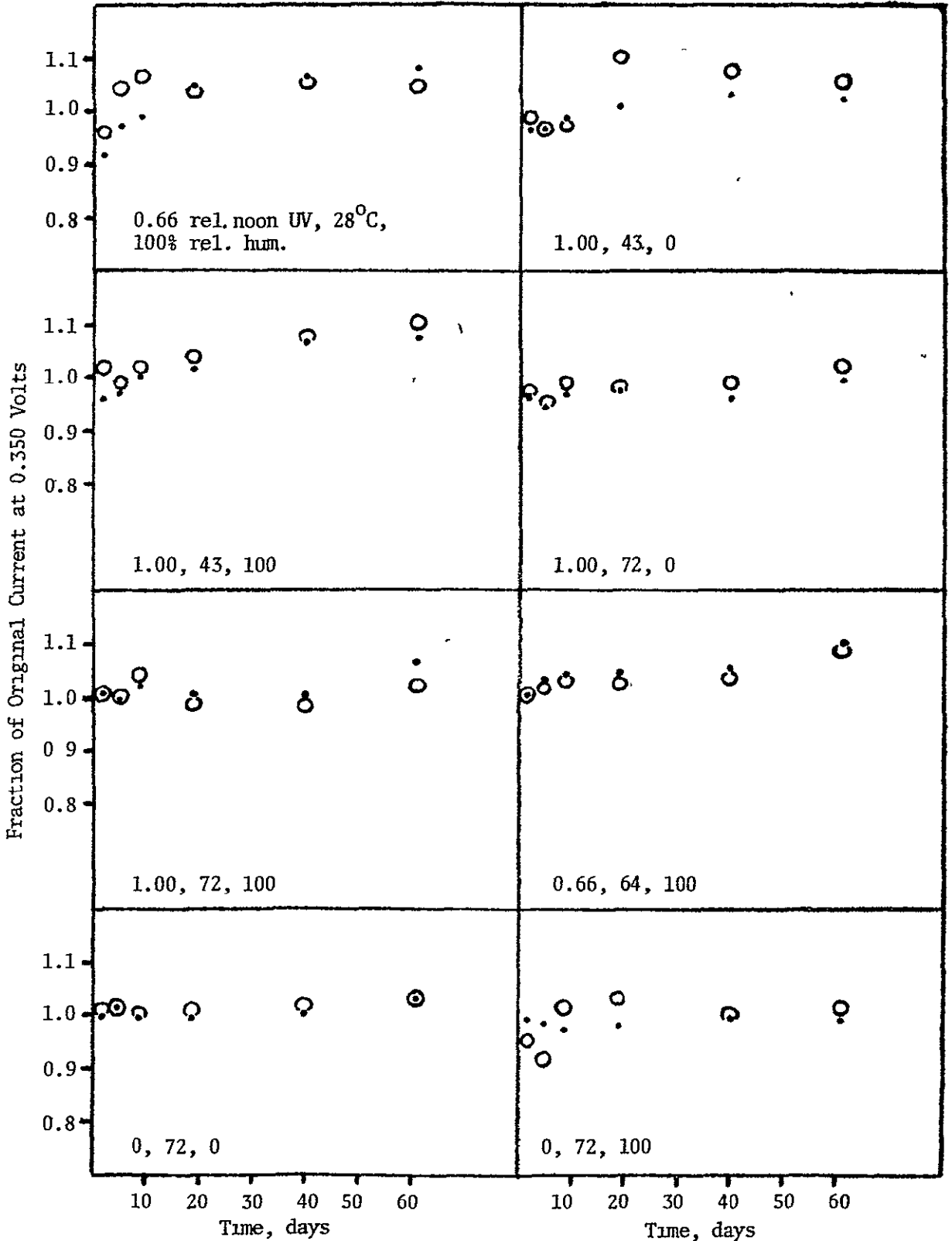
*Encapsulant: Parylene C, Substrate· ceramic, Circuitry: Mo/Mn + Cu

• = _Cell 2,   O = Cell 5

Figure A7. Change in Solar Cell Power
During Accelerated Exposure·
Array System 3*
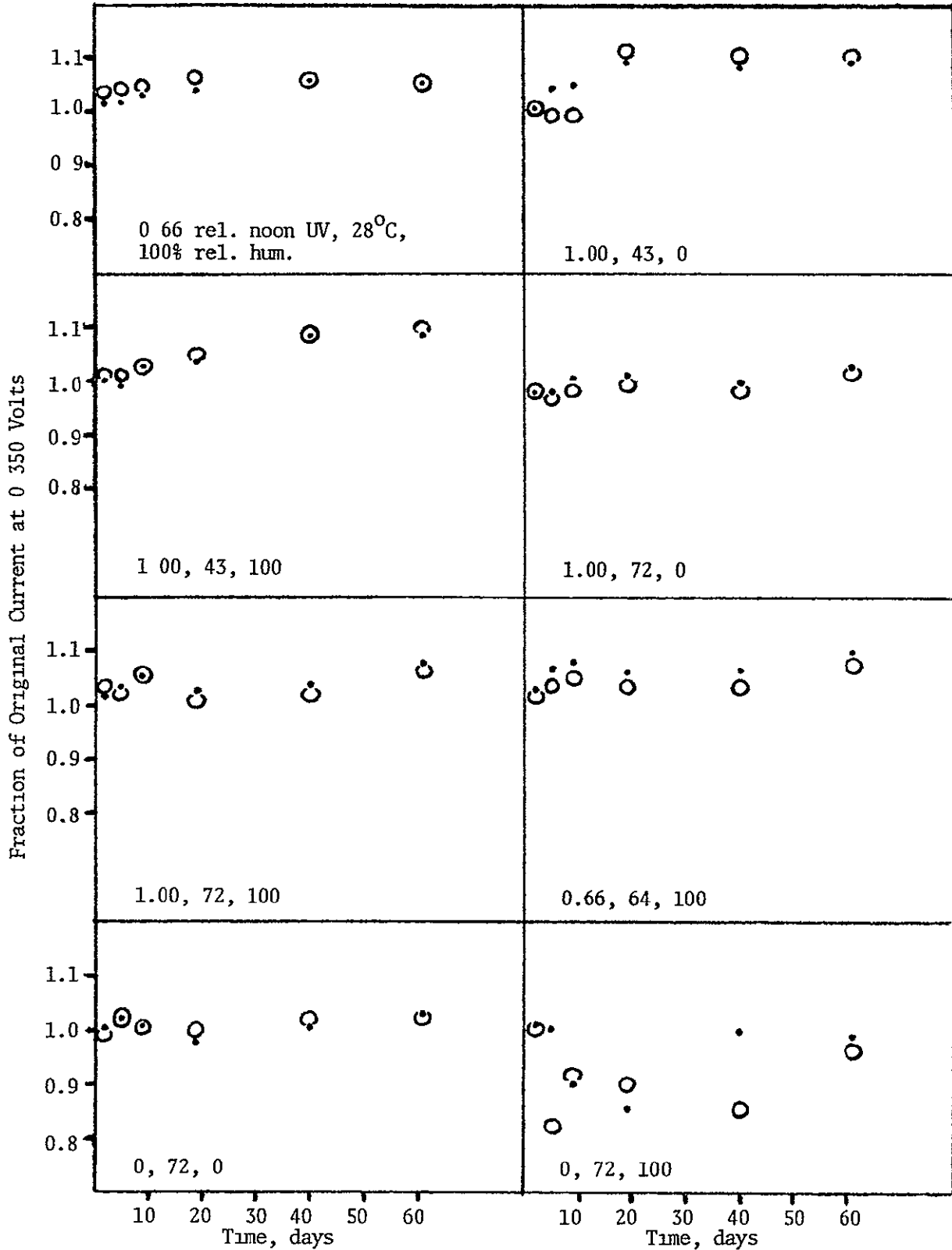
*Encapsulant 2B74 + glass, Substrate· ceramic, Circuitry Mo/Mn + Cu
• = Cell 1,   O = Cell 4

99

Figure A8. Change in Solar Cell Power
During Accelerated Exposure·
Array System 4*
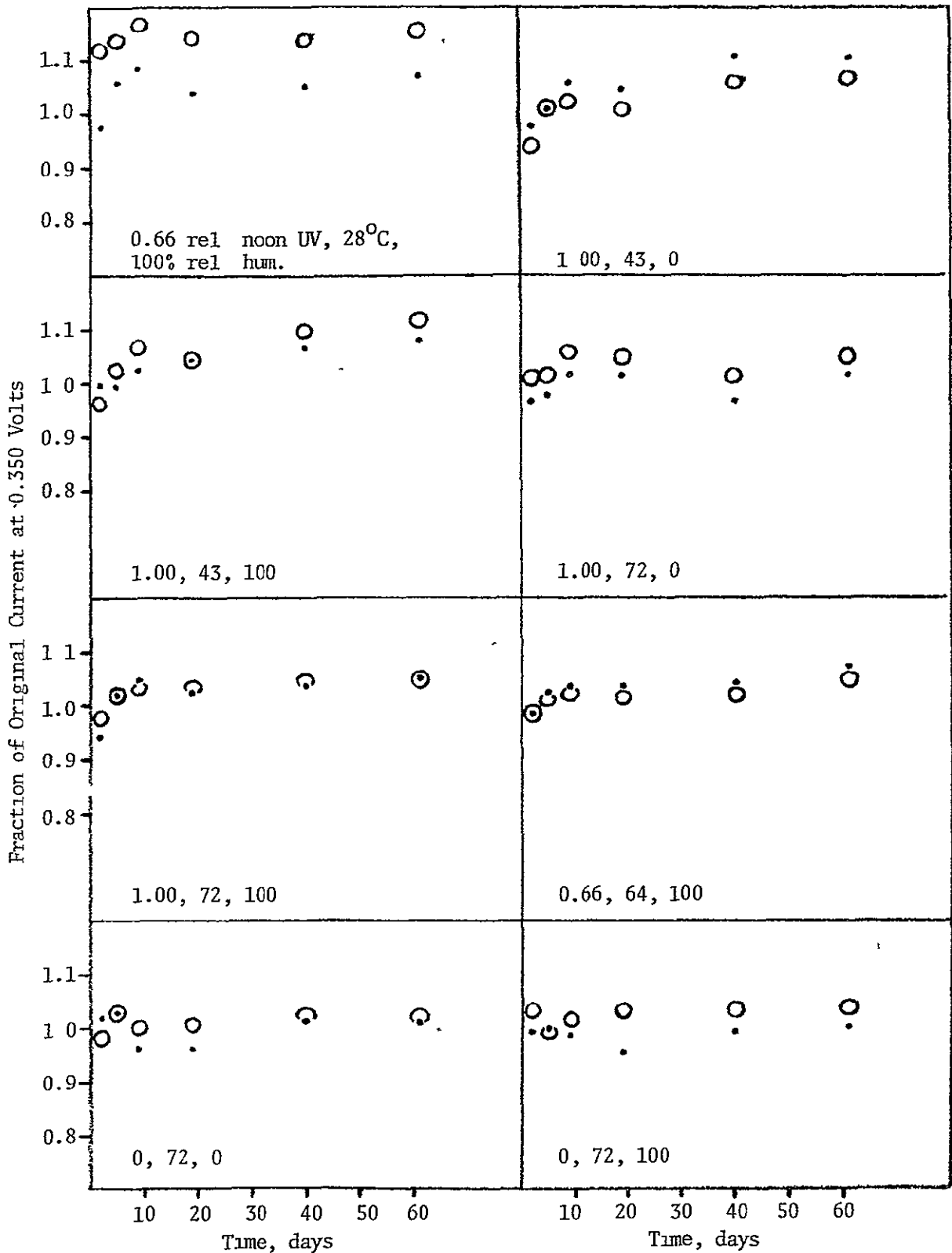
*Encapsulant. acrylic, Substrate. enameled steel, Circuitry Cu (fired)
● = Cell 3, ○ = Cell 6

130

Figure A9, Change in Solar Cell Power
During Accelerated Exposure
Array System 5*
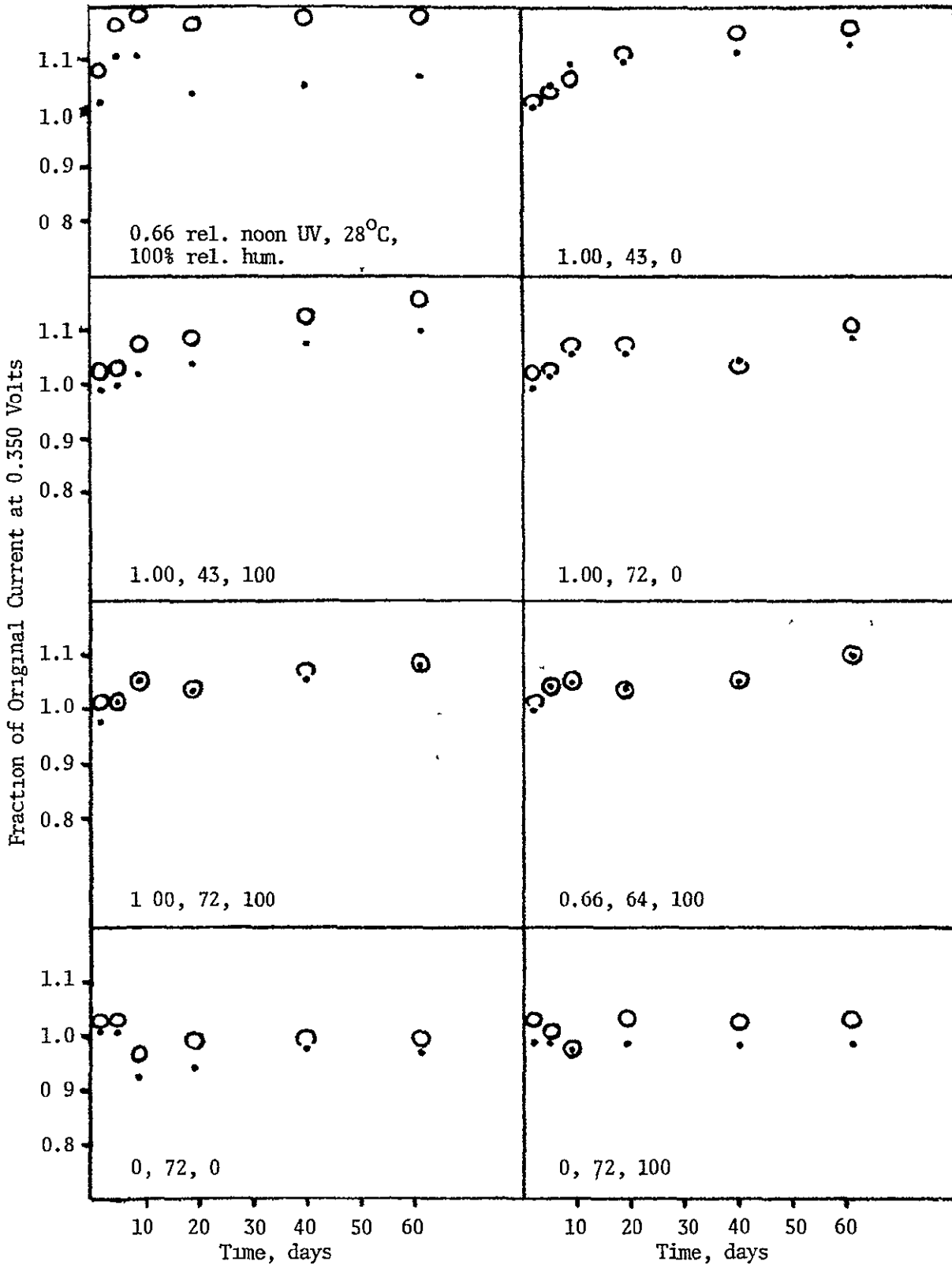
0.66 rel. noon UV, 28°C,
100% rel. hum.

1.00, 43, 0

1.00, 43, 100

1.00, 72, 0

1 00, 72, 100

0.66, 64, 100

0, 72, 0

0, 72, 100

Time, days

Time, days

Fraction of Original Current at 0.350 Volts

*Encapsulant   Sylgard 184,   Substrate   enameled steel,   Circuitry   Cu (fired)
• =   Cell 2,   O =   Cell 5

101

Figure A10   Change in Solar Cell Power
During Accelerated Exposure
Array System 6*
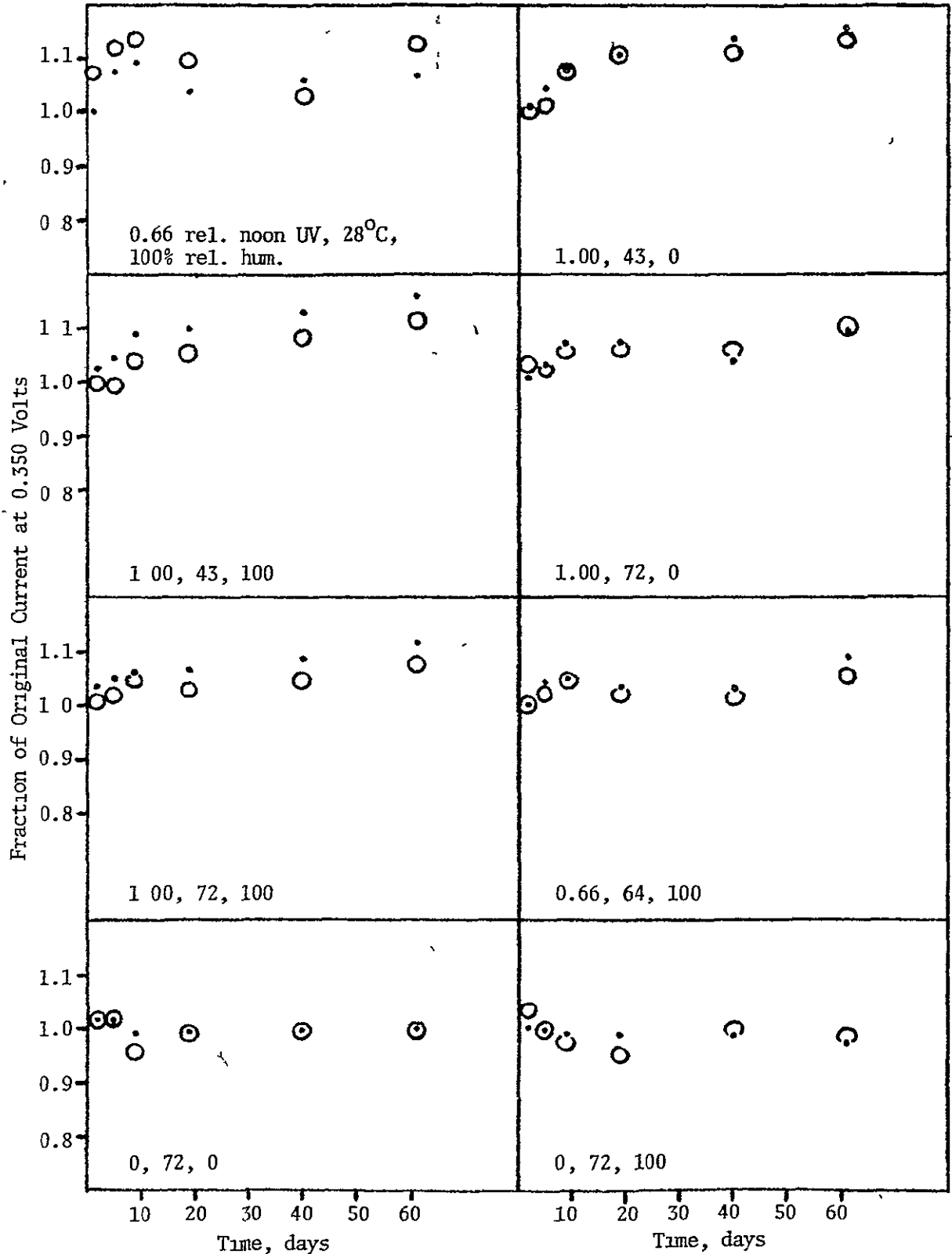
*Encapsulant   2B74 + glass,   Substrate   enameled steel,   Circuitry   Cu (fired)
● = Cell 1,   O = Cell 4

102

Figure A11. Change in Solar Cell Power
During Accelerated Exposure
Array System 7*

Fraction of Original Current at 0 350 Volts

0.66 rel. noon UV, 28°C,
100% rel. hum.

1 00, 43, 0

1 00, 43, 100

1.00, 72, 0

1.00, 72, 100

0.66, 64, 100

0, 72, 0

0, 72, 100

Time, days

Time, days

*Encapsulant   nitrocellulose lacquer,   Substrate   epoxy,   Circuitry   Cu
● = Cell 3,   O = Cell 6

103
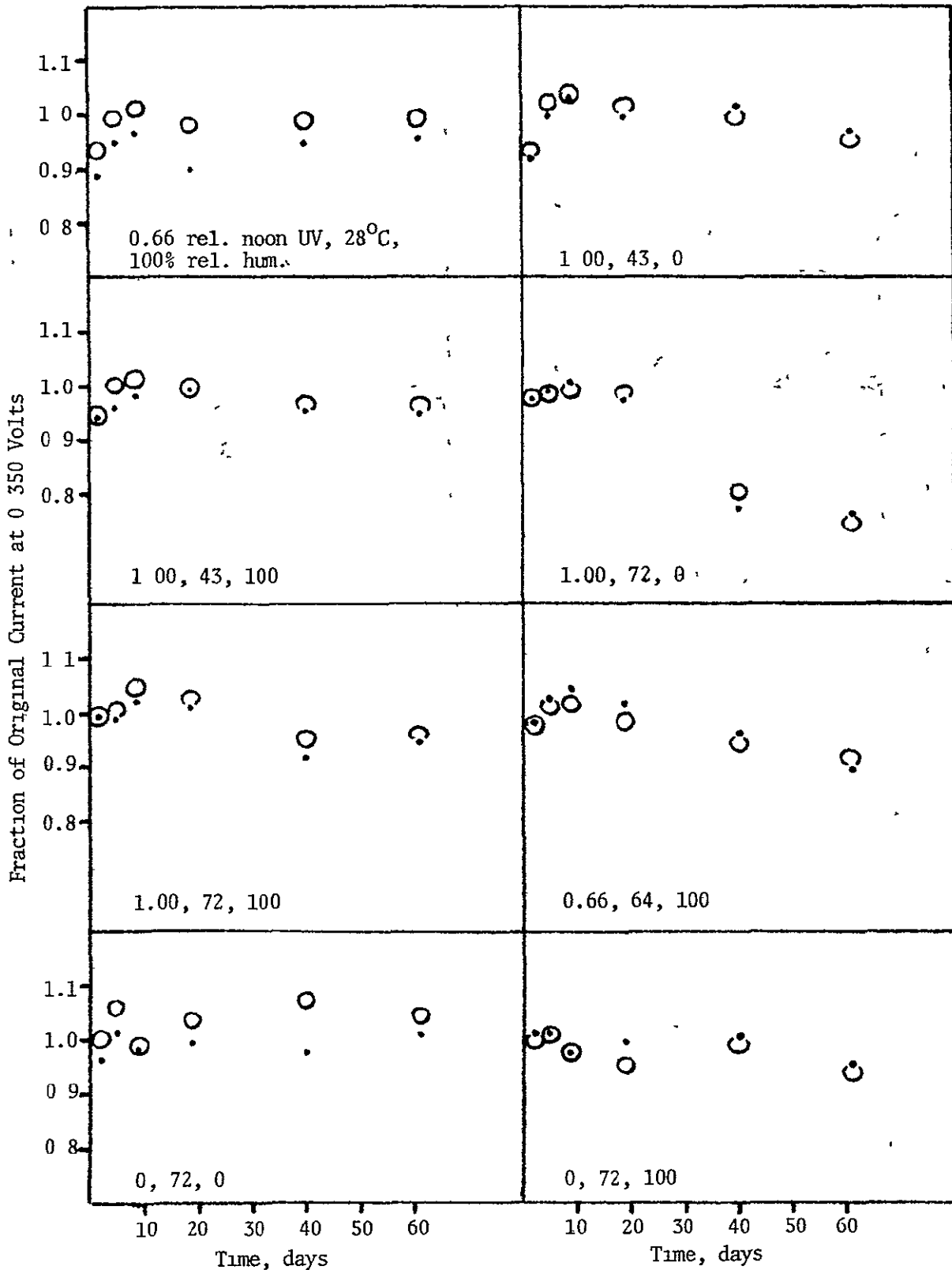
Figure A12   Change in Solar Cell Power
             During Accelerated Exposure
             Array System 8*
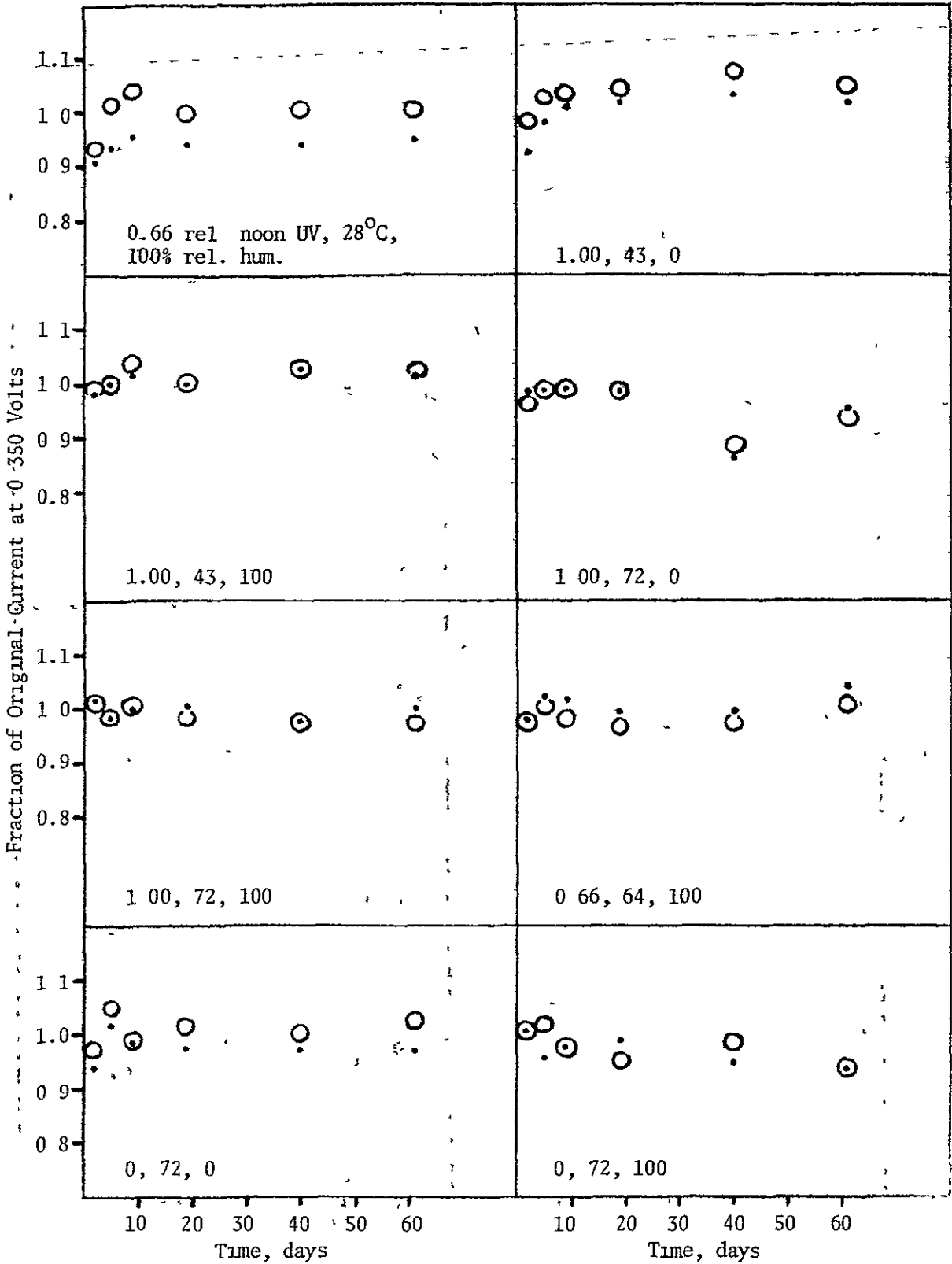
*Encapsulant   2B74,   Substrate   epoxy,   Circuitry   Cu
                    • = Cell 2,   ○ = Cell 5
104

Figure A13'. Change in Solar Cell Power
During Accelerated Exposure:
Array System 9*

0.66 rel. noon UV, 28°C,
100% rel. hum.

1.00, 43, 0

1.00, 43, 100

1.00, 72, 0

1.00, 72, 100

0.66, 64, 100

0, 72, 0

0, 72, 100

Fraction of Original Current at 0.350 Volts

Time, days

Time, days
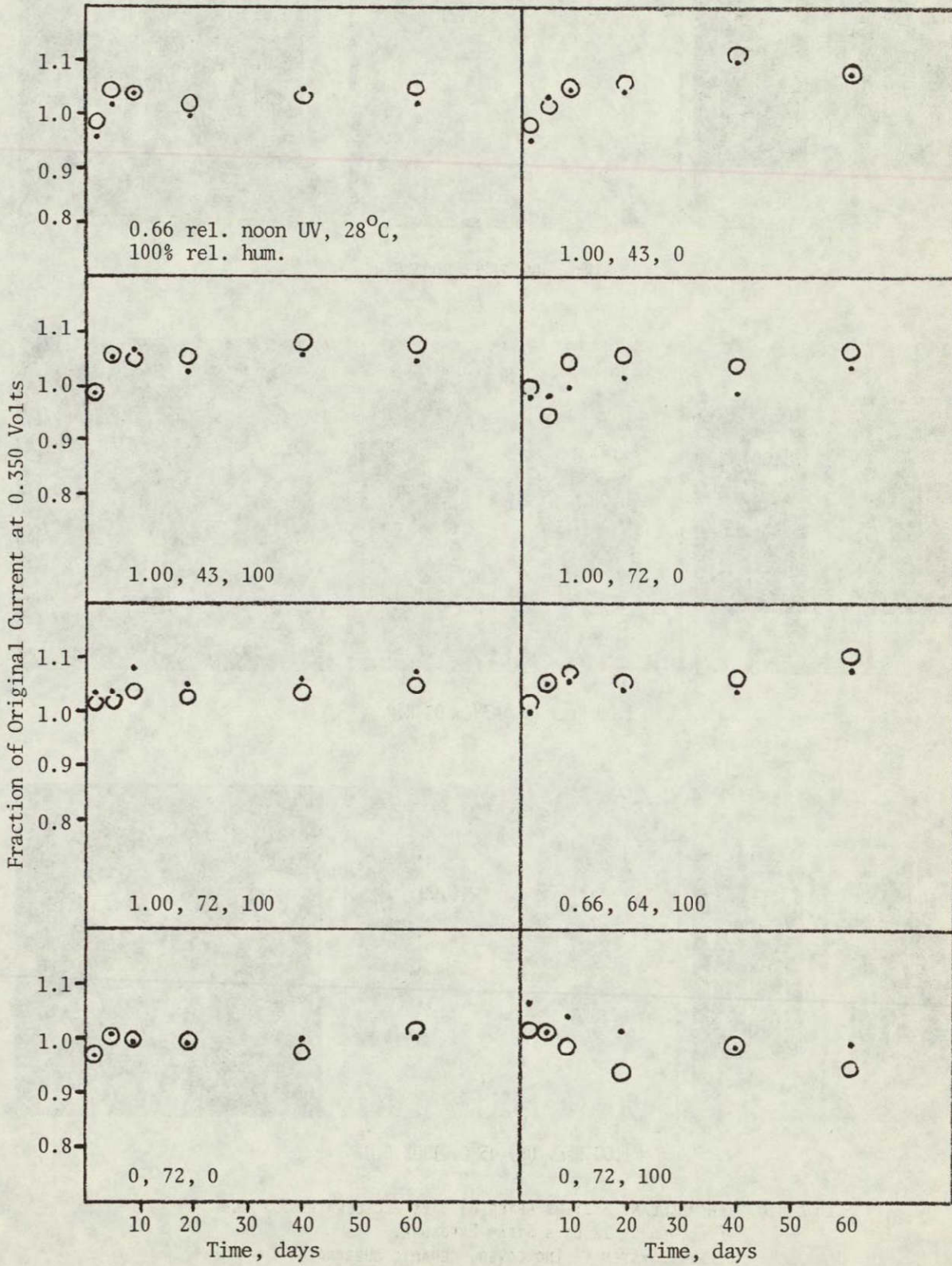
*Encapsulant: 2B74 + glass, Substrate: epoxy, Circuitry: Cu
• = Cell 1, ○ = Cell 4
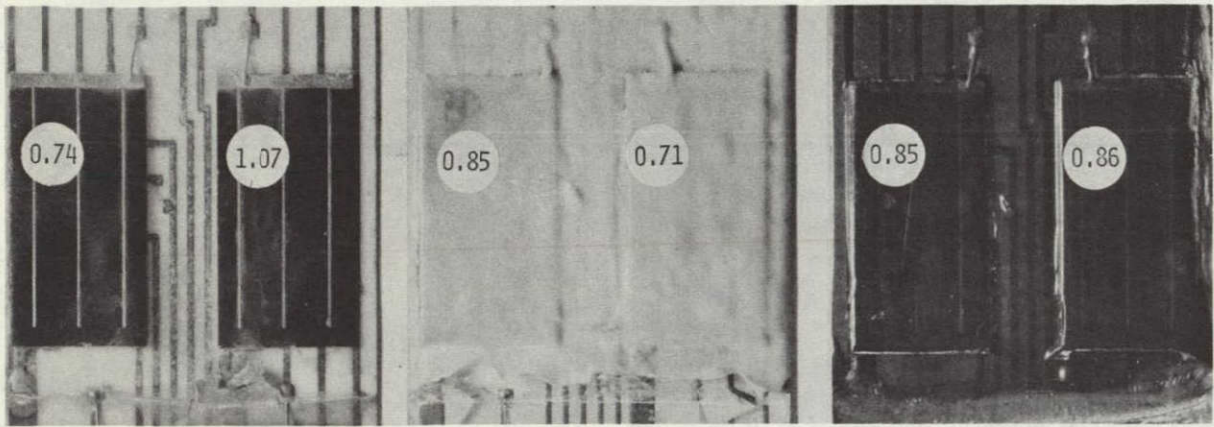
0.66 Rel. UV, 28°C, 100% R.H.
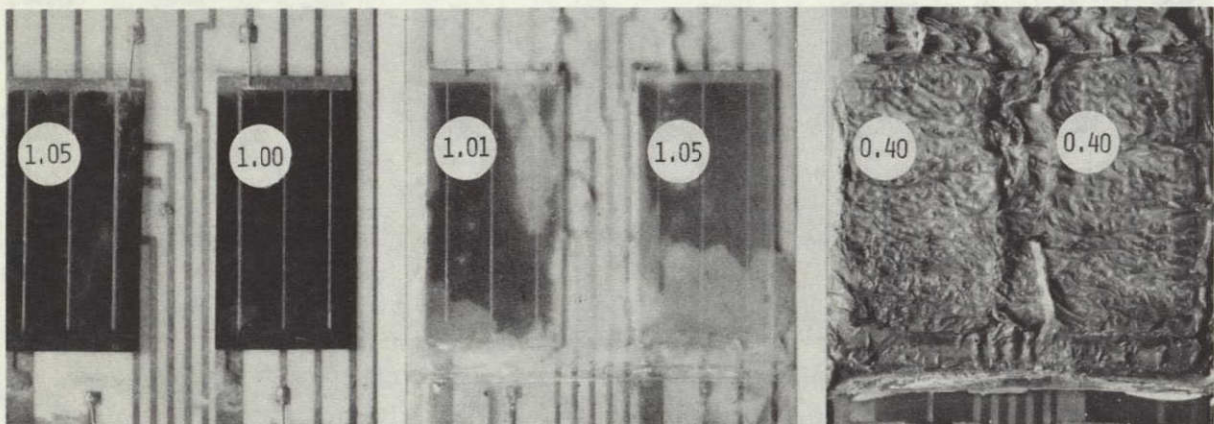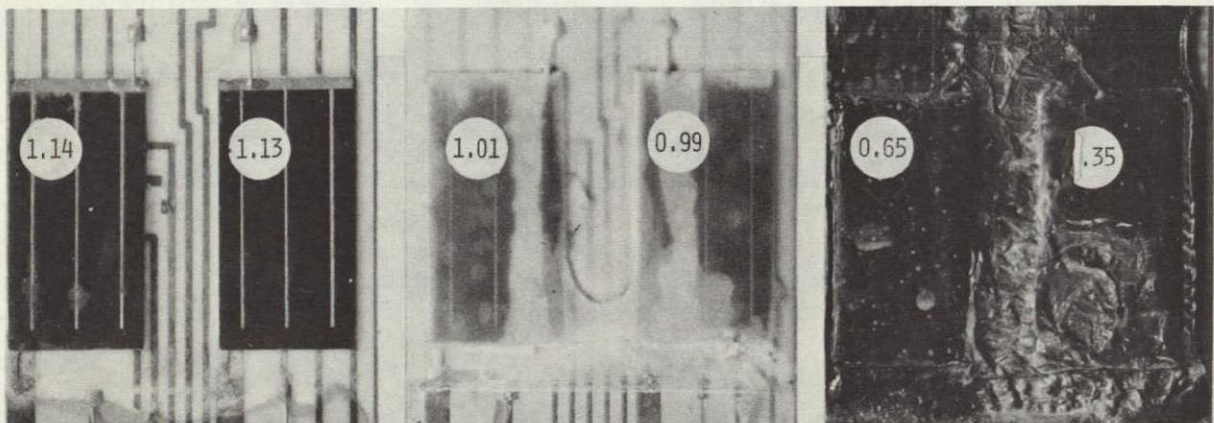
1.00 Rel. UV, 43°C, 0% R.H.

1.00 Rel. UV, 43°C, 100% R.H.

Figure A14. Encapsulant Systems After 61 Days Accelerated Exposure
Followed by 12 Days Steam Exposure.
Left: System #1 (no cover, ceramic substrate)
Center: System #4 (acrylic lacquer, enameled steel substrate)
Right: System #7 (nitrocellulose lacquer, epoxy substrate)
NOTE: Fraction of original power is shown for each cell.

106

0.83 1.07 0.96 1.01 0.35 0.31

1.00 Rel. UV, 72°C, 0% R.H.

1.09* 0.70 1.04 1.00 0.26 0.56

1.00 Rel. UV, 72°C, 100% R.H.

0.89 0.86 0.54 0.55 0.37 0.45
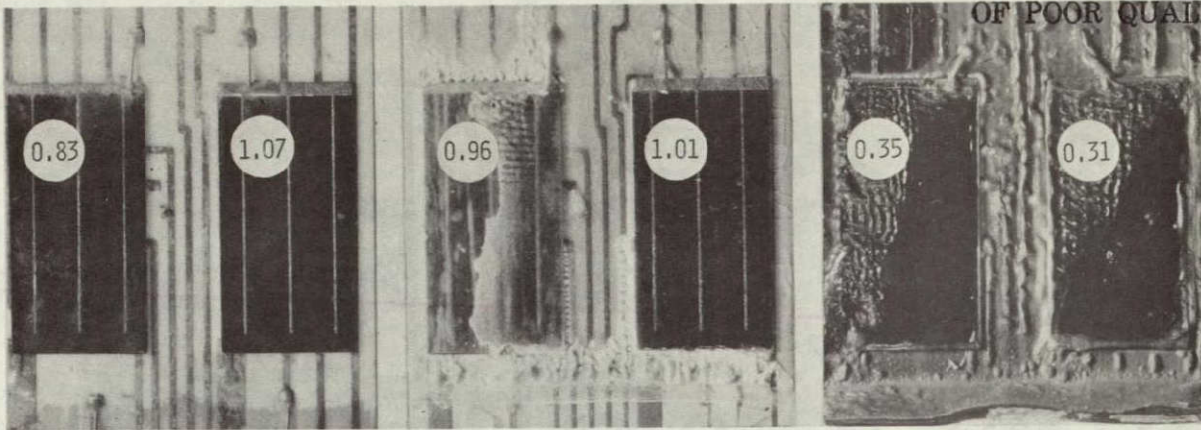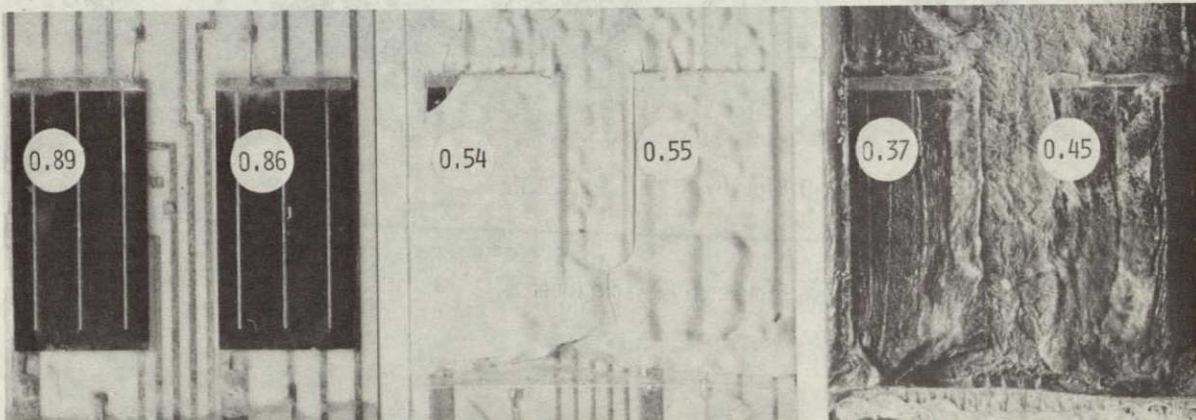
0.66 Rel. UV, 64°C, 100% R.H.

*BY PROBING

Figure A14. Continued

107
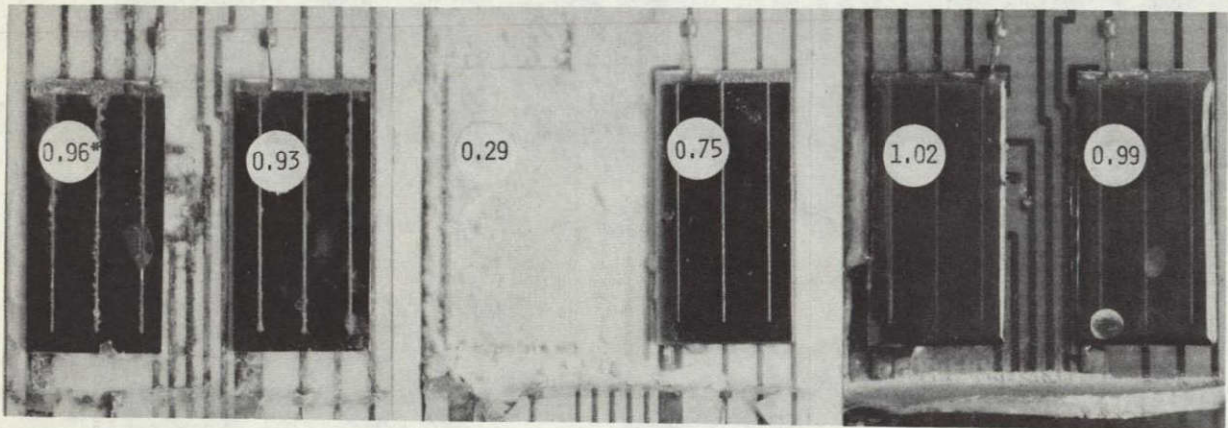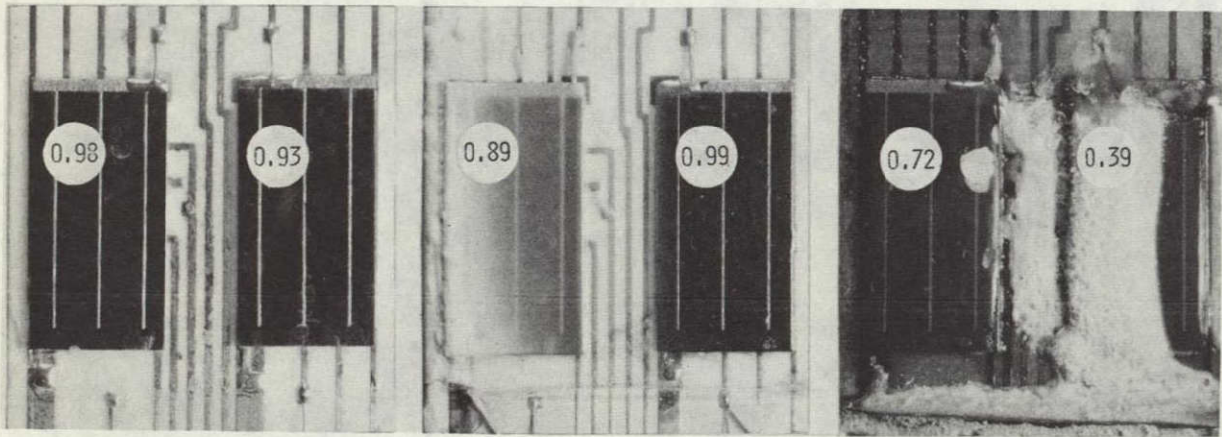
0 Rel. UV, 72°C, 0% R.H.

0 Rel. UV, 72°C, 100% R.H.

Figure A14. Continued

*BY PROBING

Figure A16   Change in Solar Cell Power During Steam Exposure
Following 61 Days Accelerated Exposure.   Array System 2*

*Encapsulant   Parylene C,   Substrate· ceramic,   Circuitry· Mo/Mn + Cu
• =   Cell 2,   O =   Cell 5

Figure A17. Change in Solar Cell Power During Steam Exposure
Following 61 Days Accelerated Exposure   Array System 3*

0 66 rel. noon UV, 28°C,
100% rel. hum.

1.00, 43, 0

1.00, 43, 100

1.00, 72, 0

1.00, 72, 100

0.66, 64, 100

0, 72, 0

0, 72, 100

(0.93 by
probing)

Fraction of Original Current at 0.350 Volts

Time, days

Time, days

*Encapsulant: 2B74 + glass, Substrate. ceramic, Circuitry Mo/Mn + Cu
• = Cell 1, O = Cell 4

111

Figure A18. Change in Solar Cell Power During Steam Exposure
Following 61 Days Accelerated Exposure   Array System 4*

0 66 rel noon UV, 28°C, 100% rel. hum

1.00, 43, 0

1.00, 43, 100

1.00, 72, 0

1 00, 72, 100

(0.69, 0.21 by probing)

0.66, 64, 100

0, 72, 0

(0 by probing)

0. 72, 100

Fraction of Original Current at 0 350 Volts

Time, days   Time, days

*Encapsulant   acrylic, Substrate   enameled steel, Circuitry   Cu (fired)
● = Cell 3, O = Cell 6

112
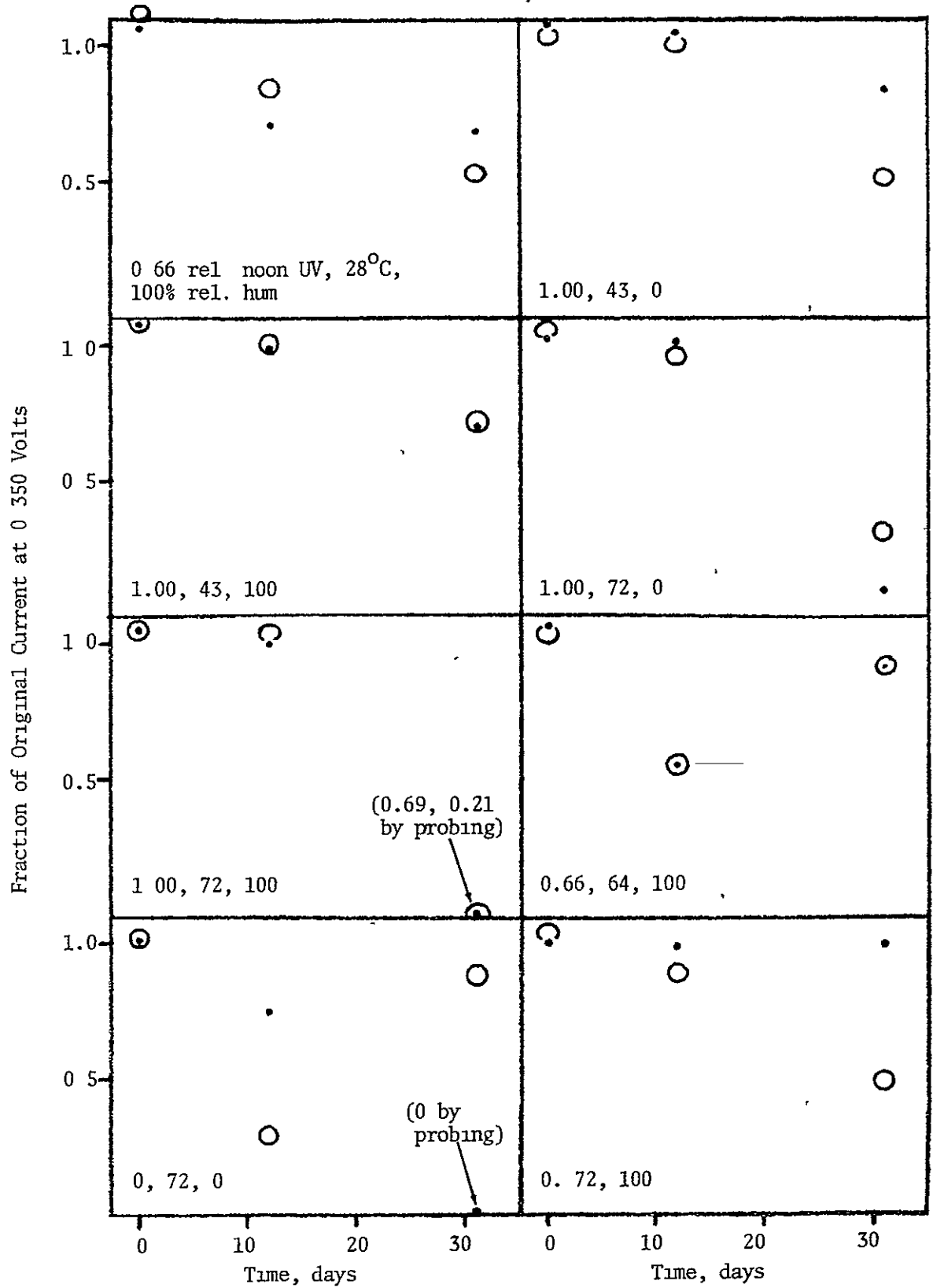
Figure A19   Change in Solar Cell Power During Steam Exposure
Following 61 Days Accelerated Exposure   Array System 5*

0.66 rel. noon UV, 28°C,
100% rel. hum.

1.00, 43, 0

1.00, 43, 100

1.00, 72, 0

1.00, 72, 100

0.66, 64, 100

0, 72, 0

0, 72, 100

Fraction of Original Current at 0.350 Volts

Time, days

Time, days

*Encapsulant   Sylgard 184,   Substrate.   enameled steel,   Circuitry   Cu (fired)
• =   Cell 2,   O =   Cell 5

113

Figure A20. Change in Solar Cell Power During Steam Exposure Following 61 Days Accelerated Exposure. Array System C*

0.66 rel noon UV, 28°C, 100% rel. hum.

1.00, 43, 0

1.00, 43, 100

1.00, 72, 0

1.00, 72, 100

0.66, 64, 100

0, 72, 0

0, 72, 100

Fraction of Original Current at 0 350 Volts

Time, days

Time, days

*Encapsulant: 2B74 + glass, Substrate enameled steel, Circuitry. Cu (fired)
● = Cell 1, ○ = Cell 4

114

Figure A21. Change in Solar Cell Power During Steam Exposure
Following 61 Days Accelerated Exposure   Array System 7*

Fraction of Original Current at 0 350 Volts

0.66 rel. noon UV, 28°C,
100% rel hum.

1.00, 43, 0

1.00, 43, 100

1.00, 72, 0

1.00, 72, 100

0.66, 64, 100

0, 72, 0

0, 72, 100

Time, days

Time, days

*Encapsulant   nitrocellulose lacquer,   Substrate   epoxy,   Circuitry: Cu
• =   Cell 3,   O =   Cell 6

115

Figure A22   Change in Solar Cell Power During Steam Exposure
Following 61 Days Accelerated Exposure   Array System 8*
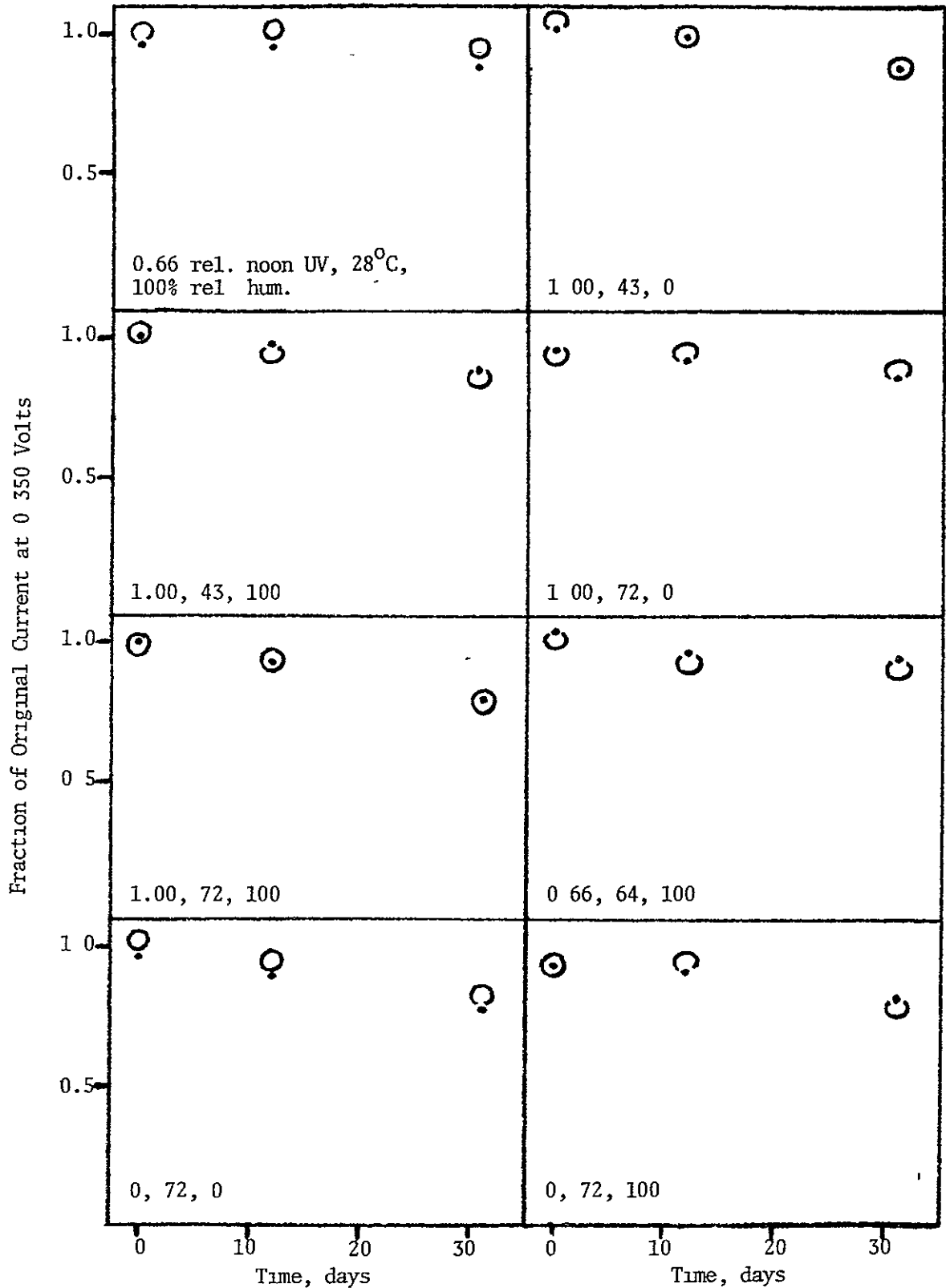
*Encapsulant   2B74,   Substrate   epoxy,   Circuitry·   Cu
● = Cell,   ○ = Cell 5

Figure A23.   Change in Solar Cell Power During Steam Exposure
Following 61 Days Accelerated Exposure: Array System 9*

Fraction of Original Current at 0.350 Volts

0.66 rel. noon UV, 28°C,
100% rel. hum.

1.00, 43, 0

1.00, 43, 100

1.00, 72, 0

1.00, 72, 100

0.66, 64, 100

0, 72, 0

0, 72, 100

Time, days

Time, days

*Encapsulant: 2B74 + glass,   Substrate: epoxy,   Circuitry: Cu
• = Cell 1,   ○ =   Cell 4

117
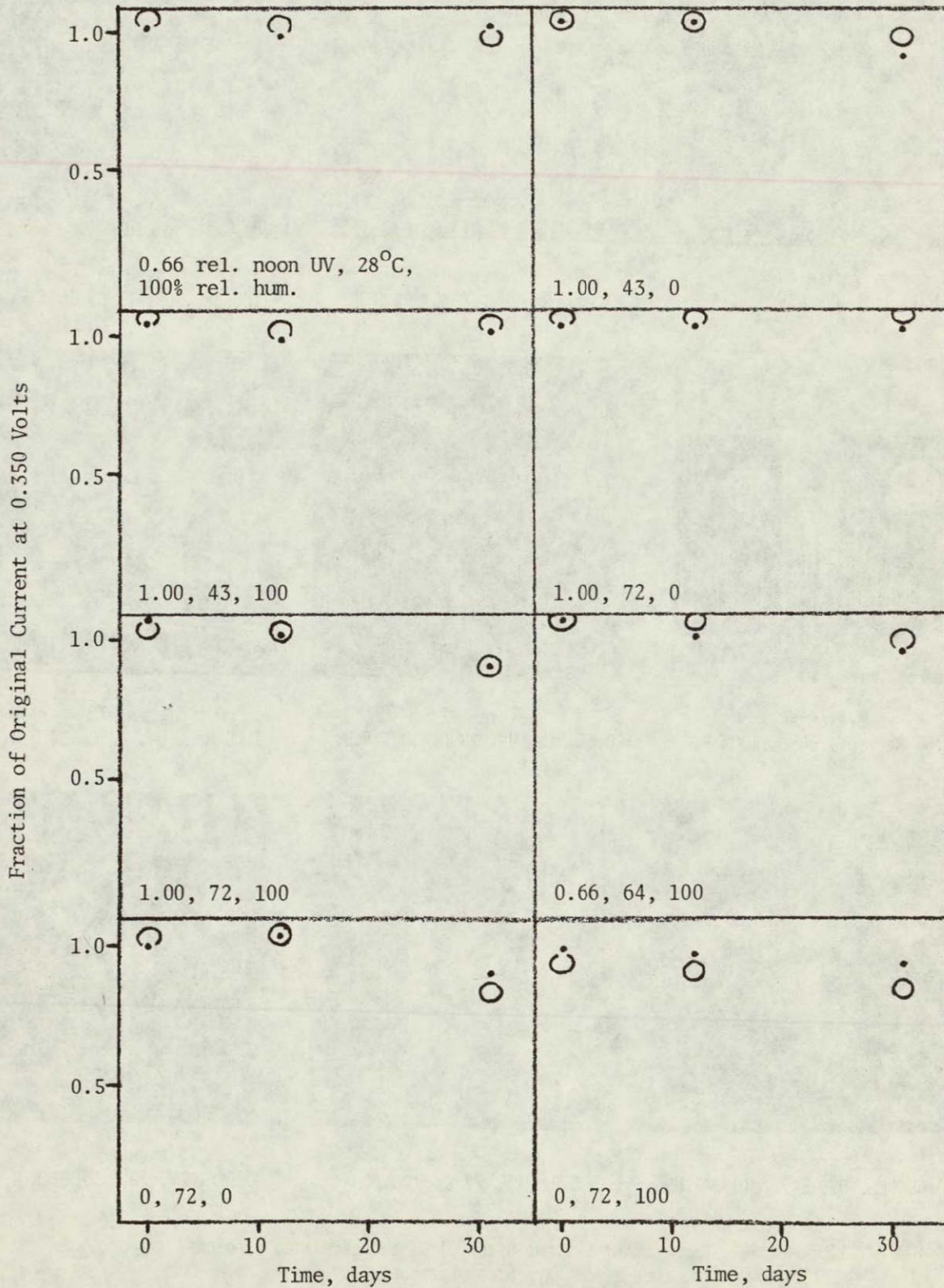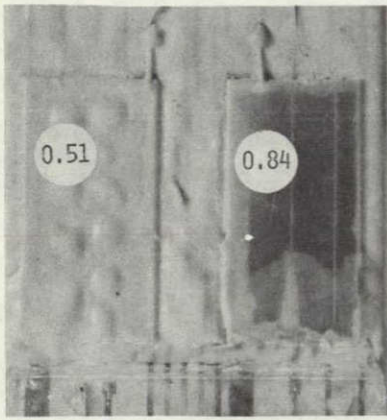
SYSTEM #4
1.00 REL. UV, 43°C, 0% R.H.
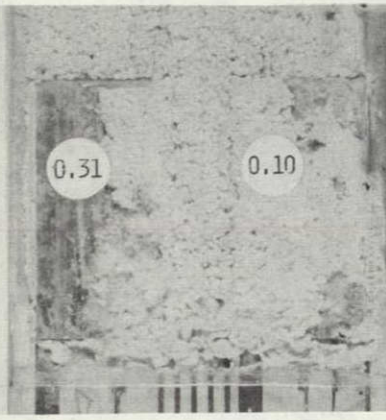
SYSTEM #4
1.00 REL. UV, 72°C, 0% R.H.
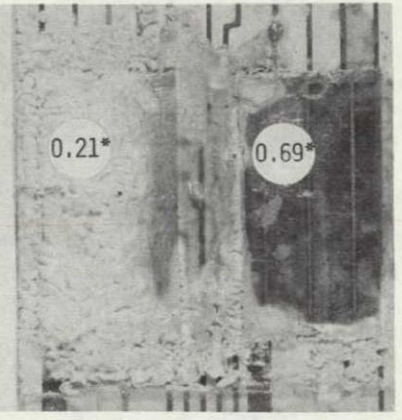
SYSTEM #4
1.00 REL. UV, 72°C, 100% R.H.
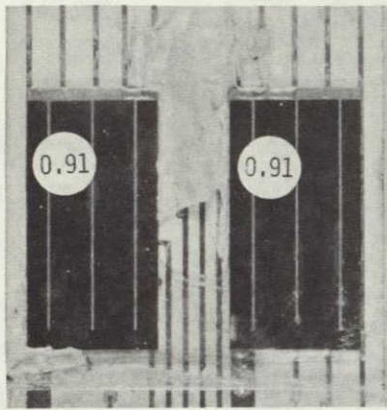
SYSTEM #4
0.66 REL. UV, 64°C, 100% R.H.
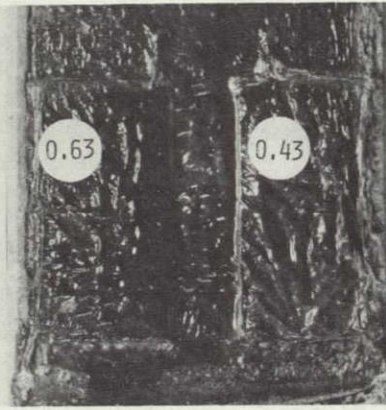
SYSTEM #7
0.66 REL. UV, 28°C, 100% R.H.
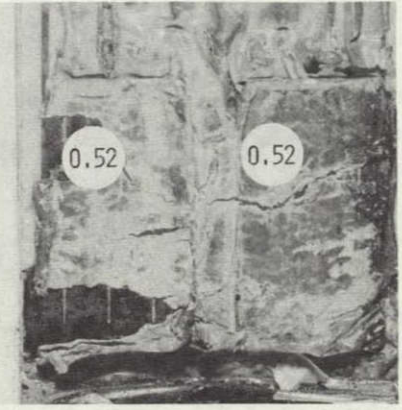
SYSTEM #7
1.00 REL. UV, 43°C, 0% R.H.
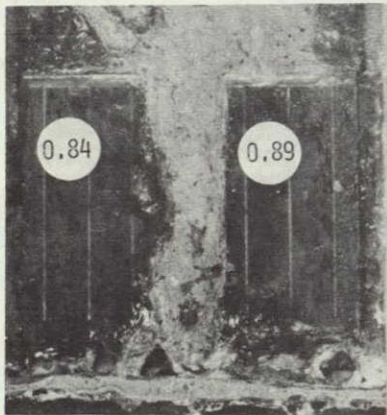
SYSTEM #7
0.66 REL. UV, 64°C, 100% R.H.
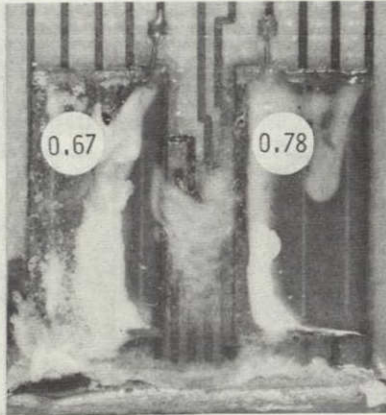
SYSTEM #7
0 REL UV, 72°C, 0% R.H.
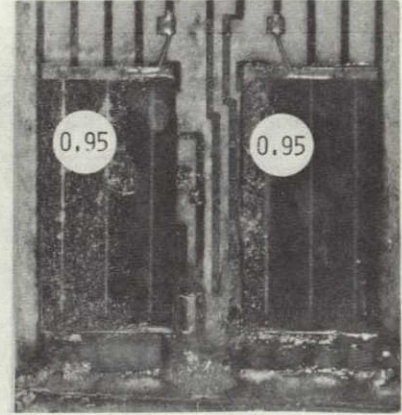
SYSTEM #7
0 REL UV, 72°C, 100% R.H.

FIGURE A24. ENCAPSULANT SYSTEMS AFTER 61 DAYS ACCELERATED EXPOSURE
FOLLOWED BY 31 DAYS STEAM EXPOSURE.
SYSTEM #4: ACRYLIC LACQUER, ENAMELED STEEL SUBSTRATE
*BY PROBING   SYSTEM #7: NITROCELLULOSE LACQUER, EPOXY SUBSTRATE
NOTE: FRACTION OF ORIGINAL POWER IS SHOWN FOR EACH CELL.
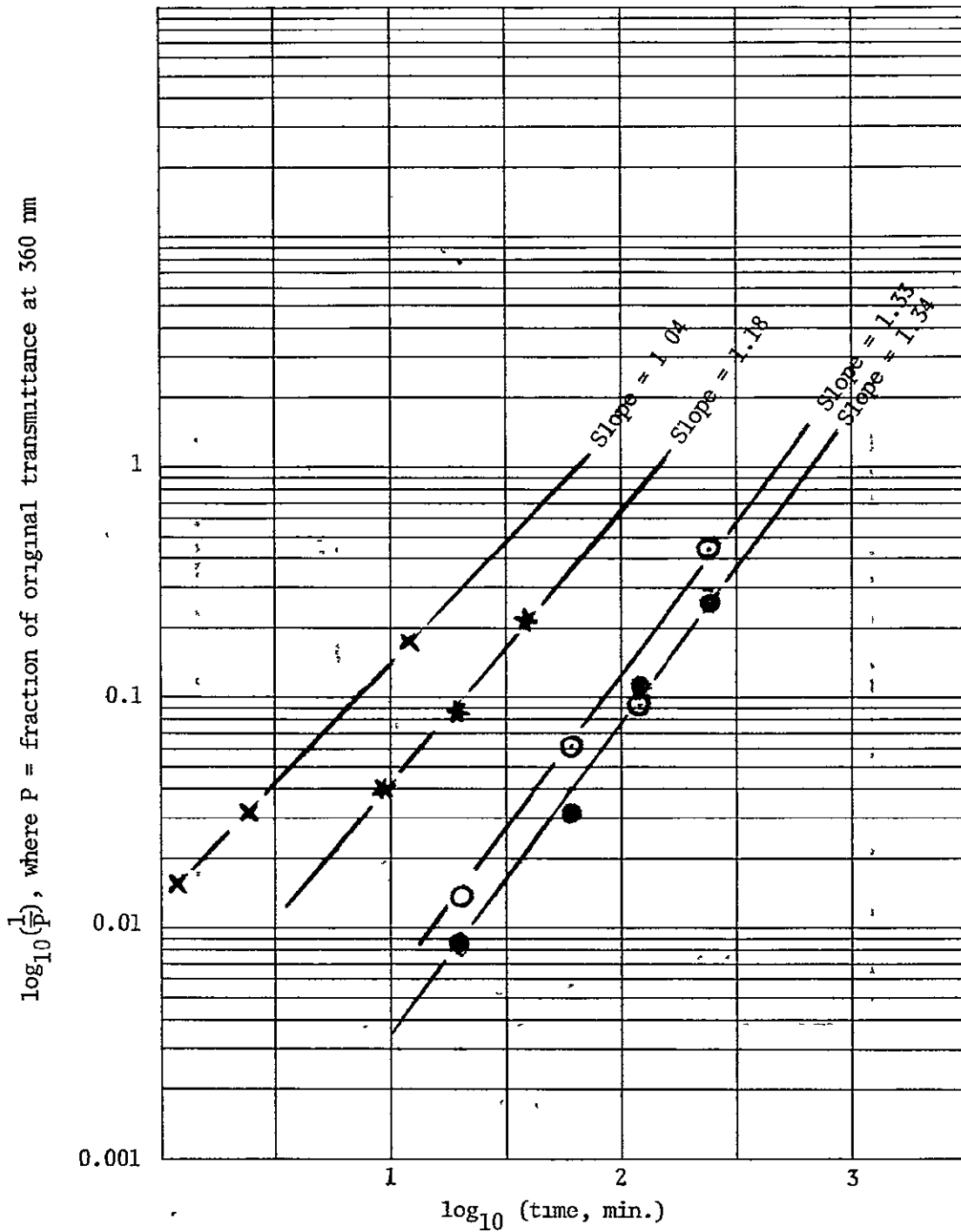
Figure A25 Increase in Absorbance of Plastic Films in Solar Furnace
at 1400 Suns vs Xenon Lamp at 1 Sun

(Polystyrene exposed to xenon lamp (1 00 rel noon UV, 26°C, 100% R.H.), arbitrary time scale.

(Lexan exposed to xenon lamp (same basis).

I Lexan in solar furnace, under water at 35°C, 33 cal./cm ^{2}/sec   (about 1400 suns).

) Polystyrene in solar furnace (same basis).
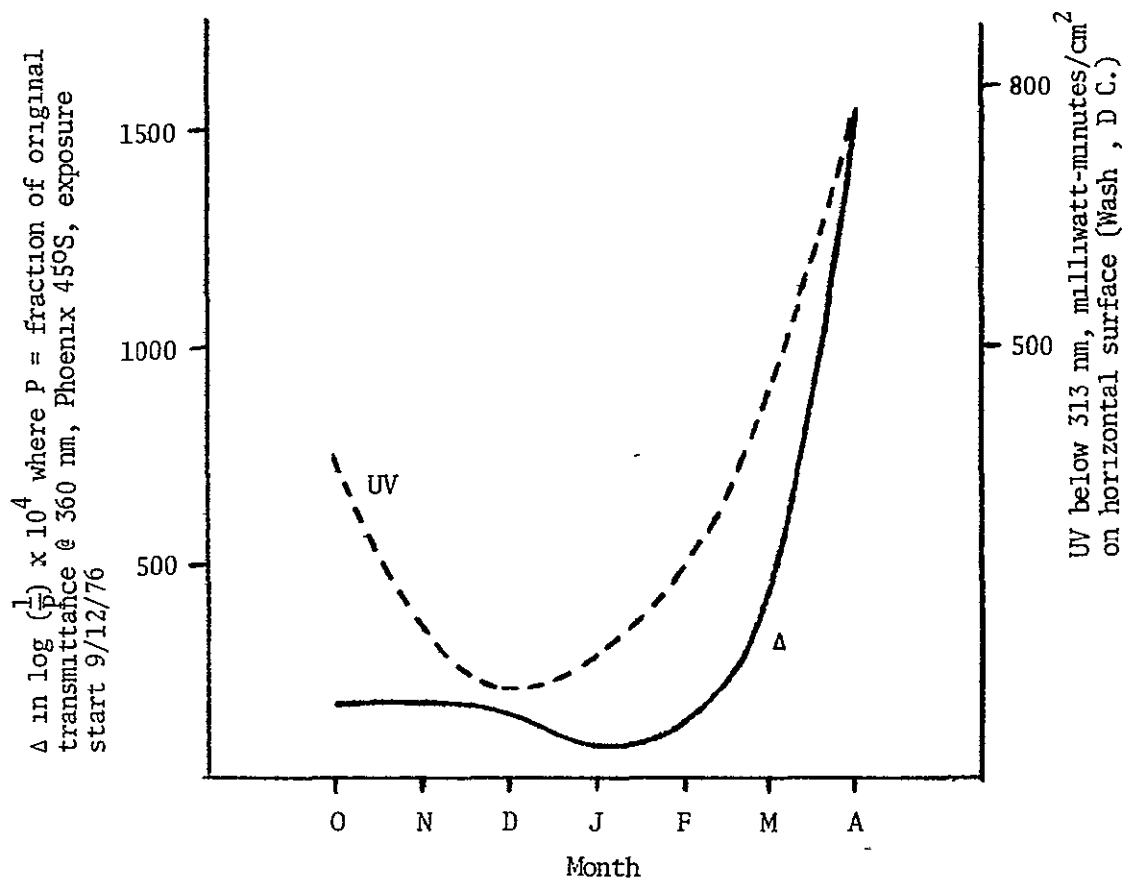
Figure A26 .   UV Intensity and Rate of Lexan Yellowing
vs. Time of Year

Figure A27

Lexan Data (Phoenix, 45°S)
vs   Cumulative UV or Calendar Time

210-day point

Calendar-time
extrapolation
from 150 days

Plot with
calendar time
on abscissa

$\log\left(\frac{1}{P}\right) \times 10^3$ where P = fraction of original transmittance @ 360 nm

-1400

1200

1000

800

600

400

200

200   400   600   800   1000   1200   1400   1600

Cumulative UV
(<313 nm)

121
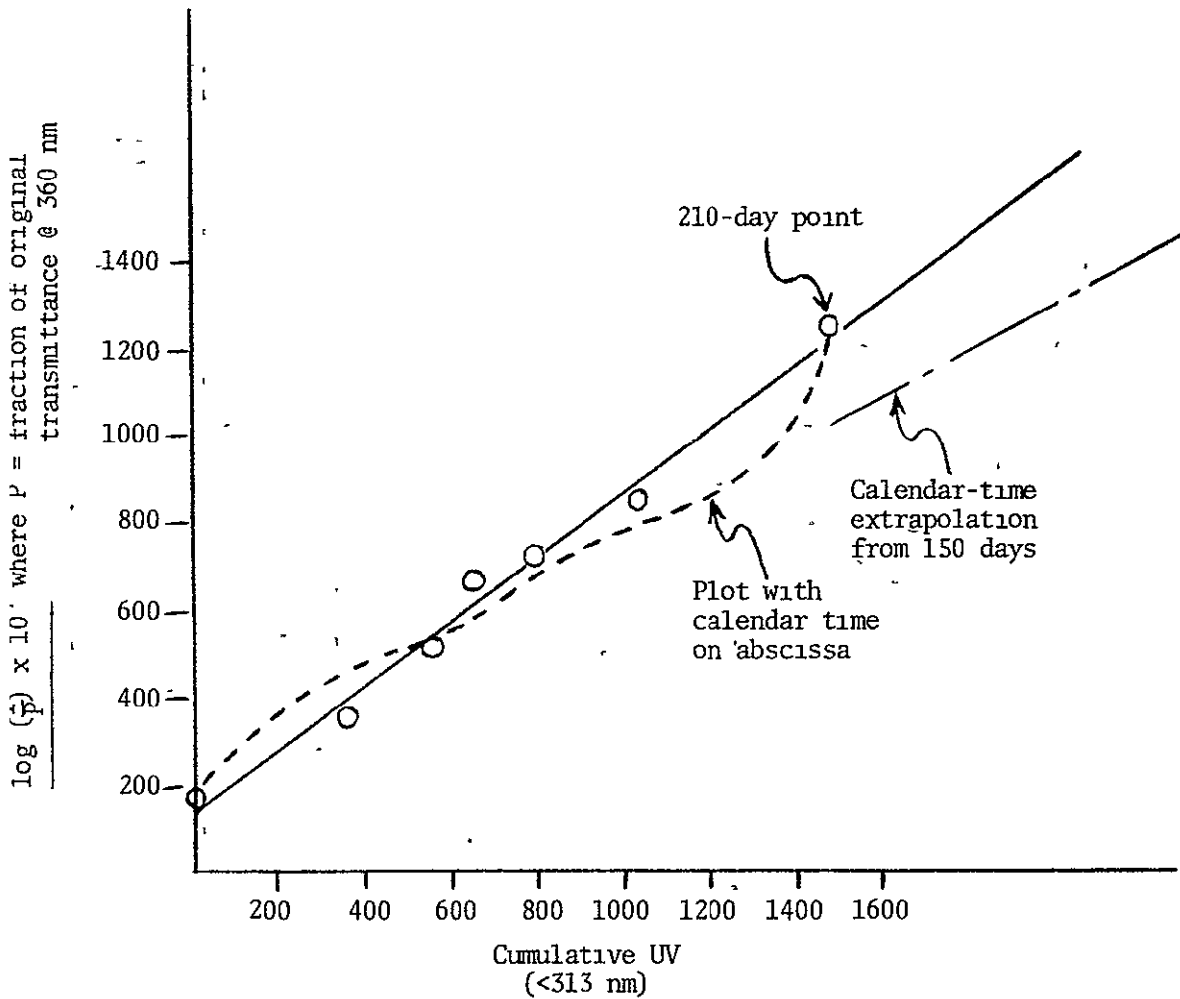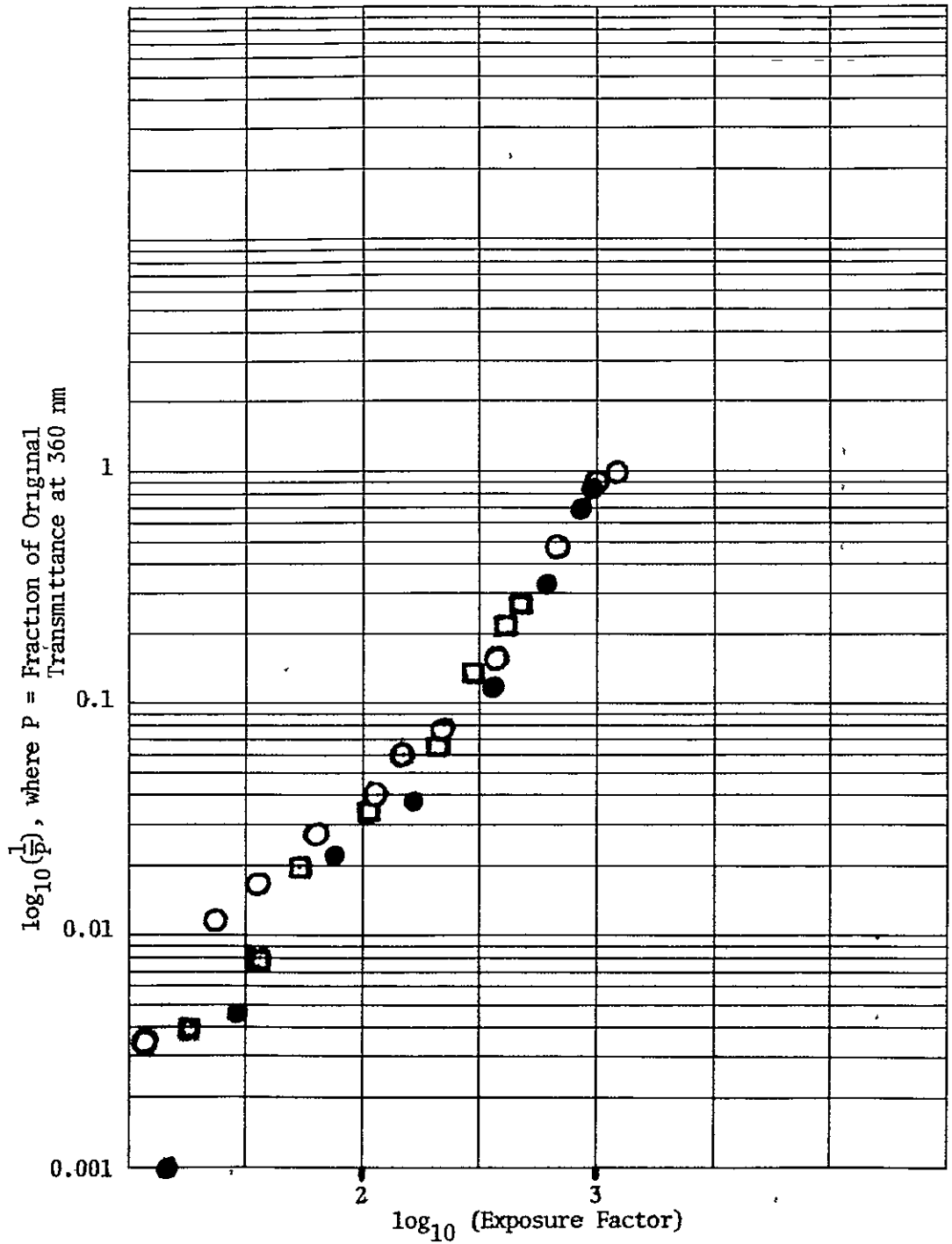
Figure A28   Yellowing of Lexan in Phoenix (45°S)

○ Exposure started 9/12/76
● Exposure started 12/22/76
□ Exposure started 6/21/77
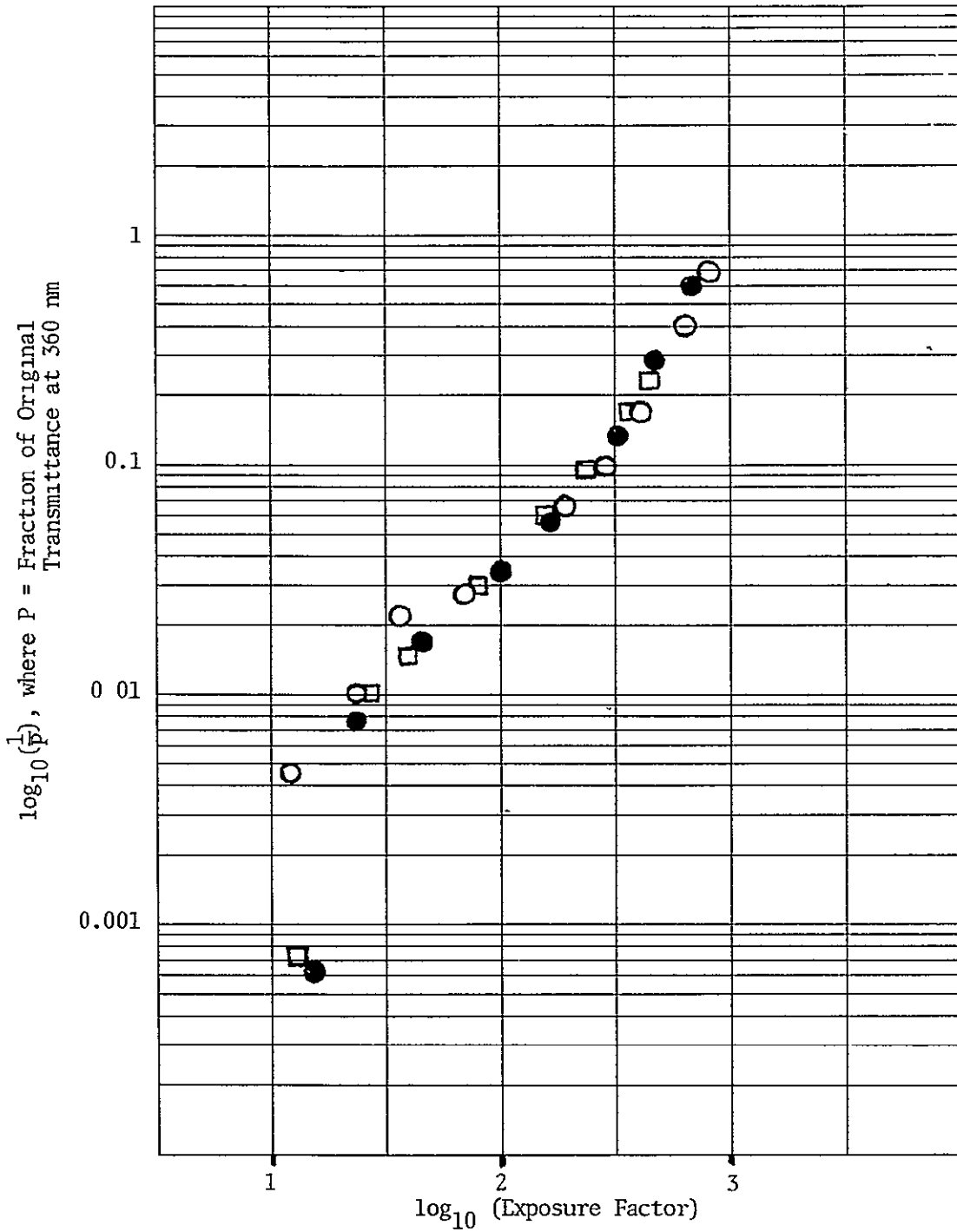
Figure A29 Yellowing of Lexan in Miami (45°S)

O Exposure Started 9/1/76
● Exposure Started 12/22/76
□ Exposure Started 6/21/77
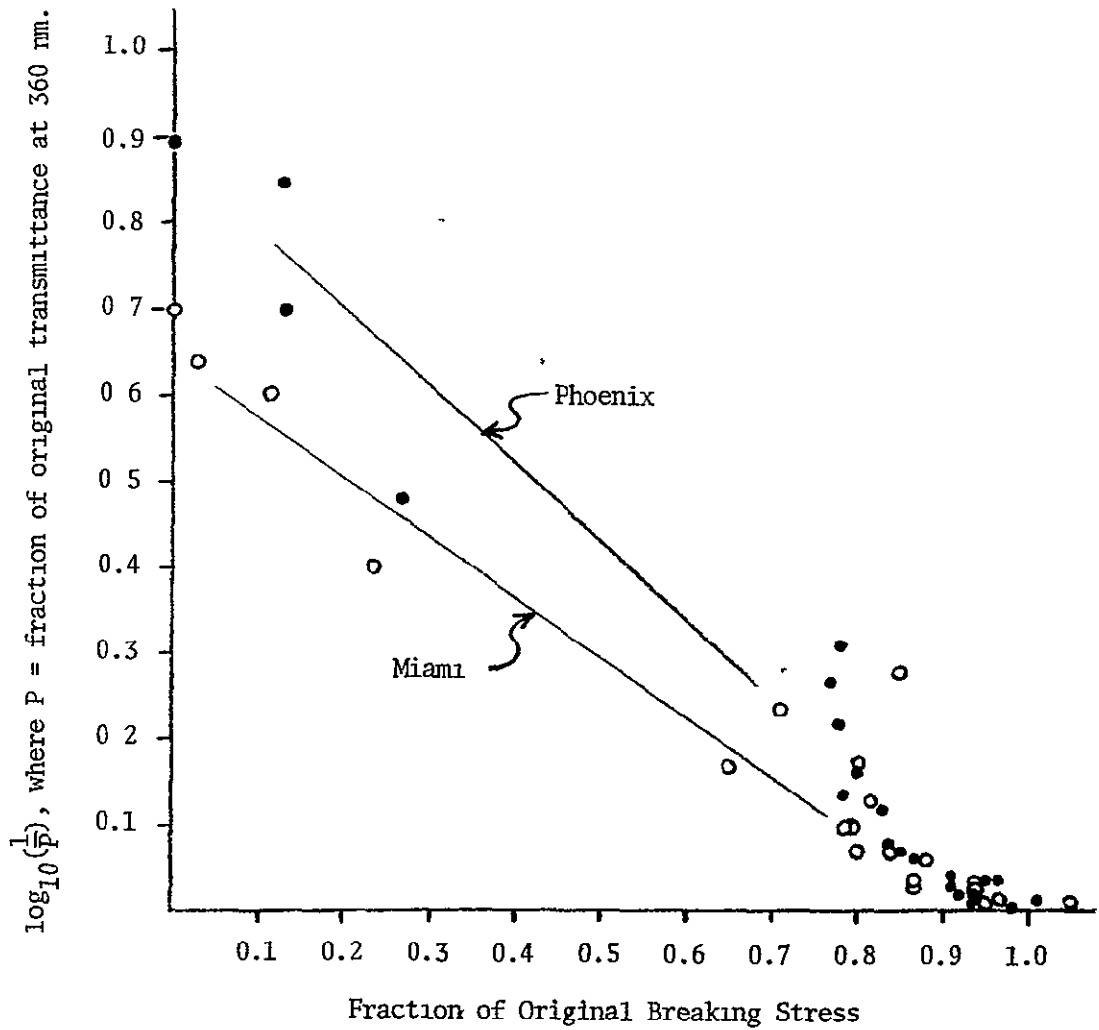
Figure A30 . Correlation of Absorbance Data with Tensile Test Data for 45°S Exposure at Phoenix (●) and Miami (o).

124
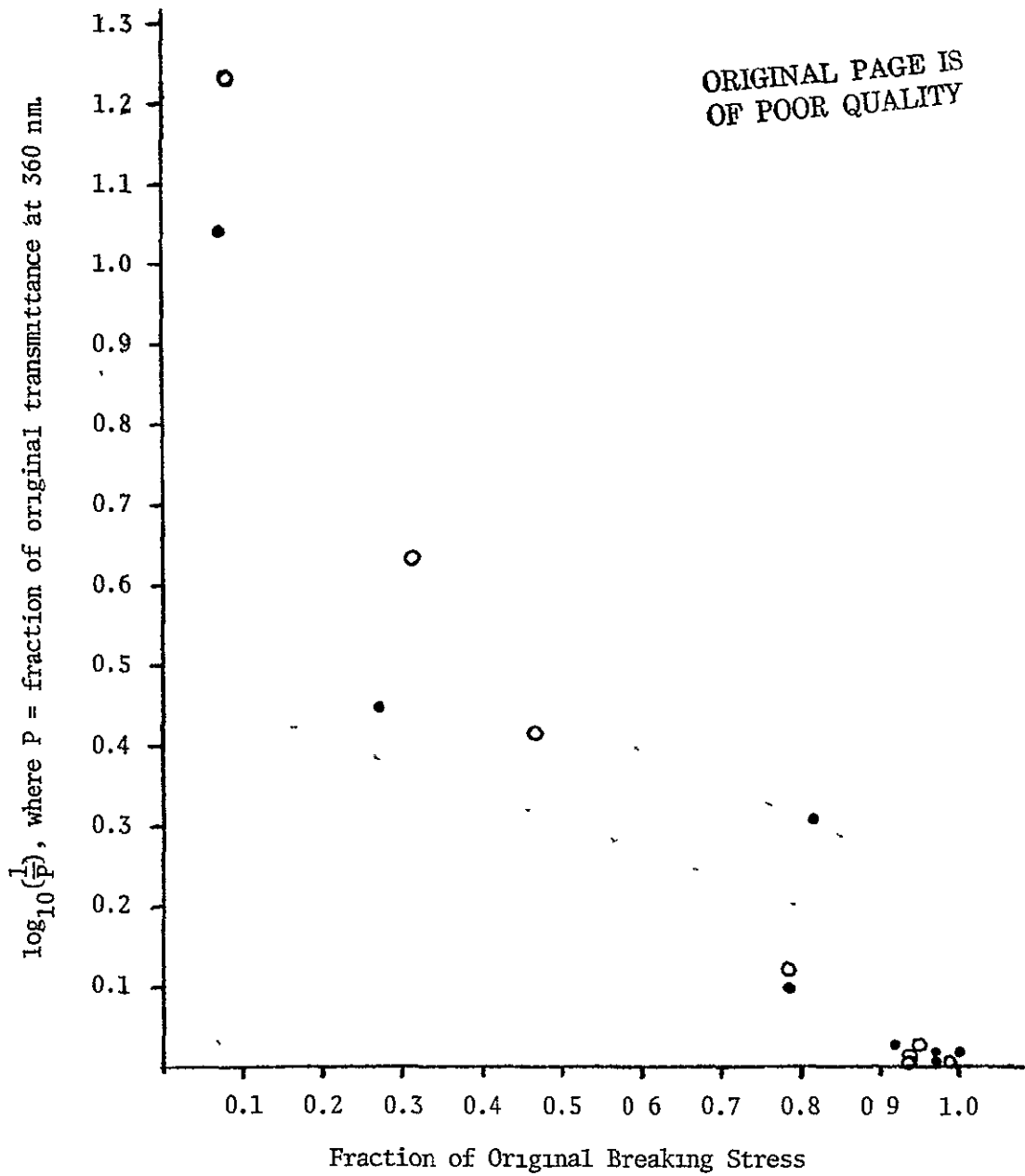
Figure A31. Correlation of Absorbance Data with Tensile Data
for Exposure on the EMMA (●) and EMMAQUA (O)
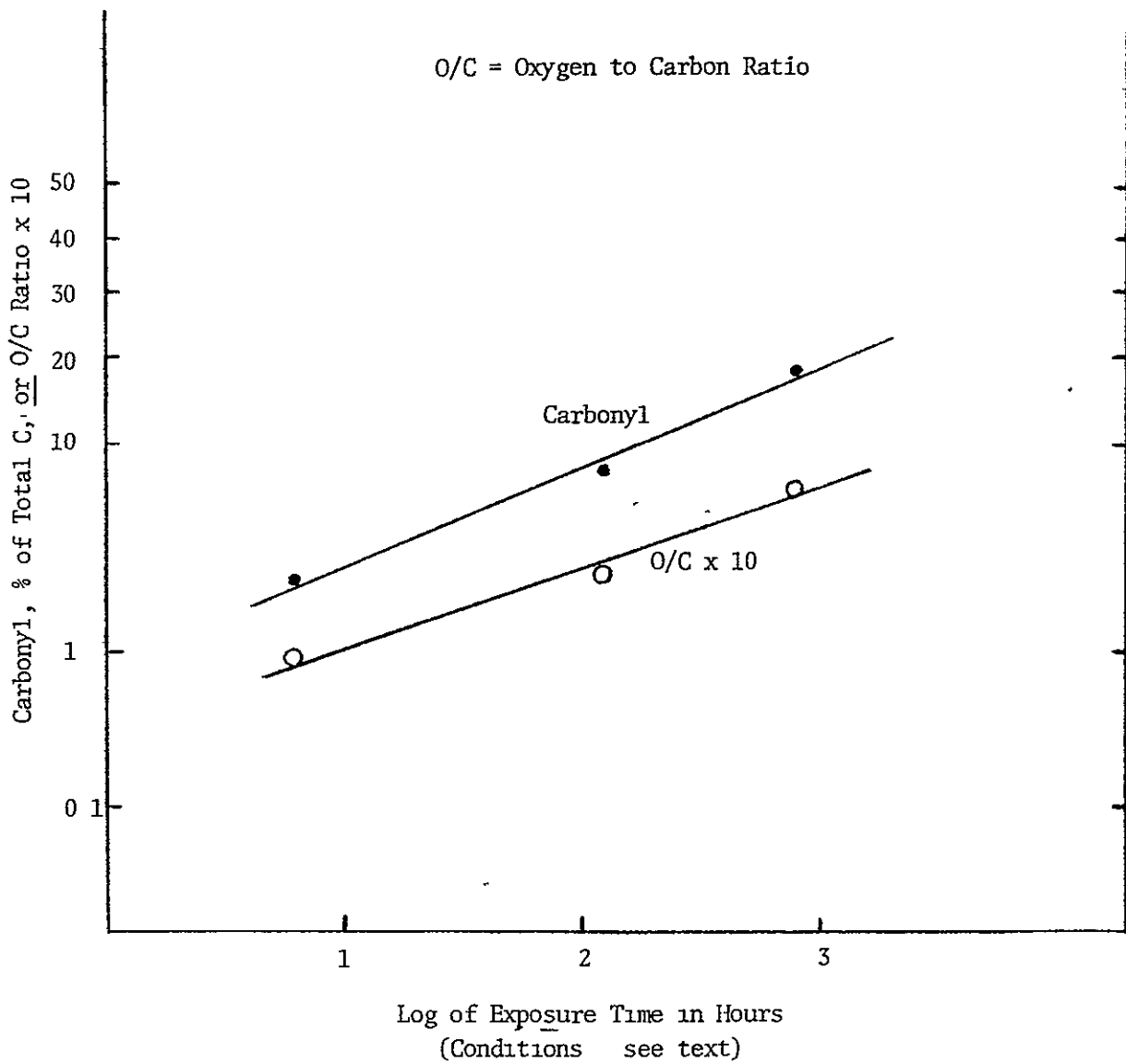
Figure A32. Lognormal Plot of ESCA Data on Polystyrene
from Accelerated Exposure

126

(Conditions   See text)
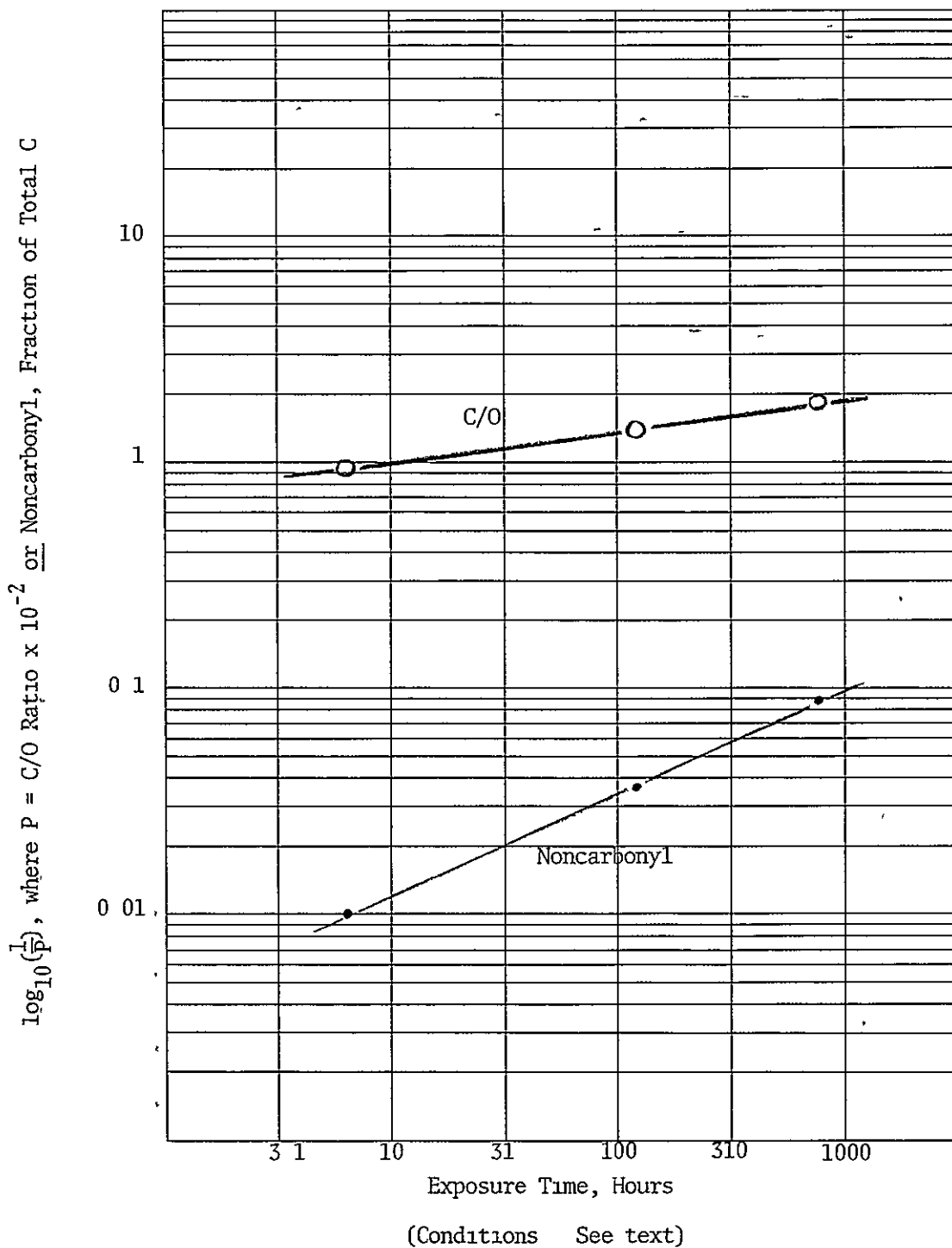
Figure A33   Weibull Plot of ESCA Data on Polystyrene
from Accelerated Exposure
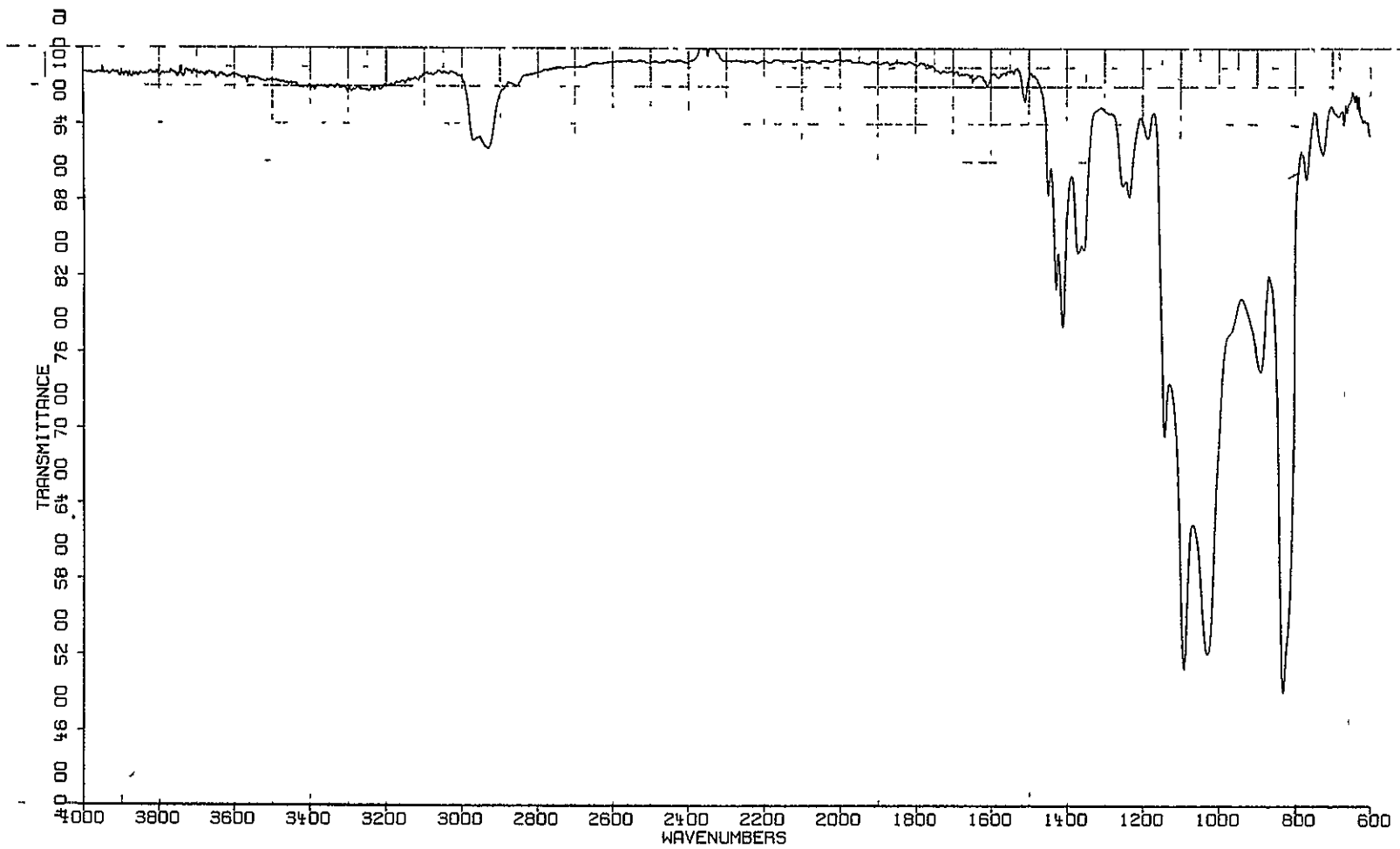
Figure A34. ATR-FTIR Spectrum of Unweathered Tedlar Film

128
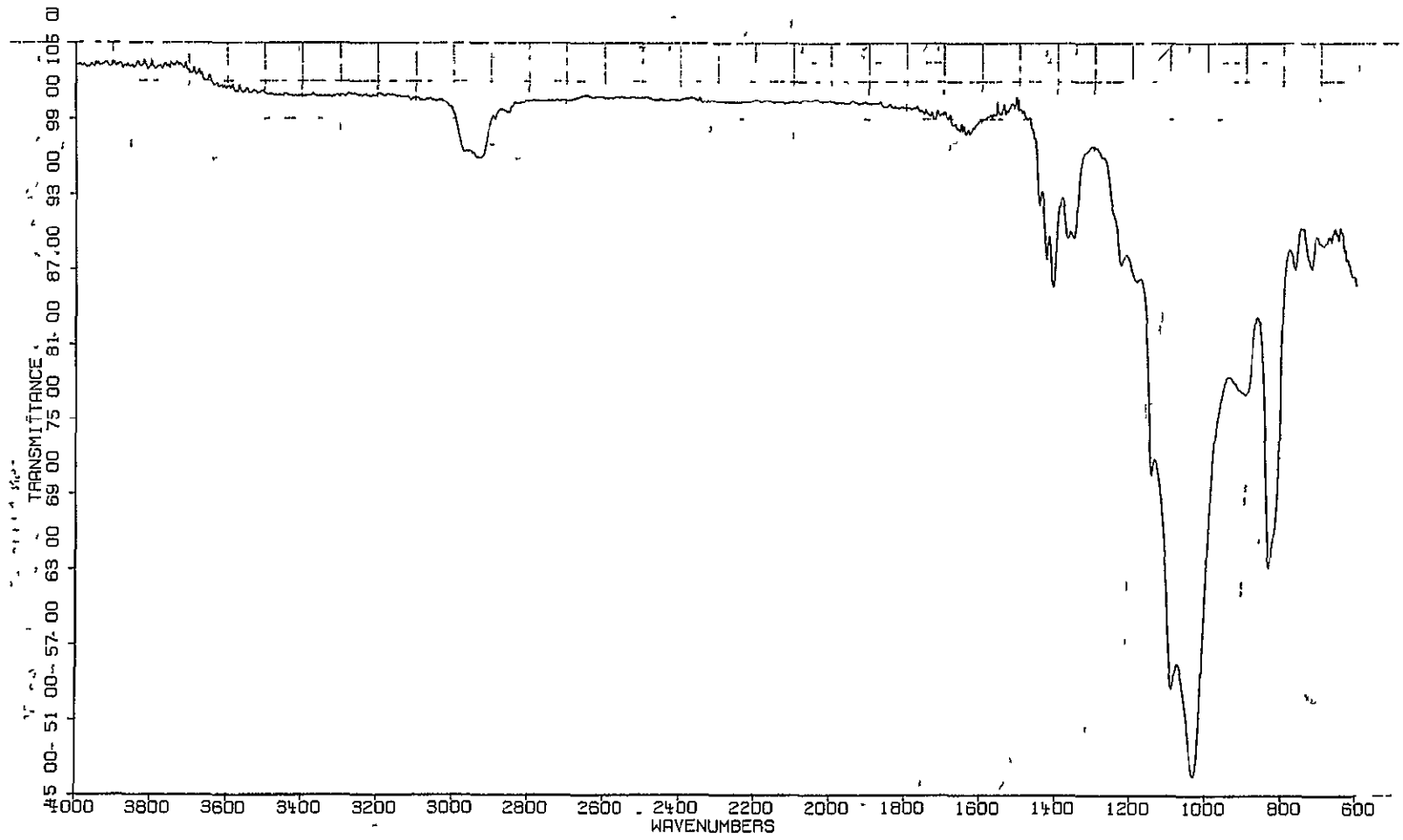
Figure A35.   ATR-FTIR Spectrum of Tedlar Film (Side Facing Away from Light)
after 540 Days on the EMMAQUA

130
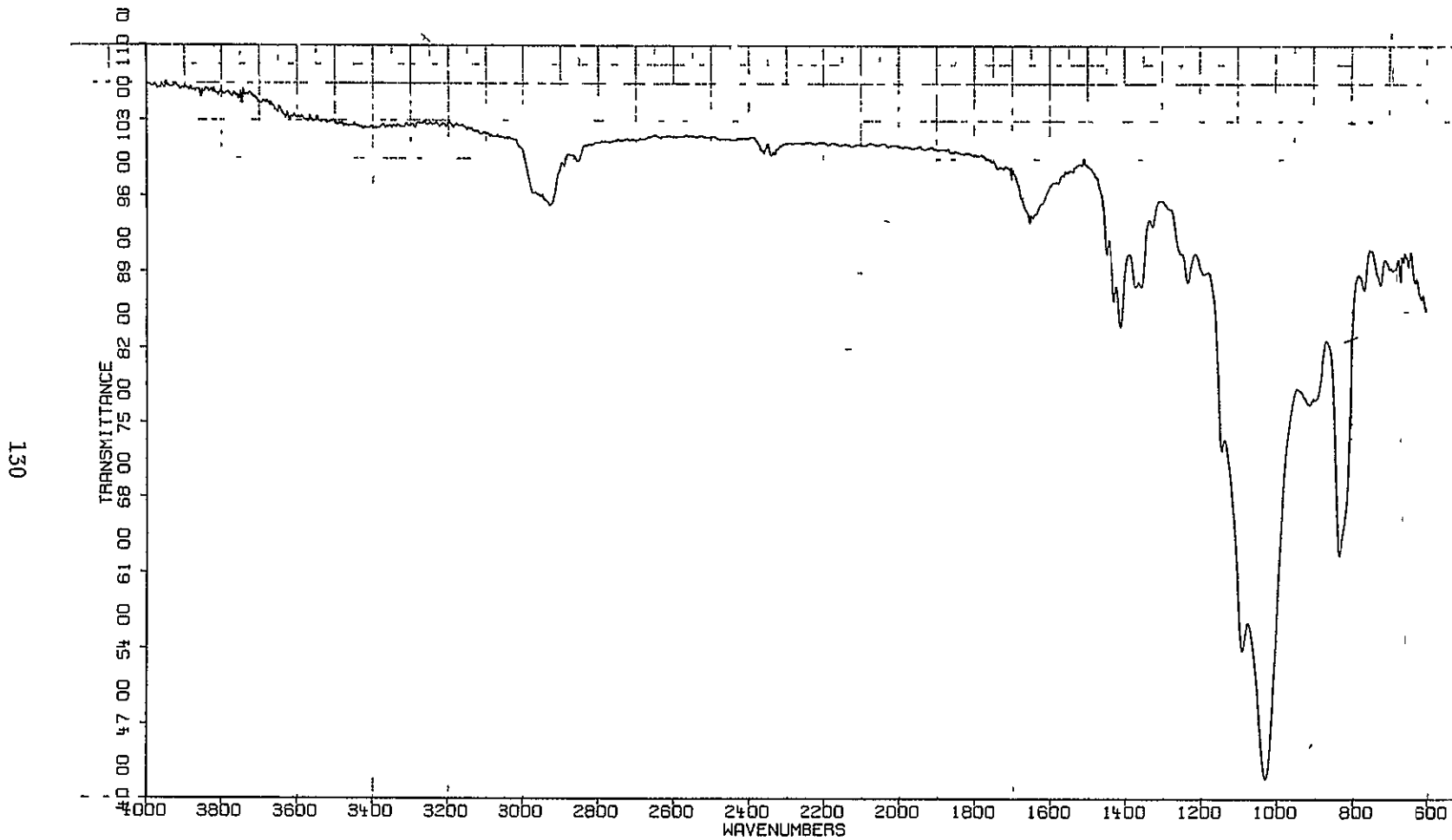
Figure A36   ATR-FTIR Spectrum of Tedlar Film (Side Facing Light)
after 540 Days on the EMMAQUA

Table A1

Array System Components

Fixed Components (Used on All Systems)	
Component	Material
Solar Cell	OCLI N210CG-9 (1 x 2 cm)
Cell-to-Circuit Contact	Tinned Cu wire, soldered with Sn 62 solder
Cell-to-Substrate Adhesive	Dow Corning 3140 RTV silicone
Cover (when used)	Window glass (2.3 mm)
Variable Components	
Component	Material
Pottant	(1) Humiseal 2B74 (polyether-type polyurethane), from Humiseal Div., Columbia Technical Corp.
	(2) Sylgard 184
	(3) Humiseal 1B73 (acrylic)
	(4) Fuller 3915 clear Silosyn (nitro-cellulose lacquer)
	(5) Parylene C (polymer of chloro-p-xylylene), from Union Carbide
Substrate	(1) Ceramic (96% alumina, 1.0 mm) from Technical Ceramic Products Div., 3M Co
	(2) Epoxy (G-10FR, 1 4 mm)
	(3) Enameled steel (carbon steel coated by Erie Ceramic Arts Co., 1.2 mm total thickness)
Circuitry	(1) Mo/Mn, plated with 2 5 microns copper (used on ceramic)
	(2) Copper, 36 microns (used on epoxy)
	(3) Thick-film copper (Cermalloy 7029), about 25 microns (used on enameled steel)

Table A2. Properties of Array System Materials

Component	Material	Dimensions (cm)			Tensile Strength (10^3 psi)	Tensile Modulus (10^6 psi)	Poisson's Ratio	Coeff. Thermal Exp. (10^{-6} cm/cm/deg C)
		L*	B*	T*				
Cell	Silicon	2	1	0.04	9	24.5	0.358	2.3
Cover	Window Glass	2.8	2.5	0.23	10	9.1	0.2	3.2
Conductors	Copper	8	0.05	Varies***	50	16	0.33	50
Bonds	Sn 62 Solder	-	-	-	7	4.5	(0.3)	25
Adhesive	RTV 3140	2	1	0.02	0.3	(0.005)	-	293
Substrate	(1) 96% Al_2O_3	10.2	2.9	0.10	25	47	0.22	6.4
	(2) Enameled Steel	10.2	2.9	E**0.013 S**0.090	(5) 62.4	(10) 28	(0.2) 0.33	(13.9) 13.9
	(3) G10 epoxy	10.2	2.9	0.14	48 (warp) 38 (fill)	4	-	10 (warp) 15 (fill) 60 (Z, vert.)
Pottant	(1) Polyurethane (Humiseal 2B74)	2.8	2.5	0.20 (no glass) 0.056 (under glass)	0.60	(0 05)	-	100
	(2) Sylgard 184	2.8	2.5	0.030	0.90	(0.01)	-	300
	(3) Acrylic (Humiseal 1B73)	2.8	2.5	0.013	(0.8)	(0.3)	-	(80)
	(4) Nitrocellulose lacquer	2.8	2.5	0.010	(1.0)	(0.3)	-	(100)
	(5) Parylene C	2.8	2.5	0.0018	1.0	(0.5)	-	35

Note: Numbers in parenthesis are estimated.

* L = Length, B = Breadth, T = Thickness (over solar cell) ** E = Enamel, S = Carbon Steel

*** 2.5 microns (on Mo/Mn) on ceramic, 36 microns on epoxy, 25 microns on enameled steel.

Table A3

Array Systems

System No.	Substrate	Pottant	Cover
1	Ceramic	None	None
2	"	Parylene C	"
3	"	2B74 (polyurethane)	Glass
4	Enameled Steel	1B73 (acrylic)	None
5	" "	Sylgard 184	"
6	" "	2B74	Glass
7	Epoxy	Nitrocellulose Lacquer	None
8	"	2B74	"
9	"	2B74	Glass

NOTE: See Table A1 for identification of components

133

Table A4

Conditions for Accelerated Exposure
of UTS's with Nine Different
Encapsulant-Substrate Combinations

Condition No.	UV Intensity Relative to Noon Summer Sunlight	Encapsulant Temperature, °C	Relative Humidity, %
1	0.66	28	100
2	1.00	43	0
3	1.00	43	100
4	1.00	72	0
5	1.00	72	100
6	0.66	64	100
7	0	72	0
8	0	72	100

Table A5

Electrical Data on Moisture-Degraded Solar Cells

(After 72 Days at 80°C and 100% Relative Humidity)

Cell No.	Power Point, milliwatts		Power Point After Exposure, % of Original
	Original	After Exposure	
1	17.7	9.33	53
2	17.7	9.98	56
3	17.9	7 38	41
4	17.4	15.4	89
5	15.1	6.92	46
6	18 7	8.72	47

Cell No.	Current, milliamperes, at 0.350 volts		Current at 0.350 volts After Exposure, % of Original
	Original	After Exposure	
1	50.5	25.7	51
2	51.0	28.4	56
3	50.5	20.7	41
4	49.4	42.8	87
5	42.3	18.3	43
6	54.3	23.5	43

Table A6. Appearance of Encapsulant (Cover) after Accelerated Exposure for 61 Days

Code: C = clear, B = blistered, Bo = bonded to glass, Br = brown, D = dull surface, 0 = orange; sl. = slight(ly), W = water-white (colorless); Y = yellow

Encaps. System No.*	Exposure Conditions: UV Intensity, Temp., Rel. Hum.							
	0.66,28 100	1.00,43, 0	1.00,43, 100	1.00,72, 0	1.00,72, 100	0.66,64 100	0,72,0	0,72,100
1	-	-	-	-	-	-	-	-
2	C, Y	C, Y	C, Y	C, light Br	D, Y - Br	C, Y, sl. D	C, W	C, W
3	C, faint Y 100% Bo	C, faint Y 100% Bo	C, W, 100% Bo	C, faint Y 100% Bo	C, faint Y 100% Bo	C, faint Y 100% Bo	C, pale Y, 100% Bo	C, Y, 90% Bo
4	C, W	C, W	C, W	C, light Br	C, light br sl. B	C, sl. Br spots	C, W	C, W
5	C, W	C, W	C, W	C, W	C, W	C, W	C, W	C, W
6	C, faint Y, 100% Bo	C, faint Y 100% Bo	C, faint Y 100% Bo	C, faint Y 100% Bo	C, faint Y 100% Bo	C, faint Y 100% Bo	C, pale Y, 100% Bo	C, Y, 95% Bo
7	sl. cloudy, W	Y-Br, with W spots	Br, with W ridges	deep Br, with W spots	part Br, part W, B	0-Br, fine ridges	C, Y	sl. cloudy, Y-Br
8	C, faint Y	C, Y	Y, D	Y, sl. cloudy	Y, D	Y, D	C. pale 0	C, 0
9	C, W 100% Bo	C, W 100% Bo	C, W 100% Bo	C, W 100% Bo	C, W 100% Bo	C, W 100% Bo	C, pale Y, 100% Bo	C, Y, 90% Bo

*Encapsulant System No.	Substrate	Pottant/Cover
1	Ceramic	None
2	"	Parylene C
3	"	2B74 (polyurethane) + glass
4	Steel	1B73 (acrylic)
5	"	Sylgard 184
6	"	2B74 + glass
7	Epoxy	Nitrocellulose lacquer
8	"	2B74
9	"	2B74 + glass

136

Table A7   Appearance of Copper Circuitry after
Accelerated Exposure for 61 Days

Code   B = bright, B- = bright with some dark specks or stains, D = dull,
D/G = dull with gray-green spots

Encaps. System No.*	Exposure Conditions· UV Intensity, Temp., Rel. Hum.							
	0.66,28 100	1 00,43 0	1.00,43 100	1 00,72 0	1.00,72 100	0.66,64 100	0,72,0	0,72,100
1	D	D	D	D	D/G	D/G	D	most D, some B
2	D	D	D	D	D	D	most B, some D	B
3	B	B	B	B-	B-	B-	B-	B-
4	B	B	B	part B, part D	B-	B-	B	B-
5	B	B	B	B	B	B	D	B
6	B	B	B-	B	B-	B-	B	B-
7	D	D	D	D	part B, part D	D	B	D
8	B	B-	B	B-	B-	B-	B	B
9	B	B-	B-	B-	B-	B-	B	B

*Encapsulant System No.	Substrate	Pottant/Cover
1	Ceramic	None
2	"	Parylene C
3	"	2B74 (polyurethane) + glass
4	Steel	1B73 (acrylic)
5	"	Sylgard 184
6	"	2B74 + glass
7	Epoxy	Nitrocellulose lacquer
8	"	2B74
9	"	2B74 + glass

Table A8. Summary of Effects of Accelerated Exposure for 61 Days

Code. Cu = copper circuitry dull, E = encapsulant brown in color,
G = 2B74 more than 10% debonded from glass cover,
Cell = power reduced more than 10%

Encaps System No.*	Exposure Conditions. UV Intensity, Temp., Rel. Hum.							
	0.66,28,100	1.00,43,0	1.00,43,100	1.00,72,0	1.00,72,100	0.66,64,100	0,72,0	0,72,100
1	Cu	Cu	Cu	Cu	Cu	Cu	Cu	Cu
2	Cu	Cu	Cu	Cu E	Cu E	Cu		
3								
4				E	E			
5							Cu	
6						G		
7	Cu	Cu E	Cu E	Cu E Cell	E	Cu E		Cu E
8								
9								

*Encapsulant System No	Substrate	Pottant/Cover
1	Ceramic	None
2	"	Parylene C
3	"	2B74 (polyurethane) + glass
4	Steel	1B73 (acrylic)
5	"	Sylgard 184
6	"	2B74 + glass
7	Epoxy	Nitrocellulose lacquer
8	"	2B74
9	"	2B74 + glass

Table A9. Appearance of Encapsulant (Cover) after Accelerated
Exposure for 61 Days Followed by Steam Exposure for 12 Days

Code C = clear; B = blistered, Bo = bonded to glass, Br = brown, D = dull surface,
M = milky, 0 = orange, sl. = slight(ly), W = water-white (colorless); Y = yellow

Encaps. System No.*	Exposure Conditions. UV Intensity, Temp., Rel Hum.							
	0.66,28, 100	1 00,43, 0	1.00,43, 100	1.00,72, 0	1.00,72, 100	0.66,64, 100	0,72,0	0,72,100
1	-	-	-	-	-	-	-	-
2	C, Y	C, Y	C, Y	C, light Br, striated 5% lost	C, Br	C, Y	C, W	C, W
3	C, W, 5% Bo	sl cloudy, W, 95% Bo	C, nearly W 0% Bo	C, faint Y, 100% Bo,"worm tracks"	C, faint Y 90% Bo	C, faint Y 5% Bo	C, Y 30% Bo	C, Y 95% Bo
4	pale Y 90% M	Y, 10% M	Y, 20% M	Y, 10% M	C, Y, many cracks, 5% M	off-white,B 100% M/over Cell 6	C,W over Cell 3, M,B	10% M (all over Cell 6)
5	C, W, B over Cell 2	C, nearly W, some dirt	C, nearly W	C, W	C, W, some dirt	C, W, sl. B over Cell 2	C, W, B over Cell 5	C, W
6	C, faint Y 20% Bo	C, faint Y, 85% Bo	C, faint Y 20% Bo	C, faint Y 100% Bo	C, faint Y 100% Bo	C, faint Y 95% Bo	C, Y 95% Bo	C, Y, 98% Bo
7	C, Br	tan, greatly B	Br, greatly 'B'	part Br part tan, B	15% C, Br, 85% tan, B, cracked	mostly tan, "furry"	C, Y	60% C, Br, 40% tan, rough
8	sl cloudy, Y	sl cloudy, 0	sl. cloudy, 0	sl. cloudy, 0	cloudy, 0-Br	cloudy deep 0	cloudy, deep 0	sl cloudy, deep 0
9	C, W 80% Bo	C, W 100% Bo	C, W 25% Bo	C, W 95% Bo	C, W 25% Bo	C, W 30% Bo	C, W 40% Bo	C, W 25% Bo

*Encapsulant System No	Substrate	Pottant/Cover
1	Ceramic	None
2	"	Parylene C
3	"	2B74 (polyurethane) + glass
4	Steel	1B73 (acrylic)
5	"	Sylgard 184
6	"	2B74 + glass
7	Epoxy	Nitrocellulose lacquer
8	"	2B74
9	"	2B74 + glass

Table A10. Appearance of Copper Circuitry after Accelerated Exposure
for 61 Days Followed by Steam Exposure for 12 Days

Code: B = bright; B- = bright with some dark specks or stains; D = dull,
D/G = dull with gray-green spots

Encaps. System No.*	Exposure Conditions. UV Intensity, Temp , Rel. Hum.							
	0.66,28 100	1.00,43 0	1.00,43 100	1.00,72 0	1.00,72 100	0.66,64 100	0,72,0	0,72,100
1	D/G	D/G	D/G	D/G	D/G	D/G	D/G	most D, some B
2	D	D	D	D	D	D	most B, some D	B-
3	B-	B-	B-	B-	B-	part B, part D	B-	B-
4	(not visible)	D	D	D	D	(not visible)	B-	B-
5	B-	B-	B	B-	B	B	D	B
6	B-	B	B-	B	B-	B-	B	B
7	D	(not visible)	(not visible)	(not visible)	(not visible)	(not visible)	D	D
8	B	B-	B	B-	seems B (hard to see)	seems B (hard to see)	seems B (hard to see)	seems B (hard to see)
9	B	B-	B-	B-	B-	B-	B	B-

*Encapsulant System No.	Substrate	Pottant/Cover
1	Ceramic	None
2	"	Parylene C
3	"	2B74 (polyurethane) + glass
4	Steel	1B73 (acrylic)
5	"	Sylgard 184
6	"	2B74 + glass
7	Epoxy	Nitrocellulose lacquer
8	"	2B74
9	"	2B74 + glass

140

ORIGINAL PAGE IS
OF POOR QUALITY

Table A11. Summary of Effects of Accelerated Exposure for 61 Days
Followed by Steam Exposure for 12 Days

Code· Cu = copper circuitry dull, E = encapsulant brown in color and/or opaque,
G = 2B74 more than 10% debonded from glass cover, Cell = power reduced more than 10%

Encaps. System No.*	Exposure Conditions· UV Intensity, Temp., Rel. Hum.							
	0.66,28,100	1 00,43,0	1 00,43,100	1 00,72,0	1.00,72,100	0.66,64,100	0,72,0	0,72,100
1	Cu Cell**	Cu	Cu	Cu Cell**	Cu Cell**	Cu Cell**	Cu Cell**	Cu
2	Cu Cell**	Cu Cell**	Cu Cell**	Cu E	Cu E Cell**	Cu Cell**	Cell**	Cell**
3	G Cell**		G Cell**	Cell**	Cell**	-G Cell**	G Cell**	Cell**
4	Cu? Cell	Cu	Cu	Cu E	Cu E (cracked)	Cu? E Cell	E Cell	Cell
5							Cu	
6	G	G	G				Cell	
7	Cu E Cell	Cu E Cell	Cu E Cell	Cu E Cell	Cu? E Cell	Cu Cell	Cu	Cu E Cell
8								
9	G		G		G	G	G	G

*Encapsulant System No.	Substrate	Pottant/Cover
1	Ceramic	None
2	"	Parylene C
3	"	2B74 (polyurethane) + glass
4	Steel	1B73 (acrylic)
5	"	Sylgard 184
6	"	2B74 + glass
7	Epoxy	Nitrocellulose lacquer
8	"	2B74
9	"	2B74 + glass

**Cells with long circuitry path gave lower power than those with short circuitry
path in 17 of 19 cases. See Table A12

141

Table A12

Effect of Length of Circuitry Path
on Solar Cell Power after Accelerated Exposure
for 61 Days Followed by Steam Exposure for 12 Days

Substrate	Approximate Percent of Original Power	
	Shorter Circuitry Path	Longer Circuitry Path
Ceramic	99	71
↑	102	80
	69	0
	80	82
	97	0
	100	0
	103	81
	99	78
	83	0
	82	0
	97	0
	98	0
	93	4
	94	67
	87	89
	96	0
	91	0
↓	91	80
Ceramic	95	0
Enameled Steel	66	74
↑	51	51
	74	28
↓	99	86
Enameled Steel	93	4
Epoxy	90	85
↑	41	42
	36	67
	41	47
	59	28
	50	40
Epoxy	41	76

NOTE: Fraction of pairs of cells in which the longer circuitry path was
         associated with lower power   ceramic 17/19, steel 3/5, epoxy 3/7.

142

Table A13. Ratio of Final to Original Leakage Current at 18 Volts
for FET's after Accelerated Exposure for 61 Days
Followed by Steam Exposure for 12 Days

Encaps. System No.*	Exposure Conditions UV Intensity, Temp., Rel. Hum.							
	0.66,28, 100	1.00,43, 0	1.00,43, 100	1 00,72, 0	1.00,72, 100	0.66,64, 100	0,72,0	0,72,100
1	(open)	(short)	(open)	(open)	(open)	(open)	(open)	17
2	(open)	22	390	(open)	(open)	(open)	(open)	(open)
3	10^6	1.7	0.4	1.1	(open)	10^6	(open)	10^5
4	(open)	(open)	0.9	0.9	1.5	(open)	10^7	2 2
5	720	8.6	13	11	8.7	14	(open)	0.3
6	(open)	1400	10^5	10^4	10^4	10^5	(short)	10^5
7	1.0	12	0.9	0.5	360	27	2	10^6
8	1.7	10^5	1900	5000	10^5	10^4	10^6	10^4
9	700	2400	1300	0.4	305	10^4	10^4	10^4

*Encapsulant System No.	Substrate	Pottant/Cover
1	Ceramic	None
2	"	Parylene C
3	"	2B74 (polyurethane) + glass
4	Steel	1B73 (acrylic)
5	"	Sylgard 181
6	"	2B74 + glass
7	Epoxy	Nitrocellulose lacquer
8	"	2B74
9	"	2B74 + glass

Table A14. Appearance of Encapsulant .(Cover) after Accelerated Exposure for 61 Days Followed by Steam Exposure for 31 Days

Code C = clear, B = blistered, Bo = bonded to glass, Br = brown, D = dull surface, M = milky, O = orange, sl. = slight(ly); W = water-white .(colorless)-, Y = yellow

Encaps System No.*	Exposure Conditions: UV Intensity, Temp., Rel Hum.							
	0.66,28, 100	1 00,45, 0	1 00,43, 100	1.00,72, 0	1.00,72, 100	0.66,64, 100	0,72,0	0,72,100
1	-	-	-	-	-	-	-	-
2	C, pale Br	C, pale Br	C, pale Br	C,light Br, striated, 10% lost	C, pale Br	C, pale Br	C, W	C, W
3	C, deep Y, 0% Bo	C,deep Y, 5% Bo	C, deep Y, 0% Bo	C, Y 0% Bo	C, Y-Br, 0% Bo	C, deep Y, 0% Bo	C, Y-Br, 5% Bo	sl cloudy, 95% Bo
4	Y, 100% M	Y, M,except over cell 3	Y, somewhat M	white, rough,M except over cell 6	white, rough,M except over cell 3	B, M, lost over cells	C,W, sl. M over part part of cell 6	C, W over cell 3, M over cell 6
5	C, sl. tint,B over cell 2	C, sl. tint	C, sl tint	C, sl. tint	C, sl. tint	C, v. sl. tint	C, v. sl. tint	C, v. sl. tint
6	C, Y, 10% Bo	C,Y at edges, 5% Bo	C, deep Y, 10% Bo	C, Y, 2% Bo	C,Y at edges, 100% Bo	C,Y at edges, 10% Bo	C, Y, 2% Bo	C, Y 98% Bo
7	cloudy, deep Br B	tan, B, some lost over cell 6	tan, B, opaque	deep Br, B	tan, rough, opaque	tan, rough, part lost over cells	rough, opaque over part of cells	C, Br, part lost over cell 6
8	red-Br, sl., cloudy	dark red-Br, sl. cloudy	dark red-Br, sl. cloudy	dark red-Br, sl. cloudy	dark Br, nearly opaque	dark Br nearly opaque	dark red-Br, nearly opaque	dark red-Br, nearly opaque
9	C, Y, 20% Bo	C, deep Y, 10% Bo	C, Y, 2% Bo	C, Y, 5% Bo	C, Br, 5% Bo	C, Br at edges, 20% Bo	C, Br at edges, 20% Bo	Y, cloudy, 60% Bo

*Encapsulant System No..	Substrate	Pottant/Cover
1	Ceramic	None
2	"	Parylene C
3	"	2B74 (polyurethane) + glass
4	Steel	1B73 (acrylic)
5	"	Sylgard 184
6	"	2B74 + glass
7	Epoxy	Nitrocellulose lacquer
8	"	2B74
9	"	2B74 + glass

144

Table A15. Appearance of Copper Circuitry after Accelerated Exposure for
61 Days Followed by Steam Exposure for 31 Days

Code· B = bright, B- = bright with some dark specks or stains, D = dull,
D/G = dull with gray-green spots

Encaps System No.*	Exposure Conditions UV Intensity, Temp., Rel. Hum.							
	0.66,28,100	1.00,43,0	1.00,43,100	1.00,72,0	1.00,72,100	0.66,64,100	0,72,0	0,72,100
1	D/G	D/G	D/G	D/G	D/G	D/G	D/G	brown
2	D, dark.	D, dark	D, dark	D, dark	D, dark	D, dark	part B, part D and dark	B, with dark spots
3	B, with many dark spots	B, with stains	B-	B, with large dark specks	mostly dark-stained	mostly dark-stained	mostly dark-stained	part B, part stained
4	(not visible)	(not visible)	(not visible)	(not visible)	D	D	D	D
5	B-	B, with dark spots	B	D	B	slightly D	D	slightly D
6	part B, part stained	B, with dark stains	mostly dark stained	B-	B, with dark stains	part B, part stained	mostly B	mostly B
7	(not visible)	D, dark	(not visible)	(not visible)	(not visible)	(not visible)	D	D, dark
8	stained	(not visible)	(not visible)	(not visible)	(not visible)	(not visible)	(not visible)	(not visible)
9	part B, part stained	some B, most dark	B, with stains	B, with much staining	D, dark	most B, some dark	part B, part stained	part B

*Encapsulant System No	Substrate	Pottant/Cover
1	Ceramic	None
2	"	Parylene C
3	"	2B74 (polyurethane) + glass
4	Steel	1B73 (acrylic)
5	"	Sylgard 184
6	"	2B74 + glass
7	Epoxy	Nitrocellulose lacquer
8	"	2B74
9	"	2B74 + glass

Table A16 Summary of Effects of Accelerated Exposure for 61 Days
Followed by Steam Exposure for 31 Days

Code. Cu = copper circuitry dull, E = encapsulant brown in color and/or opaque, G = 2B74 more than 10% debonded from glass cover, Cell - power reduced more than 10%.

Encaps System No.*	Exposure Conditions UV Intensity, Temp , Rel. Hum.							
	0.66,28, 100	1.00,43, 0	1.00,43, 100	1.00,72, 0	1.00,72, 100	0.66,64, 100	0,72,0	0,72,100
1	Cu Cell**	Cu Cell**	Cu	Cu	Cu Cell**	Cu Cell**	Cu Cell**	Cu Cell**
2	Cu E Cell**	Cu E Cell**	Cu E Cell**	Cu E Cell**	Cu E Cell**	Cu E Cell**	Cell**	Cell**
3	G Cell**	G Cell**	G Cell**	G Cell**	Cu G Cell**	Cu G Cell**	Cu G Cell**	Cell**
4	Cu? E Cell	Cu E Cell	Cu Cell	Cu E Cell	Cu E Cell	Cu E Cell	Cu Cell	Cu E Cell
5		Cell		Cu		Cu	Cu	Cu
6	G	G	Cu G	G	Cell	G	G Cell	
7	Cu E Cell	Cu E Cell	Cu E Cell	Cu E Cell	Cu? E Cell	Cu E Cell	Cu E Cell	Cu E
8	Cu E Cell	Cu? E Cell	Cu? E Cell	Cu? E Cell	Cu? E Cell	Cu? E	Cu? E Cell	Cu? E Cell
9	G	G	G	G	Cu E, G	G	G Cell	G Cell

*Encapsulant System No	Substrate	Pottant/Cover
1	Ceramic	None
2	"	Parylene C
3	"	2B74 (polyurethane) + glass
4	Steel	1B73 (acrylic)
5	"	Sylgard 184
6	"	2B74 + glass
7	Epoxy	Nitrocellulose lacquer
8	"	2B74
9	"	2B74 + glass

**Cells with long circuitry path gave lower power than those with short circuitry path in 15 of 16 cases. See Table A17.

Table A17

Effect of Length of Circuitry Path
on Solar Cell Power after Accelerated Exposure
for 61 Days Followed by Steam Exposure for 31 Days

Substrate	Approximate Percent of Original Power	
	Shorter Circuitry Path	Longer Circuitry Path
Ceramic	97	72
	93	95
	97	91
	99	0
	44	0
	102	0
	83	0
	96	32
	50	0
	98	0
	82	0
	81	67
	74	0
	83	79
	78	0
Ceramic	93	0
Enameled Steel	64	46
	76	48
	65	65
	10	30
	37	38
	0	86
	100	48
	96	97
	96	52
	96	89
	99	96
	95	90
	84	88
	84	83
	79	82
	85	88
	94	0
	86	95
	83	0
Enameled Steel	93	95

Table A17

(Continued)

| Substrate | Approximate Percent of Original Power | |
	Shorter Circuitry Path	Longer Circuitry Path
Epoxy ↑	45	64
	54	54
	30	26
	49	53
	25	18
	99	92
	78	64
	92	94
	86	84
	87	84
	90	92
	80	81
	90	90
	80	80
	88	84
	92	94
	86	91
	88	88
	90	92
	84	86
	89	91
↓	90	82
Epoxy	95	89

NOTE· Fraction of pairs of cells in which the longer circuitry path
was associated with lower power (neglecting pairs where readings
were the same)· ceramic 15/16, steel 10/19, epoxy 9/19.

148

Table A18. Ratio of Final to Original Leakage Current at 18 Volts for FET's after Accelerated Exposure for 61 Days Followed by Steam Exposure for 31 Days

Encaps. System No.*	Exposure Conditions· UV Intensity, Temp, Rel. Hum.							
	0.66,28, 100	1.00,43, 0	1 00,43, 100	1.00,72, 0	1.00,72, 100	0.66,64, 100	0,72,0	0,72,100
1	(open)	(short)	(open)	(open)	(open)	(open)	(open)	(open)
2	(open)	1300	10^3	(open)	(open)	(open)	(open)	(open)
3	(open)	10^4	7	340	(open)	(open)	(open)	(open)
4	(open)	(short)	10^5	(open)	15	(open)	(short)	11
5	840	(open)	10^5	(open)	26	286	(open)	1.0
6	(short)	(open)	10^5	(short)	10^5	10^5	(short)	10^3
7	10	12	9	5	8	10^3	(short)	10
8	(short)	(short)	(short)	10^4	10^4	10^4	10^4	10^4
9	(short)	10^5	(short)	(short)	10^4	(short)	10^4	10^5

*Encapsulant System No.	Substrate	Pottant/Cover
1	Ceramic	None
2	"	Parylene C
3	"	2B74 (polyurethane) + glass
4	Steel	1B73 (acrylic)
5	"	Sylgard 184
6	"	2B74 + glass
7	Epoxy	Nitrocellulose lacquer
8	"	2B74
9	"	2B74 + glass

Table A19

Absorbance Data for Plastic Films

Exposed in the Solar Furnace

Plastic Film (0.13 mm. Thick)	Calorimeter Reading, cal./cm.^{2}/sec.	Exposure Time, Hours	$\log_{10}(\frac{1}{P})$, where P = Fraction of Original Transmittance at 360 nm.
Lexan 8740 (not UV-stabilized)	7.0	0.20	0.0031
	12	0.083	0.0061
	12	0 33	0.0066
	12	4.0	0.0474
	33	0.33	0.0137
	33	1.0	0.0607*
	33	2.0	0.0921
	33	4.0	0.4583
Polystyrene (clear, biaxially oriented)	7.0	0.20	0.0106
	12	0.083	0.0113
	12	0.33	0.0030
	12	4.0	0.0877
	33	0.33	0.0082
	33	1.0	0.0324
	33	2.0	0.1170
	33	4.0	0.2568

*Measured 3 days after exposure. A measurement at 11 days after exposure gave 0.0645, a 6% increase over the first determination.

150

Table A20

Tensile Test Data for Polystyrene Film
Exposed in the Solar Furnace at 1400 Suns (33 cal./cm.^{2}/sec.)

Exposure Time, hours	Breaking Stress, psi	Fraction of Original Breaking Stress
0 (control)	9,900	
	9,700	
	10,450	
	10,300	
mean:	10,088	1.00
0 33 -	9,700	
	9,400	
mean	9,550	0.95
1	8,900	
	6,100	
mean	7,500	0.74
2	5,100	
	5,100	
mean.	5,100	0.51
4	7,800	
	9,100	
mean	8,450	0 84

NOTE.   To convert to megapascals, multiply values
        in psi by 0.00689476.

151

Table A21

Tensile Test Data for Lexan Film
Exposed in the Solar Furnace at 1400 Suns (33 cal./cm ^{2}/sec.)

Exposure time, hrs.		Yield Stress, psi	Breaking Stress, psi	Ultimate Elongation, %	Fraction of Original Breaking Stress
0	(control)	8,400	10,300	116	
		8,700	8,900	111	
		8,750	10,100	116	
		9,100	10,500	115	
	means:	8,738	9,950	115	1.00
0.33		8,400	9,100	92	
		8,300	9,100	85	
	means.	8,350	9,100	89	0.91
1		7,750	7,600	80	
		-	8,050	40	
	means.	7,750	7,825	60	0.79
2		-	6,700	100	
		8,200	8,000	78	
	means:	8,200	7,350	89	0.74
4		-	2,600	-	
		-	2,500	-	
	means		2,550		0.26

NOTE   To convert to megapascals, multiply values in psi by 0.00689476.

Table A22

Effect on Encapsulant
After Exposure for 30 Days

Encaps. System No.*	Exposure Condition			
	Miami, 45°	Phoenix, 45°S	EMMA	EMMAQUA
1	—	—	—	—
2	Clear yellow	Clear yellow	Clear deep yellow	Deep yellow, v. dull surface
3	Clear, v. sl. tint	Clear, v. sl. tint	Clear, v. sl tint	Clear, v sl. tint
4	Clear, color-less	Clear, color-less	Clear, color-less	
5	Clear, color-less	Clear, color-less	Clear, color-less	
6	Clear, v. sl. tint	Clear, v sl. tint	Clear, v. sl. tint	
7	Clear, color-less	Clear, color-less	Clear, color-less	Clear, color-less
8	Yellow, very sl. cloudy	Clear, yellow	Yellow, very sl. cloudy	Yellow, dull surface
9	Clear, color-less	Clear, color-less	Clear, color-less	Clear, color-less

*Encapsulant System No.	Substrate	Pottant/Cover
1	Ceramic	None
2	"	Parylene C
3	"	2B74 (polyurethane) + glass
4	Steel	1B73 (acrylic)
5	"	Sylgard 184
6	"	2B74 + glass
7	Epoxy	Nitrocellulose lacquer
8	"	2B74
9	"	2B74 + glass

153

Table A23

Effect on Circuitry
After Exposure for 30 Days

Encaps. System No.*	Exposure Condition			
	Miami, 45°	Phoenix, 45°S	EMA	EMAQUA
1	Dull	Dull	Dull	Part· dk brown, part bright
2	Dull	Dull	Dull,	Dark brown
3	Bright	Bright	Bright	Bright
4	Bright	Bright	Bright	
5	Bright	Bright	Bright	
6	Bright	Bright	Bright	
7	Dull	v. sl. dull	Bright	Sl. brown spots
8	Bright	Bright	Sl. dark-brown corrosion	Bright
9	Bright	Bright	Sl. dark-brown corrosion	Sl. brown spots

*Encapsulant System No.	Substrate	Pottant/Cover
1	Ceramic	None
2	"	Parylene C
3	"	2B74 (polyurethane) + glass
4	Steel	1B73 (acrylic)
5	"	Sylgard 184
6	"	2B74 + glass
7	Epoxy	Nitrocellulose lacquer
8	"	2B74
9	"	2B74 + glass

154

Table A24

Effect on Encapsulant
After Exposure for 60 Days

Encaps. System No.*	Exposure Condition			
	Miami, 45°	Phoenix, 45°S	EMMA	EMMAQUA
1	—	—	—	—
2	Clear yellow	Clear yellow	Clear deep yellow	Deep Yellow, v. dull surface
3	Clear, v. sl. tint	Clear, sl tint	Clear, v sl. tint	Clear, v sl tint
4	Clear, color-less	Clear, color-less	Clear, color-less	
5	Clear, color-less	Clear, color-less,sl. dusty	Clear, color-less	
6	Clear, v. sl tint	Clear, sl. tint	Clear, v. sl. tint	
7	Clear, color-less	Clear, color-less,sl. dusty	Clear, color-less	V. sl. cloudy, color-less
8	Yellow, very sl. cloudy	Clear, yellow, sl. dusty	Yellow, v. sl. cloudy	Yellow, v. dull surface
9	Clear, color-less	Clear, color-less	Clear, color-less	Clear, colorless. Debonding under glass. 0, 80%

*Encapsulant System No.	Substrate	Pottant/Cover
1	Ceramic	None
2	"	Parylene C
3	"	2B74 (polyurethane) + glass
4	Steel	1B73 (acrylic)
5	"	Sylgard 184
6	"	2B74 + glass
7	Epoxy	Nitrocellulose lacquer
8	"	2B74
9	"	2B74 + glass

155

Table A25

Effect on Circuitry
After Exposure for 60 Days

Encaps. System No.*	Exposure Condition			
	Miami, 45°	Phoenix, 45°S	EMMA	EMMAQUA
1	Dull	Dull	Dull	Most dk brown,a few spots bright
2	Dull	Dull	Dull	Dark-brown
3	Bright	Bright	Bright	Bright
4	Bright	Bright	Bright	
5	Bright	Bright	Bright	
6	Bright	Bright	Bright	
7	Dull	Sl. Dull	Bright with sl. brown specks	Some brown specks
8	Bright	Bright	Slight dark-brown specks	Bright
9	Bright	Bright	Some dark-brown stains	Slight brown stains & specks

*Encapsulant System No.	Substrate	Pottant/Cover
1	Ceramic	None
2	"	Parylene C
3	"	2B74 (polyurethane) + glass
4	Steel	1B73 (acrylic)
5	"	Sylgard 184
6	"	2B74 + glass
7	Epoxy	Nitrocellulose lacquer
8	"	2B74
9	"	2B74 + glass

156

Table A26

Effect on Encapsulant
After Exposure for 90 Days

Encaps. System No.*	Exposure Condition			
	Miami, 45°	Phoenix, 45°S	EMMA	EMMAQUA
1	—	—		
2	Clear, yellow	Clear, yellow		
3	Clear, v sl. tint	Clear, v. sl tint		
4	Clear, color-less	Clear, color-less		
5	Clear, color-less	Clear, color-less		
6	Clear, v sl. tint, yellow at edges	Clear v. sl. tint		
7	Clear, color-less	Clear, color-less		
8	Clear, yellow	Clear, pale yellow		
9	Clear, color-less	Clear, color-less		

*Encapsulant System No.	Substrate	Pottant/Cover
1	Ceramic	None
2	"	Parylene C
3	"	2B74 (polyurethane) + glass
4	Steel	1B73 (acrylic)
5	"	Sylgard 184
6	"	2B74 + glass
7	Epoxy	Nitrocellulose lacquer
8	"	2B74
9	"	2B74 + glass

Table A27

Effect on Circuitry
After Exposure for 90 Days

Encaps. System No.*	Exposure Condition			
	Miami, 45°	Phoenix, 45°S	EMMA	EMMAQUA
1	Dull	Mostly dull		
2	Dull	Dull		
3	Bright	Bright, with sl. dark stains		
4	Bright	Bright		
5	Bright	Bright		
6	Bright	Bright		
7	Dull	Dull		
8	Bright	Bright		
9	Bright with some stains	Bright with slight stains		

*Encapsulant System No.	Substrate	Pottant/Cover
1	Ceramic	None
2	"	Parylene C
3	"	2B74 (polyurethane) + glass
4	Steel	1B73 (acrylic)
5	"	Sylgard 184
6	"	2B74 + glass
7	Epoxy	Nitrocellulose lacquer
8	"	2B74
9	"	2B74 + glass

158

Table A28

Electrical Data on UTS's (First Study)

after 420 Days Outdoor Exposure

Exposure Condition	Lexan Cover		No Cover		Tedlar Cover	
	FET Ratio*	Solar Cell Power, % of Original**	FET Ratio*	Solar Cell Power, % of Original**	FET Ratio*	Solar Cell Power, % of Original**
Phoenix, 45°S	0.3	97, 106	0.3	98, 99	8.6	99, 103
Miami, 45°S	0 3	96, 99	0.2	80, 81	0 1	59, 77
EMMA	0.3	88, 91	0.3	92, 93	0.1	95, 98
EMMAQUA	0.3	97, 105	0.2	93, 99	0.1	96, 102

*Ratio of final to original leakage current at 18 volts for a field
effect transistor (FET) embedded in the Sylgard 184 pottant.

**From the power point (maximum power) on the IV curve measured by
Optical Coating Laboratory, Inc

159

Table A29

Electrical Data on UTS's (First Study)
after 540 Days Outdoor Exposure

Exposure Condition	Lexan Cover		No Cover		Tedlar Cover	
	FET Ratio*	Solar Cell Power % of Original**	FET Ratio*	Solar Cell Power % of Original**	FET Ratio*	Solar Cell Power %, of Original**
Phoenix, 45°S	4.6	87, 93	3.7	86, 88	2.5	91, 87
Miami, 45°S	1.4	56, 75	0.9	75, 68	0.3	57, 81
EMMA	1.7	90, 86	0.4	79, 79	0.1	93, 69
EMMAQUA	0.5	88, 95	0.01	89, 93	0.04	91, 91

*Ratio of final to original leakage current at 18 volts for a
field effect transistor (FET) embedded in the Sylgard 184 pottant.

**From the power point (maximum power) on the IV curve measured by
Optical Coating Laboratory, Inc.

Table A30

Effect on FET's (Ratio of Final to Original
Leakage Current @ 18 V)
After Exposure for 30 days

Encaps. System No.*	Exposure Condition			
	Miami, 45°	Phoenix, 45°S	EMMA	EMMAQUA
1	640	—	—	0.9
	—	—	—	—
2	4,300	—	0.6	2.2
	30,000	1,900	12	92
3	1.2	—	0.4	0.4
	0.7	—	0.8	71
4	0.8	0.7	0.7	
	0 6	0.9	1.3	
5	1 7	0.3	0.5	
	1.4	1 0	0.9	
6	1 4	0.7	0.5	
	2.0	0.7	—	
7	0 2	0.7	0.3	0.9
	1.4	0 3	0.8	2 4
8	1.1	1.6	0.8	1.1
	1 8	0.2	0.6	0.6
9	1.3	0.3	0.6	0.6
	0.4	0.2	0.7	0.8

*Encapsulant System No.	Substrate	Pottant/Cover
1	Ceramic	None
2	"	Parylene C
3	"	2B74 (polyurethane) + glass
4	Steel	1B73 (acrylic)
5	"	Sylgard 184
6	"	2B74 + glass
7	Epoxy	Nitrocellulose lacquer
8	"	2B74
9	"	2B74 + glass

161

Table A31

Effect on FET's (Ratio of Final to Original
Leakage Current @ 18 V)
After Exposure for 60 days

Encaps. System No.*	Exposure Condition			
	Miami, 45°	Phoenix, 45°S	EMMA	EMMAQUA
1	73,000	0 5	—	—
	—	0 6	—	—
2	200,000	780	0.9	1,700
	—	1,800	1.4	1,800
3	100	1.0	1.4	0.6
	0.6	6.7	2.0	0.8
4	0.6	0 7	1.0	
	0.4	1 1	0.9	
5	1.4	0.7	0.8	
	1.0	0.5	1 1	
6	1.0	0.8	0.6	
	1 1	0.8	0.8	
7	2.9	0.4	1.0	1,700
	0.4	0.6	1.0	—
8	0.4	1.2	1.3	1.4
	1.2	0.8	1.1	0.5
9	2.9	0.8	1.0	0.4
	1.0	0.6	0.7	0 5

*Encapsulant System No.	Substrate	Pottant/Cover
1	Ceramic	None
2	"	Parylene C
3	"	2B74 (polyurethane) + glass
4	Steel	1B73 (acrylic)
5	"	Sylgard 184
6	"	2B74 + glass
7	Epoxy	Nitrocellulose lacquer
8	"	2B74
9	"	2B74 + glass

Table A32

Effect on FET's (Ratio of Final to Original Leakage Current @ 18 V) After Exposure for 90 days

Encaps. System No.*	Exposure Condition			
	Miami, 45°	Phoenix, 45°S	EMMA	EMMAQUA
1	— —	— 42		
2	260 790	188 194		
3	1.2 2.1	1.2 1.1		
4	— —	0.9 —		
5	5.3 2.1	1.3 1.2		
6	3.6 10^5	1 0 1.1		
7	0.4 1.0	0.9 0.9		
8	1 0 0.9	0 8 0.9		
9	0.7 1 0	0.7 1.1		

*Encapsulant System No.	Substrate	Pottant/Cover
1	Ceramic	None
2	"	Parylene C
3	"	2B74 (polyurethane) + glass
4	Steel	1B73 (acrylic)
5	"	Sylgard 184
6	"	2B74 + glass
7	Epoxy	Nitrocellulose lacquer
8	"	2B74
9	"	2B74 + glass

163

Table A33

Maximum Solar Cell Power vs. Time for
Outdoor Exposure of Array System No. 1

Pottant/Cover: None

Substrate. Ceramic

Exposure Time, Days	Maximum Power, Fraction of Original*							
	Phoenix, 45°S		Miami, 45°S		EMMA		EMMAQUA	
	P.P.	0.35 V	P.P.	0.35 V	P.P.	0.35 V	P.P.	0.35 V
30	1.10	1.05	1.16	1 12	1.23	1.17	1.02	1.00
	1 33	1.33	1.09	1.05	1.04	1 04	1.03	1.02
	1.02	1.02	1 03	1.02	1 08	1 08	1.02	1.02
	1.03	1.03	1.02	1.02	1.05	1.03	1.05	1.03
	1.12	1.11	1 08	1.05	1.10	1.08	1.03	1.02
60	1.14	1.14	0.76	0 77	0.90	0.89	1 01	1.03
	0.92	0.91	0.98	0.98	0.94	0.97	0.98	1.01
	0.85	0.84	0.80	0.79	1.06	1.07	0.80	0.78
	1.05	1.04	0.78	0.76	1.03	1.03	0.93	0.95
	0.99	0 98	0 83	0 83	0.98	0.99	0.93	0 94
90	0.76	0.75	0.90	0.91				
	1.67	1.82	0.72	0 67				
	1.02	1.01	0.71	0.68				
	1.04	1.03	0.87	0.85				
	1.12	1 15	0.80	0.78				

* P.P.   = based on power point data.
0.35 V = based on current at 0.350 volts.
(Means appear under the 4 replicates.)

164

Table A34

Maximum Solar Cell Power vs Time for
Outdoor Exposure of Array System No. 2

Pottant/Cover· Parylene C

Substrate: Ceramic

Exposure Time, Days	Maximum Power, Fraction of Original*							
	Phoenix, 45°S		Miami, 45°S		EMMA		EMMAQUA	
	P.P.	0.35 V	P.P.	0.35 V	P.P.	0.35 V	P.P.	0.35 V
30	1.00	0.98	1.02	1 01	0.98	0.98	1.04	1.04
	1.00	1.00	1.17	1.20	1.03	0.99	1.07	1.08
	0.96	0.96	1.41	1.43	0.92	0 92	0.96	1.03
	1 01	1 00	1 01	1.02	1.00	1.00	1.05	1.05
	0.99	0.99	1.15	1.17	0.98	0 97	1.03	1.05
60	0.95	0.94	0.94	0.95	0.99	0 99	1.02	1.04
	0.95	0.94	0.80	0.76	0 95	0.95	1.03	1.04
	0 95	0.95	0.54	0.50	1.01·	1 02	0.77	0.77
	1.56	1.68	0.64	0.58	1 00	1.00	0.82	0.75
	1.10	1.13	0 75	0.70	0.99	0.99	0.91	0 90
90	0 81	0.76	0.88	0 90				
	0.78	0.72	0.86	0.82				
	1.20	1 00	0 85	0.86				
	1 01	1.00	0 79	0 72				
	0.95	0.87	0.85	0 83				

* P.P.· = based on power point data.

0.35 V = based on current at 0.350 volts.

(Means appear under the 4 replicates.)

165

Table A35

Maximum Solar Cell Power vs. Time for
Outdoor Exposure of Array System No. 3

Pottant/Cover: 2B74 + glass

Substrate: Ceramic

Exposure Time, Days	Maximum Power, Fraction of Original*							
	Phoenix, 45°S		Miami, 45°S		EMMA		EMMAQUA	
	P.P.	0.35 V	P.P.	0.35 V	P.P.	0.35 V	P.P.	0.35 V
30	0.99	0 98	1.11	1.07´	1.02	1.01	1 05	1.03
	1.00	0.99	1 02	1 00	1 33	1.01	1 03	1.03
	1.01	1.01	0.99	1.00	1.03	1.01	0.99	1.00
	1.36	1.38	1 01	1.01	1.03	1.05	1.02	1.02
	1.09	1.09	1 03	1 02	1 10	1 02	1.02	1.02
60	0.95	0.94	0.96	0.99	1.03	1.01	1.02	1.02
	0.83	0.77	0.70	0.64	0.79	0.77	1.09	1.03
	0.77	0.76	0.81	0.79	0.91	0.93	1 00	1.02
	1.47	1 59	0.86	0.84	0 85	0.82	1.00	0.99
	1.01	1 02	0 83	0.82	0.90	0 88	1.03	1.02
90	0.90	0.92	0.86	0.89				
	1.00	0.98	0.98	0.97				
	1.03	1.04	0.87	0.87				
	0.95	0.94	0.94	0 85				
	0.97	0.97	0.91	0.90				

* P.P. = based on power point data.

0.35 V = based on current at 0.350 volts.

(Means appear under the 4 replicates.)

166

Table A36

Maximum Solar Cell Power vs. Time for

Outdoor Exposure of Array System No. 4

Pottant/Cover: Acrylic lacquer

Substrate   Enameled steel

Exposure Time, Days	Maximum Power, Fraction of Original*					
	Phoenix, 45°S		Miami, 45°S		EMMA	
	P.P.	0.35 V	P.P.	0.35 V	P.P.	0.35 V
30	1.04	1.05	1 03	1 03	1.04	1.03
	1.05	1 04	1.04	1.03	1.03	1.02
	1.03	1.02	0 99	0 99	1.05	1.03
	0.99	0 98	1.02	1.01	1.02	1.01
	1 03	1.02	1 02	1.02	1.04	1.02
60	1.01	1 00	1.04	1.02	1.04	1.05
	1.02	1.01	1.06	1.04	0.98	0.99
	1.01	1 00	0.97	0 99	1.02	1.01
	1.00	1.01	1.01	1.01	1 00	1.00
	1 01	1.01	1.02	1.02	1.01	1 01
90	1.03	1.01	1.03	1.03		
	0.98	0.99	1 03	0.98		
	1.01	1.00	0.96	0.97		
	1 03	1.01	0.97	0 97		
	1 01	1.00	1 00	0.99		

* P.P   = based on power point data.

0.35 V = based on current at 0.350 volts.

(Means appear under the 4 replicates.)

Table A37

Maximum Solar Cell Power vs. Time for

Outdoor Exposure of Array System No. 5

Pottant/Cover· Sylgard 184

Substrate· -Enameled steel

Exposure Time, Days	Maximum Power, Fraction of Original*					
	Phoenix, 45°S		Miami, 45°S		EMMA	
	P.P.	0.35 V	P.P.	0.35 V	P.P.	0.35 V
30	1.03	1.03	1.05	.0.03	1.01	1.01
	1 04	0.02	1.05	1 05	1.01	1 00
	1.00	0.99	0.99	0 98	1.01	1.00
	1.01	1.00 ·	1.19	0.99	1.01	1 00
	1.02	1.01	1.07	1.01	1 01	1.00
60	0.99	·1.02	1.01	1.00	1.02	1.02
	1.02	1.05	1.03	1.03	1.03	1.03
	1.01	0 98	0.89	0.91	0.98	0.98
	0.99	1.01	0 99	0.99	1.00	1.00
	1.00	1.02	0 98	0.98	1.01	1.01
90	0.98	0.98	1 01	1 02		
	0.95	1.00	1.02	1 02		
	0.98	0 98	0.93	0.94		
	1.04	1.02	0.98	0.98		
	·0.99	1.00	0.99	0.99		

* P.P.· = based on power point data.

- 0.35 V = based on current at 0.350 volts.

(Means appear under the 4 replicates.)

168

Table A38

Maximum Solar Cell Power vs. Time for
Outdoor Exposure of Array System No. 6

Pottant/Cover: 2B74 + glass

Substrate: Enameled steel

Exposure Time, Days	Maximum Power, Fraction of Original*					
	Phoenix, 45°S		Miami, 45°S		EMMA	
	P.P.	0.35 V	P.P.	0.35 V	P.P.	0.35 V
30	1.04	1 04	1.07	1 05	1.02	0.99
	1.02	1.03	1.10	1 11	1.02	1 01
	1.01	1 01	1 00	1.00	1.05	1.03
	1 03	1 03	0.99	1 00	1 03	1 02
	1.03	1.03	1 04	1.04	1.03	1.01
60	1.02	1.01	1.06	1.04	1.06	1.08
	1.03	1.03	0.98	0.98	1.11	1.06
	1.07	1 01	0.95	0 96	1.00	1.01
	1.03	1.03	1.03	1 02	1.04	1 05
	1 04	1.02	1.01	1.00	1.05	1.05
90	1.00	1.00	1.04	1 04		
	1.01	1.02	1.05	1.06		
	1.03	1.02	0 97	0 98		
	1 02	1 03	0.99	1.02		
	1.02	1.02	1.01	1.03		

* P.P. = based on power point data.

0.35 V = based on current at 0.350 volts.

(Means appear under the 4 replicates.)

Table A39

Maximum Solar Cell Power vs. Time for
Outdoor Exposure of Array System No. 7

Pottant/Cover: Nitrocellulose lacquer

Substrate. Epoxy

Exposure Time, Days	Maximum Power, Fraction of Original*							
	Phoenix, 45°S		Miami, 45°S		EMMA		EMMAQUA	
	P.P.	0.35 V	P.P.	0.35 V	P.P.	0.35 V	P.P.	0.35 V
30	1.01	1.00	0.99	0.99	0.97	0.96	1.66	1.10
	1.00	0.99	1.01	0.99	1.00	0.98	1.11	1 08
	0 98	0.99	0.96	0.97	0.85	0.84	1.02	0.99
	0.99	0 98	1.00	0.99	1.01	0.98	0.98	0.98
	1.00	0.99	0.99	0.98	0.96	0.94	1.07	1.04
60	1.03	1.02	0.97	0 97	0.96	0.98	0.99	0 99
	1.05	1 03	0.99	0.98	0.98	1 01	0.98	0 98
	1.01	0.99	0.93	0 94	0.99	0.99	0 95	0.98
	0.95	0 96	0.98	0.97	0.92	0.93	0.98	0.99
	1.01	1.00	0.97	0 97	0.96	0 98	0 98	0.99
90	0.90	0.94	0.97	0 96				
	0.99	0.98	0.95	0.96				
	0 98	0.98	0.90	0.91				
	0.99	0 99	0.73	0.72				
	0.97	0 97	0 89	0 89				

* P.P. = based on power point data.

0.35 V = based on current at 0.350 volts.

(Means appear under the 4 replicates.)

170

Table A40

Maximum Solar Cell Power vs. Time for
Outdoor Exposure of Array System No. 8

Pottant/Cover: 2B74

Substrate: Epoxy

Exposure Time, Days	Maximum Power, Fraction of Original*							
	Phoenix, 45°S		Miami, 45°S		EMMA		EMMAQUA	
	P.P.	0.35 V	P.P.	0.35 V	P.P.	0.35 V	P.P.	0.35 V
30	1 00	0 98	0.98	0.99	1 01	0.98	1.17	1.11
	0.99	0.98	0.97	1.00	1.02	0.99	1.16	1.15
	1.00	0.99	1.02	1 00	0.99	0.98	0.99	0 98
	1.00	0.99	1.01	0.99	1.06	1.01	1.02	1.00
	1 00	0 99	1 00	1 00	1.02	0 99	1.08	1.06
60	1.00	1 01	1 01	1.00	1.01	1.04	1.10	1.09
	1.03	1.03	1.15	1.12	1.01	1.03	1 04	1.05
	0.97	1 00	0.95	0.99	0.99	1.00	0 99	1.01
	1.04	1.04	1.00	0.99	1.00	1.01	1.02	1.04
	1 01	1.02	1 04	1.02	1.00	1 02	1 04	1.05
90	0 87	0.90	0.97	0.96				
	1 02	1 02	1.02	1.02				
	1.01	1.00	0.95	0.96				
	1.03	1.03	-	-				
	0 98	0.99	0.98	0 98				

* P.P. = based on power point data.
0.35 V = based on current at 0.350 volts.
   (Means appear under the 4 replicates.)

171

Table A41

Maximum Solar Cell Power vs. Time for
Outdoor Exposure of Array System No. 9

Pottant/Cover: 2B74 + glass

Substrate: Epoxy

Exposure Time, Days	Maximum Power, Fraction of Original*							
	Phoenix, 45°S		Miami, 45°S		EMMA		EMMAQUA	
	P.P.	0.35 V	P.P.	0.35 V	P.P.	0.35 V	P.P.	0.35 V
30	1.03	1.02	1.02	1.01	1.02	1 01	1.17	1.13
	1.03	1 02	1 03	1.02	0.93	0.96	1.16	1.13
	1.00	0.99	1.0ᵻ	1.00	1.00	0.99	1.03	1 01
	0.99	0 98	1.02	1.00	1.00	1.01	1.03	1.02
	1 01	1.00	1.02	1.01	0.99	0.99	1.10	1 07
60	1.01	1 02	1 04	1.03	0.98	1.04	1.04	1 03
	1.29	1.26	1.04	.1 02	0.97	0.98	1.03	1.05
	1.03	1.03	0.99	1.01	1.00	1.0i	0.87	0.89
	1.05	1 04	1.01	1.02	0.92	1.03	0.90	0 91
	1.10	1.09	1.02	1 02	0 97	1.02	0.96	0.97
90	0.99	1.02	0 98	1.02				
	0.86	0.87	1.01	1.02				
	1.04	1.03	1.00	0.92				
	1.04	1.04	0.97	0.99				
	0.98	0.99	0.99	0 99				

* P.P. = based on power point data.

0.35 V = based on current at 0 350 volts.

(Means appear under the 4 replicates.)

Table A42. Absorbance Data for Lexan Weathered at Phoenix, 45°S

Exposure Time, days	Start 9-12-76		Start 12-22-76		Start 6-21-77	
	360 nm	600 nm	360 nm	600 nm	360 nm	600 nm
5	0 0902	0 0547	0.0799	0.0545	0.1032	0.0683
10	0.1011	0 0586	0.0860	0.0570	0 0963	0.0572
15	0.1074	0 0596	0.0882	0 0563	0 1152	0.0648
30	0.1208	0 0628	0.0944	0.0587	0.1352	0.0704
60	0.1342	0.0631	0.1360	0.0827	0 1681	0.0706
90	0.1588	0 0678	0.1402	0.699	0.2450	0 0730
150	0.1759	0 0678	0.2212	0 0745	0.3154	0.0693
210	0.2610	0.0724	0.4377	0.0921	0.3692	0 0681
300	0.5991	0.0869	0 8547	0 1280	0.5344	0.0748
420	1.0692	0.1408	1.0564	0 1721		
540	1.1556	0 1445				

$$A_{360} - A_{600} - 0.0309$$

Exposure Time, days				
5	0 0046		-	0 0040
10	0 0116		-	0 0082
15	0.0169		0 0010	0 0195
30	0.0271		0 0048	0.0339
60	0.0402		0 0224	0 0666
90	0.0601		0 0394	0.1411
150	0.772		0 1158	0.2152
210	0.1577		0.3147	0.2702
300	0 4813		0.6958	0 4287
420	0 8975		0 8534	
540	0 9802			

Table A43. Absorbance Data for Lexan Weathered at Miami, 45°S

Exposure Time, days	Start 9-1-76		Start 12-22-76		Start 6-21-77	
	360 nm	600 nm	360 nm	600 nm	360 nm	600 nm
0	0.0947	0 0638	-	-	-	-
5	0.0922	0.0568	0 0820	0 0561	0.1102	0.0720
10	0.0990	0.0582	0.0934	0 0619	0.1230	0.0820
15	0.1142	0.0613	0 1105	0 0723	0.1112	0.0655
30	0.1202	0.0624	0.1261	0 0783	0.1262	0.0651
60	-	-	0.1486	0.0837	0.1681	0.0706
90	0.1710	0 0749	0.1668	0.0775	0.1906	0.0640
150	0.2003	0.0712	0.2432	0.0781	0.2817	0.0777
210	0.3014	0.1009	0.3852	0.0713	0.3448	0.0748
300	0.5209	0.0916	0.7436	0.1105	0,5510	0.0775
340			0.7774*	0.1027		
379	0.8895*	0.1593				

	$A_{360} - A_{600} - 0.0309$					
5	0.0045		-		0.0073	
10	0.0099		0.0006		0.0101	
15	0 0220		0.0073		0.0148	
30	0.0269		0.0169		0.0302	
60	-		0.0340		0.0666	
90	0.0652		0.0584		0.0957	
150	0.0982		0.1342		0.1731	
210	0.1696		0.2830		0.2391	
300	0.3984		0.6022		0.4426	
340	-		0.6438			
379	0.6993		-			

*Sample embrittled; test ended.

174

Table A44. Absorbance Data for Lexan Weathered
on the EMMA and EMMAQUA

| Exposure time, days | Start 9-12-76 | | | |
| | EMMA | | EMMAQUA | |
	360 nm	600 nm	360 nm	600 nm
1	0.0900	0.0539	0 0940	0.0614
2	0 1063	0 0603	0 0912	0 0565
5	0 1043	0 0561	0 1031	0.0622
10	0.1522	0 0842	0 1334	0.0747
30	0 2128	0 0803	0 2352	0.0854
90	0.4622	0 1234	0 6341	0.1791
150	0 6359	0 1513	0 9084	0.2417
210	1.3240	0 2458	1 9190	0.6512
300	2.3380	0.5331	2.6780*	1.5230
420	2 641*	0 8261		

	$A_{360} - A_{600} - 0\ 0309$			
1	0.0052		0 0017	
2	0.0151		0.0038	
5	0.0173		0 0100	
10	0.0371		0 0278	
30	0 1016		0.1189	
90	0.3079		0.4241	
150	0.4537		0 6358	
210	1 0473		1.2369	
300	1.7740		1 1241	
420	1.6840	-	-	

*Sample embrittled, test ended.

175

Table A45

Monthly Rate Factors for Lexan Based on Early Seasonal Absorbance Data

Exposure Site	Date Exposure Started	Early Exposure Data		Time, Days, to Reach $\log_{10}(\frac{1}{P})$* = 0.02	Monthly Rate Factor = Reciprocal of Last Column Divided by 0.0187
		$\log_{10}(\frac{1}{P})$*	Time, Days		
Phoenix	12/22	0.0224	60	54	1.0
	9/12	0.0271	30	22	2.4
	6/21	0.0195	15	15	3.6
Miami	12/22	0.0340	60	35	1.5
	9/1	0.0269	30	22	2.4
	6/21	0.0302	30	20	2.7

*where P = fraction of original transmittance at 360 nm.

176

Table A46 Tensile Test Results on Lexan after Outdoor Exposure

Exposure Conditions	Exposure Time, days	Yield Stress (psi)	Breaking Stress (psi)	Ultimate Elongation (%)	Fraction of Original Breaking Stress	Fraction of Original Ultimate Elongation
Phoenix, 45°S						
(start 9/21/76)	420	-	1277	0	0 13	0
(start 12/22/76)	300	-	1278	0	0.13	0
(start 6/21/77)	90	8076	7436	77	0 78	0.95
	150	7827	7409	72	0.78	0 89
	210	8223	7365	68	0.77	0 84
Miami, 45°S						
(start 12/22/76)	300	-	1034	0	0.11	0
	340	-	238	0	0.025	0
(start 6/21/77)	90	8112	7522	76	0.79	0.94
	150	8040	6229	68	0.65	0.84
	210	7752	6777	92	0.71	1.14

177

Table A47

Molecular Weight Determinations on Weathered Lexan by
Gel Permeation Chromatography (GPC)

Exposure Conditions	Peak Molecular Weight	$\overline{Mw}$ (Weight Average Mol. Wt)	$\overline{Mn}$ (Number Average Mol Wt)	D (Dispersity = $\overline{Mn}/\overline{Mn}$)
Unexposed (control)	110,000	96,000	24,300	4 0
Phoenix, 45°S, for 540 days starting 9/12/76	95,000	80,000	13,000	6.2
Solar Furnace, 33 cal./cm.^{2}, 4 hours	40,000	36,800	6,240	5 9

METHOD

The samples were dissolved in chloroform. Standards for the calibration
are polystyrene (Waters and Associates)   No Lexan calibration standards
were available. Calculations were based on Waters Bulletin DS047.

Instrument - Waters 6000 A pump, U6K injector
Columns   - Waters μStyragel 10^5A, 10^3A, 500A
Carrier   - Tetrahydrofuran, nonstabilized UV
Chart   - 1 0 min/cm
Detector   - Beckman Model 24 Spectrophotometer set at 230 nm and 1.0 AUFS

Table A48 . Absorbance Values for Exposed Tedlar

Exposure Conditions	A_{360}	A_{600}
Unexposed	0 1297	0.0807
Accelerated test, 1.00 rel UV, 60.3°C, 0% relative humidity, 32 days	0 1161	0.0715
Same, but 100% relative humidity	0.1375	0.0734
Phoenix, 45°S, start 9/12/76, 540 days	0.1125	0.0681
Miami, 45°S, start 9/1/76, 540 days	0.1408	0.0843
EMMA, start 9/12/76, 540 days	0.1149	0.0681
EMMAQUA, start 9/12/76, 540 days	0.1674	0.0900

Table A49

Tensile Properties of Tedlar

After 540 Days Outdoor Weathering

Condition	Yield Stress, psi	Breaking Stress, psi	Ultimate Elongation, %	Fraction of Original Breaking Stress	Fraction of Original Ultimate Elongation
Control (unweathered)	4,786	14,700	86	1.00	1.00
Phoenix, 45°S, start 9/12/76	5,208	13,466	71	0.92	0 83
Miami, 45°S, start 9/1/76	5,000	11,410	72	0.78	0.84
EMMA, start 9/12/76	5,083	11,175	60	0 76	0.70
EMMAQUA, start 9/12/76	4,925	12,225	66	0.83	0.77

NOTE   Values are means of 4-7 replicates. To convert to
        megapascals, the values in psi are multiplied by 0 00689476.

180

APPENDIX B

APPENDIX B

DETAILS OF PREDICTIONS AND CALCULATIONS
FOR PROPERTIES OF LEXAN AND POLYSTYRENE FILMS
AFTER WEATHERING

181

1   Prediction of Polystyrene Yellowing Based Upon Accelerated Exposure Data
    (Weibull Model, Graphical Methods)

a. Accelerated Exposure Data (Table B1)

Fraction of original transmittance at 360 nm is plotted against exposure

time in Figures B1-B4   The plots represent different conditions of temperature

and UV intensity. Absorbance values for films were measured at 360 nm (A_{360})

and 600 nm (A_{600}) The A_{600} represents light lost by reflection and scattering,

so the corrected $A_{360} = A_{360} - A_{600}$. To obtain the increase in corrected A_{360}

due to yellowing, the corrected A_{360} for a control (unweathered) must be sub-

tracted   In the case of polystyrene, $A_{360} - A_{600}$ for the control = 0.0139.

Then, the increase in A_{360} due to yellowing = $A_{360} - A_{600} - 0.0139$. This

quantity = $\log (\frac{1}{P})$, where P = fraction of original transmittance at 360 nm

Since the data points for different humidity levels fall along the same line,

it is concluded that humidity has a negligible role in the yellowing reaction

of polystyrene   This fact simplifies subsequent calculations and predictions.

Since the slope of the line in each figure is 0 90, it is assumed that β in

the following Weibull model is constant for all values of UV intensity and

temperature

$$\log_{10} (\frac{1}{P}) = (\frac{\lambda}{2.3}) t^{\beta}$$

t   =   exposure time

λ   =   Weibull scale factor, analogous to a reaction rate constant

β   =   Weibull shape parameter

Note that when t = 1, $\frac{\lambda}{2.3} = \log_{10} (\frac{1}{P})$. Thus, we find λ from the intercept of

the line at t = 1

From the graphs (Figures B1 through B4 , the following values of "rate

constants" were computed·

Rel. UV Intensity	Temp., °C	$\dfrac{1}{Temp., °K}$	$\lambda/2.3$
0.66	18.3	0.00343	0.00108
	55.3	0.00305	0.00173
1.00	26.1	0.00334	0 00177
	60 3	0.00300	0 00245

b. Assignment of Generalized "Rate Constants" to "Environmental Cells"

Since humidity need not be considered as a factor in polystyrene yellowing, environmental cells are squares (rather than cubes) and the dimensions are temperature and insolation.

To compute the values of λ, the following method was used. First, an Arrhenius type relation was assumed between $\lambda/2.3$ and absolute temperature. Then experimental values of $\lambda/2.3$ were plotted against $1/T(°K)$ in Figure B5 The same data are shown in the following table

T, °C	1/T (°K)	1000 $\lambda/2.3$	
		0.66 UV Intensity	1.00 UV intensity
0	0.00366	0.68	1.10
5	0.00360	0.77	1.24
10	0.00353	0.93	1.40
15	0.00347	1.00	1.52
20	0.00341	1.11	1 63
30	0 00330	1 30	1 85
40	0.00319	1.48	2.07

Next, these data were plotted in Figures B6 and B7.

Approximate values from Figure B7 were used to construct the matrix of Table B1. Each "cell" has the dimensions of 1°C and 0 1 UV intensity. The UV intensity at noon in July was defined as 1.00, because our accelerated weathering chamber had the same integrated UV intensity as noon sunshine in Anaheim.

183

c. Miami Weather Data

The next step was to define Miami weather conditions. Inspection of 3-hourly data for Miami showed that the maximum daily temperature holds approximately through the afternoon. Furthermore, the mean daily temperature occurs approximately in the 7 - 9 AM period. On this basis, the temperatures in Table B3 were assigned.

Next, UV intensities were estimated. Our outdoor tests had shown a great difference in yellowing rate in winter vs. summer. Therefore, the data given by Reference B1(pg 137) were considered a reasonable approximation. The intensity of integrated UV at wavelengths less than 313 nm for each month of the year is shown in Table B4. The validity of using this data is the critical assumption in this calculation, but the correlations were good, as will be seen. To apportion the UV intensities among the 5 arbitrary 2-hour periods of the day, the data of Table B5 were used. The relative UV intensity numbers (based on noon July = 1.00) then were copied from Table B4 into Table B3.

d Assignment of Generalized "Rate Constants" to Miami by Month and Time of Day

Using the "UV" and "T, °C" data of Table B3, values of 1000 $\lambda/2$ 3 were located in the matrix of Table B2. Table B6 gives the results. Next, since λ is in units of hour^{-1}, the data of Table B6 were multiplied by 24 to change the unit to day^{-1} and divided by 1000 to remove the factor of 1000 heretofore incorporated for convenience

e. Prediction of Extent of Yellowing for Samples Exposed Outdoors in Miami

$$\log_{10}\left(\frac{1}{P}\right) = \left[\left(\frac{\lambda_1}{2.3}\right)^{1/\beta} t_1 + \left(\frac{\lambda_2}{2.3}\right)^{1/\beta} t_2 + . \quad \left(\frac{\lambda_n}{2\ 3}\right)^{1/\beta} t_n\right]^{\beta}$$

where P = property = fraction of original transmittance at 360 nm in this case.

For each "typical day" of each month,

$$\log(\tfrac{1}{P}) = \left[\left(\frac{\lambda_{7\text{-}9AM}}{2.3}\right)^{1/0.9}(\tfrac{1}{12}) + \left(\frac{\lambda_{9\text{-}11AM}}{2.3}\right)^{1/0.9}(\tfrac{1}{12}) + \dots \left(\frac{\lambda_{3\text{-}5PM}}{2.3}\right)^{1/0.9}(\tfrac{1}{12})\right]^{0.9}$$

Factoring out the $\tfrac{1}{12}$,

$$\log(\tfrac{1}{P}) \approx \left\{(\tfrac{1}{12})\left[\left(\frac{\lambda_{7\text{-}9AM}}{2.3}\right)^{1.11} + . \quad \left(\frac{\lambda_{3\text{-}5PM}}{2.3}\right)^{1.11}\right]\right\}^{0.9}$$

Thus, the $\lambda/2.3$ values for the 2-hour periods can be raised to the 1.11 power and summed. See Table B8.

To make a prediction, Table B9 is consulted. The number of exposure days in a given month is multiplied by the "total" column in Table B8 and divided by 12 (because of the 1/12 factor, above). The 1/12 factor is used because each 2-hour exposure period is 2/24 or 1/12 day. The 300-day calculation is

Month	Contents of the Parentheses in $\log_{10}(\tfrac{1}{P}) = (\dots)^{0.9}$
October 1976	(0.0212) (11/12) = 0.0194
November	(0 0112) (30/12) = 0.0280
December	(0 0081) (31/12) = 0.0209
January 1977	(0.0078) (31/12) = 0.0202
February	(0.0131) (28/12) = 0.0306
March	(0.0323) (31/12) = 0.0834
April	(0.0565) (30/12) = 0 1413
May	(0.0735) (31/12) = 0.1899
June	(0.0898) (30/12) = 0 2145
July	(0.0849) (31/12) = 0.2193
August	(0.0779) (16/12) = 0 1039
	Total = 1 0714

$(1.0714)^{0.9} = 1.0640 = $ predicted $\log_{10}(\tfrac{1}{P})$.

185

Predictions vs. actual values are

Time, days	$\log_{10}(\frac{1}{P})$ Predicted	Found
30	0.052	0.027
90	0.10	0.08
150	0 20	0.26
210	0.49	0.80
300	1.06	1.13

These data points are plotted in Figure B8. Considering the assumptions made, especially concerning UV intensity, agreement of predictions and real values is very good

2. Prediction of Polystyrene Yellowing in Miami (Lognormal Model)

In addition to the Weibull model predictions just discussed, another approach was used   The accelerated data for polystyrene yellowing were fitted to the following lognormal model (see Reference 2)

$$P = 1 - \int_{0}^{\frac{x - \mu}{\sigma}} \frac{1}{\sqrt{2\pi}} e^{-\frac{w^2}{2}} \, dw$$

where P = fraction of original transmittance at 360 nm

x = $\log_e$ of cumulative UV ("CUV" in Table B10) deposited on the sample.

μ = the median (the 50 percent point) in $\log_e$ hours of the distribution

σ = the difference (in $\log_e$ time space) between the 84th and 50th percent points.

w = variable used for integration

The accelerated data provide values of P and x.   In this case x is equivalent to exposure time because the UV level is constant.   When P is plotted vs. x on normal probability paper, μ is the value in $\log_e$ hours when p = 0.5, and σ is obtained by subtracting the value in $\log_e$ hours when P = 0 5 from the value in $\log_e$ hours when P = 0 84.

186

The 50 percent relative humidity data were used. Note that relative humidity had negligible effect in the accelerated test, so the 50 percent relative humidity data are suitable for Miami Three of the 50 percent relative humidity data sets (1 00 rel UV, 26.1°C; 1.00 rel. UV, 60.3°C, 0.66 rel UV, 18 3°C) gave good log-normal fits and yielded the following two equations for predicting μ and σ

$$\hat{\mu} = \frac{1}{k_1(UV)} + \frac{25}{T} + 3.5\,k_2$$

$$\frac{1}{\hat{\sigma}} = 0.5 + 9\,k_1(UV)/T$$

where $\hat{\mu}$ = predicted μ

$\hat{\sigma}$ = predicted σ

UV = accelerated exposure level in relative UV, either 1.00 or 0.66

T = temperature in degrees C

k_1 and k_2 = constants

The constants k_1 and k_2 are both equal to 1 in accelerated exposure In outdoor exposure, these constants depend upon the units used for UV, the exposure site, and the time of year that exposure began

For the Miami exposure (started 10-20-76), we let k_1 = 2 and k_2 = 0 86.
T = cumulative average of daily high levels of temperature from Table B3.
UV = cumulative average values from Table B4, representing the average UV level.

Thus, the equations for Miami become·

$$\hat{\mu} = \frac{1}{2(UV)} + \frac{25}{T} + (3.5)\,(0.86)$$

$$\frac{1}{\hat{\sigma}} = 0.5 + \frac{(9)\,(2)\,(UV)}{T}$$

The values of Table B10 were calculated from these equations It can be seen that agreement with actual results is good.

Sample calculation   At 90 days,

$$\hat{\mu} = \frac{1}{2(0.168)} + \frac{25}{24\,5} + (3.5)(0\,86) = 7.01$$

$$\frac{1}{\hat{\sigma}} = 0.5 + \frac{(9)\,(2)\,(0.168)}{24\,5}$$

$$\hat{\sigma} = 1\,60$$

$$\hat{z} = \frac{\log_e (CUV) - \hat{\mu}}{\hat{\sigma}} = -1.14$$

This quantity $\hat{z}$ (see Note to Table B10) is equivalent to the term t in the table on page 689 of Reference B2. F(t) in this table gives the desired result, 0.87   Note that F(t) was used because $\hat{z}$ was negative.   At 210 days, $\hat{z}$ is positive (0 98) and the 1 - F(t) column is used, giving 0.16.

3. Prediction of Lexan Yellowing Outdoors Based Upon Accelerated Exposure Data (Exponential Model, Graphical Methods)

a. Accelerated Exposure Data

The yellowing rate of Lexan decreased with time due to solarization of the xenon lamp   To correct for this effect, the following analysis was made. The efficiency of the lamp in yellowing Lexan is plotted vs. lamp age in Figure B9. Areas over the curve were used to calculate the corrected exposure times as illustrated in the figure for the 768-hour exposure.   Results are·

Exposure Time, hrs	Ratio of Integrated Efficiency to that of New Lamp	Corrected Exposure Time, hrs.
120	0 90	108
768	0 67	514
1536	0.48	742

Then, corrected exposure times and their logarithms are.

Time, hrs.	$\log_{10}$ (time)
3	0.48
6	0.78
12	1 08
24	1.38
108	2.03
514	2.71
742	2.87

The accelerated exposure data (Table B11) were plotted, using the above corrected exposure times, in Figures B10-B13.

The Weibull plot is unsatisfactory because the points define a pronounced curve. However, at 300 days the values of $\log(\frac{1}{P}) = A_{360} - A_{600} - 0.0309$ is 0.48 for Phoenix 45° exposure and 0.40 for Miami 45°S exposure   Up to this level of yellowing, the accelerated exposure data can be represented, as a first approach, by a line of slope 1.   In other words, the data follow the exponential model:

$$\frac{1}{P} = e^{\lambda t}$$

$$\text{or } \log_{10} (\frac{1}{P}) = (\frac{\lambda}{2.3}) t$$

where t = time and P = property = fraction of original transmittance at 360 nm in this case.

b. Values for Parameter λ

From Figures B10-B13, the values of $\frac{\lambda}{2.3}$, which is equal to $\log_{10}(\frac{1}{P})$ at $t = 1$, are

Relative UV Intensity	Temp., °C	Relative Humidity, %	$\frac{\lambda}{2\,3}$, hr.$^{-1}$
1 00	26.1	0	0.0119
		100	0.0146
	60.3	0	0.0165
		100	0.0165
0.66	18.3	0	0.0059
		100	0.0073
	55.3	0	0.0074
		100	0.0091

Assuming an average relative humidity of 75 percent for Miami, linear interpolation gives·

Relative UV Intensity	Temp., °C	$\frac{1}{T(^\circ K)}$	$\frac{100\lambda}{2.3}$(hr $^{-1}$) at 75% Rel Hum.
1.00	26.1	0.00334	1.39
	60 3	0.00300	1.65
0.66	18.3	0.00343	0 70
	55 3	0.00305	0.87

The value of $100\lambda/2.3$ is related to temperature and UV intensity in Figures B14-B16   From Figure B16, the matrix of Table B12 was constructed Table B13 gives Miami weather data, which includes UV levels based on Reference B1, pgs   124 and 137.   Using Table B12, $100\lambda/2.3$ values were assigned by month and time of day in Table B14

c.   Prediction for Miami

For each of the twelve "typical days", the exponential model equation is

$$\log_{10}(\frac{1}{P}) = \left(\frac{\lambda_{7-9AM}}{2.3}\right)(\frac{1}{12}) + \left(\frac{\lambda_{9-11AM}}{2.3}\right)(\frac{1}{12}) + \ ..\ \left(\frac{\lambda_{3-5PM}}{2\,3}\right)(\frac{1}{12})$$

Thus, the horizontal columns in Table B4 can be summed to give the total $\frac{\lambda}{2.3}$ for the day (Table B11).

The equation for prediction then becomes

$$\log_{10}(\tfrac{1}{P}) = \left(\frac{\lambda_{\text{month 1}}}{2.3}\right)\left(\frac{\text{exposure days}}{12}\right) + \left(\frac{\lambda_{\text{month 2}}}{2.3}\right)\left(\frac{\text{exposure days}}{12}\right)$$

$$+ \ldots \left(\frac{\lambda_{\text{month n}}}{2.3}\right)\left(\frac{\text{exposure days}}{12}\right)$$

For 300 days exposure (begun 9-1-76), the calculated degree of yellowing is

$$\log_{10}(\tfrac{1}{P}) = (0.47)\,(\tfrac{30}{12}) + (0\ 15)\,(\tfrac{31}{12}) + (0.079)\,(\tfrac{30}{12}) + (0.058)\,(\tfrac{31}{12}) +$$

$$(0.058)\,(\tfrac{31}{12}) + (0.096)\,(\tfrac{28}{12}) + (0.25)\,(\tfrac{31}{12}) + (0.49)\,(\tfrac{30}{12}) +$$

$$(0.68)\,(\tfrac{31}{12}) + (0.83)\,(\tfrac{27}{12}) = 7.779$$

The measured value for $\log_{10}(\tfrac{1}{P})$ was 0 3984.

The reason why the calculated value is 19.5 times the actual result is that the intensity of the lamp at 300 nm was much higher than that of sunlight. Experimental values were 3.4 x 10^{-3} mw/cm^2/nm vs. 8.0 x 10^{-5} in one determination (see the Interim Report, Appendix).

Table B16 lists the $\lambda/2.3$ values of Table B15 divided by 19.5. The 300-day results were recalculated as follows:

$$\log_{10}(\tfrac{1}{P}) = \frac{1}{12}\Big[(0\ 024)\,(30) + (0.0077)\,(31) + (0.0041)\,(30) + (0.0030)\,(31) +$$

$$(0\ 0030)\,(31) + (0.0049)\,(28) + (0\ 013)\,(31) + (0.025)\,(30) +$$

$$(0.035)\,(31) + (0.043)\,(27)\Big] = 0.400, \text{ which of course agrees}$$

with the measured value of 0.398

At 379 days, the sample was too embrittled for further exposure and the test was ended. At this point, the calculated $\log_{10}(\tfrac{1}{P})$ was 0.64 compared with 0.70 determined by exposure.

Results for intermediate exposure times are:

$$\log_{10}(\tfrac{1}{P})$$

Exposure Time, Days	Predicted Based on Table VI	Found
30	0 060	0 027
90	0.090	0 065
150	0.10	0.098
210	0.15	0 17

These data are plotted in Figure B17

For the exposures started on the winter and summer solstices, results

Exposure Time, Days	Exposure Started 12/12/76		Exposure Started 6/21/77	
	Predicted, Based on Table B6	Found	Predicted, Based on Table B6	Found
30	0.0075	0.017	0.10	0 030
60	0.018	0.034	0.19	0 067
90	0.045	0.058	0 027	0.10
150	0 18	0.13		
210	0.38	0.28		

d. Prediction for Phoenix

Phoenix weather data are given in Table B17   Inspection of 3-hourly data showed that the minimum daily temperature occurred about 7 - 9 AM and the mean about 9 - 11 AM, while the maximum held approximately through the afternoon. The temperatures in Table B7 were assigned on this basis. The relative UV values are the same as for Miami because the same time-of-day and seasonal variation is assumed. The general level of UV intensity is higher in Phoenix, however, and this will be corrected for below.

The mean of the monthly average relative humidities in Table B17 is 27 percent   Linear interpolation of the accelerated data gives

Relative UV Intensity	Temp., °C	$\frac{1}{T(°K)}$	$\frac{100\ \lambda}{2.3}$ (hr.$^{-1}$) at 27% Rel. Hum.
1.00	26.1	0.00334	1.26
	60.3	0.00300	1.65
0.66	18.3	0.00343	0.63
	55.3	0 00305	0 79

As for the Miami case, the plots of Figures B18-B20 were constructed, the matrix of Table B18 was derived from Figure B20, and the values of Table B11 were found by consulting Tables B17 and B18. The values of λ/2.3 for Phoenix in Table B20 correspond to the values for Miami in Table B25.

The values of Table B20 then were corrected (Table B21) using the 19.5 factor between lamp and sunlight (as discussed above) multiplied by 0 93 to give 18.1. This is done because total yearly insolation in Miami has been reported as 93 percent that in Phoenix (Reference B3). That is, sunlight was more intense in Phoenix than in Miami, so the mismatch of lamp and sunlight was somewhat less for Phoenix than for Miami.

For 300 days exposure (begun 9-12-77), the prediction calculation is

$$\log_{10}(\frac{1}{P}) = \frac{1}{12}\left[(0\ 023)\ (18) + (0.0072)\ (31) + (0.0041)\ (30) + (0.0032)\ (31) + \right.$$
$$(0.0032)\ (31) + (0.0050)\ (28) + (0.012)\ (31) + (0.024)\ (30) +$$
$$\left.(0.033)\ (31) + (0.044)\ (30) + (0\ 041)\ (9)\right] = 0\ 4086$$

The measured value for $\log_{10}(\frac{1}{P})$ was 0.4813.

Results for intermediate exposure times are

Exposure Time, Days	Predicted, Based on Table B21	Found
30	0.042	0.027
60	0.057	0.040
90	0.066	0.060
150	0 087	0.077
210	0.14	0.16

These data are plotted in Figure B21.

At 420 and 540 days the predicted results proved to be too low.

Exposure Time, Days	Predicted, Based on Table B21	Found
420	0.50	0.90
540	0.63	0.98

The reason was that the exponential model, which had been assumed, is the Weibull model with $\beta = 1$, but outdoor exposure data for 300 - 540 days indicate a higher value for β.

With β assumed to be 1 3, the method of calculation used above for polystyrene yellowing was applied. The values of Table B21 were raised to the 1/1.3 power, and the time factor x was found as follows for 300 days

$$\left[x \ (0.055 + 0.023 + 0.015 + \ldots 0.091) \right]^{1.3} = 0.48$$

$$x = 1.468$$

Then, for example, for 90 days:

$$\log_{10}(\tfrac{1}{p}) = \left[(1.468) \ (0.055 + 0.023 + 0.015) \right]^{1.3} = 0.075$$

Predicted vs. actual results for $\beta = 1.3$ are:

Exposure Time, Days	Predicted, Assuming $\beta = 1.3$	Found
30	0.038	0.027
60	0.060	0.040
90	0.075	0.060
150	0.10	0.077
210	0.16	0.16
300	0.48	0.48
420	0.90	0.90
540	1.01	0 98

Note that the value of β for the outdoor data was 1.4 as calculated by computer with a least-squares curve fitting program (see the section on mathematical models).

Also note that the data points of Figures B10-B13 are consistent with an initial slope of 1.3, or even higher, as well as with the value of 1 0 which had been arbitrarily assumed. There are not enough early points for a fine distinction.

194

4. Prediction of Loss in Tensile Strength of Polystyrene and Lexan Outdoors Using Accelerated Exposure Data (Weibull Model, Graphical Methods)

a. Polystyrene

Tensile test data on polystyrene are given in Tables B22 and B23 In Table B24, the data are converted to $\log_{10}(\frac{1}{P})$, where P = property = fraction of original breaking stress The accelerated data from Table B24 are plotted in Figure B22.

As a first approach, a line of slope 0 77 was drawn in Figure B22. This line was intended to best represent the higher levels of $\log_{10}(\frac{1}{P})$ at which data are more meaningful.

The applicable Weibull equation is

$$\log_{10}(\frac{1}{P}) = (\frac{\lambda}{2.3}) \, t^{0\ 77}$$

when $t = 1$, $\frac{\lambda}{2.3} = \log_{10}(\frac{1}{P}) = 0\ 00159$.

The corresponding value for polystyrene yellowing was 0.00177 Assuming the same UV intensity and temperature effects as for polystyrene yellowing (discussed above), the values of Table B25 were obtained by multiplying the polystyrene yellowing values by 0.00159/0.00177 = 0.90. By the method used above for yellowing,

$$\log (\frac{1}{P}) = \left\{ (\frac{1}{12}) \left[\left(\frac{\lambda_{7-9AM}}{2.3}\right)^{1.30} + \ldots \left(\frac{\lambda_{3-5PM}}{2.3}\right)^{1.30} \right] \right\}^{0.77}$$

Again, the $\lambda/2.3$ values for the 2-hour periods can be raised to the $1/\beta$ power and summed. This is done in Table B26.

195

By the method of the calculation for yellowing, the 300-day calculation

is·

Contents of the Parentheses

$\text{in } \log_{10}(\frac{1}{p}) = (.. \quad)^{0.77}$

Month				
October 1976	(0.00810)	(11/12)	=	0.00743
November	(0.00558)	(30/12)	=	0 0140
Dec.	(0.00252)	(31/12)	=	0 00651
January 1977	(0.00242)	(31/12)	=	0.00625
February	(0.00459)	(28/12)	=	0.0107
March	(0.0128)	(31/12)	=	0.0331
April	(0.0245)	(30/12)	=	0.0613
May	(0.0325)	(31/12)	=	0.0840
June	(0.0399)	(30/12)	=	0.0998
July	(0 0389)	(31/12)	=	0.1005
August	(0 0352)	(16/12)	=	0 0469

Total = 0.4705

$(0\ 4705)^{0.77} = 0.56$

Found = 0 66

For 210 days, the calculation is
                      0.00743
                      0.0140
                      0.00651
                      0.00625
                      ·0.0107
                      0.0331
                      0 0613

(0.0325) (18/12) = 0.0488

Total = 0.2160

$(0\ 2160)^{0.77} = 0.31$

Found = 0.41

196

Predicted vs. actual values are:

Time, Days	$\log_{10}(\frac{1}{P})$ Predicted	Found
30	0 042	0.066
60	0.059	0.066
90	0.070	0.056
150	0.12	0.076
210	0.31	0 41
300	0.56	0 66

These data are plotted in Figure B23. As for the polystyrene yellowing predictions, agreement is good considering the assumptions made   In the present case; these assumptions include the supposition that yellowing and tensile strength loss depend in the same way on UV intensity and temperature.

b. Lexan

    (1) Miami Exposure

        Table B27 gives accelerated exposure data   The line of the Weibull plot (Figure B24) was again drawn to emphasize the later time points.   The slope (β) = 0.55   The value of λ/2.3 was 0.0060, which is 3.39 times the value of 0 0177 for polystyrene yellowing. Again, assuming the same UV intensity and temperature dependence as for polystyrene yellowing, the values of Table   B 28   were obtained by multiplying the polystyrene yellowing values by 3.39.

        By the same method as above, the λ/2.3 values in Table B28 were raised to the power of 1/0 55 = 1.82 in Table B29.

197

The 300-day calculation for Miami exposure is.

	Contents of the Parentheses in $\log_{10}(\frac{1}{P}) = (\ .. \ )^{0.55}$		
Month			
September 1976	(0 0424)	(30/12)	= 0.1060
October	(0.0084)	(31/12)	= 0.0217
November	(0.0031)	(30/12)	= 0.0080
December	(0.0016)	(31/12)	= 0.0041
January 1977	(0 0016)	(31/12)	= 0.0041
February'	(0.0039)	(28/12)	= 0 0091
March	(0 0203)	(31/12)	= 0 0524
April	(0 0438)	(30/12)	= 0.1095
May	(0.0656)	(31/12)'	= 0 1695
June	(0.0753)	(27/12)	= · 0 1694

$$\text{Total} = 0.6538$$

$$(0.6538)^{0.55} \doteq 0.79$$

$$\text{Found} \doteq 0\ 62$$

Predicted vs. actual values are

Time, Days	$\log_{10}(\frac{1}{P})$	
	Predicted	Found
30	0.29	0.060
90	0.33	0 097
150	0.34	0 10
210	0.40	0 099
300	0.79	0 62

These data are plotted in Figure B25. Agreement is fair only at the 300-day point

(2) Phoenix Exposure

In obtaining the values of $\lambda/2\ 3$ for Phoenix (Table B30), the ratios of Phoenix to Miami relative UV intensities (see discussion of Lexan yellowing, above) were multiplied times the values in Table B28

Then these results were divided by 0.93 because total Miami insolation has been reported as 93 percent that of Phoenix as noted above. As before, the $\lambda/2.3$ values of Table B30 were raised to the power of $1/0155 = 1$ 82 in Table B31

The 300-day calculation for Phoenix exposure is

Month	Contents of the Parentheses in $\log_{10}(\frac{1}{P}) = (\ ..\ )^{0.55}$			
September 1976	(0 0348)	(18/12)	=	0 0522
October	(0.0070)	(31/12)	=	0 0181
November	(0 0031)	(30/12)	=	0.0078
December	(0.0020)	(31/12)	=	0 0052
January 1977	(0 0019)	(31/12)	=	0.0049
February	(0.0040)	(28/12)	=	0.0093
March	(0.0137)	(21/12)	=	0.0354
April	(0.0334)	(31/12)	=	0.0835
May	(0.0503)	(31/12)	=	0.1299
June	(0.0834)	(30/12)	=	0 2085
July	(0.0625)	(9/12)	=	0 0469
		Total	=	0.6017

$$(0.6017)^{0.55} = 0\ 76$$

$$\text{Found} = 0\ 57$$

Predicted vs. actual values are.

Time, Days	$\log_{10}(\frac{1}{P})$	
	Predicted	Found
30	0.22	0.041
60	0.24	0.041
90	0.25	0.060
150	0.27	0.076
210	0 37	0.096
300	0.76	0.57

As for the Miami calculation, agreement is fair only at the 300-day point.

5   Relation of Yellowing and Tensile Strength Loss for Polystyrene and Lexan in Accelerated vs. Miami Exposure

a. Polystyrene

Data are given in Tables B32 and B33   The fraction of original breaking stress is plotted against fraction of original transmittance at 360 nm in Figures B26 and B27. The same line approximately fitted both sets of data, indicating that yellowing and tensile strength loss proceed at the same relative rates in both accelerated and outdoor exposure. Presumably, both effects are induced by one wavelength region, reported to be in the vicinity of 319 nm (Reference B4).

b. Lexan

Data are given in Tables B34 and B35. The fraction of original breaking stress is plotted against fraction of original transmittance at 360 nm in Figure B28. In this case, the ratio of yellowing rate to rate of tensile stress loss was much higher in accelerated exposure than in outdoor exposure. That is, the yellowing reaction was hyperaccelerated, while loss of tensile strength proceeded at the expected rate for continuous (simulated) noon sunlight. Lexan is reported to be degraded by two wavelength regions· 295 and 330 nm (Reference B5).

The output of the lamp at about 295 - 300 nm was much higher than that of sunlight. Also, both the rate of yellowing of Lexan and the 300 nm UV intensity fell as the lamp aged due to solarization of the lamp envelope and/or Pyrex tubes containing samples. These facts suggest that the reported 295 nm region is responsible for yellowing of Lexan. On the other hand, tensile strength loss proceeded at the expected rate in accelerated exposure and so may be induced by the reported wavelength of 330 nm.

c   Conclusion

Properties may proceed at unnatural relative rates in accelerated exposure due to imperfect solar simulation This point must be checked when working with a new material.

When the relationship between two properties has been established, the more-easily measured property may be used to estimate the other For polystyrene, such a relationship was shown to hold for both accelerated and outdoor exposure. In this case, transmittance at 360 nm can be easily and precisely measured and correlated with tensile strength.

6. Acceleration Factors for EMMA and EMMAQUA Exposure

a   Yellowing of Lexan

Table B36 gives the relevant data. Assuming for the moment that an exponential model holds, the acceleration factor is the ratio of accelerated to normal-exposure values of $\log_{10}(\frac{1}{P})$ (see Table B36) for any given exposure time. Such acceleration factors are listed in Table B37   The overall average is about 5.

There is a trend for the acceleration factor to increase during the 210-day exposure period (Table B37)   This increase may be partly accounted for by the increasingly greater insolation received by samples on the EMMA/EMMAQUA vs. samples at 45°S. Figure B29 shows this effect. Using the areas under the curves of Figure B29 to obtain integrated insolation values gives

Time, days, starting 9/12	Total Insolation Received at 45°S vs. that Received on EMMA/EMMAQUA, %
30	85
90	88
150	89
210	77
300	73

For example, the EMMA acceleration factor at 90 days, corrected to be comparable to that at 210 days, is $(5\ 1)\ (\frac{88}{77}) = 5.8$.

201

The situation is complicated by the fact that up to half of the total UV

at 300 nm, the wavelength believed to cause yellowing of Lexan, is received

from the sky as opposed to directly from the sun (Reference B1, pgs. 120-123).

The sky/sun ratio varies with time of day and with season. For normal incidence,

as maintained on the EMMA/EMMAQUA, Figure 7 on pg. 121 of Reference B1 suggests

a characteristic ratio of sky/sun intensities of 0.8   That is, the sun com-

ponent is 56 percent of the total   The EMMA and EMMAQUA concentrate direct

solar radiation with 10 mirrors having a reflectance of about 80 percent. The

EMMA/EMMAQUA receive approximately 1 2 times the insolation received at 45°S,

as mentioned above. Then, the calculated acceleration factor is

$$(10) \ (0.8) \ (0 \ 56) \ (1.2) = 5.4$$

This very rough estimate is in line with the acceleration factors found.

Note that as wavelength increases, UV becomes relatively more intense in the

sun component than in the sky component (Reference B1). Desert Sunshine reports

an overall average of 88 percent from the sun for integrated UV below 360 nm

(private communication). Thus, degradations promoted by higher wavelengths,

e.g., 350 nm, would be expected to have higher EMMA/EMMAQUA acceleration

factors, approaching (10) (0.8) (1.2) = 9.6 as a theoretical maximum (all UV

from the sun). This statement assumes, of course, that the degradation rate

is directly proportional to UV intensity (exponential model).

b. Loss of Tensile Strength of Lexan

Table B38   gives the data, which are plotted in Figure B30. Judging

from these data, there appears to be an induction period   If we arbitrarily

define this period as the time to reach $\log_{10}(\frac{1}{P}) = 0\ 1$, the induction period

was 85 days for EMMA exposure vs. 200 days for Phoenix 45°S exposure. The

relative UV doses received were calculated as follows

		EMMA		Phoenix, 45°S	
Month	Rel. UV Intensity*	Months Exposed	Rel. UV Rec'd	Months Exposed	Rel. UV Rec'd
Sept.	0.73	18/30	0 44	18/30	0.44
Oct	0 34	1	0.34	1	0.34
Nov.	0.17	1	0.17	1	0.17
Dec	0.10	11/30	0 04	1	0 10
Jan.	0.15			1	0.15
Feb.	0 24			1	0 24
March	0.43			1	0.43
Totals			0.99		1.87

*Reference B1, pg 137

Assuming that the induction period is inversely proportional to rate of UV deposition, the acceleration factor for EMMA exposure vs. Phoenix 45°S exposure is:

$$\left(\frac{200}{85}\right) \left(\frac{1.87}{0.99}\right) = 4.4$$

Thus this rough calculation illustrates that the acceleration factor for tensile strength loss parallels that found for yellowing.

REFERENCES

B1. Koller, L. R., Ultraviolet Radiation, 2nd Edition, Wiley, 1965.

B2. Bennett, C., and Franklin, N. L., Statistical Analysis in Chemistry and the Chemical Industry, Wiley, 1954.

B3. Lof, G.D.G., et al, Solar Energy, 10, pg. 27, 1966.

B4. Mark, H., Editor, Encyclopedia of Polymer Science, Vol 13, pg. 239, 1970.

B5. Anon., "Outdoor Weathering of Merlon Polycarbonate," brochure from Plastics Dept., Mobay Chemical Corp., undated
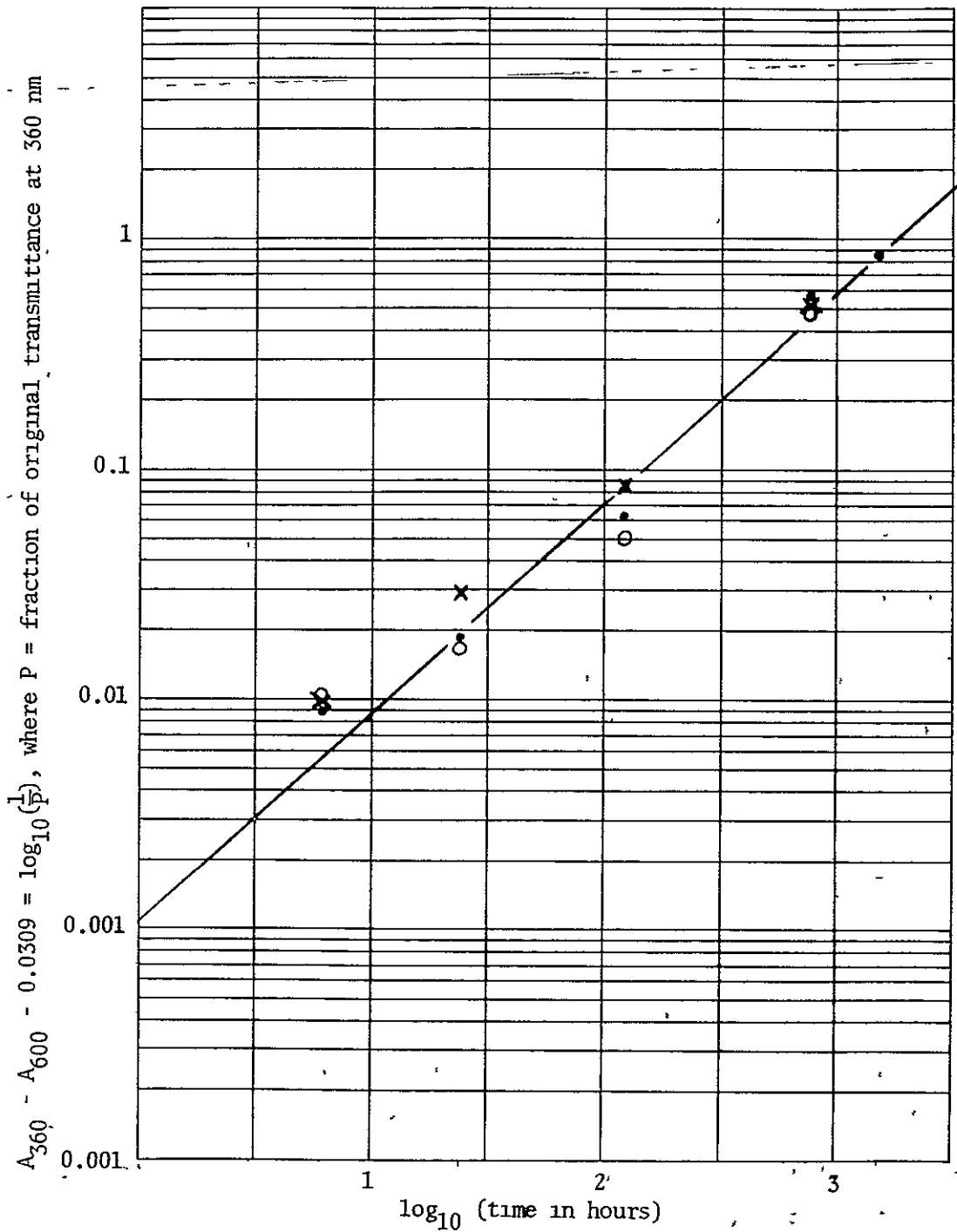
Figure B1   Accelerated Data for Polystyrene,
0.66 Relative UV Intensity, 18 3°C.

● =   0% relative humidity
○ =   50%   "   "
X = 100%   "   "

204
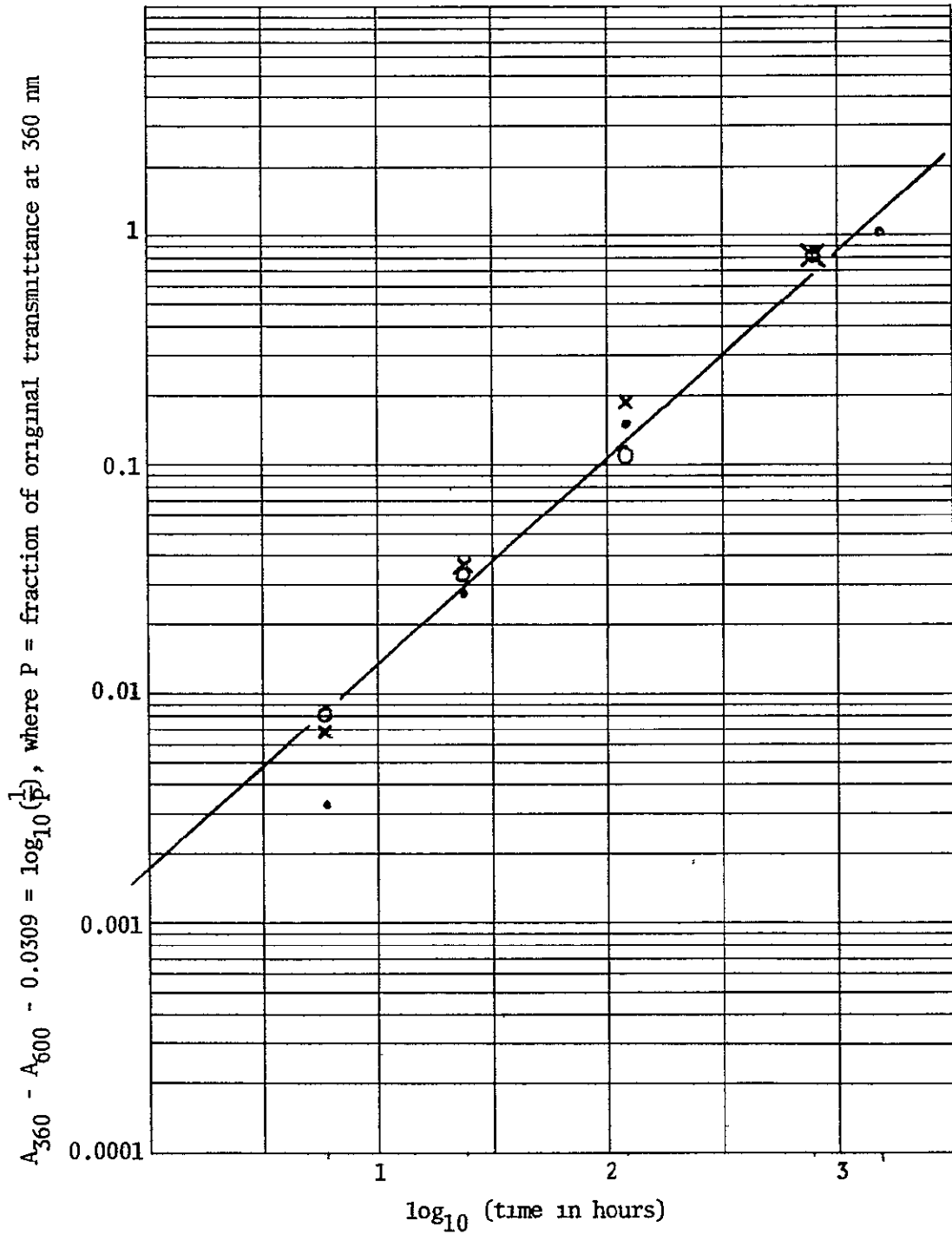
Figure B2. Accelerated Data for Polystyrene,
0.66 Relative UV Intensity, 55.5°C.

• = 0% relative humidity

○ = 50% "   "

✗ = 100% "   "

205
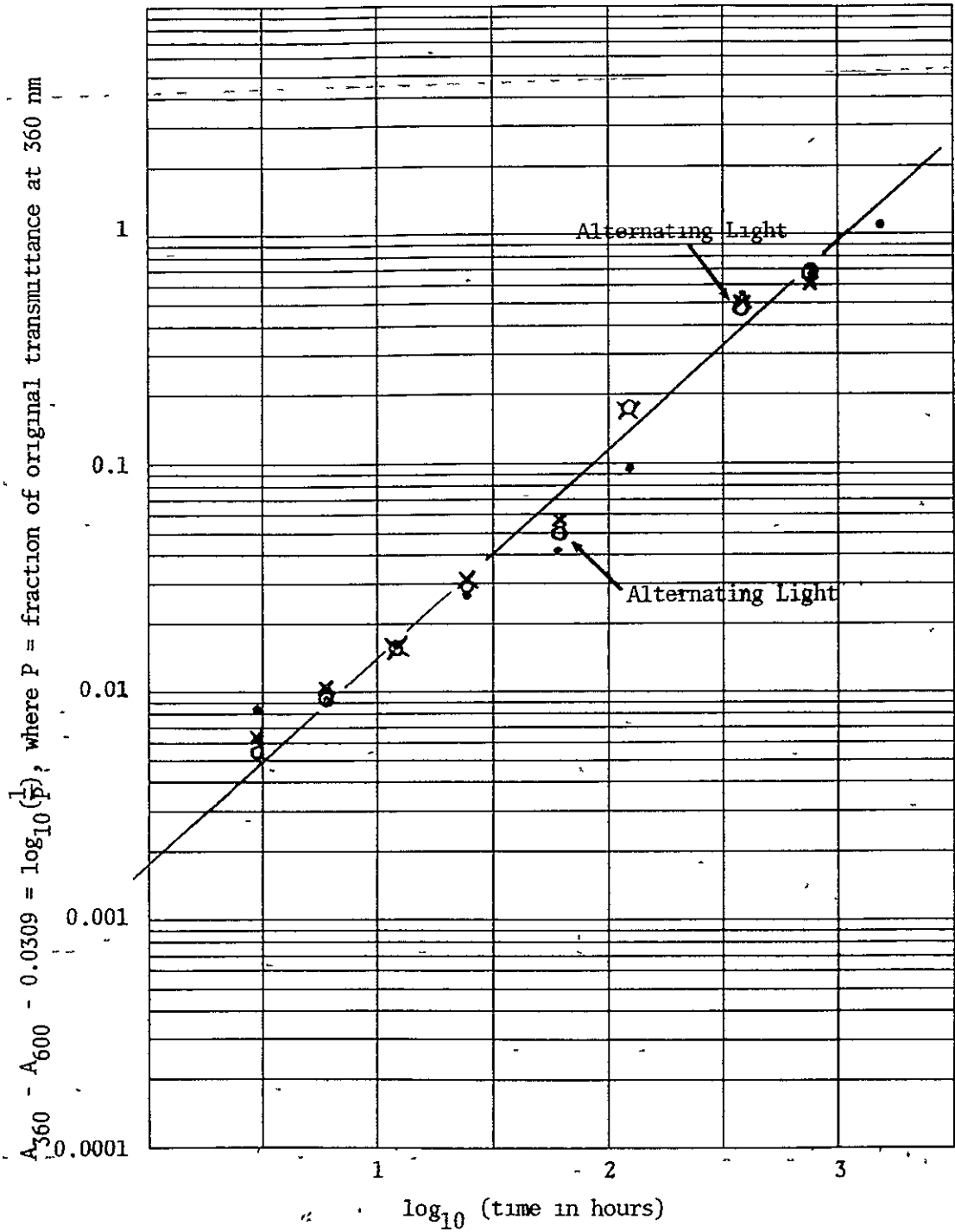
Figure B3. Accelerated Data for Polystyrene,
1 00 Relative UV Intensity, 26.1°C.

● = 0% relative humidity
○ = 50% "   "
✗ = 100% "   "
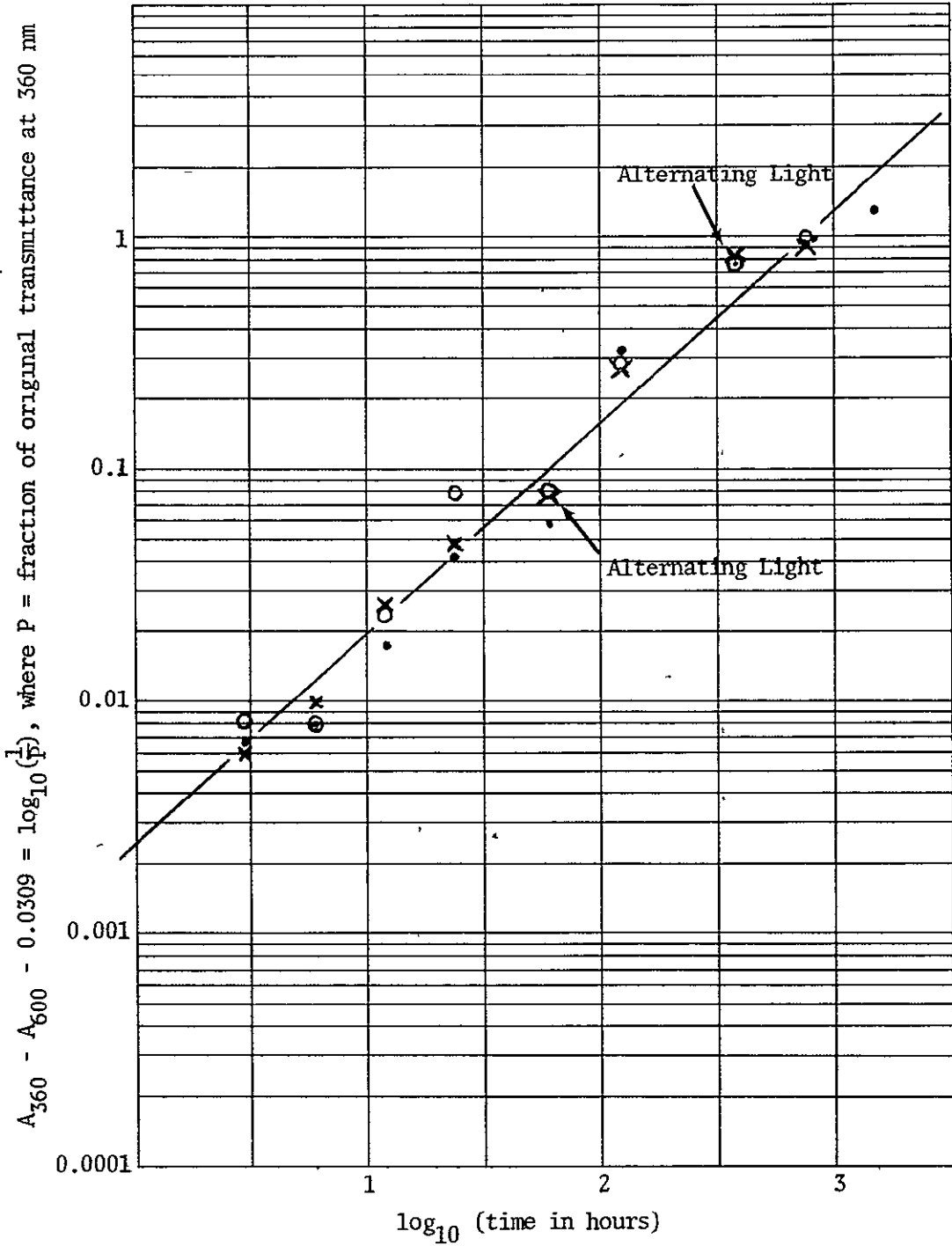
Figure B4. Accelerated Data for Polystyrene,
1 00 Relative UV Intensity, 60.3°C.

● =   0% relative humidity
O =   50%   "   "
X = 100%   "   "

207
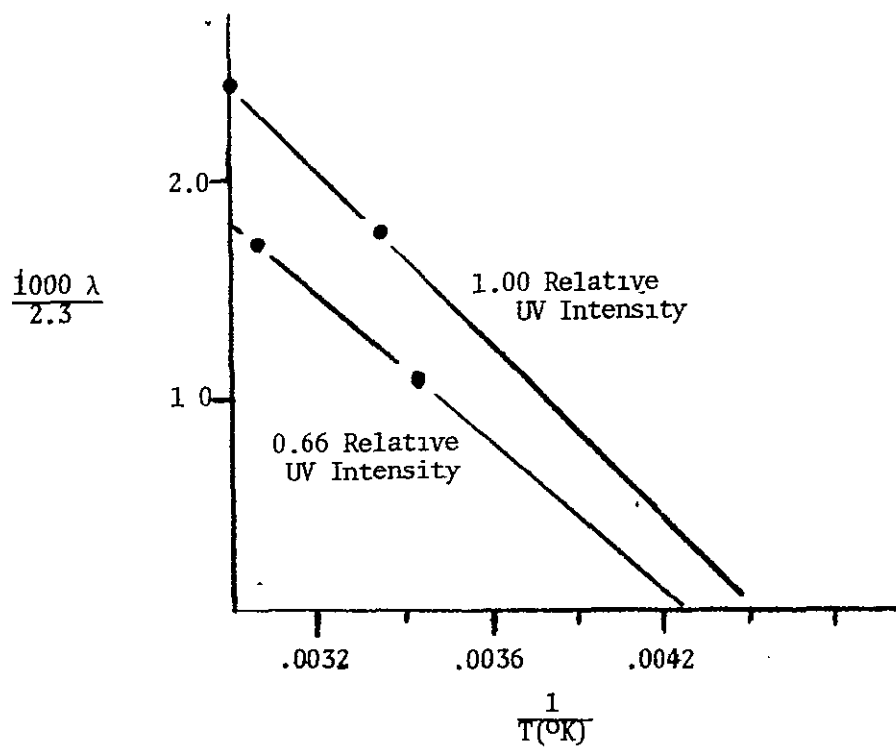
Figure B5. $\frac{\lambda}{2\ 3}$ vs. $\frac{1}{T(^oK)}$
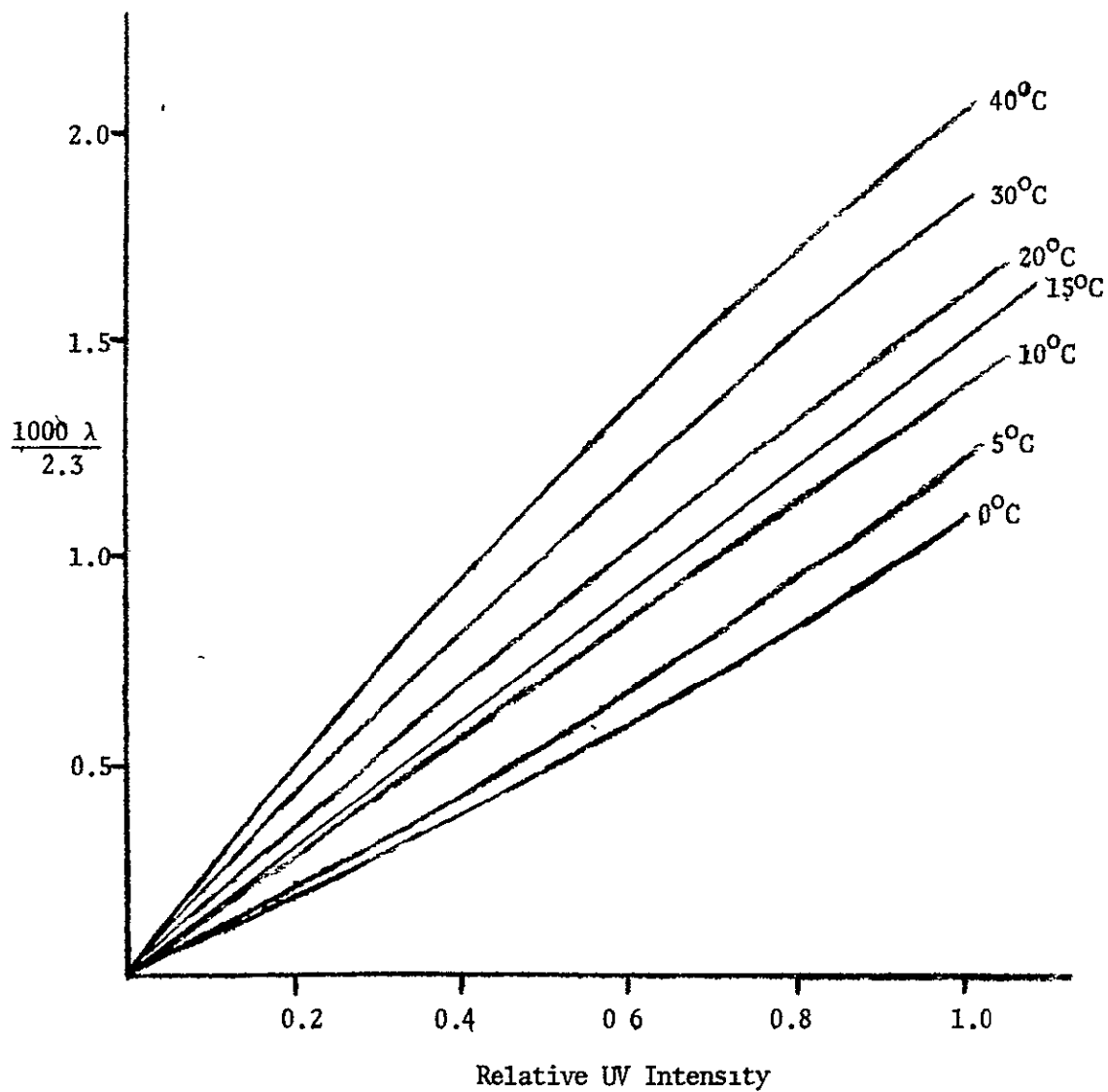
Figure B6. Relation of $\frac{\lambda}{2.3}$ to UV Intensity and Temperature
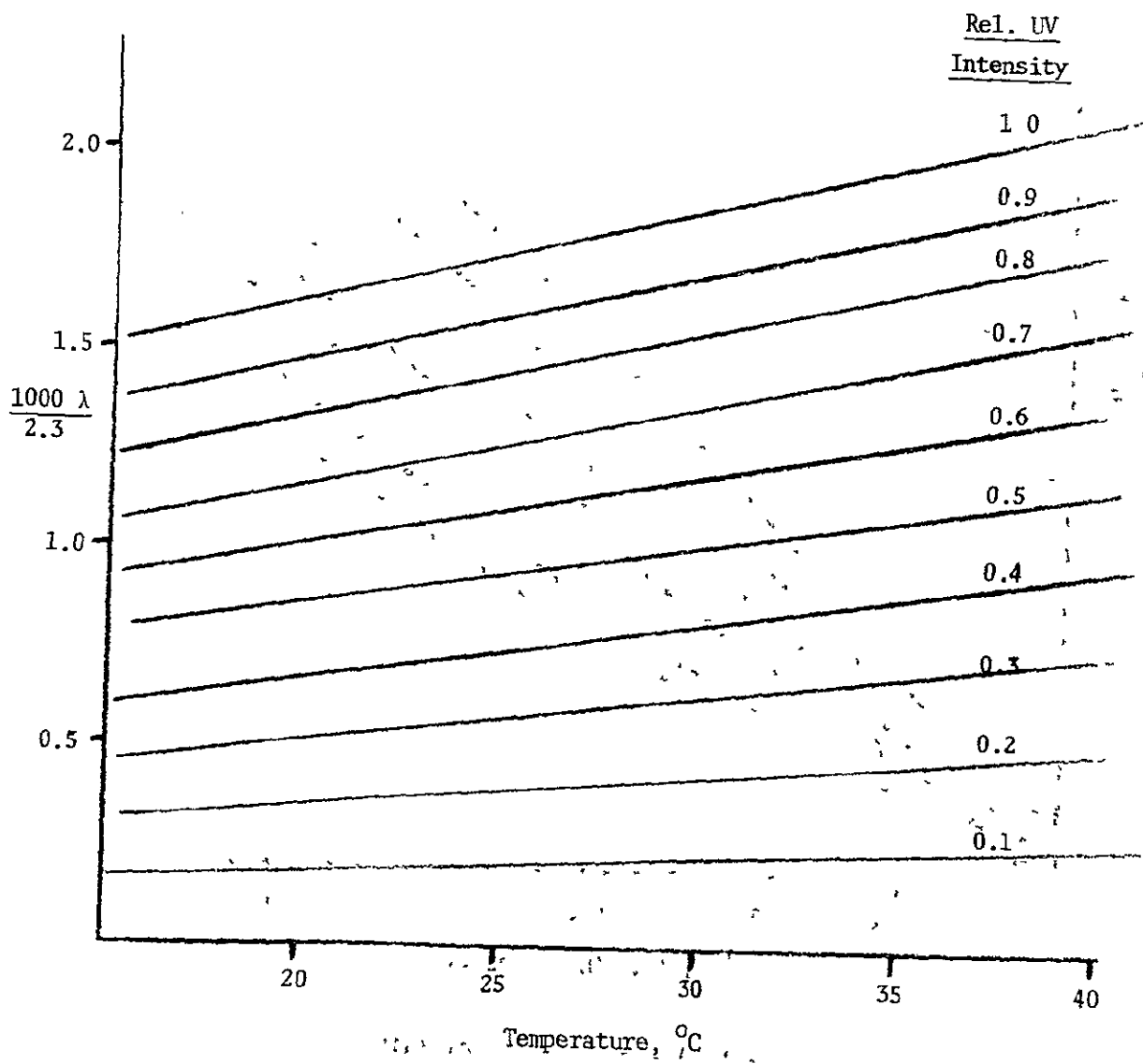
Figure B7. Relation of $\frac{\lambda}{2.3}$ to UV Intensity and Temperature

210
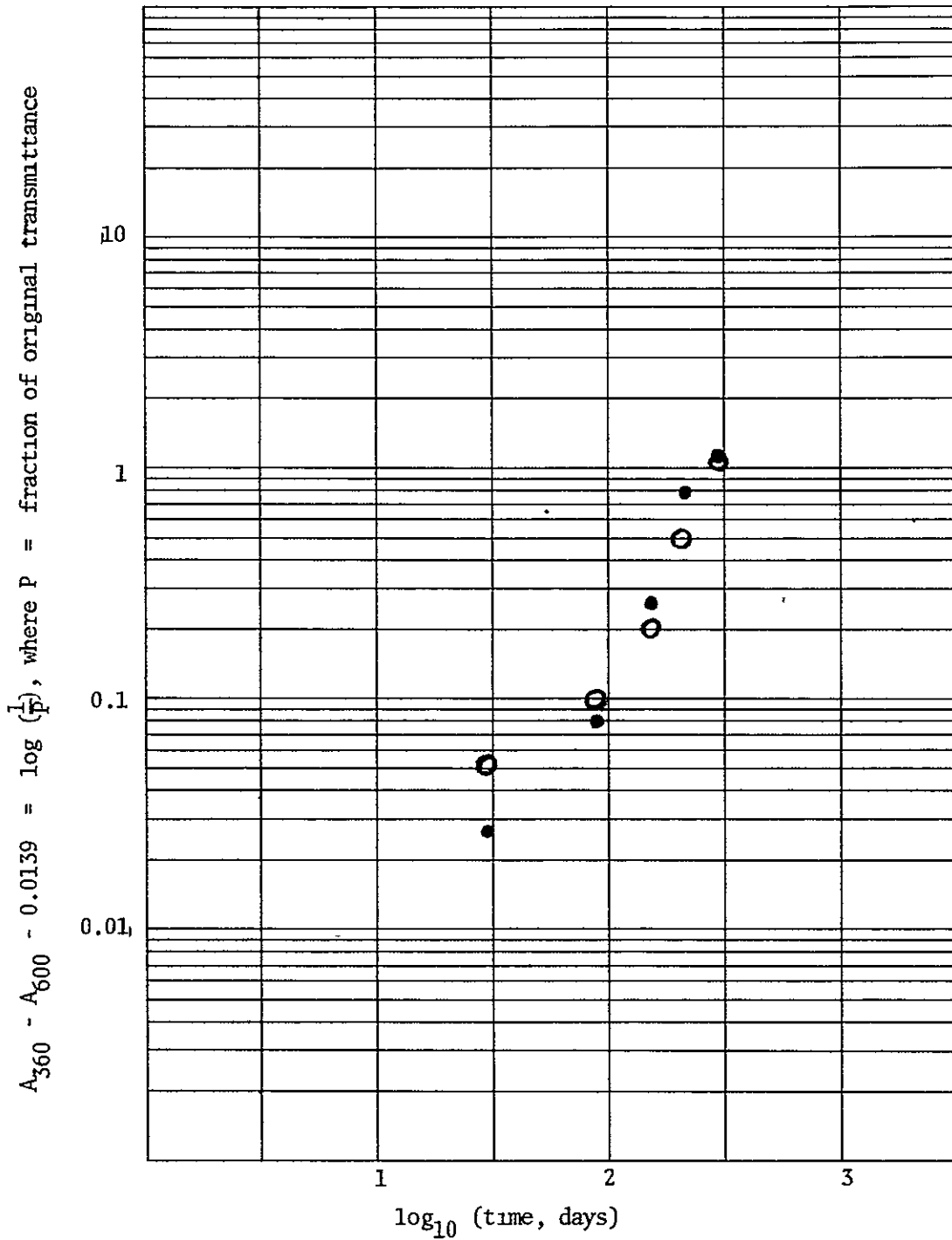
Figure B8. Predicted vs Actual Values for Yellowing of Polystyrene in Miami

● = found
O = calculated
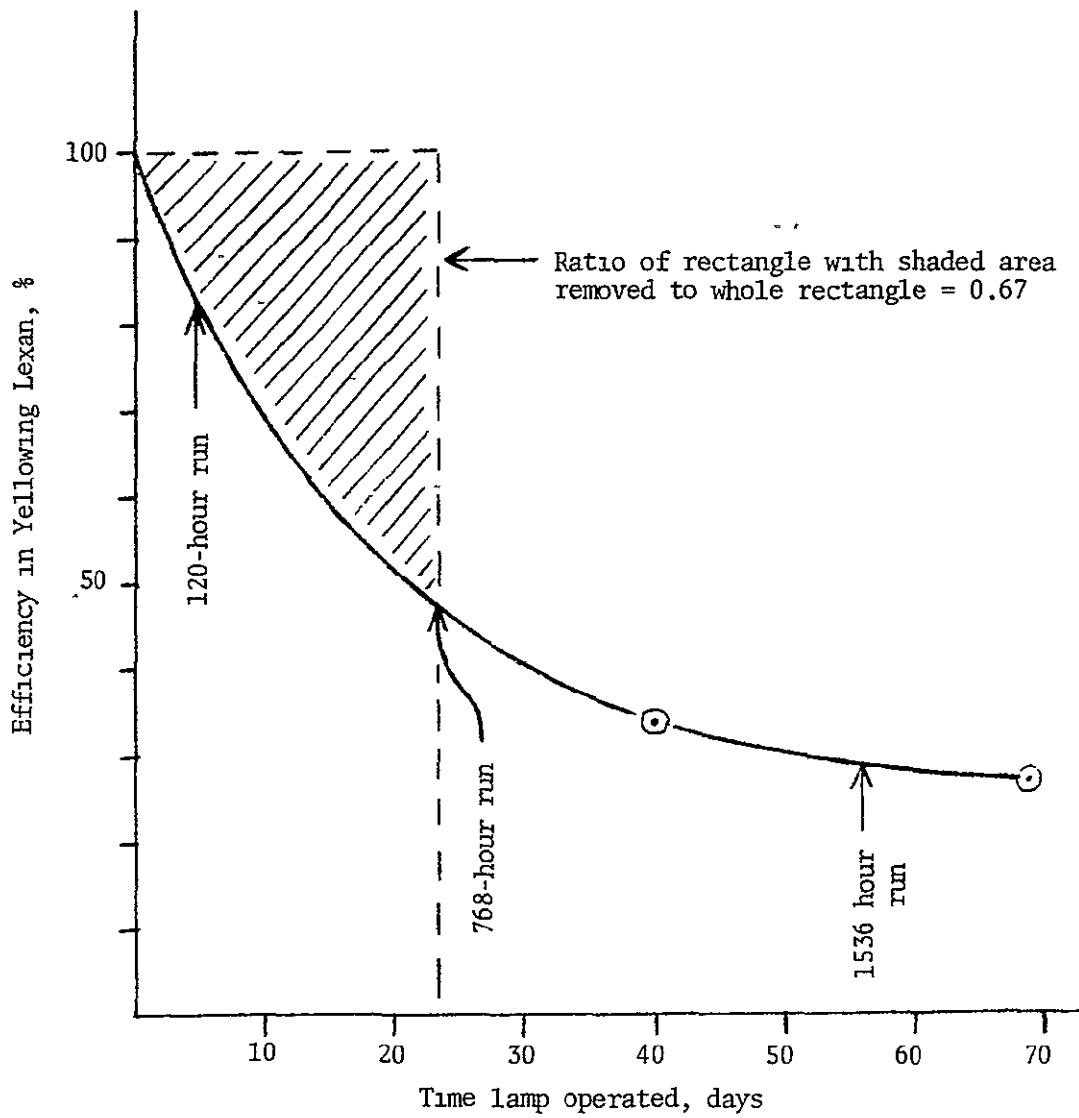
Figure B9. Efficiency in Yellowing Lexan vs. Age of Xenon Lamp

212
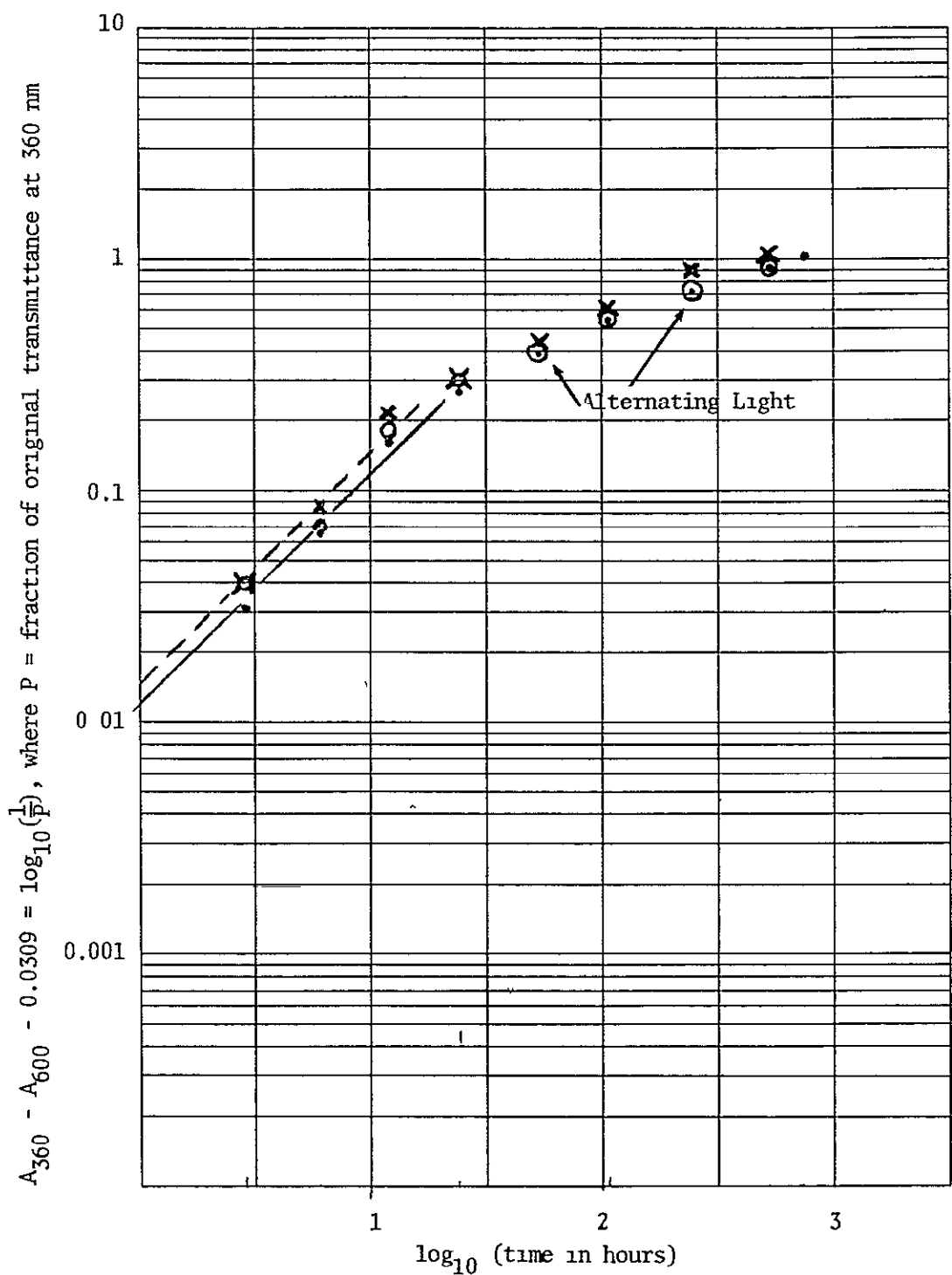
Figure B10. Lexan Yellowing vs. Time, Accelerated Exposure, 26.1°C, 1.00 Relative UV Intensity

• = 0% relative humidity (————)
O = 50% relative humidity
X = 100% relative humidity (— — —)

213
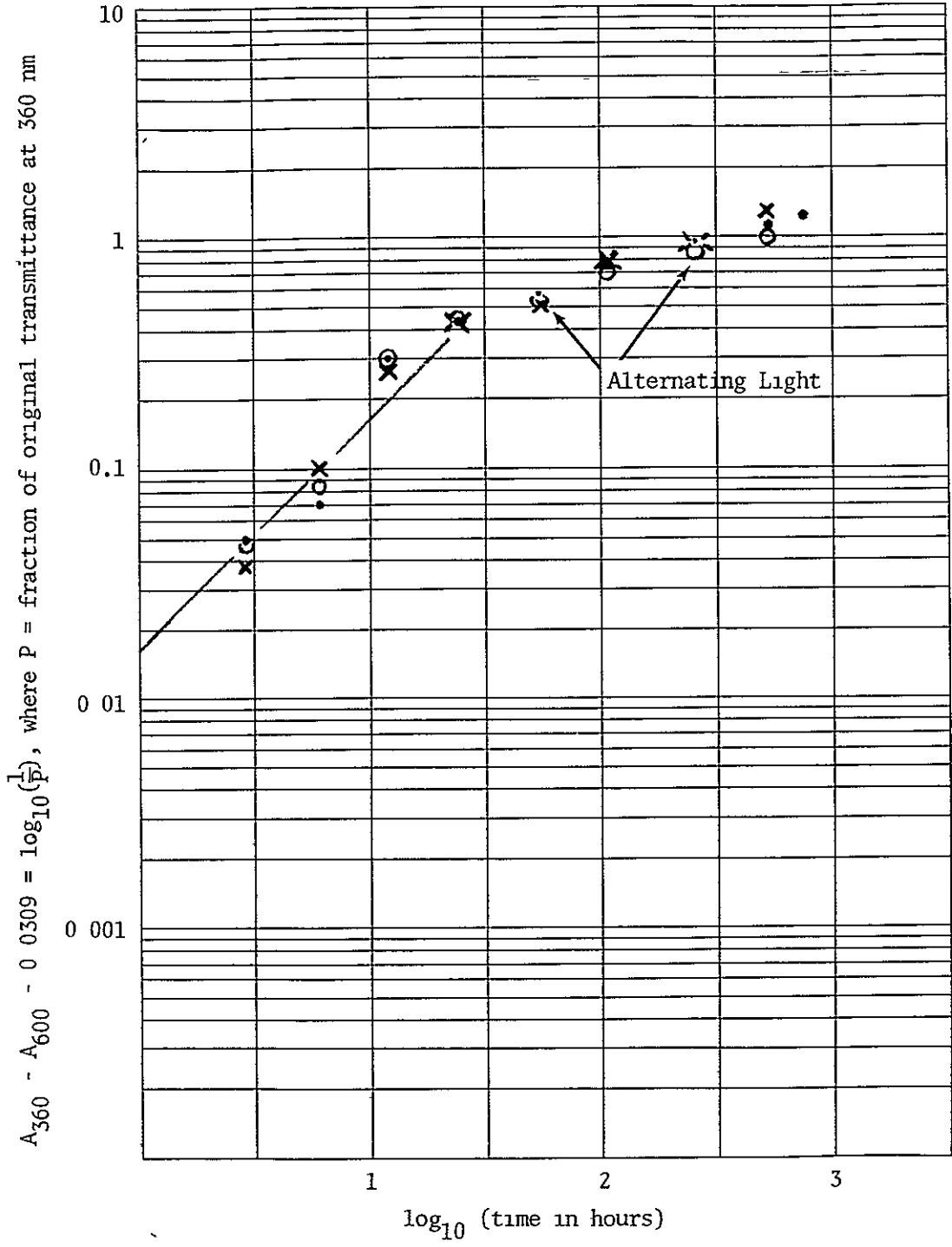
Figure B11. Lexan Yellowing vs. Time, Accelerated Exposure, 60 3°C, 1 00 Relative UV Intensity

● = 0% relative humidity (————)
○ = 50% relative humidity
✗ = 100% relative humidity (— — —)

214
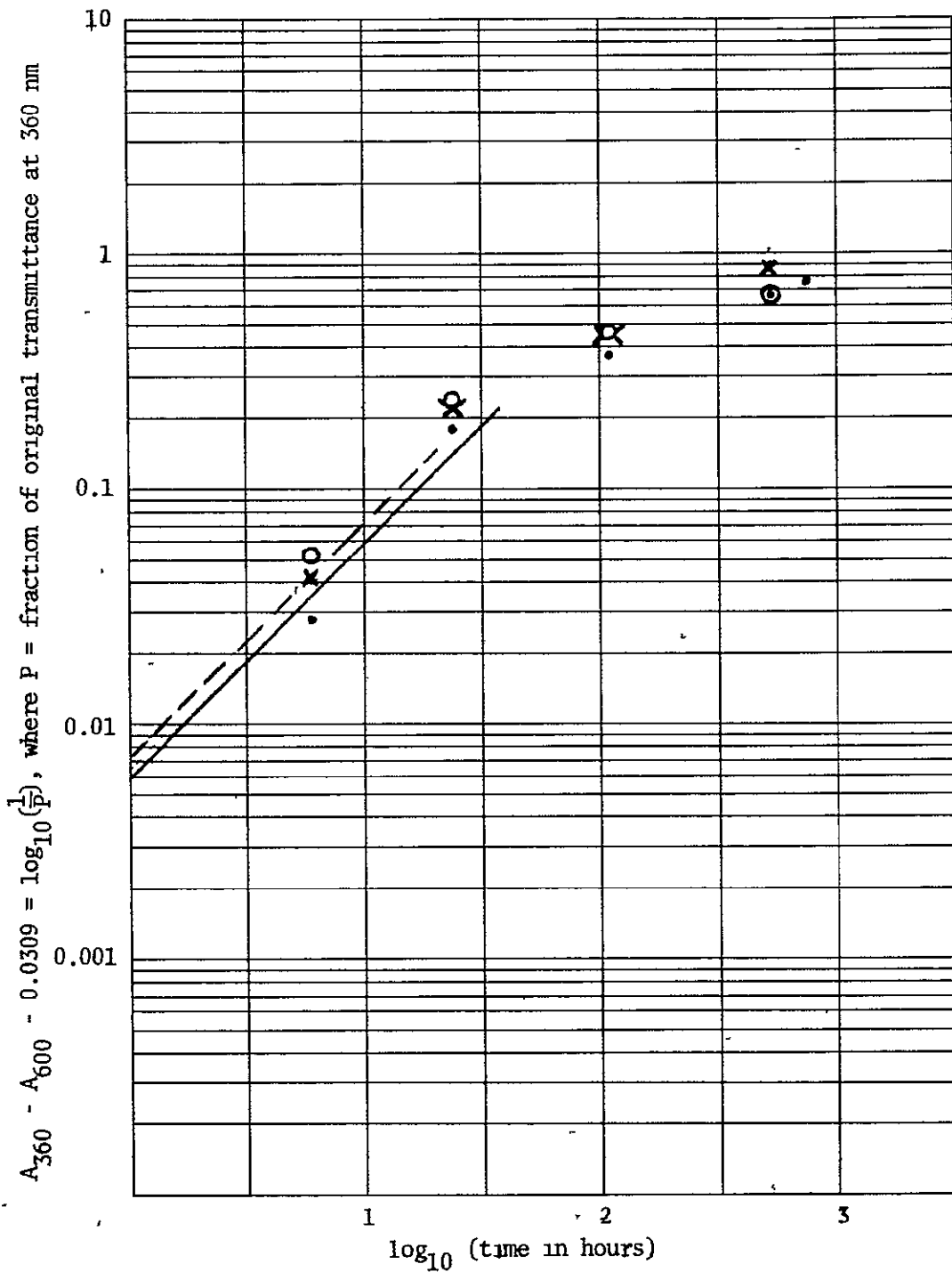
Figure B12.   Lexan Yellowing vs. Time, Accelerated Exposure,
              18.3°C, 0.66 Relative UV Intensity

• =   0% relative humidity (———)
○ =   50% relative humidity
✗ = 100% relative humidity (— ⸱⸱ —)

215
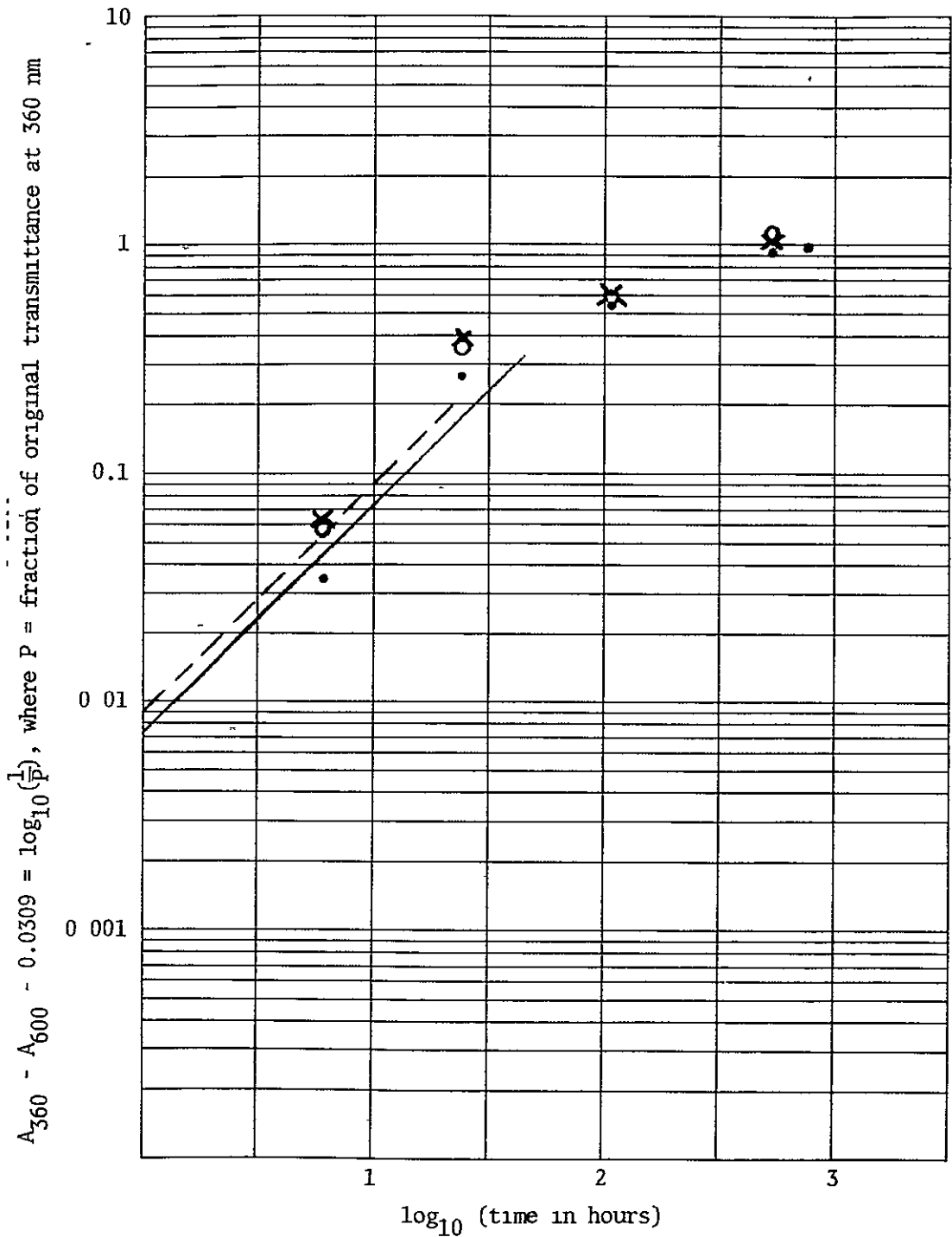
Figure B13. Lexan Yellowing vs Time, Accelerated Exposure, 55.3°C, 0 66 Relative UV Intensity

- • = 0% relative humidity (———)
- ○ = 50% relative humidity
- ✗ = 100% relative humidity (— — —)
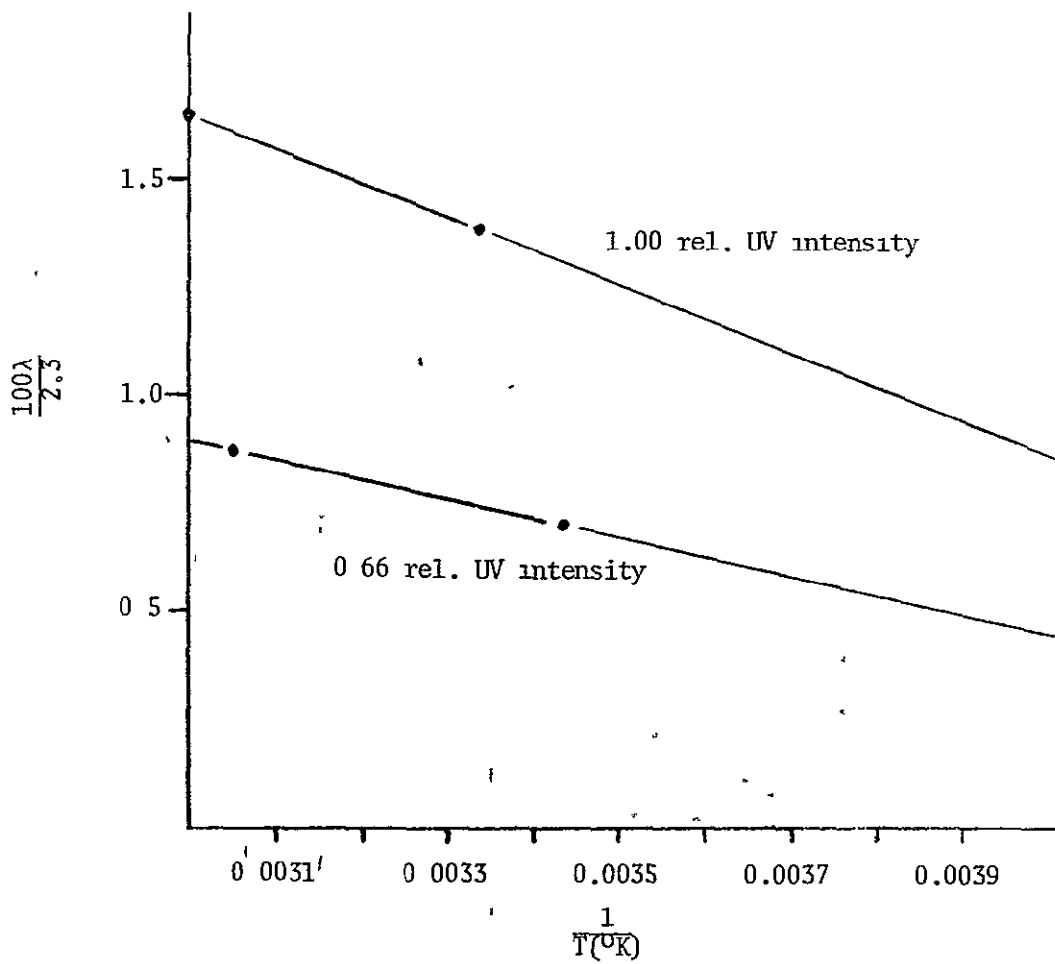
Figure B14   Relation of $\frac{100\lambda}{2.3}$ to Temperature and UV
Intensity (75% Relative Humidity)
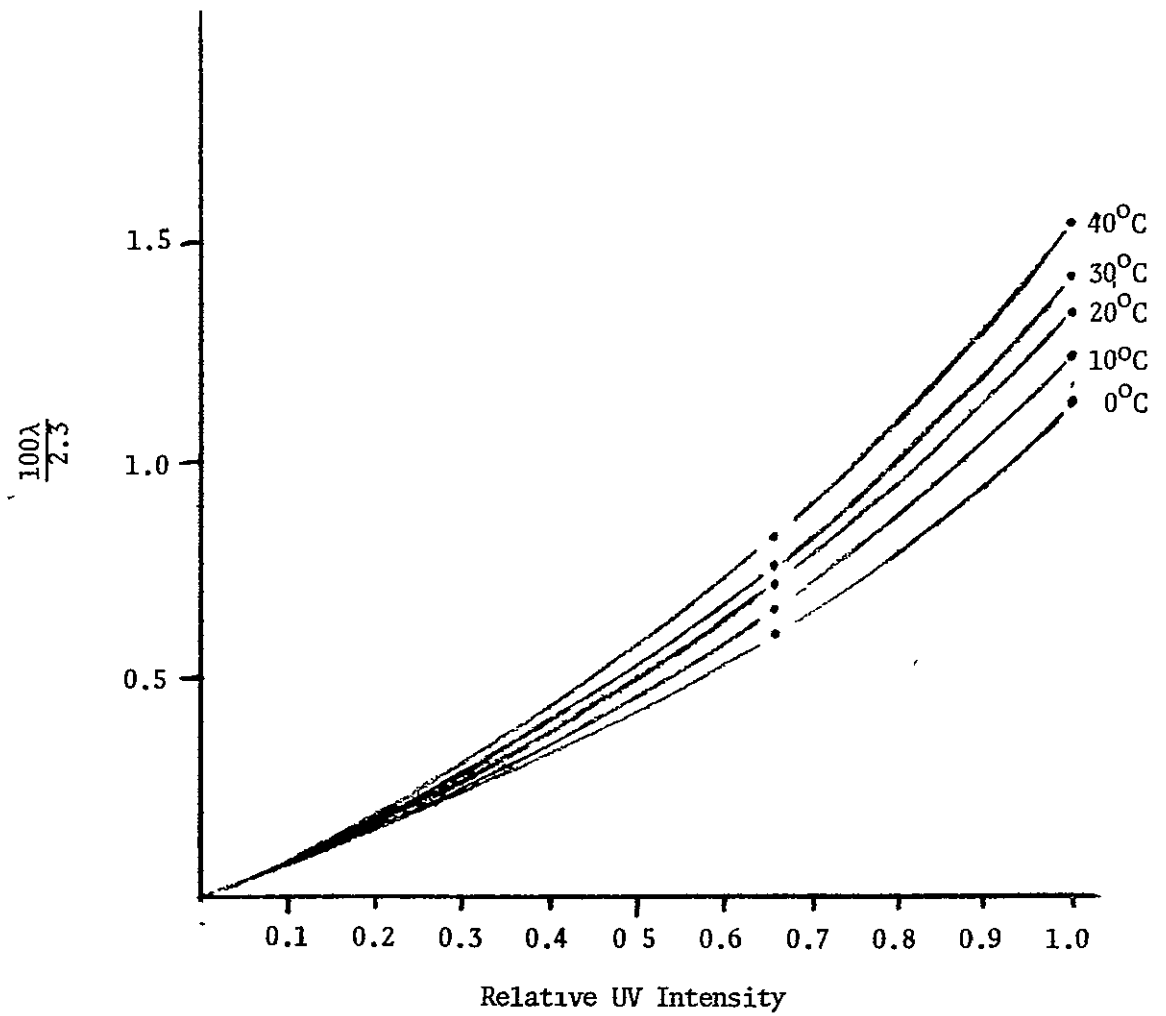
Figure B15. Relation of $\frac{100\lambda}{2.3}$ to Temperature and UV Intensity
(75% Relative Humidity)
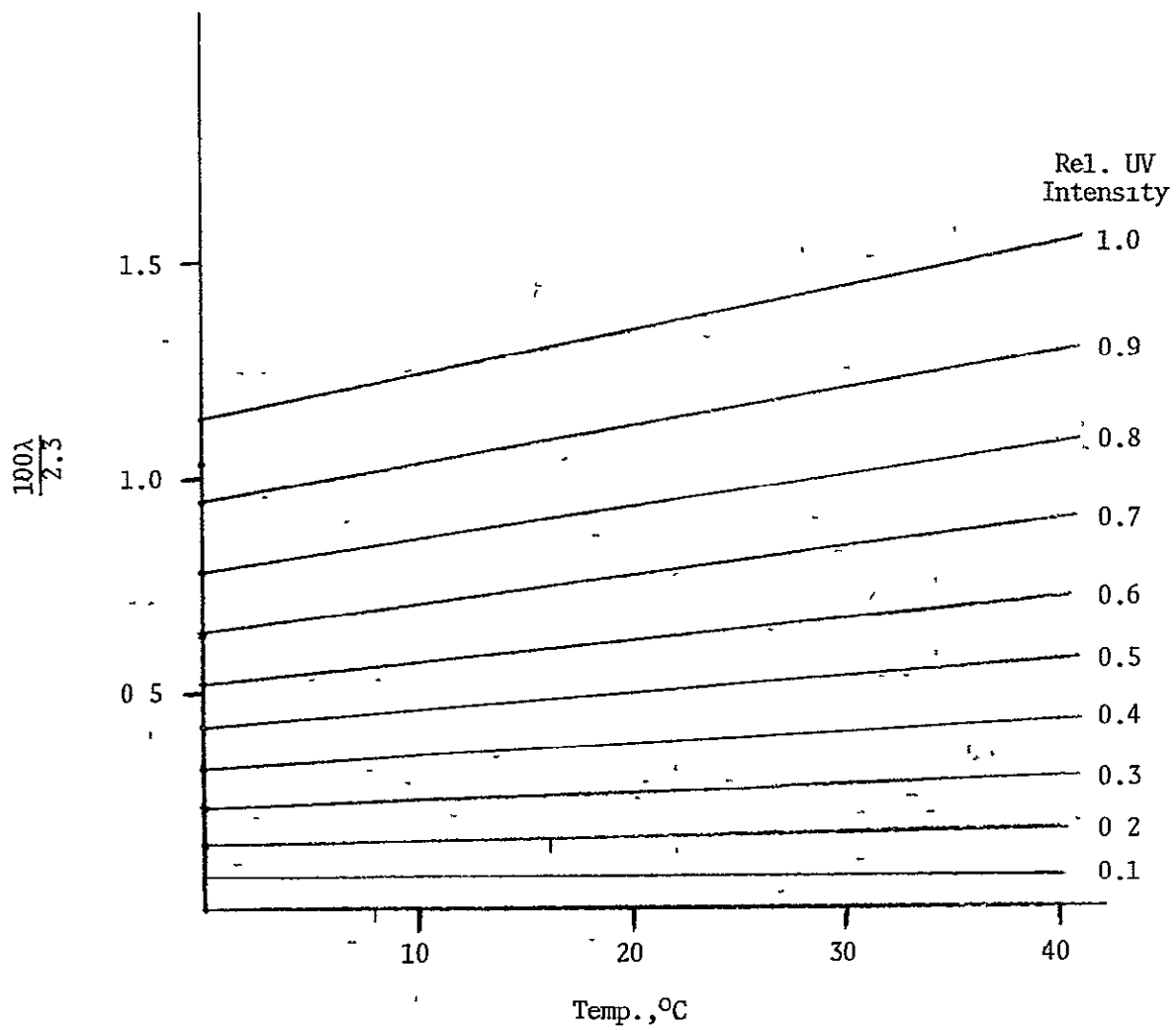
Figure B16. Relation of $\frac{100\lambda}{2.3}$ to Temperature and UV Intensity (75% Relative Humidity)
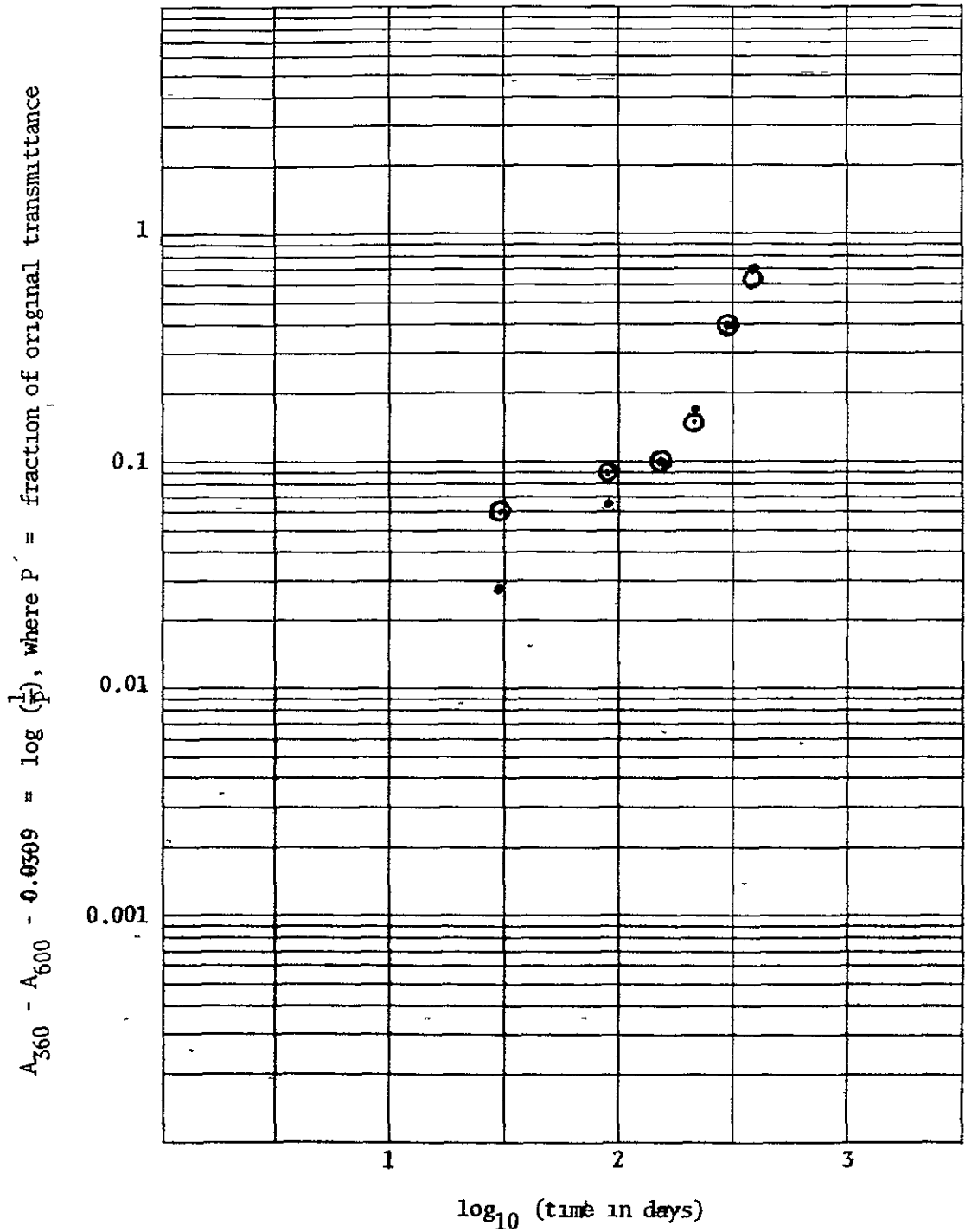
Figure B17. Predicted vs. Actual Values for Yellowing of Lexan in Miami (Exposure started 9/1/76).

● = Found

○ = Predicted
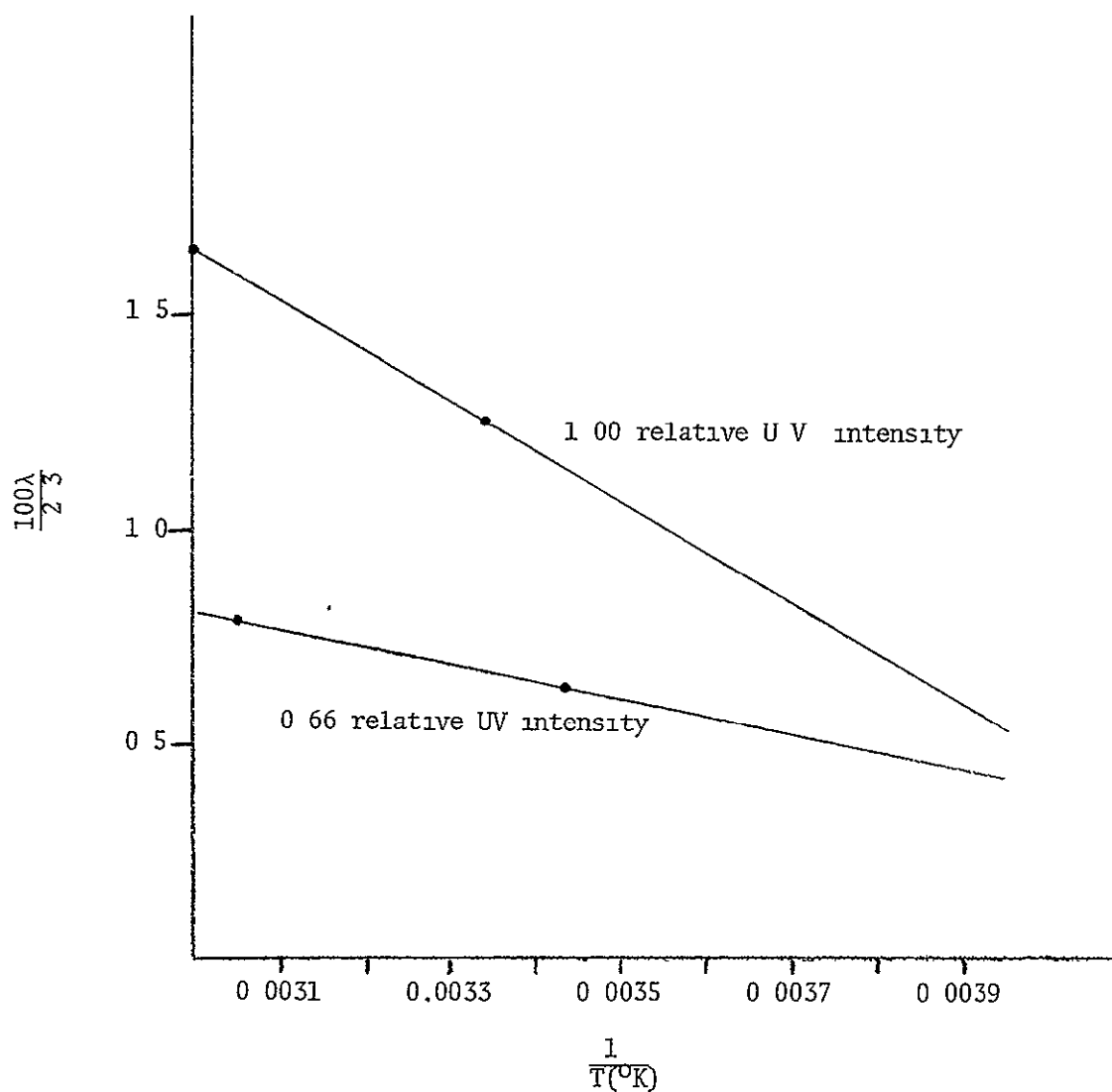
Figure B18. Relation of $\frac{100\lambda}{2\ 3}$ to Temperature and UV Intensity (27% Relative Humidity)
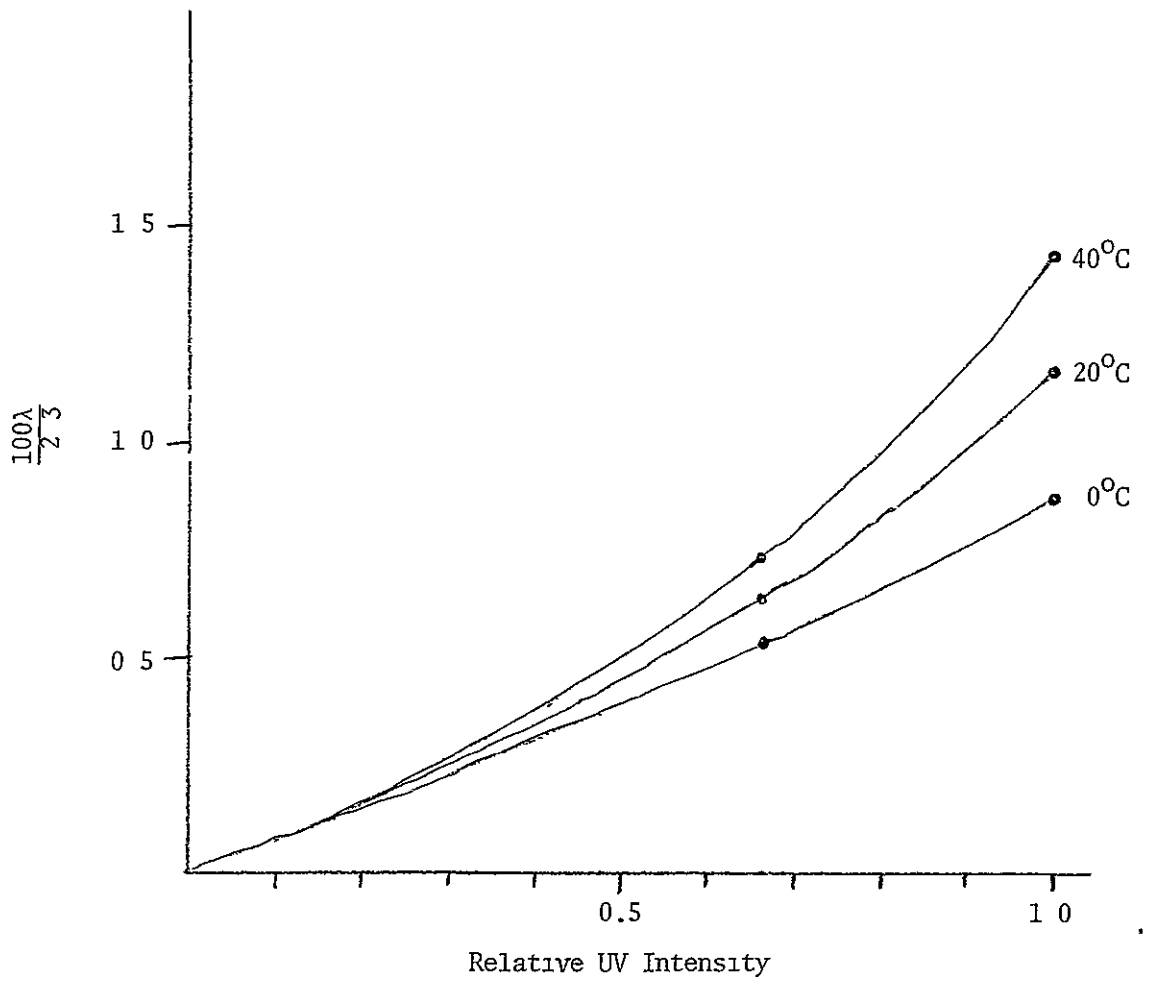
Figure B19   Relation of $\dfrac{100\lambda}{2.3}$ to Temperature and UV Intensity
(27% Relative Humidity)
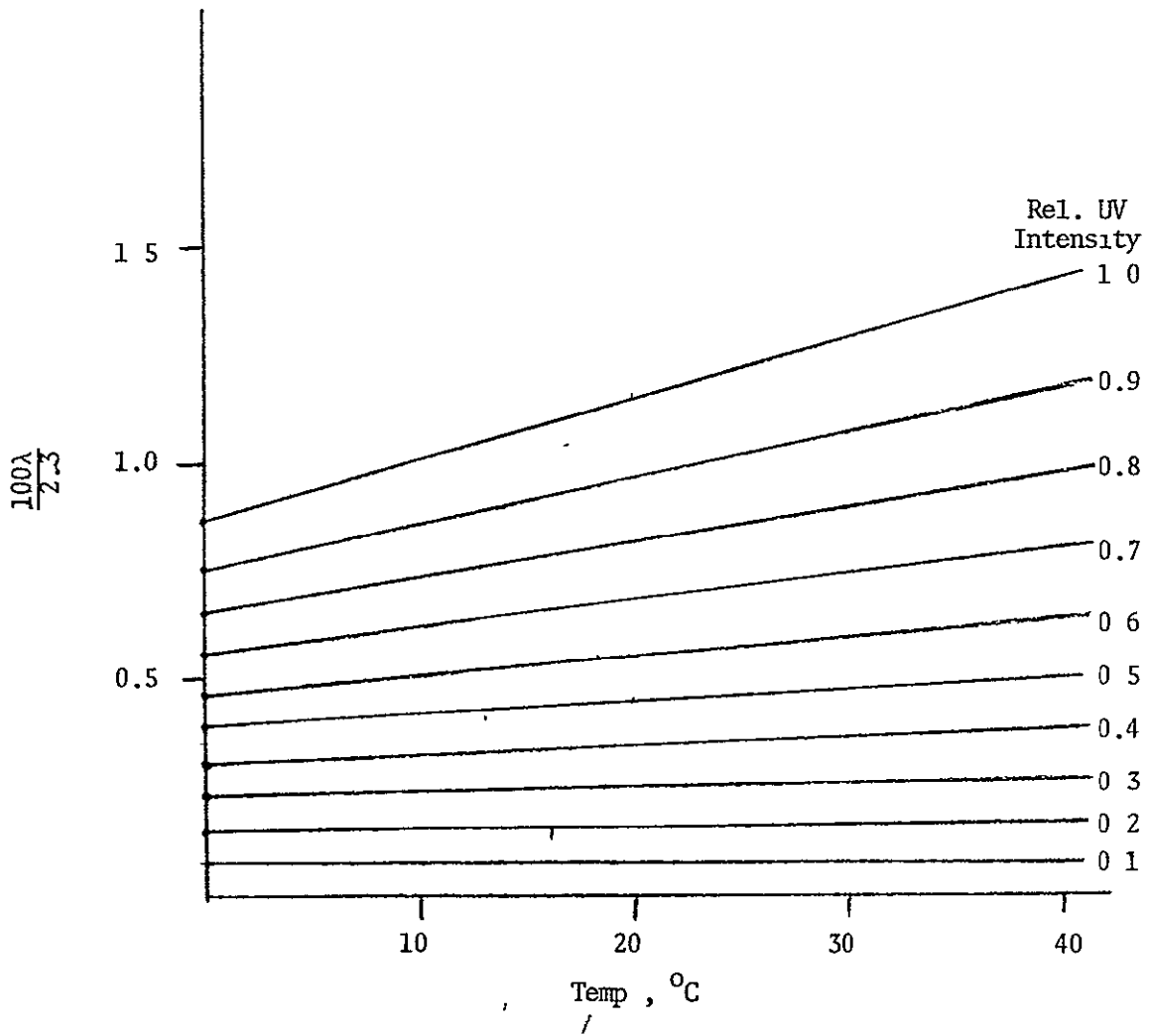
Figure B20. Relation of $\frac{100\lambda}{2.3}$ to Temperature and UV Intensity
(27% Relative Humidity)
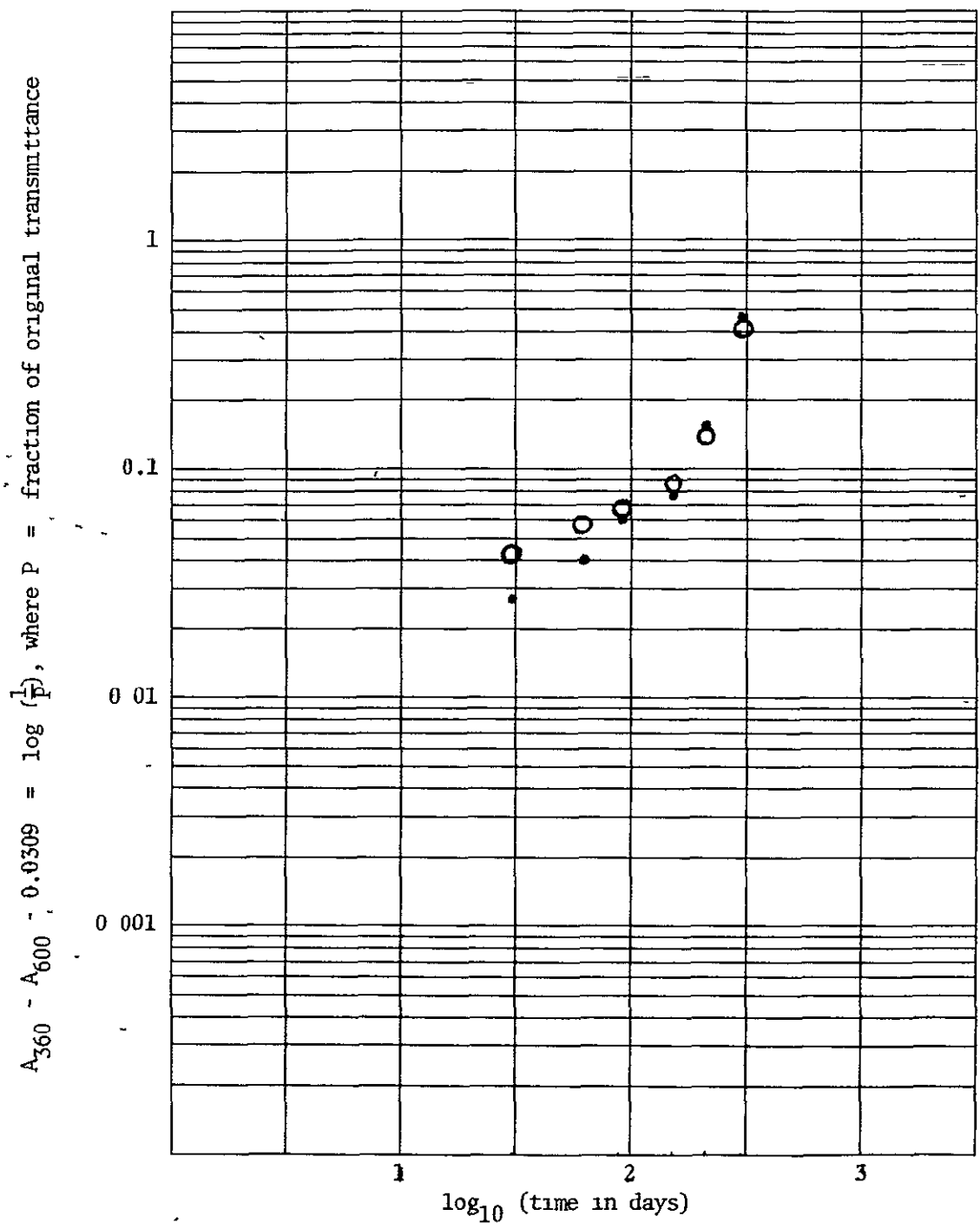
Figure B21. Predicted vs. Actual Values for Yellowing of Lexan in Phoenix (Exposure started 9/12/76).

• = Found

O = Predicted

224
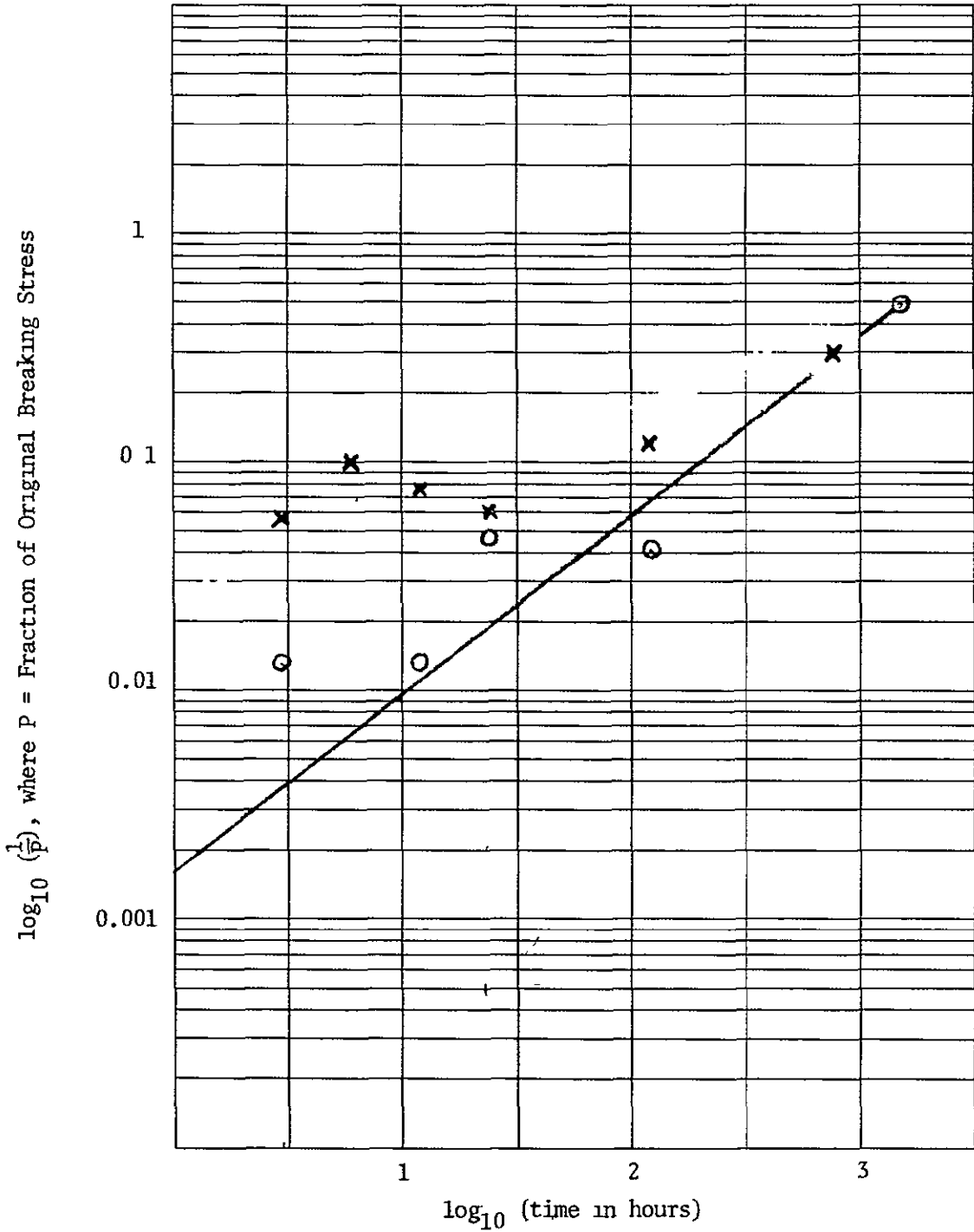
Figure B22   Accelerated Exposure Data for Polystyrene, 1.0 Relative
UV Intensity, 26.1°C

• =   0% Relative Humidity
○ =   100% Relative Humidity
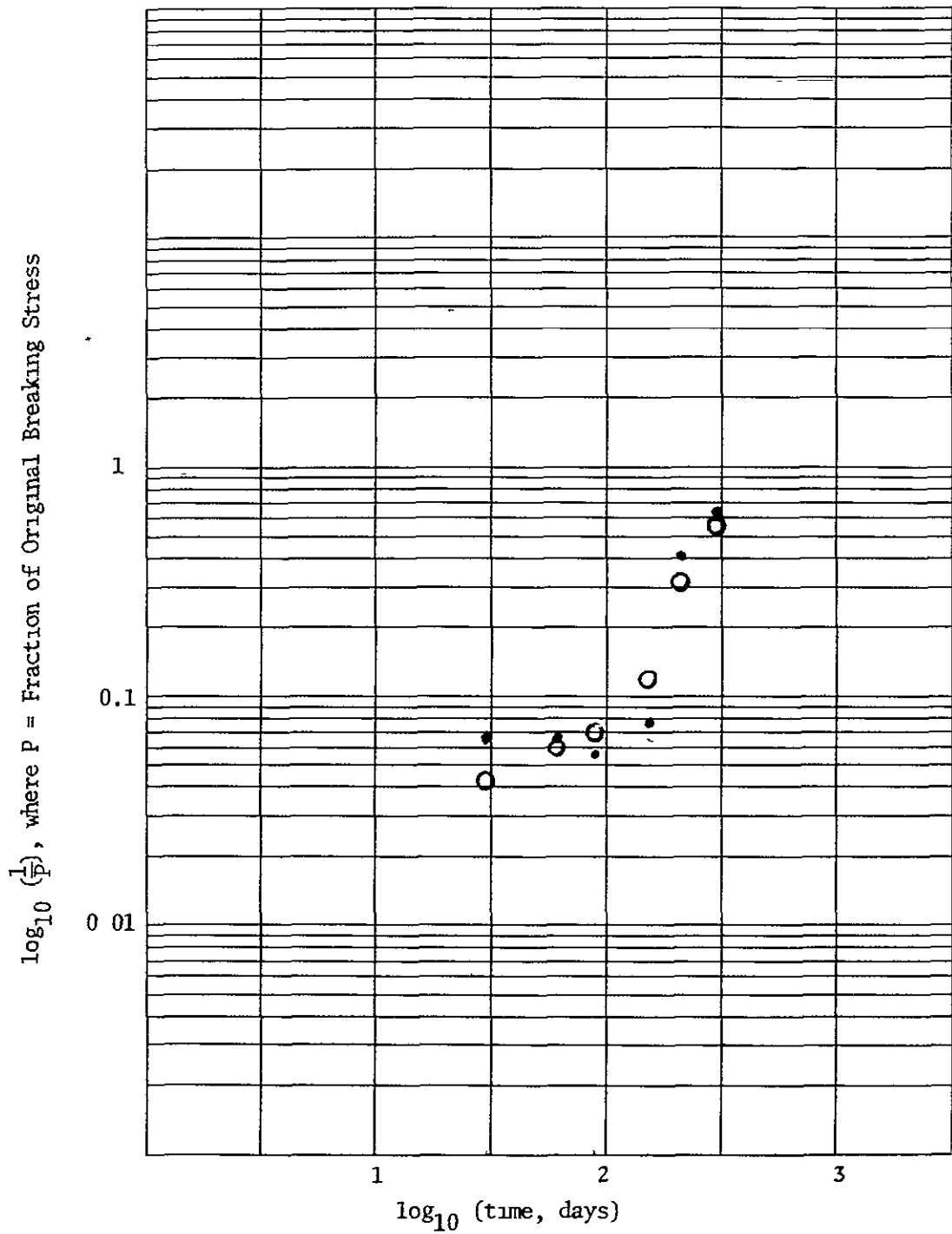
Figure B23   Predicted vs. Actual Results, Loss of Tensile Strength
of Polystyrene in Miami.

* = Found
O = Predicted

226

Figure B24. Accelerated Exposure Data for Lexan, 1.00 Relative UV
Intensity, 26.1°C.

O = 0% Relative Humidity
X = 100% Relative Humidity

227
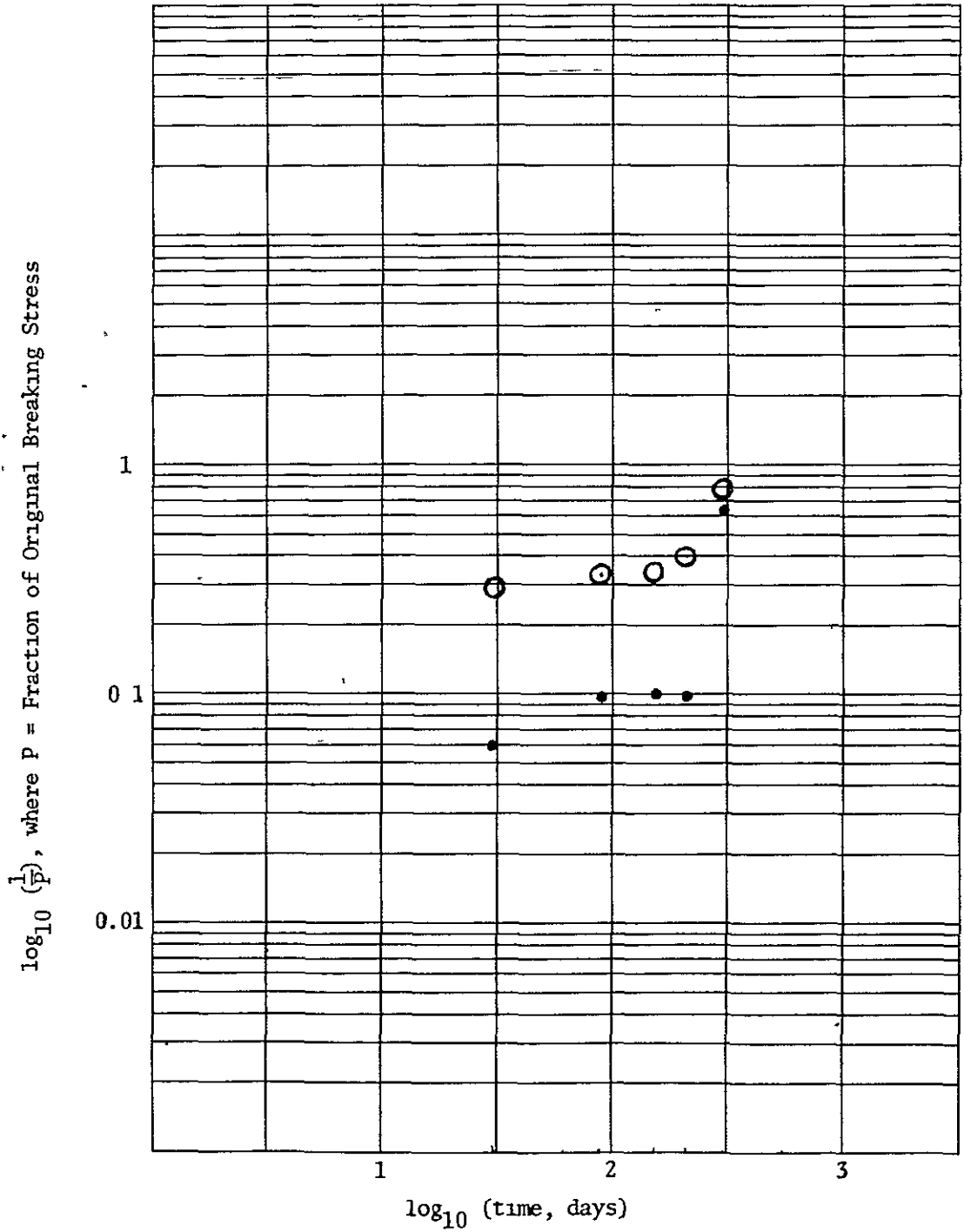
Figure B25. Predicted vs. Actual Results, Loss of Tensile Strength of Lexan in Miami.

♦ = Found
○ = Predicted

Figure B26. Relation of Breaking Stress and Transmittance at 360 nm
for Polystyrene in Accelerated Exposure,·1 00 Relative
UV Intensity, 26.1°C.

• = 0% Relative Humidity
○ = 100% Relative Humidity

229
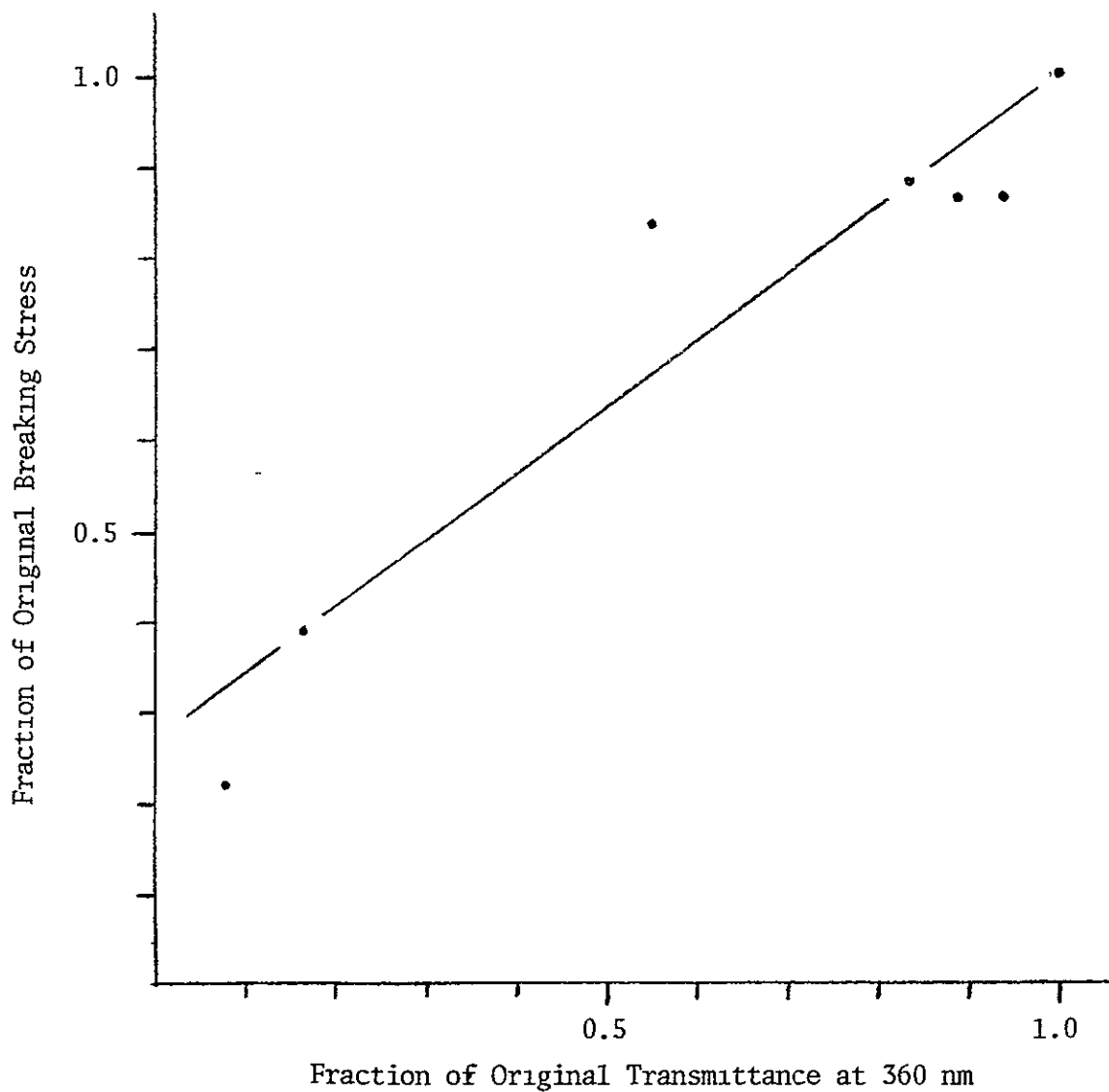
Figure B27   Relation of Breaking Stress and Transmittance at 360 nm
for Polystyrene in Miami 45°S Exposure (Started 10/20/76)

230
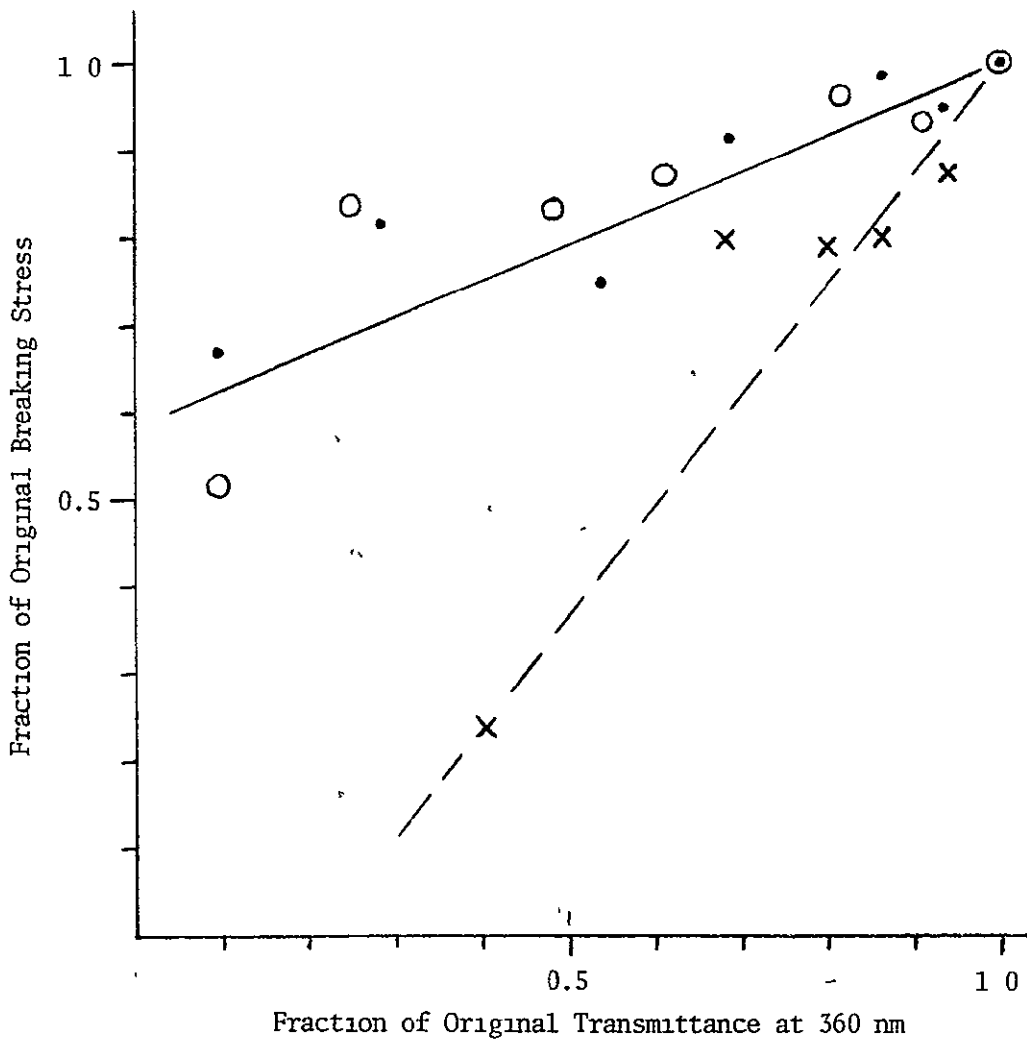
Figure B28. Relation of Breaking Stress and Transmittance
at 360 nm for Lexan

● = Accelerated exposure, 1.00 relative UV intensity,
     26 1°C, 0% relative humidity
○ = Same, 100% relative humidity
X = Miami 45°S exposure (starting 9/1/76) (— — —)

231
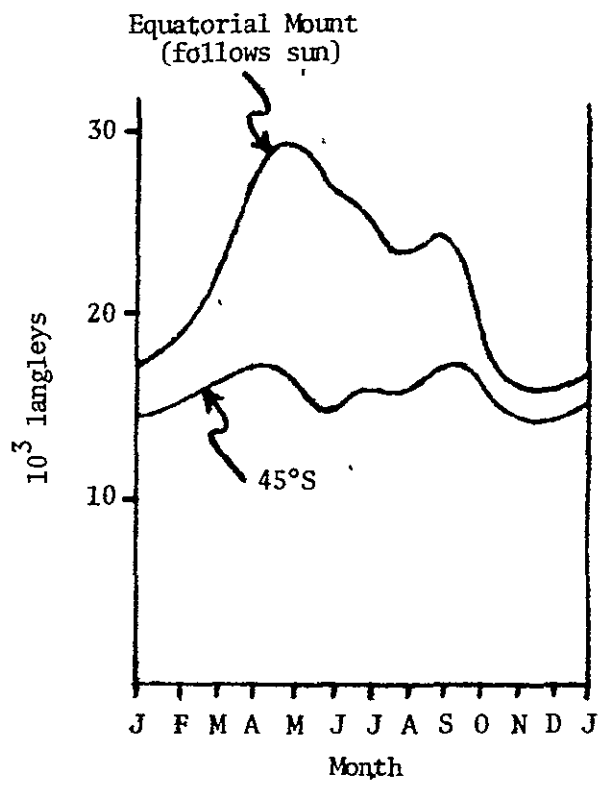
Figure B29. Monthly Insolation in Phoenix (Source· Desert Sunshine Exposure Tests, Inc.)
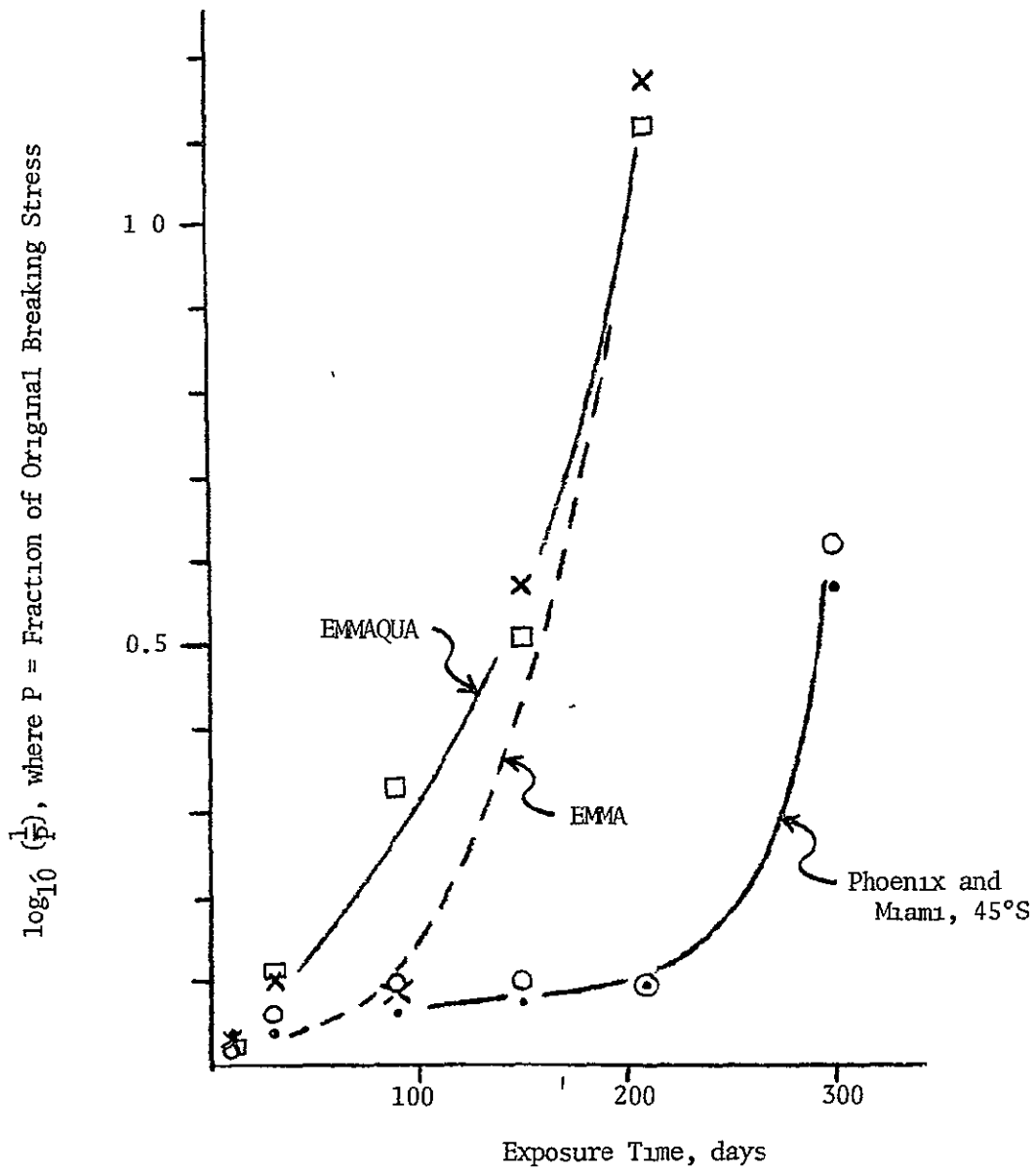
Figure B30. Tensile Breaking Stress of Lexan vs. Outdoor Exposure

- = Phoenix, 45°S
- O = Miami, 45°S
- X = EMMA
- □ = EMMAQUA

Table B1

Accelerated Exposure Data for Polystyrene

Relative UV Intensity	Air Temp., °C	Relative Humidity, %	$A_{360} - A_{600} - 0.0139$ Time, hrs						
			3	6	12	24	120	768	1536
1 00	26.1	0	0.0085	0.0094	0.0163	0 0264	0.0954	0.6677	1.0964
		50	0 0055	0.0093	0 0158	0 0283	0.1740	0.6713	
		100	0.0064	0.0102	0 0156	0.0306	0.1717	0.6135	
	60.3	0	0.0067	0.0079	0.0175	0.0414	0.3154	0 9411	1.2900
		50	0.0081	0 0081	0.0233	0.7810	0.2830	0.9924	
	/	100	0 0059	0.0099	0 0253	0.0470	0.2636	0 9114	
0.66	18.3	0		0.0088		0.0185	0 0630	0.5602	0.8546
		50		0.0104		0.0168	0.0502	0.4723	
		100		0.0098		0.0293	0.0861	0.5163	
	55.3	0		0.0033		0 0276	0.1502	0.8767	1.0315
		50		0.0081		0.0332	0.1098	0.8379	
		100		0.0069		0.0369	0 1855	0.8249	
0	40.0	0				0.0031	0.0030	0.0009	
		50				0.0041	0.0025	0.0007	
		100				0.0057	0.0019	0.0017	
	80.0	0				0.0030	0.0108	-0 0001	
		50				0.0051	0.0083	0.0019	
		100				0.0020	0 0153	0.0049	
Alt.	26.1, 6.7	0					0.0429	0.5540	
		50					0.0511	0.4880	
		100					0.0582	0 5080	
	60.3,43.9	0					0 0597	0.7505	
		50					0.0804	0.7508	
		100					0.0783	0.8120	

Table B2

Values for $\frac{1000\lambda}{2.3}$, hr.$^{-1}$

Air Temp.,°C	Relative UV Intensity									
	0 1	0 2	0 3	0 4	0 5	0.6	0.7	0.8	0.9	1.0
15	0.15	0.30	0.46	0.61	0.76	0.91	1.07	1.22	1.37	1.52
16	0.16	0.31	0 47	0 62	0.78	0 93	1.09	1 24	1.39	1.53
17	0 17	0 32	0.48	0.63	0.80	0.95	1.10	1.26	1.41	1 56
18	0 17	0.33	0.49	0 64	0.82	0.97	1.13	1.28	1 43	1 58
19	0.18	0 34	0.50	0 66	0 84	1 00	1.14	1.30	1.45	1.60
20	0.19	0.35	0.52	0.68	0.86	1.02	1 17	1.32	1 47	1.63
21	0.19	0 36	0.53	0 69	0.88	1.03	1 18	1.34	1.49	1.65
22	0.20	0.37	0 54	0.70	0.90	1.05	1.20	1.37	1.52	1.67
23	0.20	0 37	0 55	0 72	0.91	1.07	1.22	1.39	1.54	1.70
24	0.20	0.38	0 56	0.74	0.93	1.09	1 24	1 41	1.55	1.73
25	0.20	0 39	0.57	0.75	0.94	1.10	1.26	1 43	1.57	1.75
26	0 20	0.40	0.58	0 77	0 95	1 12	1.28	1.46	1.60	1 77
27	0.21	0.40	0.59	0 78	0.97	1 13	1.30	1 47	1.63	1.79
28	0.21	0.40	0 60	0 79	0.98	1.15	1.32	1.49	1.65	1.82
29	0.21	0.41	0.62	0 81	1 00	1.16	1.34	1.51	1.67	1 84
30	0.22	0.42	0.63	0.82	1.01	1.17	1.36	1.53	1 69	1.85
31	0.22	0.43	0.64	0.83	1.03	1.19	1.38	1.55	1.70	1 88
32	0.23	0 44	0.65	0.84	1.04	1.21	1 40	1 57	1 73	1.90
33	0.23	0.45	0.66	0.86	1.06	1.23	1.42	1.60	1 75	1.93
34	0 23	0 46	0.67	0.87	1 07	1.24	1.43	1.63	1.77	1.96
35	0.24	0.47	0 67	0.88	1.08	1.26	1.46	1.64	1.80	1.97
36	0.24	0.48	0.68	0 90	1.10	1.28	1.47	1.66	1.82	2.00
37	0.25	0.48	0.70	0 91	1 11	1.29	1.49	1.69	1.84	2.02
38	0.25	0.48	0.71	0.93	1 13	1.31	1 51	1.70	1.86	2.04
39	0.26	0.49	0.72	0.94	1.14	1.33	1.53	1.72	1.88	2.05
40	0 27	0 50	0.74	0.95	1 16	1 36	1.54	1.73	1.90	2.07

Table B3

Miami Weather Data

Month	Mean Rel. Humidity %	7 - 9 AM* UV	7 - 9 AM* T,°C	9 - 11 AM** UV	9 - 11 AM** T,°C	11AM-1PM*** UV	11AM-1PM*** T,°C	1 - 3 PM UV	1 - 3 PM T,°C	3 - 5 PM UV	3 - 5 PM T,°C
Sept. 1976	76	0.09	27	0.44	29	0.67	31	0.49	31	0 07	31
Oct.	75	0 04	24	0.20	27	0.31	29	0.23	29	0.03	29
Nov	75	0.02	22	0.10	24	0 16	26	0.11	26	0 02	26
Dec.	75	0.01	19	0 06	22	0.09	24	0.07	24	0.01	24
Jan. 1977	70	0.02	16	0.09	19	0.14	22	0 10	22	0.01	22
Feb.	71	0.03	18	0.14	21	0.22	23	0.16	23	0.02	23
March	69	0.05	23	0.26	26	0.40	28	0.29	28	0.04	28
April	69	0.09	23	0.46	25	0.71	27	0.52	27	0 07	27
May	71	0.12	25	0.60	27	0 92	29	0.67	29	0.10	29
June	74	0.14	27	0.69	29	1.06	31	0.77	31	0 11	31
July	74	0 13	28	0.65	30	1.00	32	0.73	32	0.10	32
Aug.	75	0.12	28	0.60	30	0.90	32	0 66	32	0.09	32

Source   South Florida Test Service, Inc., Miami,
_____   for temperature and relative humidity data.

* Average of daily means for the month.

** Average of daily means and highs, i.e , of the preceding and following columns.

*** Average of daily highs for the month.

Table B4

Relative UV Intensities

Month	Rel. UV Intensity*	Relative UV Intensity				
		7-9AM	9-11AM	11AM-1PM	1-3PM	3-5PM
Jan.	0.15	0 02	0 09	0 14	0.10	0.01
Feb.	0 24	0.03	0 14	0.22	0.16	0 02
March	0.43	0.05	0.26	0 40	0.29	0 04
April	0.77	0 09	0.46	0.71	0.52	0.07
May	1.00	0.12	0.60	0 92	0.67	0 10
June	1.15	0 14	0.69	1.06	0 77	0.11
July	1.09	0.13	0 65	1.00	0.73	0.10
Aug.	0.98	0.12	0.60	0 90	0.66	0 09
Sept.	0.73	0 09	0.44	0.67	0.49	0.07
Oct.	0.34	0.04	0.20	0.31	0.23	0.03
Nov.	0 17	0.02	0 10	0.16	0 11	0.02
Dec.	0.10	0.01	0.06	0.09	0.07	0.01

* Source   L. R Koller, Ultraviolet Radiation, 2nd Edition,
         John Wiley & Sons, N.Y., 1965, pg. 137.

Table B5

UV Intensity vs. Time of Day

Time	Relative UV Intensity	% of Total
8 AM	12	5
10 AM	64	25
Noon	100	38
2 PM	73	28
4 PM	11	4
Totals	260	100

Source   L. R. Koller, Ultraviolet Radiation,
2nd Edition, John Wiley & Sons, N Y.,
1965, pg. 124.

Table B6 Parameter Values Assigned to Miami, by Month and Time of Day

$$1000 \; \frac{\lambda}{2.3}, \; hr^{-1}$$

Month	7-9AM	9-11AM	11AM-1PM	1-3PM	3-5PM
Sept. 1976	0.21	0 81	1 38	1.03	0.22
Oct	0	0.40	0 62	0.41	0
Nov	0	0.20	0.40	0.20	0
Dec.	0	0.20	0.20	0.20	0
Jan 1977	0	0.18	0.20	0.20	0
Feb	0	0.19	0.37	0.37	0
March	0 20	0.58	0.79	0 60	0
April	0.20	0.94	1.30	0.97	0.21
May	0.20	1.13	1.67	1.34	0.21
June	0.21	1.34	1.88	1 55	0.22
July	0.21	1.36	1 90	1.40	0 23
Aug.	0.21	1.17	1.73	1.40	0.23

Table B7 . Transformed Data from Table B6

$$\text{Data of Table B6} \times 0 \; 024 = \frac{\lambda}{2.3}, \; day^{-1}$$

Month	7-9AM	9-11AM	11AM-1PM	1-3PM	3-5PM
Sept. 1976	0.0050	0.019	0.033	0.025	0 0053
Oct.	0	0.0096	0 015	0.0098	0
Nov.	0	0.0048	0.0096	0 0048	0
Dec.	0	0.0048	0.0048	0 0048	0
Jan. 1977	0	0.0043	0.0048	0 0048	0
Feb.	0	0 0046	0.0089	0.0089	0
March	0.0048	0.014	0 019	0.014	0
April	0.0048	0.023	0.031	0 023	0.0050
May	0.0048	0.027	0.040	0 032	0 0050
June	0.0050	0.032	0.045	0.037	0.0053
July	0.0050	0.033	0 046	0.034	0.0055
Aug	0.0050	0.028	0.042	0.034	0.0055

239

Table B8

Parameter Values Raised to the 1.11 Power

$$(\frac{\lambda}{2.3}, \text{day}^{-1})^{1.11}$$

Month	7-9AM	9-11AM	11AM-1PM	1-3PM	3-5PM	Total
Sept. 1976	0 0028	0.012	0.023	0.017	0.0030	0.0578
Oct	0	0.0058	0.0095	0.0059	0	0 0212
Nov.	0	0.0027	0.0058	0 0027	0	0.0112
Dec.	0	0.0027	0.0027	0.0027	0	0 0081
Jan. 1977	0	0.0024	0.0027	0.0027	0	0.0078
Feb.	0	0.0025	0.0053	0.0053	0	0.0131
March	0.0027	0.0088	0 012	0.0088	0	0.0323
April	0.0027	0.015	0.021	0.015	0 0028	0.0565
May	0 0027	0.018	0 028	0.022	0.0028	0.0735
June	0.0028	0.022	0.032	0.026	0.0030	0.0858
July	0.0028	0.023	0.033	0.023	0.0031	0.0849
August	0.0028	0.019	0.030	0.023	0 0031	0.0779

Table B9   Exposure Periods

Exposure Time, Days	Month	Days
0 (10/20/76)		0
5	Oct. 1976	5
10	Oct. 1976	10
15	Oct. 1976	11
	Nov. 1976	4
30	Oct. 1976	11
	Nov. 1976	19
60	Oct. 1976	11
	Nov. 1976	30
	Dec. 1976	19
90	Oct. 1976	11
	Nov. 1976	30
	Dec. 1976	31
	Jan. 1977	18
150	Oct. 1976	11
	Nov. 1976	30
	Dec. 1976	31
	Jan. 1977	31
	Feb. 1977	28
	March 1977	19
210	Oct. 1976	11
	Nov. 1976	30
	Dec. 1976	31
	Jan. 1977	31
	Feb. 1977	28
	March 1977	31
	April 1977	30
	May 1977	18
300	Oct. 1976	11
	Nov. 1976	30
	Dec. 1976	31
	Jan. 1977	31
	Feb. 1977	28
	March 1977	31
	April 1977	30
	May 1977	31
	June 1977	30
	July 1977	31
	Aug. 1977	16

241

Table B10

Prediction of Polystyrene Yellowing in Miami
Using a Lognormal Model

Exposure Time, Days	T	UV	$\log_e$ CUV	$\hat{\sigma}$	$\hat{\mu}$	$\hat{Z}$	$\hat{P}$	P
30	27.5	0.255	4.30	1.49	6.91	-1.75	0.96	0 94
60	25.8	0.178'	4.84	1.60	6.77	-1.21	0.89	0.91
90	24.5	0 168	5.19	1 60	7.01	-1.14	0.87	0 83
150	24.7	0.228	5.87	1.50	6.20	-0.22	0.59	0.55
210	25.6	0.405	6.46	1 27	5.21	0.98	0 16	0.16
300	27 5	0.605	7.01	1.12	4.73	2.05	0.021	0.074

NOTE   Definition of terms.

T   =   Cumulative average high temperature in °C.

UV   =   Cumulative average outdoor UV, relative value.
(See text.)   This represents the average UV level

CUV   =   Cumulative outdoor UV.   These numbers, which are based
on a different source, represent total UV deposited
on sample.

$\hat{\sigma}$ and $\hat{\mu}$ are parameters defined in the text.

$$\hat{Z} = \frac{\log_e(CUV) - \hat{\mu}}{\hat{\sigma}}$$ This is the $\frac{x - \mu}{\sigma}$ term in equation for
P in the text.

$\hat{P}$ =   Predicted fraction of original transmittance at 360 nm.

P   =   Actual fraction of original transmittance at 360 nm

Table B11

Data for Lexan Yellowing, Accelerated Exposure

Rel. UV Intensity	Air Temp., °C	Rel Hum, %	$A_{360} - A_{600} - 0.0309$ Exposure Time, hours						
			3	6	12	24	120	768	1536
1.00	26 1	0	0 0308	0 0652	0.1639	0.2693	0.5467	0.9149	1 0200
		50	0.0395	0 0699	0.1801	0.3015	0.5378	0 9369	
		100	0.0402	0 0870	0.2158	0.3171	0.6097	1 0227	
	60.3	0	0.0501	0.0712	0.2996	0 4347	0 7361	1 1135	1.2492
		50	0.0476	0.0842	0 2995	0 4558	0.6922	0 9982	
		100	0.0375	0.0995	0.2599	0 4383	0 7997	1 3134	
0 66	18 3	0		0 0278		0 1813	0.3697	0 6712	0.7582
		50		0.0533		0 2357	0.4566	0 6713	
		100		0 0418		0.2187	0 4377	0.8648	
	55.3	0		0 0352		0 2695	0.5360	0.9091	0 9714
		50		0 0575		0.3472	0 5785	1 1255	
		100		0 0642		0.3895	0 6117	1.0366	
0	40	0				-0.0049	-0 0099	-0 0117	
		50				-0 0052	-0 0106	-0 0124	
		100				-0.0097	-0 0113	-0.0121	
	80	0				-0.0087	-0 0120	-0 0147	
		50				-0.0069	-0.0114	-0 0128	
		100				-0 0104	-0 0107	-0 0051	
0 ↔ 1.00 alter-nating	26.1, 6.7	0	'	ı			0 3855	0.7279	
		50					0 4024	0 7379	
		100					`0 4458	0 9056	
	60.3, 43 9	0					0 5893	0 9578	
		50					0 5444	0 8464	
		100				.	0 5161	0 9082	

Table B12

Values for $\frac{100\lambda}{2\ 3}$ (75% Relative Humidity)

Temp., °C	Relative UV Intensity									
	0 1	0.2	0 3	0.4	0 5	0.6	0.7	0.8	0.9	1.0
15	0.08	0.16	0.26	0.37	0 48	0.59	0.74	0.90	1 07	1.29
16	0 08	0.16	0.26	0 37	0.48	0.60	0.74	0.90	1.08	1 30
17	0.08	0.16	0.26	0 37	0.48	0.60	0.75	0 91	1.09	1.31
18	0 08	0.16	0.26	0 37	0 49	0.61	0.76	0 92	1.00	1.32
19	0 08	0 16	0.26	0.37	0.50	0 61	0 77	0 93	1.11	1.33
20	0.08	0.16	0.26	0 38	0 50	0 62	0.77	0.93	1 12	1.34
21	0.08	0.16	0.26	0.38	0.50	0.63	0.78	0.94	1 13	1.35
22	0.08	0.16	0 27	0.38	0 50	0.63	0.78	0.94	1 14	1.36
23	0.08	0.16	0.27	0.38	0.51	0.63	0.79	0.95	1.15	1.37
24	0.08	0.16	0.27	0.39	0.51	0.64	0.80	0.96	1.15	1.38
25	0 08	0.16	0.27	0.39	0.52	0.64	0 80	0.97	1.16	1.39
26	0.08	0.17	0.27	0.39	0.53	0.65	0 81	0.97	1.17	1.40
27	0 08	0.17	0.27	0.39	0.53	0.66	0.82	0.98	1.18	1.41
28	0 08	0.17	0.28	0.40	0.53	0.66	0.83	0 99	1.19	1.42
29	0.08	0.17	0.28	0.40	0 54	0.67	0.83	1.00	1 20	1.43
30	0.08	0.17	0.28	0 40	0.54	0.67	0 84	1.00	1.20	1.44
31	0.08	0.17	0.28	0.40	0.54	0.67	0.84	1.01	1.21	1.45
32	0 08	0.17	0.29	0.41	0.54	0.68	0.85	1.02	1.22	1.46
33	0.08	0.17	0.29	0.41	0.55	0 68	0.85	1.03	1.23	1.47
34	0.08	0.17	0.29	0.42	0.55	0.69	0.86	1.03	1.23	1.48
35	0.08	0.17	0.29	0.42	0.55	0.70	0 87	1.04	1.24	1.49
36	0.08	0.18	0 30	0.42	0.56	0.70	0.87	1.04	1.25	1.50
37	0.08	0.18	0.30	0.42	0.56	0.70	0 88	1.05	1.26	1.51
38	0.08	0.18	0.30	0.43	0.57	0.71	0.89	1.06	1.27	1.52
39	0.08	0.18	0.30	0.43	0 57	0.71	0.89	1.07	1.28	1.53
40	0.08	0 18	0.30	0.43	0.57	0 72	0.90	1.08	1.29	1 54

Table B13

Miami Weather Data

Month	Ave R.H , %	7-9 AM		9-11 AM		11AM-1 PM		1-3 PM		3-5 PM	
		UV	T,^{O}C	UV	T,^{O}C	UV	T,^{O}C	UV	T,^{O}C	UV	T,^{O}C
Sept. 1976	76	0.09	27	0 44	29	0.67	31	0.49	31	0 07	31
Oct.	75	0.04	24	0 20	27	0 31	29	0 23	29	0 03	29
Nov.	75	0 02	22	0.10	24	0.16	26	0.11	26	0 02	26
Dec	75	0 01	19	0.06	22	0 09	24	0.07	24	0 01	24
Jan. 1977	70	0 02	16	0 09	19	0.14	22	0.10	22	0 01	22
Feb.	71	0.03	18	0 14	21	0.22	23	0 16	23	0.02	23
March	69	0 05	23	0.26	26	0 40	28	0 29	28	0 04	28
April	69	0.09	23	0 46	25	0 71	27	0 52	27	0.07	27
May	71	0.12	25	0 60	27	0.92	29	0.67	29	0 10	29
June	74	0 14	27	0 69	29	1.06	31	0.77	31	0.11	31
July	74	0.13	28	0.65	30	1 00	32	0 73	32	0.10	32
Aug.	75	0.12	28	0 60	30	0.90	32	0.66	32	0.09	32

Source   South Florida Test Service, Inc., Miami, for
temperature and relative humidity data

Table B14

$\frac{100\lambda}{2.3}$ Values for Miami, Based on Accelerated Exposure Data

| Month | $\frac{100\lambda}{2.3}$ | | | | |
	7-9 AM	9-11 AM	11 AM-1 PM	1-3 PM	3-5 PM
Sept. 1976	0.08	0.40	0.84	0.54	0.08
Oct.	0	0.17	0.28	0.17	0
Nov.	0	0.08	0 17	0.08	0
Dec.	0	0 08	0.08	0.08	0
Jan. 1977	0	0.08	0.08	0.08	0
Feb.	0	0.08	0.16	0.16	0
March	0.08	0.27	0.40	0.28	0
April	0.08	0.52	0.82	0.53	0.08
May	0.08	0.66	1.20	0.83	0.08
June	0.08	0.83	1.45	1.01	0 08
July	0.08	0.84	1.46	0.85	0.08
Aug.	0.08	0.67	1.22	0.85	0.08

Table B15

$\frac{\lambda}{2.3}$ Values for the "Typical Day" of each Month in Miami

Month	$\frac{100\lambda}{2\ 3}$, hr.$^{-1}$ Total for 7AM-5PM	$\frac{\lambda}{2\ 3}$, day^{-1}
Sept. 1976	1.94	0 47
Oct.	0.62	0.15
Nov.	0.33	0 079
Dec.	0.24	0.058
Jan 1977	0 24	0.058
Feb.	0 40	0 096
March	1.03	0 25
April	2 03	0.49
May	2 85	0 68
June	3.45	0 83
July	3.31	0.79
August	2.90	0 70

Table B16

$\frac{\lambda}{2.3}$ Values for Miami, Corrected for Mismatch of Xenon Lamp
and Sunlight at 300 nm

Month	$\dfrac{\lambda}{2.3}$, day^{-1}, total for 7 AM – 5 PM
	19.5
Sept. 1976	0.024
Oct.	0.0077
Nov.	0 0041
Dec.	0.0030
Jan. 1977	0.0030
Feb.	0.0049
March	0.013
April	0 025
May	0 035
June	0 043
July	0 041
August	0 036

Table B17

Phoenix Weather Data

Month	Ave. R H , %	7-9 AM		9-11 AM		11AM-1 PM		1-3 PM		3-5 PM	
		UV	T,°C	UV	T,°C	UV	T,°C	UV	T,°C	UV	T,°C
Sept 1976	40	0 09	18	0 44	25	0 67	32	0 49	32	0 07	32
Oct	34	0.04	14	0.20	21	0 31	27	0 23	27	0 03	27
Nov	28	0.02	10	0.10	17	0.16	23	0.11	23	0.02	23
Dec.	28	0.01	7	0 06	13	0.09	19	0.07	19	0 01	19
Jan. 1977	43	0.02	6	0.09	10	0 14	16	0 10	16	0 01	16
Feb.	20	0.03	8	0.14	14	0 22	22	0.16	22	0.02	22
March	21	0.05	7	0.26	13	0.40	20	0.29	20	0.04	20
April	19	0.09	13	0 46	21	0.71	28	0.52	28	0 07	28
May	21	0.12	14	0.60	22	0 92	29	0.67	29	0 10	29
June	15	0 14	23	0 69	32	1.06	40	0.77	40	0 11	40
July	27	0 13	27	0.65	33	1.00	41	0.73	41	0.10	41
Aug	29	0 12	22	0 60	30	0.90	37	0 66	37	0 09	37

Source. Desert Sunshine Exposure Tests, Inc. for temperature and relative humidity data.

Table B18

Values for $\frac{100\lambda}{2.3}$ (27% Relative Humidity)

Temp.,°C	Relative UV Intensity									
	0.1	0.2	0.3	0.4	0.5	0.6	0.7	0.8	0.9	1.0
6	0.08	0 15	0.23	0.32	0.41	0.49				
7	0.08	0.15	0.23	0 32	0 41	0.49				
8	0.08	0.15	0.23	0.32	0.41	0.50				
9	0.08	0.15	0.23	0.32	0.41	0 50				
10	0 08	0.15	0.23	0.32	0.42	0 50				
11	0.08	0.15	0.23	0.32	0 42	0.51				
12	0.08	0.15	0.24	0.33	0.42	0 52				
13	0.08	0.15	0.24	0.33	0 42	0 52				
14	0 08	0 15	0 24	0.33	0.43	0.53				
15	0.08	0 15	0.24	0.33	0.43	0 53	0.66	0.77	0 91	1.07
16	0.08	0.15	0.24	0.33	0 43	0.53	0 66	0.78	0 92	1.09
17	0.08	0 15	0.24	0 33	0 43	0.53	0 66	0.79	0.93	1 10
18	0 08	0.15	0.24	0.34	0.43	0.54	0.67	0.80	0.94	1.12
19	0.08	0.15	0.24	0.34	0.44	0.54	0.67	0 81	0.95	1 13
20	0 08	0.15	0.25	0.34	0.44	0.54	0 68	0.82	0.96	1 14
21	0.08	0.15	0.25	0.34	0.44	0 55	0.69	0.82	0.97	1 16
22	0.08	0.15	0.25	0.34	0.44	0.55	0.69	0.83	0 98	1.17
23	0.08	0 15	0 25	0 35	0.45	0.55	0.70	0.84	1.00	1.18
24	0.08	0 15	0 25	0 35	0.45	0.57	0.70	0.85	1 00	1.20
25	0.08	0.15	0 25	0 35	0.45	0 57	0.71	0.86	1.02	1.22
26	0 08	0.15	0.25	0.35	0.46	0.57	0.72	0.87	1.03	1.23
27	0 08	0.15	0.25	0.35	0.46	0 58	0 72	0 87	1 04	1.24
28	0.08	0.15	0.25	0.36	0.46	0.58	0.73	0 88	1.05	1.26
29	0 08	0.15	0.25	0.36	0.46	0.59	0.73	0.89	1.06	1 27
30	0 08	0.15	0 25	0.36	0.47	0.59	0 74	0.90	1 07	1.28
31	0.08	0.15	0.25	0.36	0.47	0.60	0.74	0.90	1.08	1.30
32	0.08	0.15	0.26	0.36	0.47	0.60	0.75	0.91	1.08	1.31
33	0.08	0 15	0.26	0.37	0 47	0 60	0 75	0 92	1.10	1.33
34	0.08	0.15	0.26	0.37	0.47	0.61	0 76	0 93	1.11	1.34
35	0.08	0.15	0.26	0.37	0.47	0.61	0.76	0.93	1.12	1 35
36	0.08	0.16	0.26	0 37	0 48	0.61	0.77	0.94	1 13	1.37
37	0.08	0 16	0.26	0.37	0.48	0.62	0.78	0.95	1 14	1.38
38	0.08	0.16	0.26	0 38	0.48	0.62	0.79	0.96	1.15	1.40
39	0 08	0 16	0.26	0.38	0.48	0.62	0.79	0.96	1.16	1.40
40	0.08	0.16	0.27	0 38	0 48	0.63	0 80	0.97	1.17	1.42
41	0.08	0.16	0.27	0.38	0.48	0 63	0.80	0.98	1.18	1.43

Table B19

$\frac{100\lambda}{2.3}$ Values for Phoenix, Based on Accelerated Exposure Data

Month	7-9 AM	9-11 AM	$\frac{100\lambda}{2.3}$ 11 AM-1 PM	1-3 PM	3-5 PM
Sept. 1976	0 08	0 35	0.75	0.47	0 08
Oct.	0	0.15	0.25	0 15	0
Nov.	0	0.08	0.15	0.08	0
Dec.	0	0 08	0 08	0.08	0
Jan 1977	0	0.08	0.08	0.08	0
Feb.	0	0.08	0.15	0.15	0
March	0.08	0.23	0 34	0.25	0
April	0.08	0.44	0.73	0.46	0 08
May	0.08	0.55	1.06	0.73	0.08
June	0.08	0.75	1.42	0.97	0 08
July	0.08	0.75	1.43	0.80	0.08
August	0.08	0.59	1.14	0.78	0.08

Table B20

$\frac{\lambda}{2.3}$ Values for the "Typical Day" of each Month in Phoenix

Month	$\frac{100\lambda}{2.3}$, hr.$^{-1}$, total for 7 AM - 5 PM	$\frac{\lambda}{2.3}$, day^{-1}
Sept 1976	1 73	0 42
Oct	0 55	0.13
Nov	0.31	0.074
Dec	0 24	0 058
Jan. 1977	0 24	0.058
Feb	0 38	0.091
March	0.90	0.22
April	1 79	0.43
May	2 50	0 60
June	3.30	0.79
July	3 14	0 75
August	2 67	0 64

252

Table B21

$\frac{\lambda}{2\ 3}$ Values for Phoenix, Corrected for Mismatch of Xenon Lamp
and Sunlight at 300 nm

Month	$\frac{\lambda}{2\ 3}$, day^{-1}, total for 7 AM - 5 PM 18.1
Sept. 1976	0 023
Oct.	0.0072
Nov	0.0041
Dec.	0.0032
Jan. 1977	0.0032
Feb.	0.0050
March	0.012
April	0.024
May	0.033
June	0.044
July	0.041
August	0.035

253

Table B22

Tensile Test Results on Polystyrene

After Miami 45°S Exposure

Exposure Time, days	Breaking Stress (psi)*	Fraction of Original Breaking Stress
0 (control)	10,244 (70 6 megapascals)	1.00
5	8,878	0 87
10	8,903	0 88
15	9,069	0 89
30	8,851	0.86
60	8,842	0.86
90	9,050	0.88
150	8,636	0 84
210	4,037	0.39
300	2,284	0.22

*means of 5-10 replicates.

Table B23

Tensile Data for Polystyrene in Accelerated Exposure,
1.00 Relative UV Intensity, 26.1°C

	Fraction of Original Breaking Stress	
Exposure Time, hr.	0% Rel. Hum.	100% Rel. Hum.
0	1.00	1.00
3	0.97	0.88
6	1.03	0.79
12	0.97	0.84
24	0.90	0.87
120	0.91	0.76
768	-	0.50
1536	0.32	

Table B24

Tensile Data for Polystyrene from Tables B22 and B23,
Expressed as $\log_{10} \left(\frac{1}{P}\right)$ where P = Fraction of Original Breaking Stress

Miami 45°S Data

Exposure Time, days	$\log_{10} \left(\frac{1}{P}\right)$
0	0
30	0.066
60	0.066
90	0 056
150	0 076
210	0.41
300	0 66

Accelerated Test Data

Exposure Time, hours	$\log_{10} \left(\frac{1}{P}\right)$	
	0% Rel Hum.	100% Rel. Hum.
0	0	0
3	0 013	0 056
6	-0 013	0.10
12	0.013	0.076
24	0.046	0.060
120	0 041	0.12
768	–	0.30
1536	0.49	–

Table B25

$$\frac{\lambda}{2.3}, \text{ day}^{-1}, \text{ for Polystyrene Breaking Stress, Miami}$$

Month	7-9 AM	9-11 AM	11AM-1 PM	1-3 PM	3-5 PM
Sept. 1976	0.0045	0 017	0.030	0.023	0.0048
Oct.	0	0 0086	0.014	0 0088	0
Nov.	0	0.0043	0.0086	0.0043	0
Dec	0	0.0043	0.0043	0.0043	0
Jan. 1977	0	0.0039	0.0043	0.0043	0
Feb.	0	0.0041	0.0080	0.0080	0
March	0.0043	0.013	0.017	0.013	0
April	0.0043	0 021	0.028	0.021	0 0045
May	0.0043	0.024	0.036	0.029	0.0045
June	0.0045	0.029	0.041	0 033	0 0048
July	0.0045	0 030	0.041	0 031	0.0050
August	0.0045	0.025	0.038	0.031	0 0050

Table B26

Parameter Values from Table B25 Raised to the 1 30 Power

Month	$(\frac{\lambda}{2.3}, \text{day}^{-1})^{1.30}$					
	7-9 AM	9-11 AM	11AM-1 PM	1-3 PM	3-5 PM	Total
Sept 1976	0.00089	0.0050	0.010	0 0074	0 00097	0 0243
Oct	0	0 0021	0 0039	0 0021	0	0 00810
Nov.	0	0 00084	0 0021	0 00084	0	0 00558
Dec.	0	0 00084	0.00084	0 00084	0	0 00252
Jan. 1977	0	0.00074	0.00084	0.00084	0	0.00242
Feb.	0	0.00079	0.0019	0.0019	0	0.00459
March	0.00084	0.0035	0.0050	0.0035	0	0.0128
April	0.00084	0.0066	0 0096	0 0066	0 00089	0.0245
May	0 00084	0.0078	0.013	0.010	0 00089	0 0325
June	0.00089	0.010	0.016	0.012	0.00097	0 0399
July	0.00089	0.010	0.016	0.011	0.0010	0 0389
August	0.00089	0.0083	0.014	0 011	0.0010	0.0352

258

Table B27

Tensile Breaking Stress Data for Lexan in Accelerated Exposure,

1.00 Relative UV Intensity, 26.1°C

Exposure Time, hr.	Fraction of Original Breaking Stress = P		$\log_{10} (\frac{1}{P})$	
	0% Rel. Hum.	100% Rel. Hum.	0% Rel. Hum.	100% Rel Hum.
0	1	1	0	0
3	0.95	0.93	0.022	0.032
6	0.99	0.96	0.0044	0.018
12	0.91	0.87	0.041	0.060
24	0.75	0.83	0.12	0.081
120	0.82	0.84	0.086	0.076
768	--	0.52	--	0.28
1536	0.67	-	0.17	-

Table B-28

$$\frac{\lambda}{2.3}, \text{day}^{-1}, \text{ for Lexan Breaking Stress, Miami}$$

Month	7-9 AM	9-11 AM	11AM-1 PM	1-3 PM	3-5 PM
Sept. 1976	0.017	0.064	0.11	0.085	0.018
Oct.	0	0.033	0.051	0.033	0
Nov	0	0.016	0.033	0.016	0
Dec	0	0 016	0.016	0.016	0
Jan 1977	0	0.015	0.016	0.016	0
Feb.	0	0.016	0.030	0.030	0
March	0.017	0.047	0.064	0.047	0
April	0.017	0.078	0.11	0.078	0.017
May	0.017	0.092	0.14	0.11	0.017
June	0.017	0.11	0.15	0.13	0.018
July	0.017	0 11	0.15	0.12	0.019
August	0.017	0.09	0.14	0.12	0.019

Table B29

Parameter Values from Table B28 Raised to the 1 82 Power

$$(\frac{\lambda}{2.3}, \text{ day}^{-1})^{1.82}$$

Month	7-9 AM	9-11 AM	11AM-1 PM	1-3 PM	3-5 PM	Total
Sept 1976	0.0060	0 0067	0.018	0.011	0 00067	0.0424
Oct	0	0.0020	0.0044	0.0020	0	0.0084
Nov.	0	0.00054	0.0020	0 00054	0	0.0031
Dec.	0	0.00054	0 00054	0.00054	0	0.0016
Jan. 1977	0	0.00048	0.00054	0.00054	0	0.0016
Feb.	0	0.00054	0.0017	0 0017	0	0.0039
March	0 0060	0.0038	0.0067	0.0038	0	0.0203
April	0.0060	0.0096	0.018	0.0096	0.00060	0.0438
May	0.0060	0.013	0.028	0 018	0.00060	0.0656
June	0.0060	0.018	0.032	0.024	0.00067	0.0753
July	0 0060	0.018	0.032	0.021	0.00074	0.0777
August	0.0060	0.012	0.028	0 021	0.00074	0 0677

Table B30

$$\frac{\lambda}{2\ 3}, \text{ day}^{-1}, \text{ for Lexan Breaking Stress, Phoenix}$$

Month	7-9 AM	9-11 AM	11AM-1 PM	1-3 PM	3-5 PM
Sept. 1976	0.018	0.061	0 11	0.081	0 019
Oct.	0	0.021	0 050	0 031	0
Nov.	0	0.018	0.031	0.018	0
Dec.	0	0.018	0.018	0 018	0
Jan. 1977	0	0 016	0.018	0.018	0
Feb.	0	0 017	0.030	0 030	0
March	0.018	0.044	0.059	0.047	0
April	0.018	0.072	0.10	0.074	0.018
May	0.018	0 081	0.13	0.10	0 018
June	0.018	0.11	0.17	0.13	0 019
July	0.018	0.11	0 17	0.12	0 020
Aug.	0.018	0 090	0.14	0.12	0.020

-

Table B31

Parameter Values from Table B30 Raised to the 1 82 Power

$$(\frac{\lambda}{2.3}, \text{day}^{-1})^{1.82}$$

Month	7-9 AM	9-11 AM	11AM-1 PM	1-3 PM	3-5 PM	Total
Sept. 1976	0.00067	0.0061	0.018	0.010	0.00074	0.0348
Oct	0	0.00088	0 0043	0.0018	0	0.0070
Nov.	0	0 00067	0.0018	0.00067	0	0 0031
Dec.	0	0 00067	0.00067	0.00067	0	0.0020
Jan. 1977	0	0.00054	0.00067	0.00067	0	0.0019
Feb.	0	0.00060	0.0017	0.0017	0	0 0040
March	0.00067	0 0034	0.0058	0.0038	0	0.0137
April	0.00067	0 0083	0.015	0 0088	0.00067	0.0334
May	0.00067	0.010	0.024	0.015	0.00067	0.0503
June	0.00067	0.018	0.040	0.024	0 00074	0.0834
July	0.00067	0.018	0.040	0.021	0.00081	0.0805
August	0.00067	0.012	0.028	0.021	0 00081	0.0625

Table B32

Transmittance at 360 nm and Tensile Data for Polystyrene
in Accelerated Exposure, 1.00 Relative UV Intensity, 26.1°C

Exposure Time, hrs,	Fraction of Original Transmittance at 360 nm		Fraction of Original Breaking Stress	
	0% Rel. Hum.	100% Rel. Hum.	0% Rel. Hum.	100% Rel Hum.
0	1.00	1.00	1.00	1 00
3	0 98	0.99	0.97	0 88
6	0.98	0.98	1.03	0.79
12	0.96	0.96	0.97	0.84
24	0.94	0.93	0.90	0.87
120	0.80	0.67	0 91	0 76
768	0.21	0.24	-	0.50
1536	0.080	-	0 32	- -

264

C-7

Table B33

Transmittance at 360 nm and Tensile Data for Polystyrene

in Miami 45°S Exposure (Started 10-20-76)

Exposure Time, days	Fraction of Original Transmittance at 360 nm	Fraction of Original Breaking Stress
0	1.00	1.00
30	0.94	0.86
60	0.89	0.86
90	0.83	0.88
150	0.55	0.84
210	0.16 -	0 39
300	0.074	0.22

Table B 34

Transmittance at 360 nm and Tensile Data for Lexan
in Accelerated Exposure, 1.00 Relative UV Intensity, 26.1°C

Exposure Time, hrs.	Fraction of Original Transmittance at 360 nm		Fraction of Original Breaking Stress	
	0% Rel. Hum.	100% Rel. Hum	0% Rel. Hum.	100% Rel. Hum.
0	1.00	1 00	1.00	1.00
3	0.93	0.91	0.95	0.93
6	0.86	0 82	0.99	0.96
12	0 69	0.61	0.91	0.87
24	0.54	0 48	0.75	0.83
120	0.28	0.25	0.82	0.84
768	0.12	0.095	-	0 52
1536	0.095	-	0 67	-

Table B35

Transmittance at 360 nm and Tensile Data for Lexan

in Miami 45°S Exposure (Started 9-1-76)

Exposure Time, days	Fraction of Original Transmittance at 360 nm	Fraction of Original Breaking Stress
0	1.00	1.00
30	0.94	0.87
90	0.86	0.80
150	0.80	0 79
210	0.68	0.80
300	0.40	0 24

Table B36

Transmittance at 360 nm for Lexan
vs   Outdoor Exposure Time

$$A_{360} - A_{600} - 0.0309 = \log_{10}\left(\tfrac{1}{P}\right),$$

where P = Fraction of Original Transmittance at 360 nm

Exposure Time, Days	Phoenix, 45°S (started 9-12-76)	Miami, 45°S (started 9-1-76)	EMMA (started 9-12-76)	EMMAQUA (started 9-12-76)
5	0.0046	0.0045	0 0173	0.0100
10	0 0116	0 0099	0 0371	0 0278
30	0.0271	0.0269	0.1016	0 1189
90	0.0601	0.0652	0.3079	0 4241
150	0 0772	0 0982	0.4537	0 6358
210	0 1577	0.1696	1.0473	1 2369

Table B37

Acceleration Factors for Yellowing of Lexan

Exposure Time, Days	Ratio of $\log_{10}\left(\tfrac{1}{P}\right)$ for EMMA to that for 45°S Exposure		Ratio of $\log_{10}\left(\tfrac{1}{P}\right)$ for EMMAQUA to that for 45°S Exposure	
	Phoenix	Miami	Phoenix	Miami
5	3 8	3 8	2.2	2 2
10	3.2	3.7	2.4	2 8
30	3 8	3.8	4 4	4 4
90	5.1	4.7	7.1	6.5
150	5.9	4 6	8 2	6 5
210	6 6	6 2	7.8	7 3
means	4.7	4.5	5 4	5 0

Table B38

Tensile Breaking Stress of Lexan
vs   Outdoor Exposure Time

Time, days	Phoenix, 45°S (start 9-12-76)		Miami, 45°S (start 9-1-76)		EMMA (start 9-12-76)		EMMAQUA (start 9-12-76)	
	P*	$\log_{10}(\frac{1}{P})$	P	$\log_{10}(\frac{1}{P})$	P	$\log_{10}(\frac{1}{P})$	P	$\log_{10}(\frac{1}{P})$
10	0.91	0.041	0.96	0.018	0.92	0 036	0.95	0 022
30	0.91	0 041	0.87	0 060	0.79	0 10	0 78	0.11
90	0.87	0 060	0 80	0.097	0.81	0 092	0 47	0.33
150	0.84	0.076	0.79	0.10	0.27	0 57	0.31	0 51
210	0.80	0.097	0 80	0 097	0.068	1 17	0.076	1 12
300	0.27	0.57	0 24	0 62	0	-	0	-

*P = fraction of original breaking stress.

269